Understanding
Air and Space Vehicles

Understanding
Air and Space Vehicles

Prof. H. S. Mukunda

ABETS, CGPL, Department of Aerospace Engineering
Indian Institute of Science, Bangalore.

CONTENTS

x

FOREWORD

Prof. R. Narasimha

Engineering Mechanics Unit
Jawaharlal Nehru Centre for Advanced Scientific Research, Bangalore

This is an important book, especially for students whose first encounter with aerospace engineering occurs at the Masters level (as it often happens at Indian Institute of Science where there is no undergraduate course on the subject). In many cases there are courses on the scientific fundamentals of subjects like aerodynamics, structures, propulsion, control and stability etc. Looking at this book I couldn't help recalling my own experience when I joined the Institute for what is now called the ME course, straight from a BE degree in mechanical engineering. I found that I was learning the science behind the aircraft without any real feel for the aircraft itself, till I came across a book by A C Kermode called *Flight Mechanics* (now in its eleventh edition). That book took me to a different but fascinating world, and helped make connections with the basic scientific course.

This book by Prof Mukunda serves a similar purpose but with a 21st century ring and some very important differences. First of all it handles both air and space vehicles, which is a welcome improvement as aerospace now has become a single academic discipline and its graduates can opt for a career in either aeronautics or space. Secondly, and in my view most appropriately, it has an appealing Indian flavour as it talks about not only air and space vehicles available in the interna- tional market but also about the LCA-Tejas and the PSLV and the GSLV. This gives it an Indian relevance whose value (particularly for the Indian student) should not be underestimated.

But more than all these is Prof Mukunda's infectious enthusiasm about 'the complexity and beauty of the functioning of aeronautical and space vehicles

with many aspects of aerodynamics, structural components being seamlessly integrated'. And he has succeeded in his desire 'to share this joy in a rigorous way' through a course which he has delivered at IISc several times. The book provides a lively account of how all those sub-disciplines play essential roles in designing and manufacturing a full vehicle, often with exciting performance levels. He has in particular succeeded in presenting aeronautics and space as sharing many similar-ities while at the same time having some very different objectives and performance parameters. He has therefore truly written a book on aerospace vehicles. It would be an excellent book to follow in a mandatory course on aerospace vehicles in a Bachelor's or Master's programme - particularly in India, and possibly elsewhere as well.

So I want to congratulate Prof Mukunda on this wonderful outcome of the years of hard work he has put into the preparation of this book on a fascinating subject. I hope every student, and all those potential managers who need to know some cru-cial truths about a wide variety of disciplines, will find instruction, understanding and joy in reading this book - without either the pain of too much mathematics or the frustration of hand-waving arguments.

Enjoy!

Roddam Narasimha

25 April 2017

PREFACE

Over early years as a faculty member at the Indian Institute of Science, I had always felt struck by the complexity and beauty of the functioning of aeronautical and space vehicles with many aspects of aerodynamics, structural elements, propulsive devices and navigational aids for flight control being seamlessly integrated. I wanted to share this joy in a rigorous way through a course to masters and graduate students interested in appreciating the connectivity amongst all these disciplines in achieving the remarkable performance in aircraft and missiles. While the first course on this theme with focus on aircraft was delivered in 1971, due to other commitments, it was not done again for a long time. Towards 1997, it was felt that the "general knowledge" of students appearing for their comprehensive examination was deteriorating despite major achievements in India - SLV, PSLV having had successful launches and the light combat aircraft crossing several milestones in a string of rigorous test programs before induction into the Indian Air Force. I offered a modified course that puts aircraft and space vehicles into a single package and describe with minimal mathematical content how much of the disciplines (listed above) are important for realizing a successful vehicle. This course was delivered to composite student groups for three years. I truly enjoyed delivering lectures with an occasional demonstration over three years (1998 - 2000), with assignments that involved groups to study, and describing what they learnt about select aircraft, missiles or launch vehicles and what they thought about them. I do not really know if this made a significant impact on their thinking in their professional lives, even though I hope it has. The baton of lecturing was passed on subsequently to the department to continue or modify the course as was thought fit.

Several years later after I completed the book "Understanding Aero-space chemical propulsion", it occurred to me that it would be important to communicate the essentials of what I had learnt and taught on aeronautical and space vehicles through a book. This book "Understanding Air and Space vehi-

cles" is the result of that effort. I had to ask myself if this would be different from similar books by other distinguished scientists: David W. Anderson and Scott Eberhardt's book *Understanding flight* that is widely read and appreciated; Henk Tennekes delightful book *The simple science of flight - from insects to Jumbo jets* that seeks comparisons between insect and bird flight and airplanes through "scaling laws" that are truly impressive, E. Torenbeek and H. Wittenberg's book *Flight physics, essentials of Aeronautical disciplines and technology with historical notes* that provides valuable inputs at more than a casual level for serious readers, M. J. L. Turner's book Rocket and spacecraft propulsion, principles, practice and new developments and Pasquale M Sforza's book Manned spacecraft design principles are examples of well written books and very readable on space launch vehicles.

There are a number of books that bring together air-breathing and non-air-breathing engines into discussion in one book (like what the present author has attempted). But none that the author is aware of brings together aeronautical and rocket based vehicles together to seek similarities and specialities. This book is aimed at that. The author has benefited by reading the books noted above and the style they have followed in communicating their ideas. While Tennekes' book addresses aerodynamics of birds and alongside discusses aircraft aerodynamics, the comparison between birds and aircraft is far more than just aerodynamics. Birds have structural elements that make them light and let them fly with their flexible wings, they have propulsion coming from the conversion of food to energy in moving the muscles, and they have navigational abilities that are truly amazing. The challenging aspects of work in the aeronautical field have also moved into building bird like machines and learning from them to build new small systems like micro and nano-air vehicles. It is important to bring together this knowledge base into a thinking process for a student or new initiate to let new ideas flower. Thus, this book treats aeronautical and rocket-based vehicles through the known disciplines in eight chapters.

There is one other significant way in which this book differs from others. It includes the scaling relations that will immediately help understand the way the vehicle looks and, wherever possible why, these not requiring much algebra to understand them. These include:

1. in aerodynamics, the lift and drag relationships with flight speed and wing area, lift-to-drag behavior wing geometry for various flight regimes,

2. in propulsion, the engine thrust obtained as a function of flight speed, altitude and geometric features of the system along with the role of heat release air- breathing and rocket engines,

3. in structures, bending, torsion and buckling related relations for static loading and the dependence of natural frequency and damping on the mass and material properties; (d) in aircraft performance, the dependence of range, endurance, take-off and landing lengths and the banking performance on coefficients related to aerodynamics, propulsion system and the structures,

4. in stability, the static margin for stability and stick force vs. speed and other pertinent aircraft parameters,

5. in navigation, the radar range equation expressing the dependence of range on energy of electromagnetic radiation and the geometry,

6. the relations of satellite orbits coming from space dynamics are all incredibly beautiful simple relations, the staging of launch vehicles and the simple-minded logic that has let liquid propulsion based launch vehicles perform bet- ter than solid propulsion based systems, the contemplation on all of which will reveal much on why flying vehicles have the form, structure and power they have. They are all a part of this book. Those who wish to pursue specific disciplines can and should refer to the books and references in those disciplines many of which are also cited in this book. Unlike in the past, internet allows exploration of many reference books, scientific papers and Wikipedia based information and knowledge store (extensively referred to in this book) and students have a wide arena for exploring what they seek to understand. Yet, a consolidated view of many elements can come only through a book of the kind set out here.

Arranged in the usual sequence, Chapter 1 entitled "The variety of Aero-space vehicles - what? and why?" describes all the vehicles and the basic considerations for the flight of these vehicles. I would strongly recommend a reading of this chapter before other chapters since the essence is set out here. Chapter 2 deals with Aerodynamics that spans incompressible to hypersonic flows. Chap-

ter 3 on Propusion systems describes principles and processes of the variety of propulsive devices both within the atmosphere and outside of it. Chapter 4 deals with Performance of vehicles postponing consideration of structures to (ratio of structural mass to overall vehicle mass including payload and fuel) to extract the information on the flight performance of both air vehicles as well space vehicles. Following this, Chapter 5 considers Stability and Control of vehicles. This chapter has some mathematical content and can be browsed without necessarily having to plough through the algebraic relations. Chapter 6 deals with Structures, and their static and dynamic characteristics along with aero-elastic aspects and Chapter 7 deals with Navigation and Guidance. Chapters 1, 2, 3, 6 and 7 have sections on birds seeking some relationships with how air vehicles have functioned equally well or even better in some ways. Chapter 8 provides an overview of the whole subject discussed in various chapters of this book.

Who do I think will benefit by reading this book? Engineers beginning their career in the aerospace industry needing a good understanding of the underlying principles of aeronautical and space vehicles can benefit considerably from reading this book. Engineers who have turned managers wanting to move up and shoulder greater responsibilities, overseeing more than one group, should revisit the ideas on the commonalities between vehicle systems from which they would have alienated themselves for a decade or more working hard at specific tasks. Their understanding would be considerably enhanced and they might even enjoy reading some sections since they have probably had practical insight into some systems in greater detail. There may also be interest for others outside the professional circle who want to read parts of this book to gain insight into certain finer comparative aspects of these vehicles.

In writing this book that may have taken the equivalent of 2 years of work in a total period of 10 years, I have benefited from extensively reading some material over several months and extended contemplation with derivation of relations from multiple points of view on the gross as well as subtle aspects. The only realization I have had is that the there is much more to know about many things I had known, enormously more to know about the subjects that I read up seriously only during this period. These refer to structures and material science, stability and control as well guidance and navigation.

<div align="right">
Prof. H. S. Mukunda

CGPL, Department of Aerospace Engineering
Indian Institute of Science, Bangalore
May 2017
</div>

1

The Variety of Aero-space Vehicles - What? and Why?

Table 1.1.: Principal notations

Term	Meaning
AR	Aspect ratio = b^2/A_w
A_w, A_t	Area of the wing and tail = $b\bar{c}$ (m²)
b	Span (m)
c	Chord (m)
$\bar{c}$	Mean chord in a wing with varying chord (m)
cg	Center of gravity
c_D, c_L	Coefficient of drag and lift
$c_{L,\alpha}$	$\partial c_L/\partial \alpha$
c_M	Coefficient of moment
c_{Mcg}, c_L	$\partial c_{Mcg}/\partial c_{L,}$
$c_{A,B}$	$\partial c_A/\partial B$; A = c_L, C_M, etc, B = α, V, etc
CMC, PMC, MMC	Ceramic, Polymer and Metal Matrix Composite
CFRP, GFRP, AFRP	Carbon fiber, glass fiber, and aramid fiber reinforced composites
E, UTS, YS	Elastic modulus, Ultimate Tensile and Yield Strength (N/m²)
EI	Flexural rigidity (Nm²)
F	Thrust (N, kN, MN)
GTO, GSTO, GSYO	Geo-Transfer, Geo-STationary and Geo-SYnchronous Orbit
HEO, MEO, LEO, SSO	High Earth, Middle Earth, Low Earth and Sun-Synchronous Orbit
h	Altitude
J	Polar moment of inertia (m⁴)
K_{Ic}	Fracture toughness (MPa$\sqrt{m}$)
$L, D, L/D$	Lift, Drag (N, kN, MN), Lift-to-drag ratio
M	Mach number
$m_{a,i}$	Mass of aircraft/vehicle (kg, t)
$\dot{m}_a, \dot{m}_p$	Mass flow rate of air, propellant
NP	Neutral point
p, ρ, T	Pressure (atm, N/m²), density (kg/m³) and temperature (⁰C, K)
P	Load on a structure (N)
R_e	Radius of earth (6371 km)
t/c	Thickness-to-chord ratio
x_{ac}	distance of aerodynamic center from nose
x_{cg}	distance of center of gravity from nose
α	Angle of attack
β	Glide angle
Λ	Angle of sweep back
T	Torque (N-m)
V	Flight speed (km/h), Velocity (m/s)
σ	Stress (N/m², MPa)

1.1. Introduction

World has witnessed over the last hundred years, the development and application of a variety of aeronautical, military and space vehicles for civil and military applications. There are several that started with the intent of sports, but expanded into military applications.

Paper planes and kites are made and flown largely for fun by people. Hang gliders and microlights are meant for sports; their building requires more expertise and is handled by special individuals and organizations. Their operation requires more infrastructure. Kites and hang gliders create very little noise and are also used innovatively in military applications. Piston-engine aircraft and helicopters operate at low altitudes and speeds. Jet aircraft can operate at higher altitudes and speeds. Flight beyond atmosphere is accomplished with rocket engines that have to carry their own oxidizer unlike aeronautical vehicles that have engines using atmospheric air for the oxidizer. Satellites operate beyond atmosphere and missiles can also function beyond atmosphere. Further, quite often, the look of a vehicle, the plan view or elevation can reveal the broad objectives of the vehicle. In order to do this, it is essential to understand the fundamental principles of flight vehicles. Most aeronautical movement takes place at altitudes below 12 km for civil aircraft and below 25 km for military aircraft; space launches traverse the atmosphere as soon as feasible; satellites are usually located around 400 km for the international space station, 800 km for sun-synchronous function, 20000 km for global positioning applications and at 36000 km for geo-synchronous function. Ballistic missiles go up to 70 to 90 km at which altitude the payload is launched for ballistic flight. It is important that we must become familiar with is the atmosphere in which the aerospace activities take place. Figure 1.1 shows the spectrum of air and space flight regimes around earth.

1.1.1. The atmosphere

Earth is a near-sphere with an average diameter of 12742 km. The atmosphere is largely below an altitude of 40 km and is composed of 20.9 % oxygen, 78.1 % nitro-gen, 0.93 % argon, 0.03 % carbon dioxide (and the rest some trace gases) by volume on dry basis all through (even up to 90 km). For most thermodynamic calculations a good approximation is 21 % oxygen and 79 % nitrogen. The entire plant world survives because of the carbon dioxide of the atmosphere
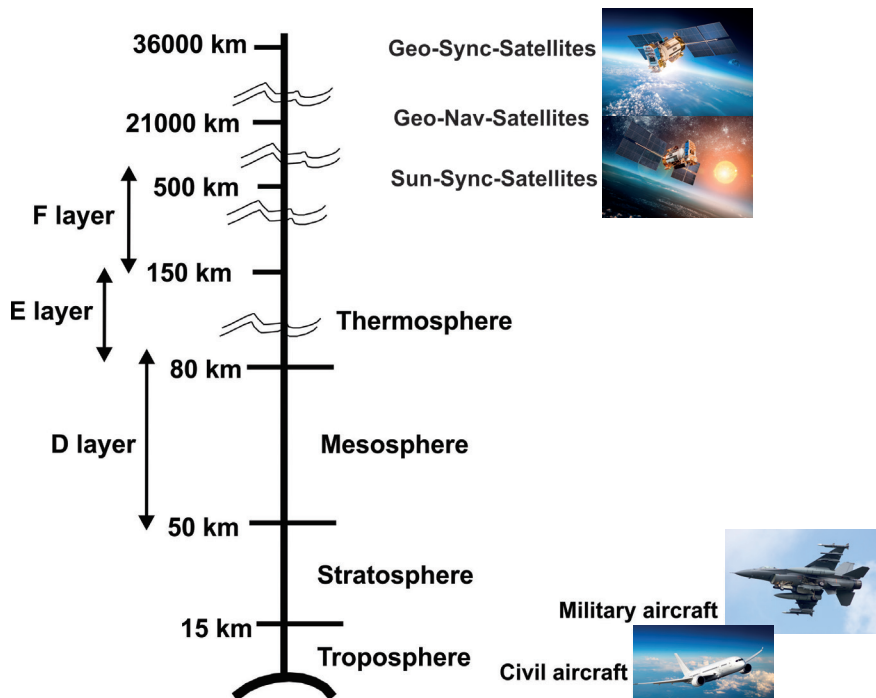
Figure 1.1.: The operational range of air and space flight vehicles in the air and space environment on the earth

(through photosynthetic reactions between carbon dioxide, water vapor in the presence of sunlight).

Between 60 and 900 km, there is ionization of the gases due to low pressure and impingement of high energy radiation from the sun. This zone is segmented into D, E and F layers (from altitudes of 60 - 90 km, 90 to 150 km and 150 to more than 500 km respectively) depending on the degree of ionization is useful to aviation for shortwave radio transmission even though not-so-relevant in
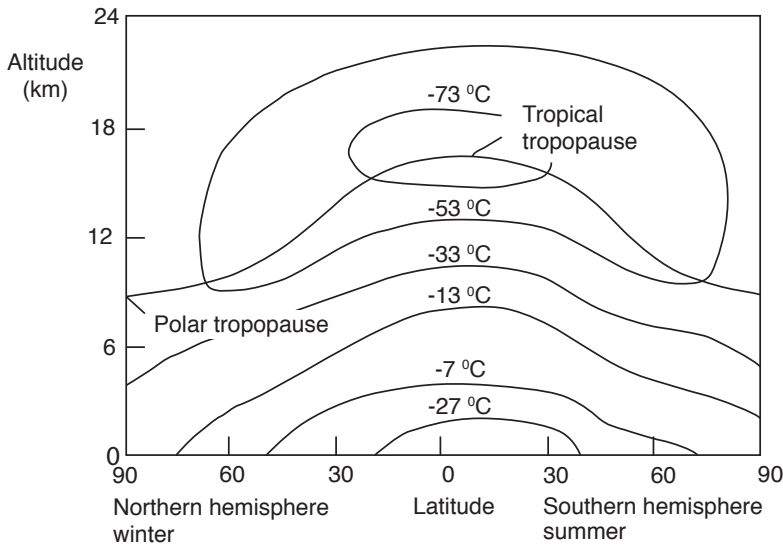
Figure 1.2.: The atmosphere, adopted from Torenbeek and Wittenberg, 2009

view of satellite communication in more recent times. Since the radiation from sun is responsible for these phenomena, there will be differences between day and night behavior with the disappearance of D and E layers and weak F layers at night.

To distinguish between air and space, the edge of atmosphere is taken at an altitude of 100 km and this level is often called Karman line (see Sforza, 2016). The variation of temperature, density and pressure with altitude is set out in Figure 1.4. The temperature decreases with altitude which is typically measured over the mean sea level as 5 to 10 K per km (lapse rate). It reaches a low at an altitude called tropopause. There is also a variation of atmospheric properties over latitudes. Figure 1.2 shows the variation of atmospheric temperatures over the globe. As can be noted, tropopause occurs at an altitude of 17 km in the equatorial zone (latitudes of $\pm 30^0$) and about 10 km in the polar region. Since the exploitation of atmospheric flights largely occurred in the west (Europe and the USA), efforts to standardize the atmospheric characteristics took place there largely. This resulted in the adoption of international standard atmosphere in the design process of air-craft and the engines. The
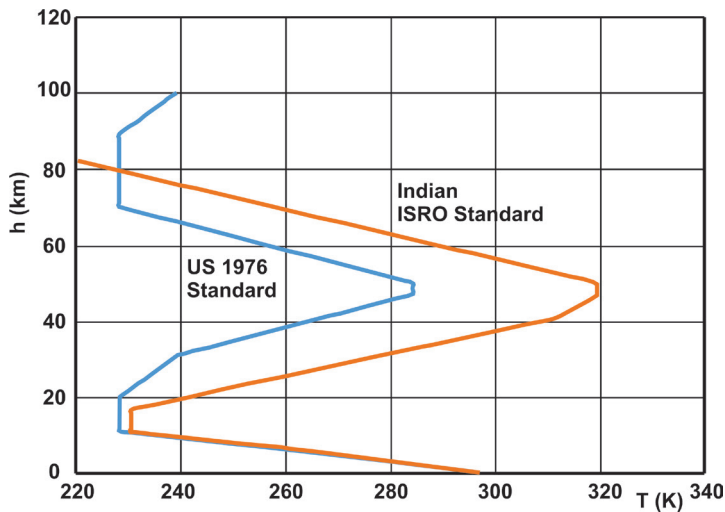
Figure 1.3.: Atmospheric temperature with altitude for International standard atmosphere, Indian standard atmosphere and international tropical reference atmosphere

nature of variation of thermodynamic properties with altitude is different in equatorial zone and this calls for the consideration of what may be more appropriate standards in the equatorial zone. Much work has been done in this area. Ananthasayanam and Narasimha (1979) consolidated the data from several sources including many early ones from India and created first a Indian Standard Tropical Atmosphere (ISTA) and later extended it to International Tropical Reference Atmosphere (IRTA) in 1985. The early work on this subject was also taken up by Indian Space Research Organization (ISRO) to adopt it to space vehicle design (Sasi and Sengupta, 1979). All the three standards are set out in Figure 1.3. There are significant points to note: consistent with the fact that temperatures in the tropical region are higher than in temperate climate, the standard chosen for Indian standards is 300 K as different from ISA set at 288 K. The lapse rate is about the same (-6.5 K/km) up to 10 km. In the case of ISA, tropopause is reached and the temperature remains same at 216.6 K up to 20 km. Beyond this, the temperature increases. In the case of ITRA, the tropopause is at 16 km and so the atmospheric temperature goes down to 195.6 K (-78^0C) and increases beyond that altitude. While ISA is adopted for all con-
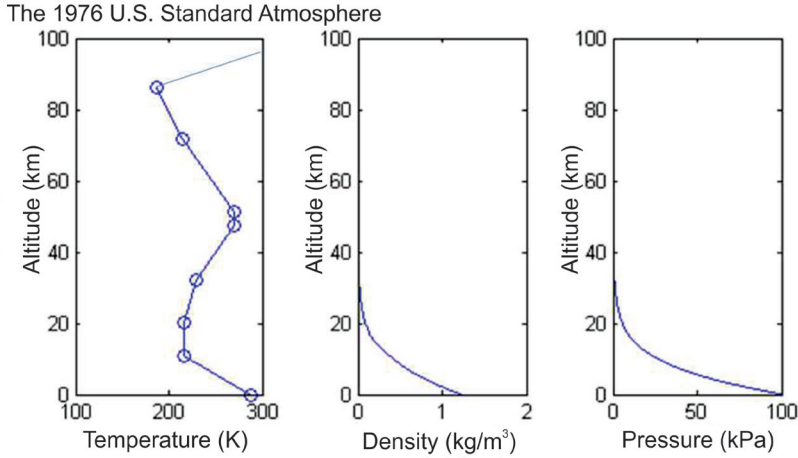
Figure 1.4.: Temperature, density and pressure with altitude, adopted from Chapman et al (1985)

tractual definitions on performance for aeronautical and aero-space products marketed from the west, the position adopted for procurements for tropical operations in India is to specify ISA+ 15^0C as the reference temperature. Indian Air force has adopted the ITRA for the Indian operational transactions. Regions beyond a few hundred kilometers above the earth are largely beset with solar activity and these are extensively studied and documented (Chapman et at, 1985). The variation of various properties for ISA are set out in Figure 1.4. Density and pressure fall off rapidly with altitude.

We first concern ourselves with the behavior till an altitude of 20 km. The behavior can be derived by noting that the pressure gradient is caused by the weight of air above a certain location. Thus,

$$\frac{dp}{dh} = -\rho g$$

(1.1)

Now the equation of state, $\rho = p/RT$ is used to replace the density. Experimentally, it is known that atmospheric temperature decreases linearly with height. This is given by $T = T_{ref} - L_{lr}h$ where T_{ref} is the reference mean sea level temperature (288.16 K) and L_{lr} is the lapse rate - rate at which temperature

decreases with height measured as 6.51 K /km up to a height of 10 km, *the tropopause*. The above equation can be recast as

$$\frac{dp}{p} = -\frac{g}{R}\frac{dh}{dT}\frac{dT}{T}$$

(1.2)

which can be integrated to lead to

$$\frac{p}{p_{ref}} = \left[\frac{T}{T_{ref}}\right]^{g/(RL_{lr})}$$

(1.3)

If we now introduce the values, g = 9.81 m/s², R = 287.0 m²/s² K, L_{lr} = 0.00651 K/m, we get

$$\frac{p}{p_{ref}} = \left[\frac{T}{T_{ref}}\right]^{5.256}$$

(1.4)

One can deduce the density after the pressure is obtained. The data are listed below in Table 1.2. From 11 km onwards, the temperature is constant up to an altitude of 20 km. The equation (1.1) can be used to obtain the pressure from 11 to 20 km from the following equation.

$$p = p_{11km}exp[-1.735(h/10 - 1)]$$

(1.5)

where h is in km. These data are also presented in Table 1.2 as corresponding to ISA. The data on ITRA is also set out in the table. There are differences between the two standards in the data up to 20 km, but they are minor.

1.1.2. Molecular and kinematic viscosity, and Reynolds number

One of the fluid properties that makes an impact on aerodynamics and propulsion is the viscosity. Molecular viscosity, μ is a property of the fluids that decreases with temperature for liquids and increases with temperature for gases. Its fundamental characteristic is to transfer momentum from regions with higher value to those with lower value; it is an equalizer of momentum. In steady flow streams with differing velocities (like say a stream of jet in air) its absence implies that the stream will continue to move with the different velocities. In practice however, this is not the case. The fact that the fluid has viscosity leads to smoothening of the gradients.

Table 1.2.: The properties of international standard atmosphere,*h, p, T , ρ, a =* altitude, static pressure, temperature and density and local acoustic speed; 1 atm. = 101.325 kPa

h	ISA				ITRA			
	p	T	ρ	a	p	T	ρ	a
km	atm.	K	kg/m³	m/s	atm.	K	kg/m³	m/s
0.0	1.000	288.16	1.225	340.3	1.005	300.15	1.166	347.3
1.0	0.887	281.65	1.112	336.4	0.896	294.15	1.061	343.8
2.0	0.785	275.15	1.007	332.5	0.793	288.15	0.963	340.3
3.0	0.692	268.66	0.909	328.6	0.704	282.15	0.873	336.7
4.0	0.608	262.17	0.819	324.6	0.623	276.15	0.789	333.1
5.0	0.533	255.68	0.736	320.5	0.550	270.15	0.712	329.5
6.0	0.466	249.19	0.660	316.4	0.484	264.15	0.641	325.8
7.0	0.406	242.70	0.590	312.3	0.425	257.65	0.577	321.8
8.0	0.352	236.21	0.526	308.1	0.371	251.15	0.517	317.7
9.0	0.304	229.73	0.467	303.8	0.324	244.65	0.463	313.6
10.0	0.261	223.25	0.413	299.5	0.281	238.15	0.413	309.4
11.0	0.224	216.77	0.365	295.1	0.243	231.65	0.367	305.1
12.0	0.191	216.65	0.312	295.1	0.209	225.15	0.325	300.8
13.0	0.164	216.65	0.267	295.1	0.179	218.65	0.287	296.4
14.0	0.140	216.65	0.228	295.1	0.153	212.15	0.253	292.0
15.0	0.120	216.65	0.195	295.1	0.130	205.65	0.221	287.5
16.0	0.102	216.65	0.166	295.1	0.111	199.15	0.193	282.9
17.0	0.087	216.65	0.142	295.1	0.093	201.65	0.161	284.7
18.0	0.075	216.65	0.121	295.1	0.078	204.15	0.134	286.4
19.0	0.064	216.65	0.104	295.1	0.066	206.65	0.112	288.2
20.0	0.054	216.65	0.089	295.1	0.056	209.15	0.094	289.9

Viscosity appears in fluid flow analysis through the Newton's linear stress -strain rate relationship given by $\tau = \mu\, du/dy$ where τ is the tangential stress, u, the stream velocity and y, the distance coordinate normal to the direction of the stream flow. The quantity, du/dy constitutes a strain rate and viscosity can be thought of as the ratio of stress to strain rate (this is similar to elastic modulus in stress-strain relationship in elastic materials).

Viscosity expresses itself in the fluid flow by causing zero difference in velocity between the fluid and the body. This implies that for a stationary body in a flowing stream, the fluid velocity at the surface is 0. *For a flying vehicle, the velocity of the fluid at the surface equals the speed of flight*. The fluid velocity changes between the surface and the free stream in a distance that is small ~millimeters (compared to the size of the flying object - meters). This is called boundary layer, the layer that is most influenced by viscosity.

It was recognized long ago that the flow behavior is captured by a dimension-less number called Reynolds number (due to Osborne Reynolds, the British Physicist at the University of Manchester who discovered it in 1883). *Re* is defined as $Re = \rho V\, l/\mu$ where V and l refer to the characteristic velocity and length scale and constitutes the ratio of inertial to viscous forces because it can also be represented as $[\rho V^2/2]/[\mu V/l]$. The numerator represents inertial component and the denomina-tor viscous stress. The quantity, l, in the expression for Reynolds number is taken as the wing chord for flying vehicles, diameter in the case of spherical or cylindrical objects. The quantity $\nu = \mu/\rho$ is referred to as kinematic viscosity. Its role becomes significant when comparing the momentum transfer with those of heat and species. Like ν, heat transfer is characterised by thermal diffusivity, α defined by $\alpha = k/\rho c_p$ where k and c_p refer to conductivity and constant pressure specific heat respectively. Similarly, species transport in flows with multiple species is characterized by mass diffusivity, D. A conventional approximation made in many analysis aimed at capturing essential behavior is $\nu = \alpha = D$. Like viscous boundary layer, one may have thermal boundary layer and species boundary layer. It is useful to recognize that all the three transport mechanisms are caused by random motion of molecules producing effects in a fluid stream with velocity, temperature and species concentration gradients. Fluid flow, combustion and propulsion are all influenced by them.
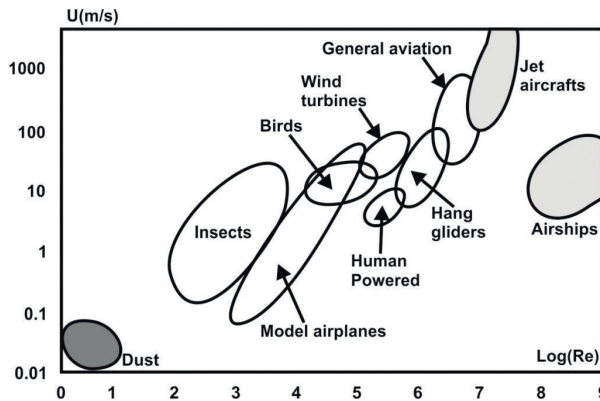
Figure 1.5.: The flight range of flying objects - natural and man made on speed vs. log10 Re plot, adopted from Lissaman, 1983

It may be useful to estimate the value of Re for select cases. For a Boeing 747 aircraft with a mean wing chord of 5 m flying at 250 m/s (900 km/h) at an altitude of 10 km ($\rho = 0.4$ kg/m^3 and $\mu = 1.5 \times 10^{-5}$ kg/m.s $= 1.5 \times 10^{-4}$ N s/m^2), we get $Re = 3.3 \times 10^7$. For an insect with wing size of 20 mm flying at 1 m/s near ground, Re works out to 1600. This range from a thousand to tens of millions constitutes the range in Reynolds number in flying objects - both natural and man-made.

Figure 1.5 shows on a speed of flight vs. Reynolds number, the operational domain of most flying objects. Reynolds number is used to distinguish the nature of flow over bodies (or through them, as well). When the flow properties, implying velocity and pressure, say, have little fluctuations, the flow is termed laminar. When these quantities have fluctuations that are random with the energy in the fluctuations having a wide spectrum (range of frequencies not related to any geometric features of the object), the flow is termed turbulent.

Laminar flows are observed at low Re. As Re increases, disturbances naturally present in the flow get amplified linearly first, nonlinearly later, become three-dimensional and break down into a flow with chaotic distribution of fluctuations. There is also a process of transition from laminar to turbulent flow that occurs over a Re range depending on the smoothness of the geometry and resident free stream turbulence. The role of Re in aircraft dynamics is that the lift distribution is little affected by it, but the drag is influenced significantly.

Table 1.3.: Aerospace vehicles, purpose and importance of disciplines involved; edu = education, C = Civil, M = Military, Ae = Aerodynamics, St = Structures, Pr = Propulsion, Co = Controls, Av = Avionics; El = Electronics; UAVs = Unmanned air vehicles, MAVs = Mini and micro air vehicles

	The aero vehicle	Purpose	Important Disciplines	Alt. km	Speed km/h
1	Paper planes, Walk-wing gliders	Fun, edu.	Ae and Stability	0.01	< 10
2	Kites, Gliders	Sport, C, M	Ae, St, Co, Av	1	< 300
3	Hang-gliders, Wing-suit diving	Sport, C, M	Ae, St, Co	< 5	< 150
4	Micro-lights, home-builts	Sport, C, M	Ae, Pr, St, Co	< 5	< 200
5	UAVs and MAVs	C, M	Co, Av, St, Ae	< 5	< 100
6	Civil transport, Executive, Short & Long range passenger & cargo	C, M	Ae, St, Pr, Co, Av	5 to 12 / 5 to 12	900 / 900
7	Military a/c sub- & supersonic	M	Ae, St, Pr, Co, Av	5 to 20	3000
8	Air cushion vehicle	C, M	Ae, St, Pr, Co	< 5	< 200
9	Gyrocopter, helicopter	C, M	Ae, St, Pr, Co	< 5	< 300
10	Tactical Missiles (A-A/S-A/S-S)	M	Pr, Co, St, Ae, El	5 to 20	3000
11	Long range missiles, strategic	M	Pr, Co, St, Ae, El	< 500	20000
12	Launch vehicles	C	Pr, Co, St, Ae, El	Space	20000
13	Spacecraft	C, M	Co, Pr, St, El	Space	100000
14	Reusable launch vehicle (RLV)	C, M	Ae, Pr, St, Co	Space	-

Also local flow behavior - between fuselage and wing joint region, flows in the tail region are strongly affected by viscous effects. This is why, in actual design, occasional small changes in the geometry lead to avoidance of buffet or vibrations that were otherwise caused due to disturbed flow interactions with the body. Also, under certain circumstances, trubulent flows become laminar, a phenomenon known as reverse transition. These create new features that need to be understood for better flow management.

1.2. The Variety of Aerospace Vehicles

The vehicles described in Table 1.3 cover a wide range of altitudes and speeds with some of them flying outside the atmosphere. It should be noted that the values of maximum altitude and speed presented in Table 1.3 can be taken as indicative.

Glider | Hang Glider

Para Glider | Wing suit Glider

Figure 1.6.: Various types of gliders: The large standard glider, hang-glider, paraglider and wingsuit glider

1.2.1. Paper planes, Walk-along gliders

Paper planes and walk-along gliders have been discussed in a large number of sites on the internet (Wikipedia1, 2011). Just shaping a paper into the right form and shooting it at the right angle provides the momentum for the plane to fly around. If it is not rightly shaped, the glider may tumble.

A walk-along glider is made from paper or plastic like Styrofoam of an appropriate shape and is kept flying by upward force (technically called lift) produced by a sheet held behind the moving plane by a person who walks along with the paper plane as it flies. Just presenting hands or even the forehead behind the flying object will do even if it requires some technique to accomplish this. Several of these designs have names like air surfer, wind-rider, tumble-wing and follow-foil.

1.2.2. Kites

Kites have a rich history connected with the east - China, Indonesia and India going back to 3000 years used for both fun and military applications. Silk fabric and bamboo were used to make the kite and fine silk thread (fine materials have high strength - see section 6.5.2 in Chapter 6) was used for the flying line. Apart from applications for sport, China appears to have used it for measuring

distances, testing the wind, lifting men, signalling, sending messages for rescue missions and communication for military operations. Kites have also been used to demonstrate that lightning implies electrical discharge. The entry of kites into Europe appears to have been from the east in the sixteenth century. NASA Langley center maintains a very good site on scientific and related aspects of kites [Kites, 2011].

1.2.3. Gliders, hang-gliders and wingsuit diving

Figure 1.6 shows the four types of gliders (see Wikipedia2, 2011). While the top left is the standard glider that has the largest gliding capability (implying that it remains flying with the lowest sink rate), other variants got developed largely due to sporting interests, but also have had uses in other spheres.

Glider is essentially a flight vehicle without any engine. It is a product of aerodynamics which guides the shape and size, stability that is affected by shape as well as control surfaces, some fixed and some variable and structures that allow the creation of a light, but strong physical entity. The most crucial part is the wing which helps lift the body because of forces on the wing due to wind against which it must fly. If there is no wind, it cannot fly. To lift it, the glider is pulled by a rope- winch arrangement through a speed range at which the glider is lifted and carried to a comfortable height (50 to 100 m) at which stage the rope link is released and the glider can be autonomous in its flight. Once reaching an altitude, the glider moves up when there is an upward current and sinks when there is none. It can be navigated into going up, moving down, turning or banking or side-slipping as decided by the pilot using the control surfaces - ailerons for turning and side-slipping, ailerons and rudder for a coordinated turn, and elevators for moving up or down (see Figure 1.7 for the location of various control surfaces).

The forces on a glider are shown in Figure 1.7. Various terms used in aerodynamics of flying systems are set out in Table 1.1. The three principal forces are Lift (L), Drag (D) and Weight (W). *Lift is the force normal to the flight direction* and is produced by air flow past the airfoil of the wing. The airfoil is so shaped that at the flow angles under normal flying conditions, the air pressure on the top surface will integrate to much lower values than in the bottom surface so that there is a net force in the upward direction. The component of the force in the vertical direction balances the weight of the glider. This is how it is able to be in sustained flying condition.
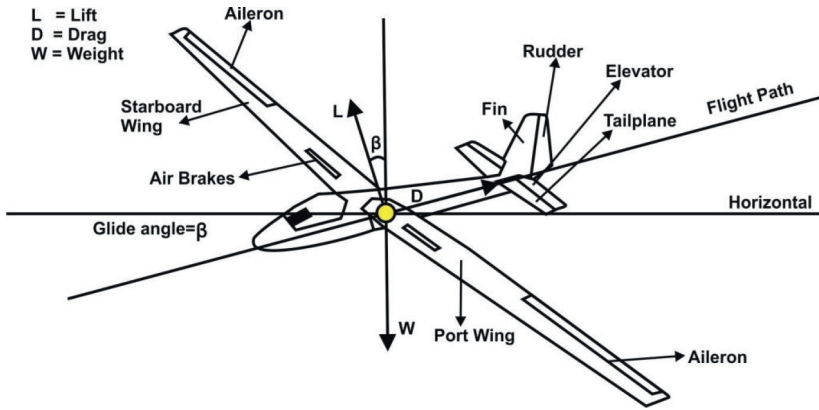
Figure 1.7.: A Glider: Various flying and control elements and the force diagram; moving elevator down allows the craft to move up, applying left aileron that causes left aileron up and right one down causes the craft to turn clockwise, but also bank towards left. This motion can be offset by using the rudder to the left suitably allowing a smooth coordinated turn. Air brakes are applied during landing to ensure touching the surface at the last stage before touchdown. The tail plane provides stability

The vertical and horizontal force balance as well as moment balance around the center of gravity (M_{cg}) will become

$$L cos\beta + D sin\beta = W \text{ (Vertical)}; \quad L sin\beta = D cos\beta \text{ (Horizontal)}; \quad M_{cg} = 0 \quad (1.6)$$

In the above equation, β is called the glide angle - the flight path angle with horizontal (it is also the angle between the vertical and the lift vector). From the force balance on the horizontal line, we get $\tan\beta = D/L$. The ratio of vertical drop to horizontal distance travelled is approximately given by $\tan\beta$ which is the same as D/L. Thus designing the vehicle for large L/D will reduce the sink rate under still wind conditions. This will in fact the objective of the design of a glider if other requirements or constraints do not limit the choice.

Lift and Drag (profile drag) are essentially the pressure, p integrated over the wing area. Thus L or $D \sim pA_w$, where A_w is the wing area. We can replace p by $\rho V^2/_2$ (V = free stream velocity) following the relationship between pressure and velocity. These are put together as

$$L = c_L \frac{\rho V^2}{2} A_w; \quad D = c_D \frac{\rho V^2}{2} A_w; \quad M_{cg} = c_{M,cg} \frac{\rho V^2}{2} A_w \bar{c} \quad (1.7)$$

In the above equations, the quantities c_L, c_D, and c_{Mcg} are called lift, drag and moment coefficients with $\bar{c}$ referring to the mean chord. Both the lift and drag coefficients depend on the geometry and the angle of attack (the angle between the mean chord and the flow direction). They are expressed approximately as

$$c_L = \frac{2\pi}{(1 + 2/eAR)}; \quad c_D = c_{D0} + \frac{c_L^2}{\pi eAR}$$

$$(1.8)$$

where c_{D0} is the combination of profile and frictional drag and the second term on the right hand side refers to lift induced drag (see for more discussion Chapter 2, section 2.2). The drag coefficient, c_{D0} can be reduced by avoiding sharp changes in geometry, making the surfaces very smooth both of which contribute to reducing c_{D0}.

The term AR called the aspect ratio is defined by $AR = b^2/A_w$ where b is the "length" of the wing and A_w is the projected surface area of the wing given by the product of the length and mean chord ($\bar{c}$) of the wing; the term $\bar{c}$, referring to mean chord is relevant for a non-rectangular wing. For a rectangular wing, $AR = b/c$, the ratio of the length to the chord of the wing $c = \bar{c}$. Large aspect ratio and so, large b/c reduces the lift induced drag. The quantity e is called Oswald's efficiency related largely to the aspect ratio and is about 0.9. How does the wing produce lift? and high L/D ? Most wings look like somewhat warped rectangular flat plates from a distance. However, they contain a smooth circular contour towards the nose end and are sharp towards the tail end. To appreciate why this geometry is important, explanations are provided in Chapter 2, section 2.2. The key result that is of impor-tance in the present discussion is the ratio of lift to drag which is the same as the ratio of the coefficients given in equations 1.8. We have

$$\frac{L}{D} = \left[\frac{c_{D0}}{c_L} + \frac{c_L}{\pi eAR} \right]^{-1}$$

$$(1.9)$$

where c_L is the lift coefficient, c_{D0} is the drag coefficient composed of profile and friction components, Typically for gliders, $c_L = 0.12\alpha$ where α is the angle of attack in degrees, c_{D0} is about 0.004 to 0.006, e is about 0.8 to 0.9. The aspect ratio AR is 20 to 30 for gliders (it is lower, about 10 to 15 for other sub
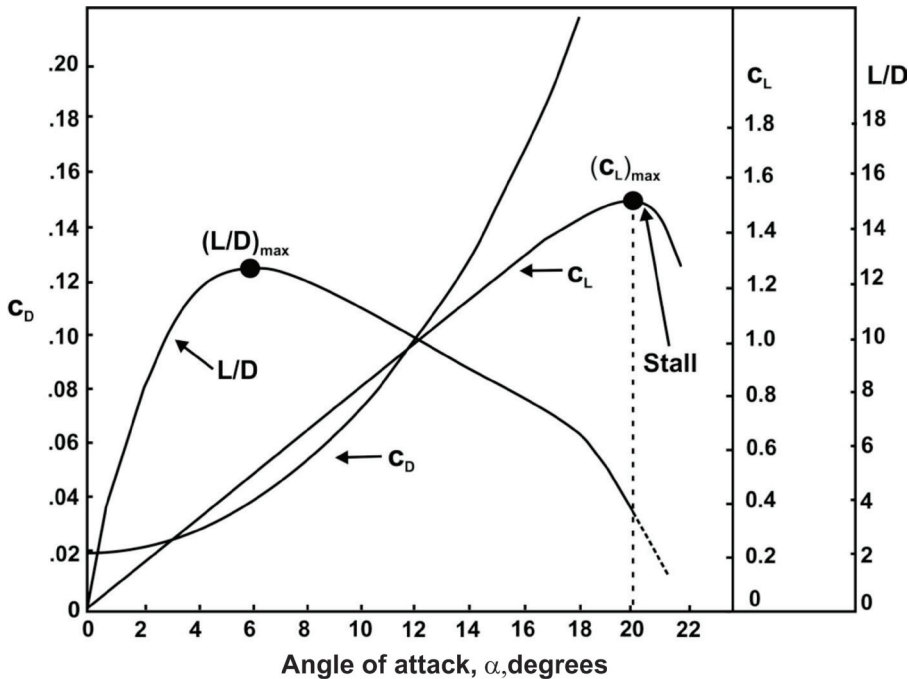
Figure 1.8.: The variation of lift coefficient, drag coefficient and L/D with angle of attack

sonic aircraft and even lower for military aircraft). The broad behavior of these quantities for a specific choice of parameters is shown in Figure 1.8. This figure has many aspects that need discussion.

Lift coefficient: The lift coefficient, c_L is 0 at zero angle of attack, a feature usually valid for symmetrical airfoils. Most usual airfoils have a positive lift coefficient of 0.05 to 0.1 at zero angle of attack. The slope of the c_L - α curve, $dc_L/d\alpha$ is about 2π per radian - implying 0.11 per degree of α. The variation of c_L with α is nearly linear till high angles of attack. It reaches a peak and curves down, a condition known as stall.

Wing stall: As the angle of attack is increased, the flow turning demanded will be so large that viscous forces cause separation of the flow from the surface of the wing. This will happen whether the flow over the airfoil is laminar or turbulent corresponding to small or large flying vehicles. There will be flow re-

versal beyond this point over a significant region. In this relatively low velocity region, the pressure is uniform and more than what would be the case without separation (in the mean). This feature leads to reduced wing lift and enhanced drag. In low speed aircraft with nearly constant wing cross section across, the drop in the lift can be sharp. For a well designed aircraft (implying stable here, see below), the nose of the aircraft drops reducing the angle of attack and hence recovery from stall occurs. In aircraft with swept back wings, the stall phenomenon can occur over patches on the wing; this is not always considered to be better, because if it occurs over an area involving control surfaces, there will be loss of control.

In any case, every flying device must loose its lift before it begins to do high speed deceleration on the ground. Relatively small aircraft stall just before landing. However, large aircraft that need to land in varying conditions of cross wind fly into the runway at speeds above stall. Just before touchdown a flare is performed and descent rate reduced to allow smooth touchdown. Almost immediately afterwards, spoilers are deployed to bring down the lift drastically. The relationship between the velocity at stall and other parameters is set out as

$$V_{stall} = \sqrt{\frac{2m_{a,i}g}{\rho A_w c_{L,max}}}$$

(1.10)

where $m_{a,i}$ is the aircraft mass. Reduction in stall speed implies landing at lower speeds allowing smoother landing with a shorter landing field length. However, the stall speed is higher for heavier aircraft and can be brought down by increasing the wing area and maximum lift coefficient. Both are achieved firstly by extending the wing surfaces and then by causing curvature; these are done by high lift devices that aircraft possess (see section 2.7 for greater discussion). This is why during the landing segment, high lift devices are deployed to ensure that the speed of the aircraft at the time of landing is minimum (just above the stall speed). The wing surfaces called spoilers are brought into operation to cause sudden loss of lift so that aircraft touches the ground, beyond which reverse engine thrust followed by the application of brakes. Thus stall is a very crucial phenomenon which must be mastered by a pilot for avoidance in normal flight and for exploitation during landing.

Table 1.4.: Glide ratios of several flight vehicles

Flight vehicle	Fight condition	Glide ratio (L/D)
Sailplane	Gliding	40 - 60
Hang glider	Gliding	10 - 15
Paraglider	High performance	10 - 12
Gimli glider	Aircraft (no engine)	10 - 12
Wingsuit	Gliding	2 - 3
Powered parachute	Rectangular	4 - 5
Flying squirrel	Gliding	2
Lockheed U-2	Cruise	28
Albatross	Cruise	18 - 20
Arctic tern	Cruise	12 - 15
Boeing 747	Cruise	17
Concorde	Cruise	7
Space shuttle	Landing	4.5

Drag coefficient: (c_D): The drag coefficient is minimum at zero α and increases rapidly with α. This is an indication of a contribution of both profile and viscous effects. The combination of profile and viscous drag components is also called parasite drag. Because of the peculiar way c_L and c_D, increase with α, L/D ratio peaks around $\alpha = 5$ to 9° and this is the reason why the wings are fixed on the fuselage such that when aircraft is taxiing, the angle of attack perceived by the aircraft is in this range. This choice of the angle of attack fixes the lift coefficient of the wing, typically about 0.3 to 0.5 for steady clean configuration. Given the weight of the payload consisting of the passenger(s) largely and the inert mass of the glider, the use of $W = L = c_L \, (\rho V^2_2)A_w$ will give the steady speed at which the glider can fly.

Quite often, from the data of c_D, and c_L versus α as in Figure 1.8, a cross plot of c_D, vs. c_L is made. This plot is called drag polar and is used by designers to understand the aerodynamic behavior of the airfoils. Figure 1.9 shows the drag polar for a specific airfoil (NACA 23012).

Glide ratio *(L/D)*: It is useful to compare the glide ratios (the same as L/D) of several flight vehicles. Table 1.4 presents the data for several vehicles. Gliders designed for best glide have L/D as large as 60. This implies that one can tra-

verse 60 m for a drop of 1 m. Hang-glider is operated by a human being holding on to a frame over which there is a light weight structure and a fabric. Because of the construction, the aspect ratio cannot be large and this is why the glide ratio is limited to 15. Paragliding also leads to L/D up to 12.

Gimli glider is a nickname of the Air Canada aircraft that was involved in an aviation incident in which Boeing 767 aircraft ran out of fuel at a high altitude half-way through the flight and had to be brought in an emergency mode on glide to the nearest airport (Gimli). It can be noted that the L/D on this mode is as large as 12. Wingsuit diving is a variation of skydiving. The geometry of the suit is such that a larger wing area is presented during the drop from an aircraft. While sky-diving leads to free fall, aerodynamics helps achieve a glide ratio up to 3. Powered parachute is essentially a rectangular parachute that carries a motorised propeller and also has wheels. This sport is considered least expensive and is used for low flying. A flying squirrel is provided for reference of a naturally evolved species. Several other birds that engage in long distance cruise and subsonic aircraft have cruise L/D values of 12 to 17. Lockheed U-2 is a special aircraft that flew at very high altitudes and was required to remain in cruise for long times. This is the reason for much larger values of L/D for this aircraft. Concorde aircraft is a supersonic aircraft that was designed for cruise at very high altitudes. Because of its deep delta wing configuration, its L/D is much lower. Space shuttle uses glide mode during landing and because of the geometry of swept wings has a low aspect ratio and hence low L/D. It lands at high speeds (350 km/h compared to 250 km/h for jet liners) and needs a longer runway despite a drag-parachute being used to decelerate it.

Moment coefficients: In equation 1.7, the moment coefficient is around an axis passing through the center of gravity and refers to the flight vehicle since what is indicated therein is c_{Mcg} with particular reference to steady flight at constant altitude. We need to consider first the airfoil itself. A large number of airfoils have been experimentally investigated and set out in an excellent book by Abbot and von Doenhoff (1949). The results of one airfoil are set out in Figure 1.9. The left ordinate of the figure presents the lift and moment coefficients of an airfoil as a function of angle of attack and the right ordinate of the figure shows the drag and moment coefficients as a function of lift coefficient. The plot of c_D, vs. c_L constitutes the drag polar. The changes in the drag polar with Reynolds number are essenta-ially due to changes in the character of the flow over the airfoil. The slope of the lift coefficient with the angle of attack ($\partial c_L / \partial \alpha$) can be obtained quite accurately from a simple theory of thin airfoils and has
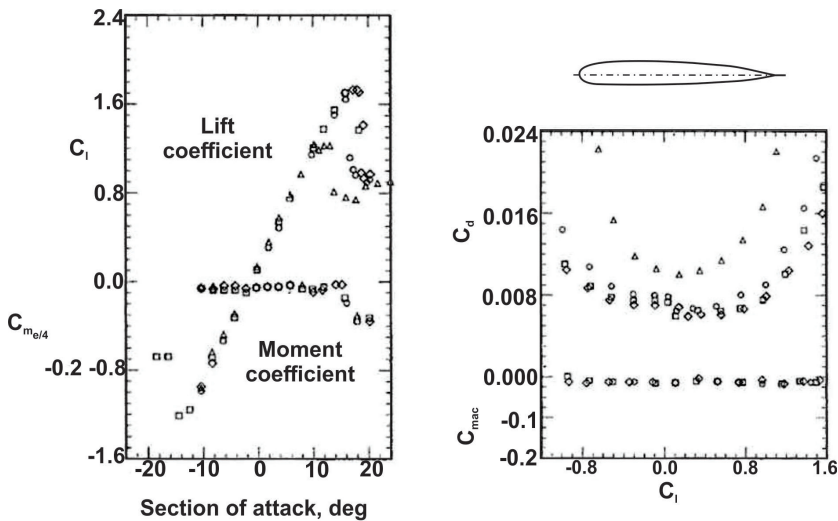
Figure 1.9.: The lift, drag and moment coefficients about quarter chord points and aerodynamic centre $(c_L, c_D, c_{M,a/4}$ and $c_{M,ac})$ with angle of attack at various chord based Reynolds numbers (Re) for NACA 23012 aerfoil drawn from Abbot and von Doenhoff (1949); Data points: circle - Re = 3 million, square: Re = 6 million, diamond: Re = 8.8 million, Triangle: Re = 6 million, standard roughness

been set out in equation 1.8 till large angles of attack - near to wing stall, as evident from a near-linear character of the behavior. While parts of drag coefficient can be similarly estimated, the drag coefficient is best obtained from experiments; so also the moment coefficient that is composed of both these parts. The moment coefficient is sometimes described around quarter chord axis and some times around aerodynamic center which is defined as the axis such that moment coefficient does not vary with the lift coefficient. For most aerfoils with moderate camber the aerodynamic center is not far from the quarter chord point. As can be seen from Figure 1.9, the moment coefficient is near zero for this airfoil (NACA 23012). For symmetric airfoils it is zero and for cambered airfoils it varies between −0.02 to −0.3.

These two previous figures have additional information on lift and drag coefficients. The lift coefficient is non-zero at zero angle of attack because the airfoil is cambered. The lift coefficient at negative angle of attack follows the same slope as for positive angles of attack. The values of the lift coefficient for moderate angles of attack do not depend on Reynolds number or the roughness.

That the Reynolds number dependence of drag coefficient is similar is also clear from the Figure 1.9 on the right ordinate. Only at high angles of attack dominated by separation, do Reynolds number and roughness matter.

1.2.4. Stability and Control - importance

In order to appreciate the aspects of stability, it is useful to examine the path of the glider or an aircraft from take-off to cruise conditions. In the case of a glider, an auxiliary arrangement is provided to accelerate the vehicle on the runway till the take-off speed is achieved - lift being larger than the weight. At that time, elevator is moved so that the tail produces a downward force. This causes a moment around the center of gravity for the vehicle to become airborne. In the case of an aircraft, the pilot (and the co-pilot) taxi along the runway using engine power and accelerate the aircraft to a speed for lift to be larger than the weight using the elevator so that the aircraft lifts off from the ground. Then onward, aircraft accelerates under the power of the engines and the elevator angle is reduced slowly over the next period - typically about ten minutes or so when the the aircraft reaches the specific cruise altitude. Later, for the duration of several hours, the aircraft moves steadily unless air traffic control indicates a change in the corridor for the flight to higher or lower altitude or specific direction to help avoid major clear air turbulence issues or traffic realted matters. When the aircraft moves steadily over a long time, the flight parameters are set using what are known as trim tabs. Under this condition, the net lifting force equals the weight, the thrust equals the drag and the moment of all the forces around the axis through the center of gravity is zero. The trim tabs are relatively small surfaces, part of elevator located towards the aft end which cause the small changes to restore the flight parameters that vary because of the consumption of the fuel that alters the center of gravity of the aircraft or other disturbances.

The question of stability is posed thus. The aircraft is flying steadily at constant altitude - called the trimmed condition. If the aircraft gets impinged by a gust for a brief while, will its flight path get restored after the gust passes? The answer to this question is a part of the study of static stability. The next question that is asked is: how long does it take for the aircraft to come back to its original flight path?An alternate way of posing this question is: under the
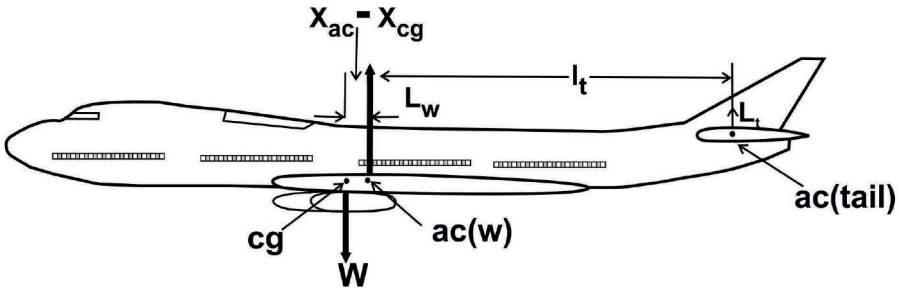
Figure 1.10.: The principal forces on an aircraft. The stability is obtained by the moment around the center of gravity being balanced by the tail plane lift

usual oscillatory recovery of divergence, what is the duration of period halving or doubling? The answers to this class of questions are covered under dynamic stability.

A simple way to begin understanding stability is thus: suppose you consider a rectangular wing in the form of say, a typical envelope and launch it with some speed axially from a height, the cover will move in a tumbling mode till it reaches the ground. If now you add a weight in the form of a long pencil into the cover near quarter chord point or so, you can notice that the cover will glide smoothly to the ground. This changed behavior is due to stability. To appreciate this we look at the force balance of a flying vehicle (see Figure 4.6).

We first note that the force balance $L_w + L_t - W = 0$ satisfies the vertical equilibrium requirement (vertical upward taken positive). Thrust *(F)* equals drag *(D)* for the horizontal equilbrium. It is not considered further here because it is not as significant as of vertical forces located at widely different points (here, tail lift is positioned at a distance of l_t from that of L_w). If we take the moments about the center of gravity (clock-wise moments taken as positive), we get

$$M_{cg} = M_0 - L_w(x_{ac} - x_{cg}) - L_t(l_t + x_{ac} - x_{cg}) \qquad (1.11)$$

Here, M_0 is the moment due to wing pressure distribution, L_w is the wing lift, L_t is the tail plane lift acting at a point l_t from the wing aerodynamic center, x_{ac} and x_{cg} are the distances of the aerodynamic center and the center of gravity from a reference position that is taken here as the nose of the aircraft. The precise reference location does not influence the results since what matters is
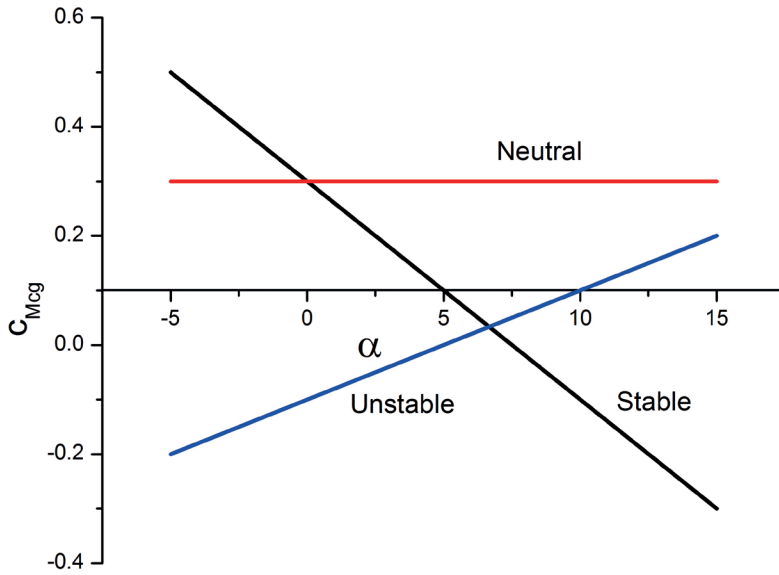
Figure 1.11.: The moment coefficient as a function of the angle of attack, α for a number of cases

the relative location. If we render the terms dimensionless as done earlier (eqns. 1.7), we get

$$c_{Mcg} = c_{M0} - c_L \frac{(x_{ac} - x_{cg})}{\bar{c}} - c_{Lt} \frac{A_t l_t}{A_w \bar{c}} - c_{Lt} \frac{A_t}{A_w} \frac{(x_{ac} - x_{cg})}{\bar{c}}$$

(1.12)

where c_{M0} is the moment coefficient of the wing and tail combination around the aerodynamic center, $c_L = L_w / (\rho V^2 / 2) A_w$, $c_{Lt} = L_t / (\rho V^2 / 2) A_t$ and it must be understood that the tail has generally zero moment coefficient around its aerodynamic center because most airfoils chosen are symmetric. The term $(A_t l_t) / (A_w \bar{c})$ is called the tail volume ratio denoted by V_t. The value of V_t is typically about 0.5 to 0.65 for most aircraft. This relation is used to obtain the tail area required for providing the required stability margin (see Chapter 5). The above equation can be rearranged as

$$c_{Mcg} = c_{M0} - \left[c_L + c_{Lt} \frac{A_t}{A_w} \right] \frac{(x_{ac} - x_{cg})}{\bar{c}} - c_{Lt} V_t$$

(1.13)

Figure 1.11 shows schematically the variation of c_{Mcg} with the α, the angle of attack of the main wing. All the lines start from some value of c_{Mcg} at zero angle of attack and decrease, stay at the same level or increase. Each of these cases refers to stable, neutral and unstable condition. If, in particular, we examine the stable curve, we consider the behavior at the trim condition where $c_{Mcg} = 0$. Now the occurrence of a gust may increase the angle of attack slightly. At this condition c_{Mcg} is negative. This means that the tendency is to return the angle of attack to 0. This implies stability; stated differently, the change of moment coefficient with angle of attack must be negative. Instead of the angle of attack we can choose the lift coefficient as their relation is linear to write for the derivative of the moment coefficient with the lift coefficient as $c_{Mcg,cL} = \partial c_{Mcg}/\partial c_L < 0$. For neutral stability $c_{Mcg,cL} = 0$ and instability $c_{Mcg,cL} > 0$. We can now express the derivative as

$$c_{Mcg,cL} = \frac{\partial c_{Mcg}}{\partial c_L} = - \left[1 + c_{Lt,cL}\frac{A_t}{A_w} \right] \frac{(x_{ac} - x_{cg})}{\overline{c}} - c_{Lt,cL}V_t \tag{1.14}$$

where $c_{Lt,cL} = \partial c_{Lt}/\partial c_L$. The point at which neutral stability is obtained is called the neutral point (NP). To obtain this value, we set $c_{Mcg,cL} = 0$ in equation 1.14 to get

$$\frac{x_{NP}}{\overline{c}} = \frac{x_{cg}}{\overline{c}} + \frac{c_{Lt,cL}V_t}{(1 + c_{Lt,cL}A_t/A_w)} \tag{1.15}$$

We introduce this expression for the neutral point in eqn. 1.14 to obtain an expression for $c_{Mcg,cL}$ as

$$c_{Mcg,cL} = -\frac{(x_{NP} - x_{cg})}{\overline{c}}(1 + c_{Lt,cL}A_t/A_w) \tag{1.16}$$

In the above equation, the quantity $(x_{NP} - x_{cg})$ is the stability margin and as long as it is positive, there will be stability. The neutral point can also be interpreted as the aerodynamic center of the airplane in view of the fact that moments about this point do not change with angle of attack even if the magnitude of the lift force itself is altered.

The role of the position of centre of gravity (x_{cg}) is two fold:

The currently more evident one concerns stability. If $(x_{NP} - x_{cg})$ is more positive, greater is the stability. Thus civil aircraft that do not need to do sharp maneuvers will have a reasonable value for the margin of stability. Military aircraft that are expected to be very agile will have very low value of $(x_{NP} - x_{cg})$ or some of them even negative. The stability margin has a direct effect on the control forces required to maneuver an aircraft. Small aircraft can manage with the control stick in the cockpit directly linked to the operating control surface. Larger aircraft have hydraulic devices to manage the control surfaces. More recent times have seen electrical systems; such aircraft are supposedly using fly-by-wire approach for control. Those aircraft that have little margin or even unstable cannot function unless they are flown by fly-by-wire due to need for fast responses. More on both these aspects will be the subject of Chapter 5.

The less known role of the center of gravity concerns performance optimization towards fuel consumption. If the center of gravity if ahead allowing for more stability, the tail forces required to maintain the equilibrium will be larger and this increases the wing lift and so, the drag and consequently the fuel consumption. Thus one cannot design for too much stability either. More on this is discussed in Chapter 4, section 4.8.

1.2.5. Microlights and home-builts

Microlight aircraft are adaptations of hang glider. Instead of a person hanging from the rod, there will be regular seat(s) and a reciprocating engine driven propeller. The propeller provides the thrust for the flight. The aerodynamic features are similar to those we have discussed in the earlier section. Home-builts are aircraft or flying vehicles built by amateurs for personal use or for participation in air races (the famous annual Oshkosh experimental air flight races in the USA) classified under experimental aircraft. While the accident rates in these aircraft are about double of commercial flight operations, they have contributed immensely to public interest and encouragement to innovations in flying machines.

1.2.6. Dirigibles and Aerostat

These are lighter-than-air technology including balloons and powered airships. The word dirigible comes from a French word meaning "steerable" and the word aerostat implies remaining in the atmosphere with aero-static buoyancy

Figure 1.12.: Typical tethered balloon built with a kite attached and aerostat built by ADRDE, India

created by using a lighter gas inside the balloon. Typical gases used are hydrogen and helium. Because of fire safety reasons, helium is a preferred gas. There are many variants in the technologies. Airships with no structural framework using only a lighter gas inside are called "blimp". Rigid and Semi-rigid airships use structural framework fully or partially. There are also systems that combine aero-static buoyancy with aerodynamic lift. The balloons may be untethered or tethered. Tethering can be "live" implying that the power and gas links are drawn from the ground support system and it can be "dead" if power support for the payload is carried on board. Live tethering allows carrying greater useful payload. They have multitude of uses both in civilian and military sector. They can be used as stationary systems located at an altitude with payload available for communications in difficult terrains, infrastructure protection, border and maritime reconnaissance and surveillance. The systems are set aloft from mobile or fixed system. Typical altitude of operation goes up to 7 km and operational range up to 400 km with higher altitude allowing for better range. They can be built in a variety of shapes and sizes (Anonymous, 2017). Two of these are shown in Figure 1.12.

Aerostats need to stand up to speeds up to 40 m/s (150 km/h) and air ships move at these speeds. The force balance is given by

$$F_v = \mathcal{V}(\rho_a - \rho_g)g - m_{str}g + c_L \frac{\rho V^2}{2} A_{c-s}$$

(1.17)

$$F_h = c_D \frac{\rho V^2}{2} A_{c-s}$$

<div align="right">(1.18)</div>

where F_v and F_h are the vertical and horizontal forces, V is the volume of the aerostat, ρ_a and ρ_g are the densities of air and gas (say, helium), m_{str} is the structural mass proportional to the surface area of the aerostat with a cross sectional area A_{c-s}. The first term on the right hand side of the equation for F_v is due to buoyancy. The net forces must be taken up by the tether attached to the ground system. This leads to the equation for the force on the tether as $F_{tether} sin\,\theta = F_v$ and $tan\,\theta = F_v/F_h$. When we consider airships moving steadily, the speed of movement V is given by $F_v = 0$ and $F_h =$ thrust due to propeller.

1.2.7. UAVs, MAVs and Bird-like vehicles

In the last twenty years progressively sophisticated unmanned air vehicles from mini to micro to nano variety have been built for a number of uses. These have been possible because of miniaturization of electronics and computing hardware as well as sophisticated optical devices. A relatively tiny vehicle directed and maneuvered from a large distance can accomplish tasks of seeing the battle field or a target area closely and in some cases, fire laser guided precision missiles with telling effect.

There are basically three types of micro-air vehicles - (a) those based on fixed wing design that has higher L/D and so, allowing for longer flight times (b) those that use rotary-wing principle that permits hovering and movement all round but for much shorter flight times and (c) those that use flapping wing idea similar to insects and birds with great maneuverability that demands very inventive strategies on all aspects - aerodynamics, control, structures and propulsion. Control system design to obtain matching maneuverability with wind turbulence and tight surroundings will hold the key; some new ideas known as optical flow are integrated in these designs (see Chapter 5 and section bird-control-law for more details) Figure 1.13 shows four different types of smart vehicles developed in recent times (Wikipedia3, 2016).

Raven is a battery powered light weight (20 N ~ 2 kg mass) vehicle with a color day video camera, or a two color infrared night camera that can stay in the air for 80 minutes at a time (built by a company AeroVironment in the USA). The cameras broadcast real-time video back to an operator who can control the ve-
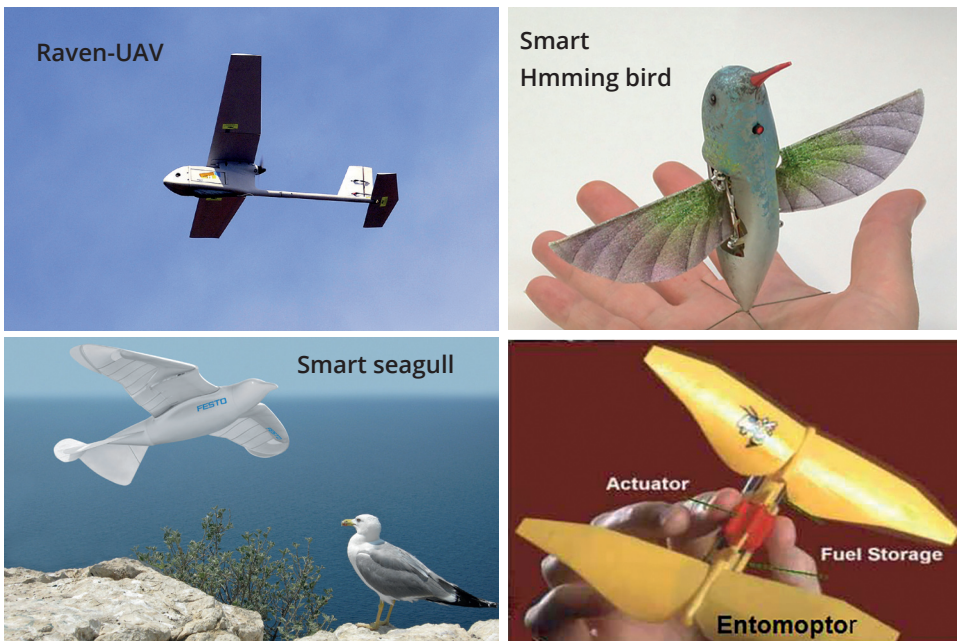
Figure 1.13.: Top left: Raven, the US built hand-managed surveillance flying aircraft, top right: US built Smart hummingbird; bottom left: German built Smart bird; bottom right: US built Entomopter

hicle through a laptop. Its cruise speed is about 40 km/h but can reach 90 km/h at the peak. Launched by turning on the motor and being thrown into the air, it flies within a range of 15 kilometers on a pre-programmed route with GPS for-navigation. They land by coming back to ground at a designated GPS location. Made of Kevlar they survive on an average about 200 landings.

While some Ravens have got shot down, the most common cause of loss is the loss of communications link (as the aircraft flies out of range) or a software/hardware failure on the aircraft. Since it is launched and managed by troops on their own, apparently, the lost aircraft are recovered by putting a label on each aircraft, indicating in the local language that the return of the hardware would be rewarded; several lost aircraft were indeed recovered this way. (see Wikipedia3, 2016) The Nano Hummingbird designed and built by the company AerVironment, USA weighs 0.19 N and has a wing span of 160 mm. It flies around at 18 km/h for about 11 minutes with noise level slightly larger than a real hummingbird, though it could be mistaken for a real bird. It uses its wings

for propulsion and steering, and can move in any direction or rotate in a fixed place like a helicopter. It carries cameras and communication equipment and can be controlled remotely. It has gone through development and is likely to be used in some battle field environment in coming times.

A German company, Festo (see Fischer and Stoll, 2016) designed the robot weighing 4.5 N with a wing span of 2 m that not only flap up and down, but bend at specific spots just like the way wings of a normal bird do in flight. When flying, a lever mechanism increases the degree of deflection from the tor-so to the wing. The wings can also twist in such a way that during the upwards stroke, the leading edge of the wing is slightly upwards to provide a positive angle of attack. Direction is changed by the opposing motion of the head and torso of the bird. This movement is synchronised by cables and two electric motors. The movements of the tail also help change directions. It can tilt left or right to initiate turns or move left to right to generate yaw. The tail also acts as stabilizer and a pitch elevator. Modern technology of lightweight carbon fiber is used for the body of the bird. One of the key features is that the development of this technology with its functional integration of coupled drive units provid-ed significant insights that can then be applied to hybrid drive technology.

Entomopter is a smart insect that produces lift by flapping wings (Wikipedia3, 2016). There are two wings, front and rear, which are coupled to the fuselage in an X configuration. These wings are made of a thin film maintaining stiff-ness with flexible veins to give the wings the curve they need to generate lift on both the up-and downstrokes. The flapping is provided by a reciprocating "chemical" muscle. A monopropellant is injected into the body, causing a chem-ical reaction that releases a gas. The gas pressure build-up pushes a piston in the fuselage. This piston is connected to the pivoted wings, causing them to flap rapidly. Some of the gas is exhausted through vents in the wing and can be used to change the lift on either wing so the vehicle can turn as well. In a fuselage like arrangement, the power source and primary fuel tank are located in the central zone. There are also sensors and navigational aids located in the central zone and surface locomotors designed to provide anti-roll inertia and auxiliary fuel storage.

The field of nano, micro and mini flight vehicles is very active particularly because the investment in research and development is not as heavy as in major aircraft and the developments in miniaturization are being continuously

bootstrapped into the development of these vehicles. The principles of force development for flapping wings like humming bird will be discussed in Chapter 2, section 2.5. The relatively smooth and stable flight of tiny birds like bats and insects through gusts and complex terrain has evoked aeronautical attention particularly on aerodynamics and control system elements over the last decade. Ideas of optic flow have been integrated into the control system elements to produce very elegant formation flights of a fleet of quad-copters. More on the relationship of bird flight with control systems is discussed in Chapter 5, section 5.8.2.

1.2.8. Civil transport aircraft

Civil transport for passengers and freight is one of the most important segments of flight industry. Optimization of the performance demanding a safe transport at as high a speed as possible with the greatest fuel economy is the objective. Comfort is essential but is secondary to the other demands. Both high speed and fuel economy are covered by aerodynamics. The maximum speed possible is determined by what is known as drag rise Mach number (the ratio of speed of flight to the local speed of sound) that determines the increasing role of compressibility of the fluid. Analysis of flows with increasing speed shows that as one approaches the speed of sound, sound waves caused by the body, particularly in the front area accumulate close to the flying object and at a flight speed to the speed of sound (Mach no = M = 1), the sound cannot propagate into the front of the flying object and creates a strong wave across which pressure rises significantly. This pressure rise creates a force called wave drag. The wave drag, D_w divided by the dynamic pressure, $(1/2)\rho V^2$ is the wave drag coefficient, $c_{D,w}$. Compressibility effects on drag begin to dominate at around free stream Mach number, $M\sim0.85$ because around this mach number, the speed over the thicker part of the wing reach M = 1 leading to additional drag. A simple way has been found to extend the range of flight speeds to obviate the problem of drag rise. The approach lies in making the wing swept - forwards or back, back mostly.

Figure 1.14 shows the transition to the form of the vehicle as one moves from a glider to an aircraft at low speeds and then at higher speeds. While the first one is a micro-light, the most elementary form of an autonomous flying device, and the second, a glider modified to include an engine that can be brought into operation as desired, the business-jet and the long range air liner as examples

Microlight

Glider with retractable
jet engine

Business jet

Long distance
airliner

Figure 1.14.: Modifications of gliders to aircraft: The microlight that is a glider with an engine, a standard glider with a retractable engine, a business jet with slight sweepback and a long range civil aircaft with sweep=back of about 45⁰

of civil transport aircraft designed to operate at as high speeds as feasible. One distinguishing feature is that wings that are normal to the fuselage become "swept back" as speeds increase. Boeing 747 is a long range air liner with a swept back wing with a sweep back of about 38⁰. It flies at a flight Mach number (M) of 0.85. In comparison, Boeing 737 and Air bus A 320 are designed to fly at $M = 0.78/0.79$. Other aircraft like Boeing 757, 767 fly at $M_0 = 0.80$, A330 and A 340 at $M = 0.82$ and Boeing 777 is designed for $M = 0.84$.

How does sweep back enable raise the speed for limiting the drag rise? When sweep back is enabled and the air flows over the wing, the straight flow encounters a wing with longer chord for the same thickness. This implies that the thickness-to-chord ratio is brought down. This enables reducing the peak speed achieved by the fluid over the surface. Since this is a geometrical effect,

an alternate way of accounting for the behavior is to take the effective Mach number as $M cos \Lambda$ where Λ is the sweep back angle. It is the angle between the line normal to the axis of the aircraft and quarter-chord line of the wing. While sweep back is a definite choice for aircraft flying at high speeds including those at speeds larger than of sound (called supersonic flying), its effects on the flying qualities are many. Among the downside effects are (i) lower lift at lower airspeeds, (ii) higher stall speed, (iii) higher angle of attack at stall, (iv) tendency for the tip-stall to occur earlier leading to pitch-up at stall and (v) poor oscillatory stability and other minor effects. Nonetheless, these ill-effects are moderated through other changes or simply accepted; for instance, the higher landing speed is dealt with by providing a longer runway.

Civil transportation also includes freight of goods. Many variants of civil aircraft are built for this purpose. In special cases, aircraft are built only for transportation of airworthy equipment. An example is the C-140 aircraft to transport the space shuttle.

One of the key aspects on which great attention is paid is the safety of operations. While it is generally true to say that flying vehicles have always derived greater attention to safety because any small deviation sometimes is very critical to safety, it is particularly true of passenger aircraft. Airliners carry 200, 300, 500 and 800 people over long distances and almost no deviation affecting the safety is tolerated. All component designs are reviewed, tests are conducted on the components extensively and the test results are reviewed and clearance is obtained for use in flight worthy vehicles.

1.2.9. Military aircraft

Aircraft for military applications cater to a wide range of demands: transport, reconnaissance, bomber, fighter and a single aircraft fulfilling multiple roles. While the aerodynamic features of transport and reconnaissance remain the same as was discussed for subsonic aircraft for civilian needs, the fighter, the bomber and those fulfilling multiple roles are able to fly supersonic and in some instances from shorter runways. The fact that speeds of these aircraft are as high as $M = 3$ demands vastly different configuration for their wings and bodies. The bodies are made sharp edged instead of being smooth and rounded as for subsonic aircraft. This is because the lift has to be generated through differential forces caused by shock waves unlike in the subsonic regime. The drag

LCA - India

F22-Raptor-USA
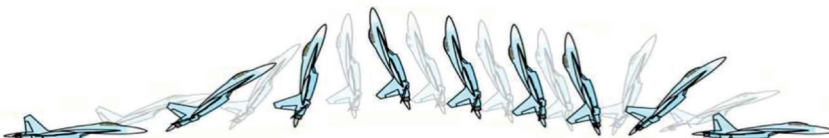
Sukhoi 30, cobra Maneuver - Russia

Hawkeye - USA

F-22-Raptor-USA

Figure 1.15.: Top left: LCA - Tejas multi-role fighter developed by India; top bottom right: Two different views of F-22, one of the most advanced stealth fighters developed by the USA; the middle left one the Russian Sukhoi 30MKI aircraft in various stages of a Cobra maneuver and the bottom left is the US built Hawk-eye, the very advanced reconnaissance aircraft

too is controlled by shock waves and frictional forces play a minor role. Sharp edged designs are good for high speeds, but not so for low speeds. Since any supersonic aircraft has to traverse low speeds before getting to higher speeds implies that the flow behavior will be inferior to what happens in subsonic regime.

This is accepted as an inevitable feature. The payload characteristics will be very different from a civil aircraft. The human component of the flying aircraft is limited to a pilot and in addition, a co-pilot and the payload consists of weapons – bombs and air-to-air or air-to-surface missiles. High acceleration and maneuverability are principal demands limited by the ability of the pilots to withstand longitudinal and lateral accelerations for certain durations as well as the physical integrity of the aircraft. In fact, being a pilot of a military

aircraft has demands on physical fitness far in excess of those for other flight vehicles. Figure 1.15 shows five different types of military aircraft.

The Light Combat Aircraft (LCA) developed in India (see Wikipedia4, 2016). It is a tailless compound delta-wing design powered by a single engine. It has the delta wing configuration, with no tail-planes or canards and a single vertical fin. It integrates technologies such as relaxed static stability, fly-by-wire flight control system, advanced digital cockpit, multi-mode radar, integrated digital avionics system, advanced composite material structures and a flat rated engine.

The top and bottom right shows the F-22 *stealth* aircraft also called Raptor designed and built in the USA (Wikipedia5, 2016). The front view shows the angular design to lower the radar cross section. Its complex aerodynamics, advanced controls, thrust vectoring nozzles, and high thrust-to-weight ratio contribute to its super-maneuverability. It can cruise at *M = 1.5* without using afterburners- known as super-cruise. This feature greatly expands the range and speed over other fighter aircraft. Its airframe design and avionics together make it very difficult for radar detection.

The left middle aircraft is Russian Sukhoi 30MKI aircraft (Wikipedia5, 2016) that has an aerodynamic configuration is an unstable longitudinal triplane. The canard increases the aircraft lifting ability and deflects automatically to allow high angle-of-attack flights allowing it to perform Pugachev's Cobra maneuver shown in the figure. The integral aerodynamic configuration combined with thrust vectoring makes it highly maneuverable with good take-off and landing features. The high agility helps rapid deployment of weapons in any desired direction. The canard assists in controlling the aircraft at large angles-of-attack and bringing it to a level flight condition.

The bottom left aircraft is US built reconnaissance aircraft, Hawkeye, E-2 (Wikipedia5, 2016) provides all-weather airborne early warning, command and control capabilities (also termed AWACS) for all aircraft-carrier battle groups. In addition, its other purposes include sea and land surveillance, the control of the aircraft carrier's fighter planes for air defense, the control of strike aircraft on offensive missions, the control of search and rescue missions for naval aviators and sailors lost at sea, and for the relay of radio communications, air-to-air
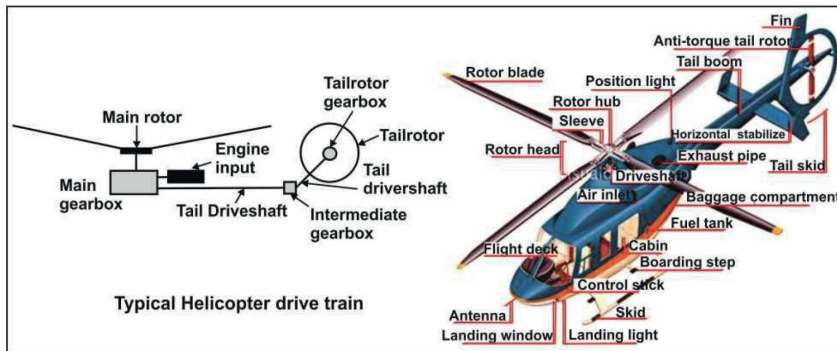
Figure 1.16.: The picture of a helicopter on the left and tiltrotor craft on the right, drawn from open internet sources on helicopter drive train

and ship-to-air. A distinguishing feature of the Hawk-eye is its large diameter (7.3 m in this case) rotating dome that is mounted above its fuselage and wings. This carries the primary antennas for long-range radars.

The key aerodynamic features of many of these aircraft are large sweepback with a delta wing planform and a low aspect ratio. The engines develop required thrust because of high speeds even with relatively smaller values of the lift coefficient. The thrust for which the engines will be designed will be such as to enable the aircraft to climb at a vary fast rate, make a high speed dash from subsonic flight conditions and take deep turns and rolls as desired, all of which are very different from a civil aircraft. In all these aircraft, the engine(s) is(are) located in the fuselage, since this area is freed from occupancy of passengers as in civil aircraft. Most of these aircraft have high quality avionics to enable them to be always better in the event of war or war-like situations.

1.2.10. Helicopter and Rotorcraft

The idea of a helicopter appears to have old connections to devices like the Chinese top as early as in 400 B. C. with children playing with homemade tops of slightly twisted feathers attached to the end of a stick. The stick would be rapidly spin between their hands and released to find that that the stick climbed rapidly to a height in free flight. While many inventions were made later including those of Leonardo da Vinci (Wikipedia, 2016) in 1480 A. D. who thought of the fundamental aspects of providing an air screw for lift, one remarkable invention was by a French naturalist in 1783 (Intnet2, 2017) who

produced the Chinese top with two sets of feathers at both ends of a stick in which the top and bottom feathers rotated in opposite directions. This eliminated the torque created by one set of rotors and allowed vertical climb.

The humming bird that can hover in one place and fly backwards is another example of a helicopter from nature. Figure 1.16 shows schematically the power drive arrangement to enable controlled propulsion as well as the principal components of an actual helicopter. The principal power generator is a turbo-shaft engine operating at very high speeds ~ 5000 to 10000 rpm. This power is taken through a gear train to the main rotor drive and a shaft drive to the tail rotor through additional gear trains designed to get the appropriate operating speeds. The tail rotor is a smaller rotor mounted so that it rotates in a vertical or near-vertical plane at the end of the tail of a traditional single-rotor helicopter. Its rotation provides a force which will provide a torque in opposition to the main rotor torque either completely or partly. The partial compensation allows the rotation of the helicopter while being stationary. The tail rotor is encased in a duct looking like a ducted propeller. This provides reduced noise and enhanced safety for operating personnel.

The differences between the operation of a helicopter and an aircraft can be best understood by examining the operational aspects of an airplane and what is known as the autogyro. In an airplane, as discussed earlier, the lift is provided by the fixed wings; in the autogyro, a free rotor which rotates due to the air-flow caused by the forward motion of the aircraft leads to lift. The forward movement in both the airplane (that uses a propeller) and an autogyro is obtained from the thrust created by an ordinary propeller that absorbs the power of the engine. But in the case of a helicopter, the ability to hold on to altitude and forward movement is provided by the engine-driven rotors. The rotors generate a force that largely constitutes lift with a component going towards the forward movement. One can also look upon a helicopter as an airplane with its fixed wings removed and its propeller shifted overhead in the form of much longer rotor blades (much longer because of the need to generate a much larger force than an aircraft propeller; also, the rotors are horizontal and are not limited by the small space between the engine axis and the ground) turning about a vertical axis that permits tilt of the axis of rotation to help obtain propulsion. Figure 1.17 shows the pictures of a helicopter and a tilt-rotor aircraft together to see the analogy concerning the generation of a lifting force. The helicopter

shown on the left side is built by HAL (helicopter division) and is built to fly and land at extremely high altitudes (in this case, Leh in India) The helicopter blades experience a complex aerodynamics with forward movement. When the blades are rotating, one part cuts into the flow and the other is receding. This implies the effective speed faced by one part is different. The effects of these varying forces influences the motion of a helicopter. As the helicopter accelerates to higher forward speeds, the rotor blades change their pitch throughout the 360° rotation using an articulated mechanism.

Helicopters are most critically deployed whereever and whenever vertical lift from nearly unprepared areas is required particularly in mountainous terrains both for civilian and military applications. The fact that their fuel consumption for transportation is much higher than for aircraft is simply understood as follows.

Suppose, we consider the total mass to be transported by the helicopter and aircraft to be the same. We know that the aircraft needs to generate a thrust that is weight divided by the L/D of the wing. Since civil aircraft have L/D of 10 to 15, the thrust needed is about 6 to 10 % of the weight of the aircraft. In the case of helicopter, the thrust required is at least equal to the weight (in reality, more than the weight because there is also a horizontal component that contributes to forward movement) and so the engine will be needed to be ten to fifteen times powerful compared to that of an aircraft. Consequently, the fuel consumed will be that much larger in a helicopter. A significant part of the disadvantage is removed through the use of an aircraft with tiltable engines. Only when vertical take-off is required the engines operate at full power generating the thrust vertically and once the craft is airborne, the engines are tilted to horizontal mode and operate like aircraft engine (Osprey aircraft is an example). Despite the availability of tilt-rotor aircraft, the popularity and the demand for helicopters remains very high since unprepared grounds can also be accessed by helicopter.

1.2.11. Hovercraft (Air cushion vehicle)

A hovercraft (air-cushion vehicle, ACV) is an amphibious craft capable of travelling over land, water, mud or ice and other rough surfaces both in a stable manner while also being stationary. The principle of operation is illustrated in Figure 1.18. A cushion of high-pressure air is created in the bottom area above

Figure 1.17.: The picture of a helicopter on the left designed and built in India and tiltrotor craft built in USA on the right
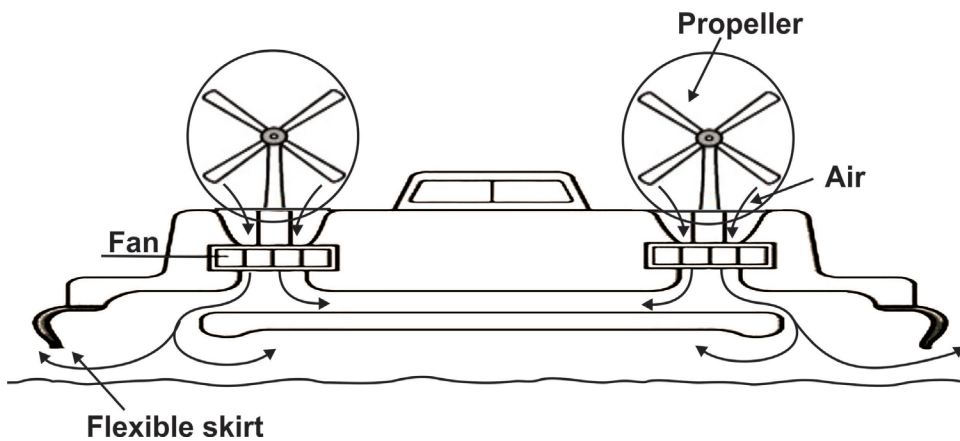
Figure 1.18.: The elements of an air cushion vehicle. The air from the fans is direted to the bottom area creating a cushion of air at pressures larger than the ambient and this air flows out through the skirt. The difference in pressure multiplied by the area provides the force to maintain the craft above the ground/bottom surface the popularity and the demand for helicopters remains very high since unprepared grounds can also be accessed by helicopter.

the ground/water surface. The craft is provided with a skirt to enable air flow out of the bottom region. The skirt is made flexible so that a plenum is maintained inside the bottom area even when the craft is negotiating uneven surfaces including waves. The difference in pressure between the bottom area and the ambient multiplied by the area provides the force required to maintain the craft above the ground. The forward movement is provided by the propellers

Figure 1.19.: Tactical missiles Prithvi and Dhanush, Strategic missile AGNI all of DRDO, India and PSLV and GSLV of ISRO, India, drawn from open internet sources

mounted over the craft. The hover height is typically 200 to 600 mm above any surface and the speed is 30 to 60 km/h and can go over gradients of 20 degrees. These craft are used as specialised transport passenger service, military, disaster relief, coast guard and other civilian applications and sport. Hovercraft are largely operated as an aircraft rather than as a marine vessel even when traversing water bodies (like the English channel, for instance over which it has been extensively used). In terms of fuel efficiency, it is about half as efficient as a passenger car and thrice as expensive in terms of first cost. Its ability to handle multiple terrain conditions makes its value high for special applications.

1.2.12. Missiles and Satellite launch vehicles

Both missiles and satellite launch vehicles are discussed together because of several common elements. Many developments of missiles for launch vehicle applications can be almost directly used for satellite launch vehicles and vice versa. Missiles are classified as tactical and strategic. The tactical systems can be further classified in terms of applications as air-to-air, surface-to-surface, surface-to-air, air-to-surface and ship based systems, short range and long range. Strategic systems are special in their ability to carry nuclear warheads and are generally long range surface-to-surface systems. They also go under the broad name of IRBMs and ICBMs (inter-mediate range as well as in-

ter-continental ballistic missiles), with range typically 1000 to 10,000 km. It is the propulsion systems that can almost directly be exchanged between missile systems and satellite launch vehicles because both the vehicles use multi-stage propulsion systems as can be seen in Figure 1.19. The first stage carries the vehicle up to a certain altitude and drops off. The next stage ignites and burns for additional time, takes the vehicle farther and higher and is then dropped off (this process called staging is discussed in Chapter 4, section 4.16.3). In this manner, the payload is taken to the planned orbit with each stage operating for a minute or two. The individual propulsion systems can be based on different class of propellants - solid, liquid or hybrid, tested and qualified before integration. Since the objectives of a large missile or a launch vehicle are long range and altitude, the individual propulsion segments can be adopted for either of the applications. Of course, the control and navigational elements also allow adaptation.

Figure 1.19 presents pictures of tactical missile - Prithvi and Dhanush and the straegic missile, AGNI and the satellite launch vehicles - PSLV and GSLV, all these developed in India. The elements of the tactical missile are a cylindrical shaped vehicle with the payload (a warhead), a guidance system that becomes a part of the payload, small size control surfaces and propulsion system. The launch vehicle is made of many stages each of which contains a propulsion system, and the payload section that contains a satellite along with a propulsion system for controlling the satellite during the launch operations as well as subsequently. The complexity is very much more, but the essential elements the same. In comparison with an aircraft, the shape is largely cylindrical with *the design being largely controlled by propulsion and guidance systems rather than aerodynamics and structural aspects*. This is because the vehicles are largely accelerating with propulsive thrust much in excess of the weight of the system - typically the ratio between the launch thrust and weight is 1.5 to 2 for launch vehicles and 4 to 10 for tactical systems. Due to this reason, structural optimization is important but not as crucial to performance as in an aircraft. Aerodynamics plays a role in ensuring stability of the flight; for launch vehicles, this constitutes a small segment of the flight. For tactical systems that usually work within the atmosphere, the role of aerodynamics is much larger, but again it is in terms of ensuring the stability of the flight in the pathway of the missile to the target.

Satellites have to be in specific orbits around the earth. The purpose of the launch vehicle is to deliver the satellite to this orbit. The orbits are are set out in Figure 1.20.

The orbits of importance are several:

1. High-earth orbits (HEO) like Geo-synchronous (GSYO) and Geo-stationary orbits (GSTO) at 35780 km altitude, and a period of near 24 hours

2. Mid-earth orbits (MEO) at 20200 km altitude for helping locating positions on earth or for flight operations with a period of 12 hours

3. Polar orbits, also called sunsynchronous orbits (SSO) at 500 to 800 km altitude for earth observations with a period of 1.5 to 2 hours

4. Transfer orbits, principally Geo-transfer orbits (GTO)

5. Low-earth orbits (LEO) at about 200 to 400 km altitude for several applications including the international space station with a period of about 1.5 hours

The orbital periods set out as above are very simply derived by first determining the velocity of the satellites in these orbits. The equilibrium motion in a circular orbit is due to a balance between centrifugal and gravitational forces. This balance gives $mV^2/r = mg$ where m is the mass of the satellite (or any object), V, its velocity, r the radius of the orbit with the center of the earth as the center and g, the acceleration due to gravity at the orbit location which decreases with altitude as $g = g_0/(1 + h/R_e)^2$. In this expression g_0 is the acceleration due to gravity at the surface of earth, h is the altitude of the orbit above earth and R_e is the radius of earth taken as 6371 km at equator. If we note that $r = h + R_e$ and rearrange the result we get

$$V = \sqrt{\frac{g_0 R_e}{\left[1 + \frac{h}{R_e}\right]}}$$

This gives the period, $P = 2\pi(h + R_e)/V$ as

(1.19)

$$P = 2\pi \sqrt{\frac{R_e}{g_0}} \left[1 + \frac{h}{R_e} \right]^{\frac{3}{2}}$$

<div align="right">(1.20)</div>

The results of calculations from this equation for P are set out in Figure 1.20. As shown in the figure, the inclination is the angle between the plane of the orbit and equator.

1.2.13. GSYO, GSTO and MEO

Geosynchronous orbit (GSYO) is located at an altitude of 35790 km above earth so that the satellite has the same period of rotation as earth, P = 23 hours 57 minutes; it can have any inclination with respect to the equator. When the inclination becomes zero implying that it is orbiting at equator, one gets geostationary orbit (GSTO) so that it is stationary with respect to earth (another way of expressing this is that GEO is an equatorial geo-synchronous orbit). Middle earth orbits are between 2000 km to 20000 km.

Geosynchronous satellites have the advantage of remaining permanently in the same area of the sky, as viewed from a particular location on Earth, and so permanently within view of a given ground station. The operational success of the first Geosynchronous satellite (GSYO), Syncom 2 in 1963 is credited to Mr. Harold Rosen, an engineer at Hughes Aircraft Company (Wikipedia8, 2016). Each geo-stationary satellite can provide a coverage of about 40 % of the earth's surface. Multiple (a minimum of 3) can provide adequate coverage over most of the habited earth. Yet, geosynchronous satellites at some orbit inclinations in tandem are used for better coverage including monitoring in times of conflict.

Some satellites carry color and infrared cameras to image storms day and night, and a sounding device to collect temperature, humidity and ozone data in different layers of the atmosphere. They can can also relay observations from remote weather station and ocean buoys to forecast centers, and monitor distress signals from ships, airplanes and others for rescue.

There are four commonly used satellite transmission bands termed C (4 - 8 GHz), X (8 - 12 GHz), Ku (12 - 18) and Ka (20 - 40 GHz). While the larger frequency range (part of X, Ku and Ka bands) is meant for military communica-
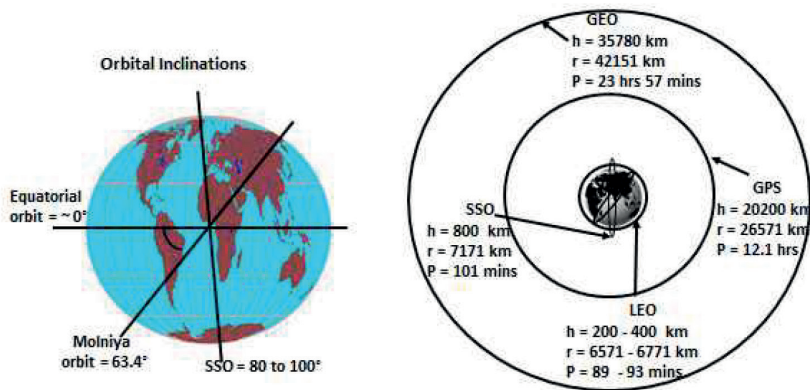
Figure 1.20.: The most important orbits that are used in the service of people and nations

tions and radars, direct-to-home (DTH) television services also use a part of this range (10 to 14 GHz in India). Use of higher frequencies helps in reducing the antenna size (domestic dish size in India ~ 0.67 m). The uplinking and downlinking frequencies are separated to enable better reception.

The distance that an electromagnetic signal must travel to and from a geo-stationary satellite is nearly twice the orbital altitude amounting to 71,600 kilometers and causes a signal delay of about 0.25 s for a round trip simply due to the travel of the signal (technically termed latency). This will not matter for television or data transmission, but uncomfortable for telephone conversations. Through the use of multiple satellites in the middle earth orbits low earth orbit (LEO), latency has been brought down to as low as 70 ms.

Middle earth orbits between 2000 km and 20000 km has been used for positioning multiple satellites for communication, Global Positioning System (GPS, USA), or Global Navigation Satellite System (GLONASS) and similar systems with limited objectives. To ensure reliability of service, a large number of satellites are deployed for this purpose. GPS uses 4 satellites each in 6 orbital planes (24 totally) all at 20218.0 km altitude at 55° inclination GLONASS also has 24 satellites with 8 each in three orbital planes at an inclination of 64°8´ with a 12 hour period (see Fig 1.20. The latter orbit is nearly the same as Molniya orbit (whose inclination is 63.4 degrees). At this inclination, the orbit is highly elliptic with the perigee not rotating so that the satellite spends nearly

11 hours of its 12-hour period over the Northern Hemisphere needed by Russia before it travels very fast over the southern hemisphere. The disadvantage of not having sufficient launch vehicle energy for putting their satellites into equatorial orbit was taken advantage of by inventing this orbit needing much less launch energy. A further advantage is that with multiple satellites the coverage of higher latitudes is much better than can be provided by GEO satellites. The disadvantage is that the ground stations need a steerable antenna to track the spacecraft and that the spacecraft will pass the Van Allen radiation belt four times per day leading to possible EMI.

The IRNSS (Indian regional navigation satellite system) equivalent of GPS or GLONASS consisting of 3 satellites in GEO and four in GSO at 55° inclination has been operationalized to provide position information for civilian use of 10 to 20 m accuracy and in an encrypted form with an accuracy much finer than 10 m for military needs. This development permits independence for India in obtaining positioning information largely in the Indian region.

The exact position of a geostationary satellite relative to earth location varies slightly because of gravitational interaction (even if it were weak) among the satellite, the earth, the sun, the moon and other planets. This wander which gets corrected by station keeping maneuvers by small thrusters on the satellite can on occasion limit the sharpness of the ground reception. Also, there will be an inevitable increase in electromagnetic interference (EMI) due to the influence of the Sun in times of equinoxes.

1.2.14. GTO

Geo-transfer orbit (GTO) which is a deep elliptical orbit of 10 to 11 hours period with the closest point to earth called perigee is typically around 200 km altitude and the farthest point called apogee is closest to geosynchronous altitude. It is called transfer orbit because by increasing the satellite speed at the apogee using thrusters (solid or liquid, but usually the latter because it provides for better control) the orbit is circularised at the GSYO or GSTO at the equatorial latitude. The perigee is so arranged to optimize the energy demand and reduce the space junk resulting from separated segments left behind; they will need to de-orbit and be consumed during re-entry. This orbit is termed a Hohmann transfer orbit (due to the German scientist Walter Hohmann who invented it in 1925) and requires a few days to reach the geosynchronous orbit.

The initial injection into the GTO can occur with an inclination. Achieving the GSYO can occur by circularising the trajectory (or reducing the eccentricity of the elliptic orbit to zero). Achieving GSTO calls for reducing the inclination as well. These can be done in two separate maneuvers or in a single maneuver. Adoption of the latter reduces the needed energy (or velocity increment of the vehicle). With the greater crowding being experienced in the GSTO, there is a new trend to tolerate some level of inclination in order to accommodate more satellites at the cost of operational inconvenience. As seen from a ground system, these satellites trace a figure of eight in the sky.

It is important to know that most launchers release their payloads into GTO even if the launcher has an overall responsibility to place the satellite into GSYO or GSTO. The operations on the spacecraft required to place the satellite into the final geostationary orbit will be conducted differently. Most often, the intervening time is long and is used to unfurl the solar array and generate enough power (of 2 to 5 kW) so that the on-board systems can be functional for subsequent actions required to reduce the inclination and also circularize. Also, some launchers (like PSLV C-23 mission launched five satellites, C-34 mission, 20 and C-37, 104 satellites) carry several satellites in a single launch to reduce overall costs; the approach optimizes the mission when the payloads are destined for different orbital positions.

1.2.15. LEO/SSO

Low earth orbits constitute a range of altitudes between 200 to 2000 km at a range of inclinations. Inclination is the angle between the plane of the orbit and equatorial plane. When the inclination is close to 90°, the orbit becomes sun-synchronous - one will observe the land mass at the same time every day. Lower segments around 200 km are the region that have advantages for satellites in terms of communication needing less powerful transmission devices. The use of VHF and UHF frequency bands permits low cost antennas for hand-held terminals for communication. They have also much less latency (10 to 100 ms depending on the altitude of choice and other parameters) than GSYO and GSTO and much higher band width. These satellites can also act as observational posts when used in sufficient numbers because their orbital period is about 75 to 100 mins (see Figure 1.20).

An important example of LEO is the international space station located at an
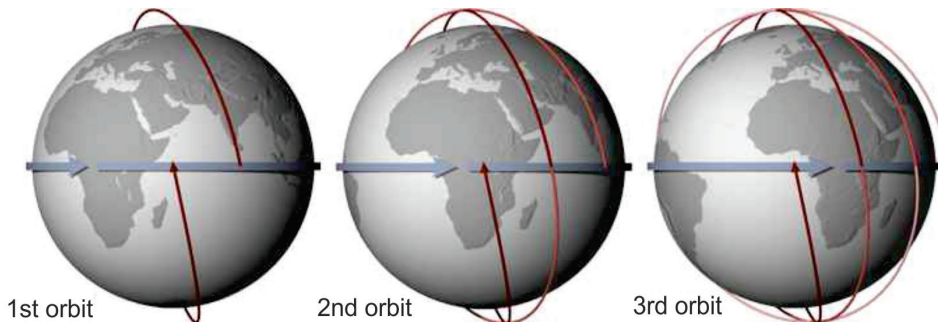
Figure 1.21.: The orbits of sun-synchronous satellite orbiting around the poles at around 90 to 100 minutes shown for three orbits; drawn from Wikipedia7 (2016)

average altitude of 350 km. Established in 1998 due to multinational effort (primarily USA, Russia, Japan, Europe and Canada) it is a unique space laboratory with a crew of six and some visitors. Unmanned spaceflights deliver cargo and these have largely been performed by the Russian Progress spacecraft using the Soyuz launch vehicle. European Automated Transfer Vehicles, Japanese vehicles as well as the American Dragon and Cygnus spacecraft have also docked into the space station. Approximately 230 people have made 390 space flights to the international space station till the end of 2016.

Sun-synchronous orbit is preferred for remote sensing in which the satellite is in a circular orbit between 500 to 1000 km altitude with an inclination of about 90° to the equator. The period of these satellites, P is about one and half hours. The earth below is moving around at the rate of 15 degrees per hour and therefore the satellite track will intersect the zone only once in a day around the same time.

The most important application of this orbit is to estimate the properties on the surface, typically, the productivity of agricultural crops, state of forests, sea surface temperatures, and some weather patterns, particularly the variations over several years since there is consistency in the images from the same season. In launching these satellites (and others), a maneuver termed dog-leg (shown in Figure 1.22) in which a powered turn during ascent phase is sometimes deployed. A dogleg is necessary if the desired launch azimuth, to reach a desired orbital inclination, would take the ground track over land or over a

populated area or if the vehicle is trying to reach an orbital plane that does not reach the latitude of the launch site. In this instance, the landmass of Srilanka is in the pathway of spent stages of PSLV (India) and so this maneuver was considered mandatory. If the maneuver could be avoided, the satellite payload could be increased by 20 to 25 %.

The use of LEO particularly for communication purposes requires a large number of satellites with accompanying problem of their maintenance and management. One important issue is that these satellites undergo eclipse several times a day, and so, there is a need for robust on-board battery system for the satellite for operations without solar power during eclipse. There are several satellite operators in the communication area: Iridium with 66 satellites (several non-functional now), Globalstar with 48 satellites, and Orbcomm with 35 satellites are all currently operational in the LEO orbit. Because of the density and some becoming dysfunctional, the possibility of collisions is not insignificant. In fact, in 2009, an active Iridium 33 collided with a dysfunctional Russian satellite Kosmos 2251. One of its in-orbit spares, Iridium 91 was moved in to replace the destroyed satellite (wikipedia9, 2016). There are more than ten thousand objects in the orbits, largely in the low earth orbits. About a few thousand of these are active. Those whose life has ended will still float around; those in GSYO and GSTO are not as bothersome as those in LEO. Those in lower range of LEO can come down also because of drag and other. Figure 1.23 contains the picture of objects in space in all the orbits as well low earth. The density is surprisingly large. Collisions take place occasionally as already indicated. in the low earth orbits. About a few thousand of these are active. Those whose life has ended will still float around; those in GSYO and GSTO are not as bothersome as those in LEO. Those in lower range of LEO can come down also because of drag and other. Figure 1.23 contains the picture of objects in space in all the orbits as well low earth. The density is surprisingly large. Collisions take place occasionally as already indicated.

All the launch vehicles need a velocity increment between 9 to 12 km/s, the lower values for SSO and larger values for GTO. This velocity increment is obtained from rocket based multi-stage vehicles. Detailed discussion of the need for multi-stage arrangements, the choice of the propulsion systems for obtaining higher payload for the same lift-off weight will be discussed in Chapter 4, section 4.16.3.
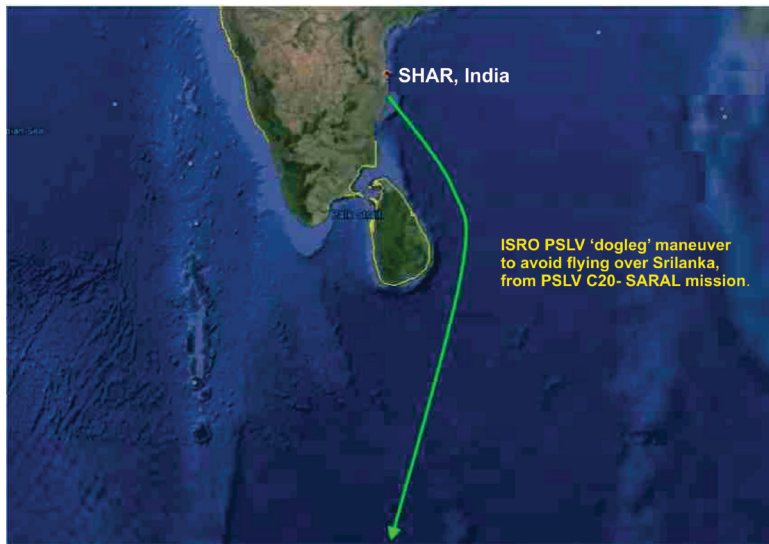
Figure 1.22.: A typical dog-leg maneuver used for a mission by ISRO; from open internet sources

1.3. Weight Decomposition and Performance

The decomposition of the mass amongst payload, fuel and inerts (structures) for a number of different types of vehicles is set out in Table 1.5 constructed from actual data for many aeronautical and space vehicles is very instructive. All aircraft have structural fraction that is between 25 to 55 % controlled by two factors - the size of the aircraft and demand on maneuverability. Smaller size and the demand on maneuverability lead to higher structural fractions. Long range civil aircraft have adopted in recent times advanced materials and reduced the average structural fraction (see section 6.4.1 in Chapter 6 for discussion on Boeing 787 and AB 380 both of which have used advanced materials).

The fuel fraction in aircraft depends on the mission. Long range aircraft carry considerable amount of fuel while military aircraft carry much less fuel since the payload is meant for armaments. However, some extra fuel can be carried in lieu of external armament load if the specific mission requires deep penetration, as is the case of LCA and F 16. In the case of helicopters, the structural mass is about 50 % of the total mass. Here also, the fuel load and payload can
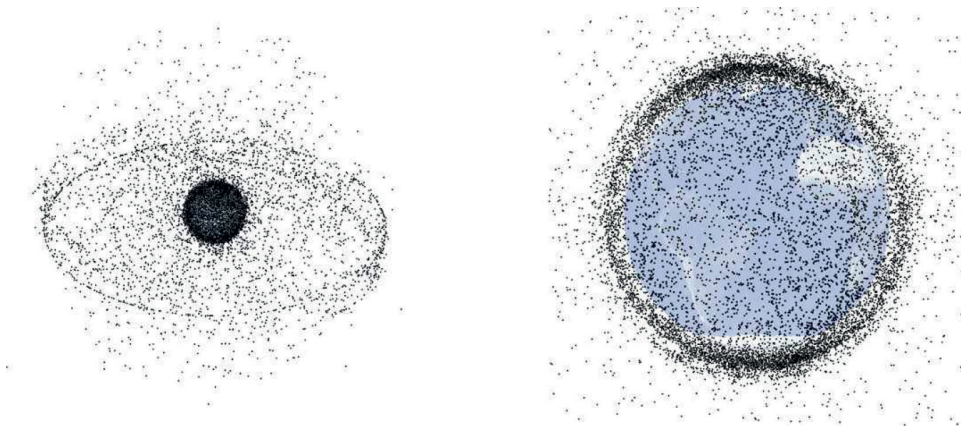
Figure 1.23.: Satellites active and defunct in space - over all the orbits (left) and LEO (right); drawn from Wikipedia7 (2016)

Table 1.5.: Mass decomposition of air and space vehicles and performance; stft = structural fraction; plf = payload fraction; ff = fuel fraction

Vehicle	Total mass, t	Payload (pl), t	Fuel mass, t	Str. mass,	stft	plf	ff	speed M
Civil transport, turboprop								
Metro	7.5	1.7	2.6	3.2	0.42	0.22	0.36	0.46
ATP	22	7.0	5.1	10.9	0.49	0.32	0.19	0.44
AN 32	27	6.7	5.4	14.9	0.55	0.25	0.20	0.42
Jet transport-200 series, high bypass turbo-fa								
A320	74	20.0	24.0	30.0	0.40	0.27	0.33	0.78
B757	100	26.1	42.3	31.6	0.32	0.26	0.42	0.80
B747	379	92.3	198.3	88.4	0.23	0.25	0.52	0.85
B777	230	54.4	117.3	58.3	0.25	0.24	0.51	0.87
Military aircraft, low bypass turbo-fan								
LCA	13.3	2.3	2.4	6.6	0.50	0.17	0.23	2.0
F 16	19.2	7.6	3.1	8.5	0.44	0.39	0.17	2.0
Rafale	24.5	11.3	4.7	8.5	0.35	0.46	0.19	1.8
Military helicopter, turbo-shaft								
Apache	10.0	3.0	1.8	5.2	0.52	0.32	0.18	0.28
Mi26	56.0	19.0	9.0	28.0	0.50	0.34	0.16	0.28
Launch vehicle, rockets								
PSLV (SSO)	320	1.8	261.8	56.4	0.18	0.005	0.82	-
GSLV (GTO)	414	2.0	361.0	51	0.12	0.005	0.87	-
SOYUZ-SSO	320	4.4	271.0	49.0	0.15	0.013	0.85	-
Ariane5 (GTO)	777	10.5	650.0	118.5	0.15	0.013	0.84	-

Table 1.6.: Mass fraction of various elements of a satellite; typical satellite mass = 1.5 to 2 t; AOCS = Attitude and orbit control system; TT&C = Telemetry, tracking and command system

	Payload	Power	Structure	Propulsion	Thermal	AOCS	TT&C
%	25	30	20	10	5	5	5

be exchanged to a limited extent depending on the range to be covered. For instance, if the aim is to lift a heavy load to a top of a mountain from the bottom, one can keep a minimum fuel load and carry the desired payload. Quite differently, if injured people have to be immediately moved to a distant hospital, what is important is to have a larger range rather than the level of payload.

Satellite launch vehicles have lower structural fractions between 8 to 17 %. The payload fraction indicated for PSLV vis-a-vis SOYUZ and GSLV vis-vis Ariane 5 launch vehicles are such that Indian vehicles have much lower payload fraction. The primary reason for this is the choice of the propulsion system. Liquid stages used in SOYUZ and Ariane 5 vehicles perform far more effectively than solid stages of PSLV/GSLV. Unlike airbreathing engines, propellant fraction for rocket vehicles is very large because the rockets have to carry oxidizer as well. It must also be noted that the satellite itself has many elements in it and if we decompose the weight of a satellite in terms of its elements, we have the data set out as in Table 1.6. It can be noted that while the functional payload is about 25 % of the mass of the satellite, the power generation system consisting of solar arrays and the power conditioning system take up about 30 % of the mass. The propulsion system consisting of the propellant tanks and zero-g acquisition devices, micro thrusters located at several points on the satellite structure constitutes about 10 % of the mass. Other elements involving thermal protection, attitude and orbit control system as well as telemetry, tracking and command system packages constitute the remaining mass.

The life of the satellite is dependent on how much of propellant is available for station keeping purposes. This is typically 10 to 12 years for geosynchronous satellites. However, in recent times, the demand for the design life of these satellites has moved up to 14-16 years. The use of hybrid propulsion integrating non-chemical propulsion systems with the chemical propulsion had been enabling substantial increase the life and payload fraction of communication satellites has moved up to 14-16 years. The use of hybrid propulsion integrat-

ing non-chemical propulsion systems with the chemical propulsion had been enabling substantial increase the life and payload fraction of communication satellites.

1.3.1. Air-breathing vs. Rocket vehicle based vehicles

A question may come up: Can an air-breathing engine replace a rocket engine for specific missions? Or the other way round?

The answer is that it is not possible to swap one for the other for any mission that one of them is currently in vogue. Rocket engines discharge their function in minutes (if not seconds all the time). Air-breathing engines take that kind of time to get to full power and maintain it for several hours at least. Further, the density of the fuel-oxidant system (both being solids or liquids) for a rocket engine is 1000 to 1700 kg/m³, but the equivalent density for an air-breathing engine is about 1 kg/m³. Thus replacement of a rocket engine for the thrust it produces by an air-breathing engine is not feasible. Air breathing engines can even operate for long durations and even on 24 x 7 basis as the prime movers for power generation. In fact, high bypass ratio turbine engines in turbo-shaft mode are ideally suited for this. The high bypass ratio turbofans on wide body airliners can operate for fourteen hours and their life is several thousands of hours. The operational duration of any launch vehicle for ICBM or a sat-ellite does not exceed twenty minutes. Therefore rocket engines can be used in aircraft applications whenever a short duration enhancement of thrust is demanded. The propellant usage in a rocket engine is at least ten to fifteen times higher than for a air-breathing engine for the same thrust and hence is avoided for use in aircraft. A slightly different way of expressing these is that non-air-breathing engines should be used to deliver "impulse" - implying large thrust for short duration and air-breathing engines for delivering work moder-ate thrusts for very long durations; the roles cannot be interchanged.

1.4. Reusable Launch Vehicles

Aircraft are reusable flight vehicles. Satellite launch vehicles are not reusable. The cost of putting a payload into space is estimated variously to be 6000 to 10000 USD/kg payload. In the case of an aircraft, the cost of transportation of a payload (passenger or cargo) is estimated to be between 1 to 5 USD per kg. If space has to be made affordable for satellite delivery into transit orbits (like a deep elliptic orbit of few hundred km perigee x 36000 km apogee), the cost of
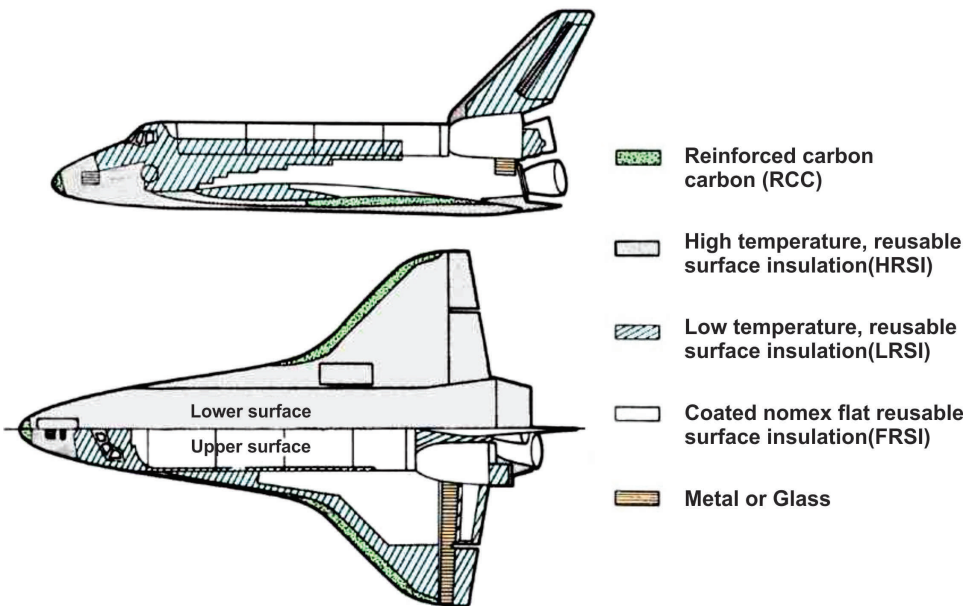
Figure 1.24.: Thermal protection systems on the Orbiter of the space shuttle

such a delivery must be brought down by at least a factor of ten if not more. Recognizing that the only expendable in an aircraft is the fuel (apart from changes during periodic preventive maintenance) on which the cost of transportation is very strongly dependent, attempts have been made to evolve strategies for reusing as much of hardware as possible yet retaining the rocket as the basis of the propulsion system.

This effort is the design, evolution and operation of Space shuttle. It is a very interesting man-rated vehicle – it is launched (or can it be said, takes off) as a rocket but lands as a glider. Its configuration has an aircraft like appearance but riding on rocket boosters. Five vehicles were built and were totally involved in 135 space missions. Two of these vehicles were destroyed and three remaining ones are mothballed. The orbiter, which includes the main engines, and the two solid rocket boosters, are reused after several months of refitting work for each launch. The external drop tank containing both fuel and oxidizer in separate containers is discarded, but it is possible for them to be re-used in space for various applications.

Over a period of time, the degree of re-usability came down significantly and hence even the idea of partial re-usability could not be fulfilled. Its technological elements were perhaps the most advanced at any point of time. The space shuttle main engine working on liquid hydrogen and liquid oxygen operated at a combustion chamber pressure of 200 atm and the peak pressure attained in the pumps would go up to 550 atm. It used a staged combustion cycle and is one of the most elegant and complex propulsion systems built till date. Space shuttle undergoes a very high level of thermal loading during the reentry that is one of the most critical segments of the mission. In order to meet with the very hostile thermal environments of entry speeds (M = 25 to 35), various portions of the vehicle are provided thermal protection systems. These are illutrated in Figure 1.24 that shows four kinds of thermal protection systems used in the orbiter. Towards the aft end is seen the nozzles of the Space shuttle main engine (LOX-LH$_2$).

One of the more daring attempts in recent times is one of building a reusable space accessible aircraft by Burt Rutan (Scaled composites, see Rutan, 2004 who made an exciting demonstration of the plane termed "SpaceShipOne"; this effort won the X-prize competition for space flight in a man rated reusable vehicle for successfully reaching an altitude in excess of 100 km and returning to earth. This system involves a rocket engine based space plane (similar to Space shuttle in terms of landing like a glider) that is taken by a mother plane dropped at an altitude. Shortly after the drop, the space plane fires the rocket engine to reach an altitude of 100+ km, altitude that qualifies for being out of atmosphere and being in space. After a short duration of weightless stay in space, it makes a reentry, maneuvers the aircraft into the landing area and lands like a glider. This system used a hybrid rocket engine with a solid rubbery fuel and nitric oxide oxidizer. This oxidizer was carried in the space plane at take-off. This successful mission created a milestone in the human aspiration to access space including space tourism in an affordable manner. This kind of a vehicle is conceptually akin to *two-stage-to-orbit vehicle*.

Greatest optimization in creating affordable access to space can be achieved by making use of the most appropriate possibilities for each segment of the flight in what can be termed as a *single stage-to-orbit* approach. One cannot live without carrying the oxidizer as well when flying into space. One should not use any oxidizer other than air when flying within the atmosphere. And it is

most desirable not to carry what one should not. This implies that the aircraft has both an air-breathing engine and a rocket engine right at take-off. It carries liquid fuel for both aeronautical and space operations, but only an empty oxidizer tank at take-off. Once an altitude of 10 to 15 km is reached, the plane will receive aerial transfer of the oxidizer (like the routine aerial fuel transfer for long duration operating planes). Once the oxidizer transfer is complete, it will operate the rocket engine to get into space. In the return segment, the air-breathing engine comes into operation to help the aircraft operate in an autonomous mode much like any other aircraft. Ideas of such a nature have been pursued (Jayan et al, 2004) to determine the crucial parameters that affect the ability to accomplish the mission. It has been determined that low structural ratio and high specific impulse (performance parameter of a rocket engine) are crucial to the operability of the mission. Two key aspects in the realization of such a plane are the true and perceived reliability and safety of operations. The space operations are yet to acquire these features; the current check out system of rocket launches that takes a long time must be brought down to values similar to aircraft. It may be expected that more developments will occur in coming decades.

1.5. Summary

Table 1.3 is central to appreciating the whole range of vehicles that are currently prevalent. Items 1 to 3 in the Table refer to vehicles that do not need propulsion.

These vehicles are "pure" flying systems; they depend on the atmospheric conditions. Paper planes and Walk-wing gliders need careful handling. When wind is still kites cannot be flown. Gliders need wind and also warm plumes so that they can use the vertical winds to soar. Demand on autonomous flight implies invoking propulsive units. The importance of propulsive units acquires a quantum change with missiles and launch vehicles.

The de-marking line is below item 8. All flying vehicles above item 8 have aerodynamics (and stability) as the most important feature and those below that have propulsion as the primary element. The use of aerodynamic principles will aid in reducing the propulsive requirements significantly (items 4 to 8) and hence the amount of fuel consumed in accomplishing what is intended. The developments of civil aircraft with the great demands of low maintenance, low

fuel consumption, very high reliability and long life are intertwined with very demanding performance in terms of maneuverability, high speed and stealth characteristics at the conceptual level as well as component development.

For vehicles below item 9, propulsion, guidance and control become vital. Making the vehicle slightly heavier will only reduce the efficiency of the mission. The entire aerospace industry has many cross-links and on occasions low cost development has benefited from off-the-shelf reliable utility components developed for other civilian uses. Equally, the special developments in aerospace have also entered utility market.

The mass distribution of specific segments in Table 1.5 reveals several important aspects of aero and space vehicles developed till date. The key feature is that all flying vehicles must be as light as permitted by structural integrity for a specific mission - military vehicles that have to face severe g-loads have to have greater structural mass fraction than vehicles built for civilian applications. In most flight vehicles the fuel carried can be swapped with payload to a limited extent decided by operational or commercial considerations. The life cycle of military aircraft is much smaller than for civil aircraft because of geopolitical compulsions on the part of individual nations to stays ahead in military hardware.

Any aerospace vehicle is a synergestic integration of aerodynamics, structures, propulsion and avionics. All flying vehicles need to be weight and volume optimised for the purpose for which they are designed by factoring into the design, robustness, reliability and life. Even so, for vehicles that fly subsonic the demand for integration between various elements is not strong. One can choose comparable but different propulsion systems for the same aircraft and obtain the desired performance. Slight loss in structural efficiency will not disable flying but its fuel efficiency may be non-optimal. As one moves to supersonic flight regime, the integration becomes far more important. Minimizing supersonic drag may demand that the engine be inside the fuselage largely. And, if external stores are to be carried as a part of the functional role, their position and integration must be given great thought for, the flight stability under maneuvering conditions will be deeply affected by it.

Missiles, tactical and strategic depend on rocket engines and are developed by many nations. Strategic missiles that are sub-orbital and satellites that

function in orbits have many aspects of the launch vehicle and payload that are common. The developments in air and space vehicles need to get integrated by combining winged vehicles with air-breathing propulsion as well as rocket engines to achieve low cost access to space with high reliability and safety.

Understanding bird flight and design of small flying systems similar to them has occupied great deal of attention in recent times. These have also defense applications being explored in many laboratories and industries. The succeeding chapters are concerned with the science of each of the disciplines just listed earlier to understand technological achievements better.

Bibliography

[1]   Ananthasayanam, M. R., and Narasimha, R., (1985) A proposed interna-
      tional tropical reference atmosphere up to 80 km, Advances in Space Re-
      search, volume 5, pp. 145 - 154; see an early report 79 FM-5 of the depart-
      ment of Aeronautical engineering, Indian Institute of Science, Bangalore,
      Nov, 1979

[2]   Anonymous (2017) https://wildtech.mongabay.com/2016/03/a-beginners-
      guide-to-aerostats/

[3]   Champion, K. S. W., Cole, A. E., and Kantor, A. j, Standard and reference
      atmospheres, Handbook of Geophysics, 1985 http://www.cnofs.org/Hand-
      book_of_Geophysics_1985/Chptr14.pdf

[4]   Fischer, M and Stoll, W., (2016) Festo AG & Co., KG https://www.festo.
      com/net/SupportPortal/Files/46270/Festo_SmartBird_en.pdf

[5]   Intnet (2016) www.n2yo.com/space-station/; also see a similar site from
      European Space Agency

[6]   Intnet2 (2017) http://www.century-of-flight.net/Aviation%20history/heli-
      copter%20history/Early%20Helicopter%

[7]   Gupta, S., and Malik, S., (2002) Report on Envelope details for demo air-
      ship, Aeriel delivery research and development establishment (ADRDE)

[8]   Jayan, N., Biju Kumar, K. S., Gupta, A. K., Kashyap, A. K., Venkatraman,
      K., Mathew, J., and Mukunda, H. S., (2004), Studies on an aerial propel-
      lant transfer space plane (APTSP), Astronautica Acta, v. 54, pp. 519 – 526.

[9]   Kites (2011), small http://www.grc.nasa.gov/WWW/K-12/airplane/kitefly.
      html

[10] Lissaman, P. B. S., (1983) Low Reynolds number Airfoils, Annual Review
      of Fluid Mechanics, v. 15, pp. 223 - 239

[11] Rutan, B, (2004), http://www.scaled.com/projects/tierone/

[12] Sasi, M. N., and Sengupta, K., (1979) A model equatorial atmosphere over the Indian zone from 0 to 80 km, Scientific report, ISRO-VSSC-SR-19-79

[13] Sforza, P. M., (2016) Manned spacecraft design principles, Elsevier

[14] Torenbeek, E and Wittenberg, H., (2009) Flight physics (essentials of aeronau-tical disciplines and technology with historical notes), Springer

[15] Turner, M. J. L, (2006), Rocket and Spacecraft propulsion, principles, practice and new developments, 2nd Edition, Springer

[16] Wikipedia1, (2011), http://en.wikipedia.org/wiki/Walkalong_glider; see a youtube http://www.youtube.com/watch?v=S6JKwzK37_8 on how to fly. This site is accessi-ble through the wikipedia URL.

[17] Wikipedia2, (2011) http://en.wikipedia.org/wiki/Glider_(sailplane)

[18] Wikipedia3, (2016), http://en.wikipedia.org/wiki/AeroVironment_RQ-11_ Raven; http://en.wikipedia.org/wiki/Entomopter; http://www.avinc.com/ nano

[19] Wikipedia4, (2016) https://en.wikipedia.org/wiki/HAL_Tejas

[20] Wikipedia5, (2016) https://en.wikipedia.org/wiki/Lockheed_Martin_F-22_ Raptor; https://en.wikipedia.org/wiki/Sukhoi_Su-30MKI https://en.wikipedia.org/wiki/Northrop_Grumman_E-2_Hawkeye

[21] Wikipedia6, (2016) https://en.wikipedia.org/wiki/Helicopter

[22] Wikipedia7, (2016) http://earthobservatory.nasa.gov/Features/OrbitsCat-alog/

[23] Wikipedia8, (2016) https://en.wikipedia.org/wiki/Geosynchronous_satel-lite

[24] Wikipedia9, (2016) https://en.wikipedia.org/wiki/Iridium_satellite_con-stellation

2
Aerodynamics

2.1. Introduction

This chapter is devoted to a discussion of aerodynamics of vehicles as driven by the needs of performance. Aerodynamics is of paramount importance to "form and shape" for aeronautical applications when the flight of the vehicle is within the atmosphere. For autonomous flight of an aircraft, the role of lift would be to reduce the force required for propulsion. Propulsion that overcomes atmospheric drag and provides in addition, force for maneuver, is controlled by the lift-to-drag ratio, L/D called finesse (Tennekes, 2005). Gliders and very low speed flying vehicles will all benefit from obtaining high L/D by having large aspect ratio (AR = square of span divided by the wing area) wings that are rectangular. Flying until the second world war was largely in subsonic conditions in the 100 to 150 m/s (360 to 540 km/h) range. Occasional diving resulted in high speeds and heavy vibrations, the speeds being close to that of sound; it was thought that perhaps, speed of sound was a barrier. Of course, it was known that V2 missile (of Germans) did cross the speed of sound and may have required large amount of thrust to go through the "barrier". Even though there were many flights in the WW II scenario that were suspected to have touched or just crossed the speed of sound, the recorded indications of aircraft crossing the sound barrier in a steady flight belong to Chuck Yaeger for flying ex-perimental aircraft X-1 (termed Glamorous Glennis) beyond the speed of sound in October 1947. Basically, unsteady transonic aerodynamics dominant in transonic flow conditions led to vibrations called buffeting and if this regime was crossed, the supersonic segment of the flight was found steady.

The rectangular wings of medium aspect ratio ($AR \sim 8$) were shaped with a sweep (largely, sweep-back up to 45^0) to enable reaching as high a subsonic speed as possible such that drag coefficient does not increase significantly. This is the speed at which all long-distance passenger air transportation takes place. Military demands for high speed and greater agility demanded that the AR be limited (to 1.5 to 4) with excess demand on drag being accounted for by more powerful engines. This would also allow greater maneuverability including slam acceleration. The geometry would be altered from swept back wings to delta shaped wings with sweep back of 60^0 and in addition ogive leading edge. This shaping helped achieve Mach numbers of 2 or more. The large variety of shapes seen with military aircraft is due to the fact that some aircraft are

designed for a brief supersonic dash and others for cruise and maneuver at supersonic speeds.

While all these developments took place over the last five decades, miniaturization of electronics, communication and optics coupled with the demand for unmanned autonomously functioning or at least, remotely controlled vehicles led to the development of unmanned mini-, micro- and nano-vehicles. Some use cruising wing shapes and others flapping wings. These have been helped by examining the insect and bird flight behavior. These developments are currently continuing and will continue through the coming times.

In order to truly understand and appreciate the flight behavior, it is important to explore the fundamental aspects of fluid flow over bodies, how lift and drag are generated, what these components are at subsonic and supersonic flight conditions. These are explored in the following sections.

2.2. Aerodynamical Aspects

The subject of the generation of forces of flying bodies has been addressed in a number of books, some very well known. Anderson (1984) has written a widely read book on Aerodynamics; Anderson and Eberhardt (2010) have written a more readable account. The lift generation mechanism seems to have received much misinterpretation from many writers. Some of the references and additional insight into the lift generation process are set out in Appendix 1. The essential summary is that the pressure distribution on any body with inviscid flow integrates to zero force. The presence of a sharp trailing edge is considered essential along with the presence of non-zero fluid viscosity, however small, to cause the flow to move off the trailing edge and this creates a pressure distribution leading to net force - both lift and drag. In so far as flow of air over aircraft wing like objects is concerned, these conditions are obeyed and hence we obtain the forces in proportion to the dynamic pressure on the wings. We now move on to the details of a wing cross section.

Figure 2.1 shows the various features of an airfoil. The chord, c is the distance from the leading edge to the trailing edge. Maximum thickness (or thickness-to-chord ratio, t/c) and its position and camber are the important parameters of a two-dimensional wing. The angle of attack is defined as the angle between
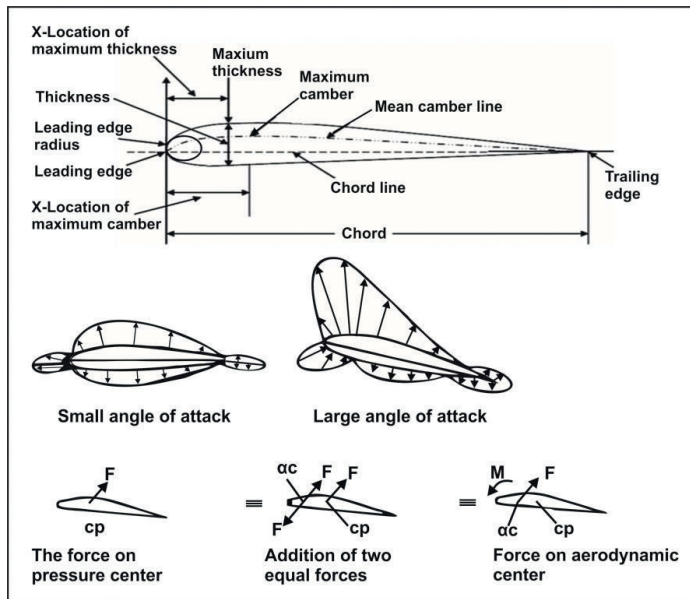
Figure 2.1.: The definitions of airfoil geometry; the distribution of the difference between the local pressure over the airfoil and the free stream static pressure at low and high angles of attack with the arrows indicating whether the pressure is larger than the ambient or otherwise; the composition of the net forces, lift, drag and moment around the aerodynamic center; adopted from open internet sources

the wind direction and the chord of the airfoil. The pressure distributions at two angles of attack are shown below the airfoil. The pressure is smaller on the top part of the airfoil than that on the bottom zone. The difference between the top and the bottom sections is more at larger angle of attack. The zone in which flow occurs from low pressure to increasing pressures is termed adverse pressure gradient region. In this zone, viscous effects become important and aspects like separation, transition to turbulent boundary layer come into picture. The integrated lift and drag forces on the airfoil pass through an axis around which the pitch moment is zero; such a point is called centre of pressure.

The forces are transferred to a point such that moment around an axis through this does not change much with angle of attack. Such a point is called "aerodynamic center (AC)". Thus, the lift and drag forces along with the moment around the aerodynamic center constitute the force system on the wing. The
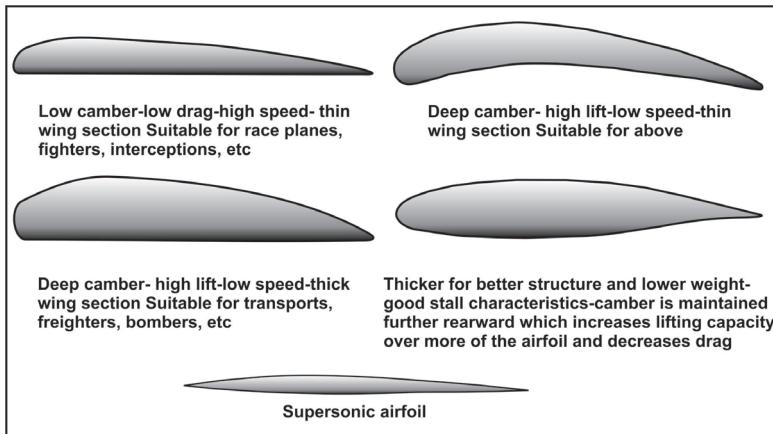
Figure 2.2.: Airfoil sections used on various classes of aircraft

aerodynamic center is located typically at about 25 % of the chord from the leading edge. It shifts the position on the chord only with substantial compressibility effects (see later). In addition to the lift and drag coefficients, c_L and c_D, a moment coefficient, c_M is defined such that $c_M = M_{AC}/[\rho v^2 A_{wc}/2]$ where M_{AC} is the moment of the forces around the aerodynamic center and c is the chord. Based on a number of tests of various shapes of airfoils designated suitably depending on maximum t/c and its position along the chord and camber, a large amount of data on c_L, c_D, cc_M with angle of attack have been documented by NACA and other organizations in Europe.

The NACA system consists of a series of 4, 5 and 6 digit airfoils. The meaning of these is as flows: 4-digit airfoils - for example, NACA 2415 means the following:

2 - maximum camber is 0.02 % over the chord, 4 - the location of the maximum camber along the chord line given as 0.4 c, 15 - the maximum thickness, here 0.15 c, Take 6-digit airfoils, for instance. NACA 632215 airfoil. This 6-digit series has the following meanings: The second digit 3 - maximum pressure location, here, 0.3 c, 2 - minimum drag at design lift coefficient, 0.02 here, 2 - design lift coefficient, 0.2 here, 15 - the maximum thickness, here 0.15 c. The tail surfaces of an aircraft are generally symmetric and are made with thin airfoils like NACA 0012. (zero camber, 12 % thick).
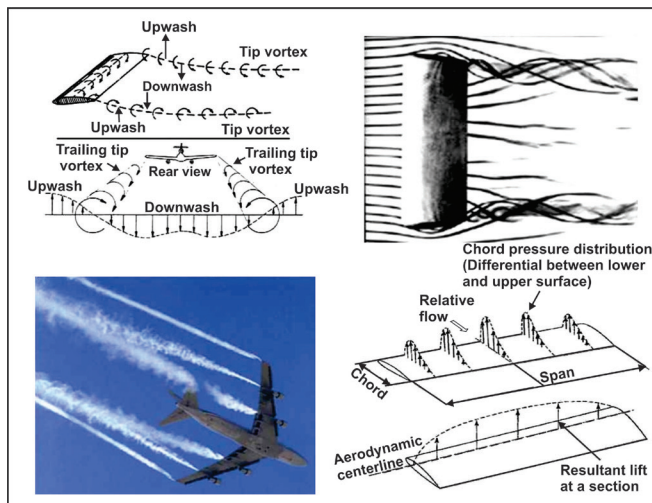
Figure 2.3.: Left-top: The vortical structure from wing shapes; Right-top: Laboratory demonstration of the vortical structures; bottom left: the trailing vortices from a flying aircraft; bottom right: the net pressure distribution over the chord at different span-wise stations and the load distribution over the span passing through the aerodynamic center; compiled from open internet sources

Figure 2.2 shows several sections of airfoils with a suggested broad application. Thick and thin airfoils are meant for low speed and high speed applications, respectively. Those with a smooth near-flat top profile minimizes the flow acceleration and so pressure gradient holds on to laminar flow for much longer distance along the chord and allows better lift characteristics. Such airfoils are called super-critical or laminar flow airfoils.

There is the third component of drag called lift induced drag that arises because of finite size of the wing. At the ends of the wing, the fact that the *bottom portion has a higher pressure compared to the top surface causes a flow from bottom to the top region* around the tips of the wing. This process causes vortices being shed from the wing tips, a feature that can be seen from the aircraft during take-off particularly in winter when the rotating vortex is made visual in a foggy environment or when there is significant atmospheric moisture (see Figure 2.3). The top left part shows the trailing vortex system. Top right shows a caricature of the vortical system. Bottom left shows the vortical structures
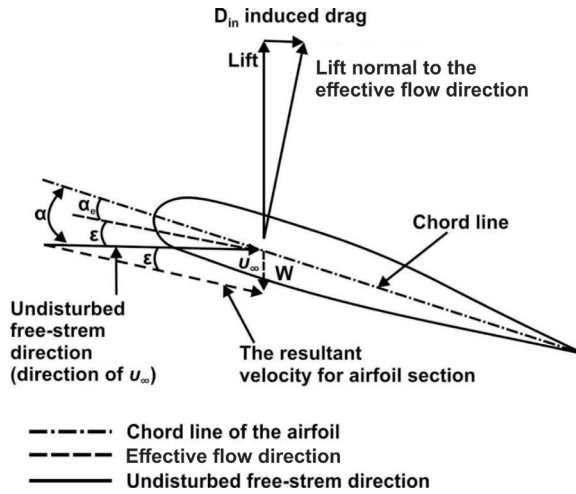
Figure 2.4.: The various aspects of a finite wing in which the effects of wing tip vortices are taken into account. The effective angle of attack is changed and the lift vector normal to this will have a component along the free stream lift induced drag; α is the angle of attack, ε is the tilt caused by wing tip vortices called the downwash angle; adopted from Torenbeek and Wittenberg, 2009

shed from wing tips and other locations where fluid was injected to help visualisation of the trailing flow and the bottom right, the pressure distribution over the wing section at various span-wise stations as well as the integrated load at each span-wise location.

The influence of this will be small for long wings. A parameter that characterises this feature is called "Aspect ratio *(AR)*". It is defined by $AR = b^2/A_w$ where b is the span of the wing and A_w is the projected surface area of the wing given by the product of the length and chord *(c)* of the wing. This implies that for a rectangular wing, $AR = b/c$, the ratio of the length to the chord of the wing. Larger the AR, smaller will be the lift induced drag.

The wing deflects the flow leaving behind a trailing wake. This wake in turn has an effect on the flow over the wing inducing a flow which modifies the local angle of attack (from α to α_o because of downwash angle ε as in Figure 2.4). For

a level flying aircraft this "downwash" causes the aircraft to behave as though it were flying through a downdraft.

The lift at a given station acts perpendicular to the local flow angle, and this change in the local angle of attack causes the lift vector to tilt backward as shown in Figure 2.4, resulting in a force component that is parallel to the free stream direction.

This creates the lift induced drag. A simple approach to dealing with finite size effects is to consider a reduction in the angle of attack due to downwash. From an analysis of the forces due to downwash, the reduction in the angle of attack is obtained as $\varepsilon = c_L/(\pi e AR)$, where the efficiency factor e is added to account for the approximations made in the theory (see Anderson, 1984 or Torenbeek and Wittenberg, 2009 for more details). The theory leads to

$$c_L = \frac{2\pi}{(1 + 2/eAR)}; \quad c_D = c_{D0} + \frac{c_L^2}{\pi e AR}$$

(2.1)

where c_{D0} is the combination of profile and frictional drag and the second term on the right hand side refers to lift induced drag. It is also important to know that the lift coefficient drops from the two-dimensional value to a lower value because of these three-dimensional affects.

The three-dimensional distribution of pressure when integrated over each section gives the load at that section. This distribution over the span of the wingshown as a representative case in the bottom right side of Figure 2.3 depends on the planform. While moderate wing taper produces a near parabolic distribution, high taper makes the load distribution more uniform over the wing with sharp tail-off towards the tip, and low taper makes the distribution with near-uniform fall-off from the root to the tip. Sweep-back makes the distribution near flat over the span. Figure 2.5 shows a comparison between the shapes of wings at the root, mid-span and tip of a bird (in this case, pigeon) and a typical swept wing airplane. As can be noticed, the wing chord decreases in both cases, but the change in camber in the case of pigeon from the root to tip is more than in an airplane.
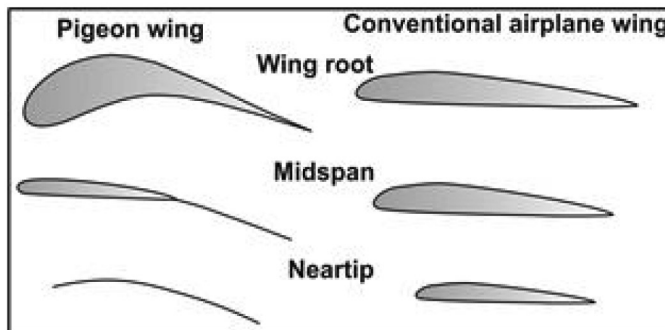
Figure 2.5.: Comparison between the wing shapes of a bird (in this case, pigeon) and an airplane. Notice more significant changes in camber in the case of pigeon while the span-wise chord reduction is about similar; adopted from Shyy et al (2008)

2.3. Compressibility Effects

The discussion on the lift and drag aspects of the wing in the previous section is largely for incompressible flows - flows with flow speed very small compared to local acoustic speed - very small Mach number. The effects of compressibility become significant as M goes beyond about 0.3. Increase in Mach number leads to decrease in lift, increase in drag and an aft-shift of the center of pressure.

It is useful to understand the physical aspects of what happens when the Mach number keeps increasing through the sonic condition ($M = 1$) to supersonic ($1 < M <$ about 5) and hypersonic conditions ($M >$ about 5). As discussed in section 1.2.8, sweep back is used to obtain higher cruise speeds in aircraft without significant drag rise. By managing to fly near critical Mach number (discussed below) and below the drag divergence Mach number, the deleterious effects of compressibility are brought down. Figure 2.6 provides the definition of sweep back and oil flow visualization pattern over the wing.

The flow over a swept wing behaves differently than a straight fixed wing. Instead of flowing straight along the chord of the wing in a two-dimensional fashion, air is also directed along the wing parallel to the leading edge as seen on the oil flow visualization. Due to three-dimensional nature of the flow, the boundary layer on swept wing is affected by cross flow instability. This bound-
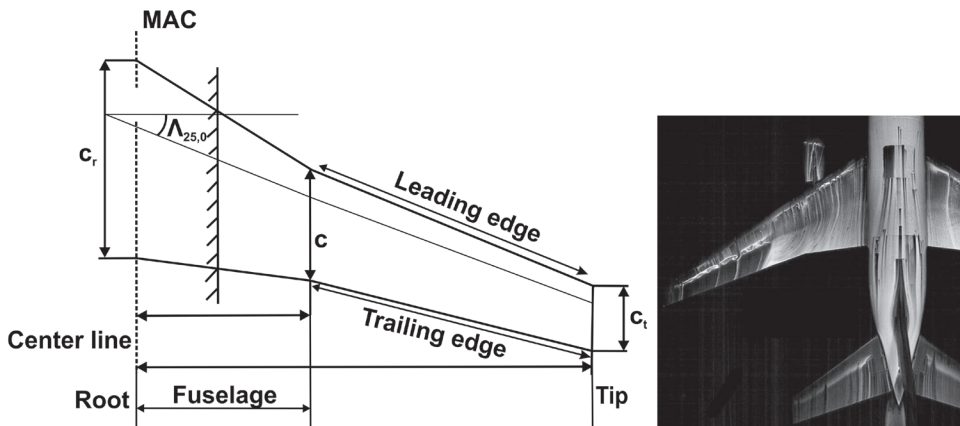
Figure 2.6.: Left: Definitions of a swept back wing shape; Right: Oil flow pattern over the wing

ary layer instability can lead to turbulence and/or flow separation in the outer regions of the wing towards the trailing edge. This leads to tip stall, which may lead to partial loss of aileron control at low speeds. The stall on the outer part of the wing with the flow over the inner part intact causes the airplane to pitch up, a feature that must be taken care. The more sharply sweptback the wing is, the stronger this pitching behavior becomes.

Several passive arrangements like vortex generator, notched or dogtooth leading edge, boundary layer fence, underwing pylon or vortilon as shown in Figure 2.7 are all employed to get better aerodynamic performance even though each of these has some penalties in some aspect of the performance or the other. The way vortex generators work is shown in the right part of Figure 2.7. The small protuberances create vortices that bring in the higher momentum fluid from the outer part of the flow into the near stagnant lower parts that enabling better control of ailerons or flaps; there will, however, be additional contribution to drag.

The question of how sweepback helps limit the drag rise and hence allow aircraft to fly at higher Mach numbers compared to straight wings has been discussed in Chapter 1, section 1.2.8. A further important feature of a swept back wing is that it has higher longitudinal stability (by pushing back the aerodynamic center of the wing) allowing for the adoption of smaller tail plane even if not dispensed with. This arises from the fact that under a gust or lateral dis-
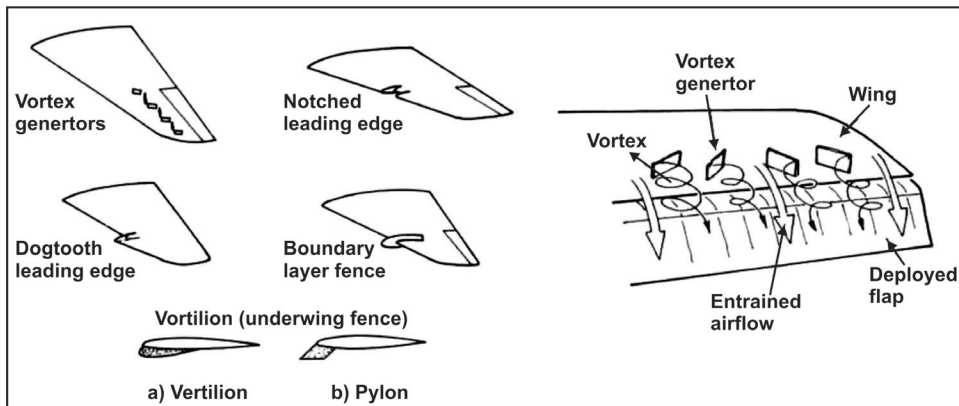
Figure 2.7.: Left: Various wing aerodynamic passive control arrangements; Right: Oil flow pattern over the wing
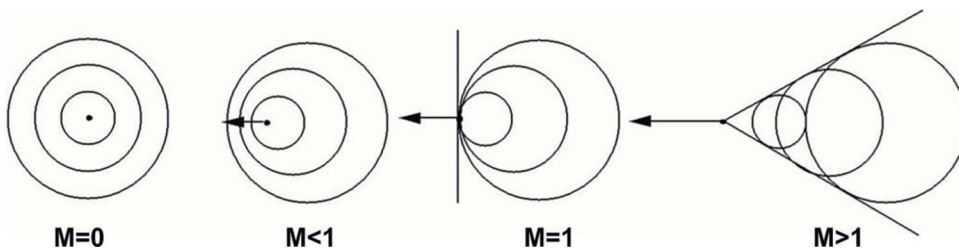
Figure 2.8.: Depiction of sound propagation process: the pressure peaks identified by the circular lines, from the left: $M = 0$, $M < 1$, $M = 1$, and $M > 1$; the cone angle in the last figure is 2θ

turbance, if the aircraft were to be subject to yaw, the differential movement of one wing moving into the wind and the other away from it causes a restoring force. Because of enhanced stability, there are examples of the tail plane having been dispensed with - B-2 or the flying wing.

While *swept back* wings are most commonly used, some experimental planes have used *swept forward* wings that make these aircraft move towards lower stability zone and may even need a fly-by-wire control to cover the entire flight envelope. One redeeming feature is that if sweep back is switched, the root willstall before the tip, this aspect providing for better low speed tail control. Even with these minor benefits, this design has rarely been used because of serious aero-elastic problems (see Chapter 6, section 6.14).

2.3.1. Sound wave propagation with moving sources

Figure 2.8 shows the movement of sound waves under various conditions. The first figure is for a stationary sound source (implying *M = 0*). Under this condition, the sound waves propagate in a spherically symmetric manner. The distance between the peaks divided by the time taken gives the speed of the sound wave. Any point that sound has reached is at a distance of at where a is the sound speed and t is the time elapsed after the sound is generated. When the source moves at a speed less than that of sound (*M < 1*), the sound waves get bunched together like in the second figure. This leads to frequency shift (similar to Doppler shift). The wave speed ahead of the source is $(a - V)$ where V is the source velocity. When the source moves at the same speed as the speed of sound (third part of the top figure – *V* = a or *M* = 1), sound cannot travel beyond the source. The wave are bunched at one place. Sound waves travel only behind the wave. This implies that if an aircraft were to be flying towards a person at this speed, the person will be able to see it flying noiselessly and will begin hearing it only when it is just overhead. If the aircraft were flying supersonic, then, the sound is heard only after the aircraft passes beyond the location of the person, the subtended angle smaller with increasing flight Mach number. The loudness of the sound depends on how high it is flying. In order for the inevitable noise not to create great discomfort, the aircraft must be really flying high. In fact, there is usually an advisory indicating the minimum altitude at which one can reach *M* = 1. Typically, such sound levels do not exceed 120 dB for about 2 s or so for the aircraft flight is ensured to be over land mass with little habitation.

The natural question would be why is all this so? Sound waves are essentially pressure waves. The deviation in pressure compared to the ambient pressure which is not far from 1 atm (or 101.32 kPa or 10^5 Pa approximately) is indeed very small. This is measured by the well known decibel scale (dB for short). Based on the nature of sound perception by the ear, the sound pressure level is measured as

$$\text{SPL (dB)} = 20 \, log_{10} \left[\frac{p}{p_{ref}} \right]$$

$$(2.2)$$

where SPL is the sound pressure level, p and p_{ref} are the actual sound pressure and a reference sound pressure. The reference pressure, p_{ref} is taken as 20 μPa (20×10^{-6} Pa). The reference pressure is chosen on the basis of this sound pressure leads to the lowest audibility. Normal conversation is a pressure of 0.002 to 0.02 Pa (40 to 60 dB), jet engine at 100 m is about 6 to 200 Pa (110 to 140 dB), acoustic tests on a rocket launch 4000 Pa (165 dB), threshold of hearing 63 Pa (130 dB) and theoretical limit for undistorted sound at 1 atm is as large as 1 atm (194 dB). At $M = 1$, the stagnation pressure is 1.9 atm. At speeds more than this, nonlinear acoustics plays a very significant role and can rattle and breakup window glass panes and is obviously unbearable for human hearing. To prevent such occurrences in the areas of human habitation, military aircraft achieve supersonic conditions at very high altitudes. The acoustic disturbance travels through the atmosphere and decays in strength before the surface of earth is reached.

For $M > 1$ (supersonic condition), the waves move back such that the entire acoustic propagation of the source is restricted to a cone with a cone angle, θ given by $\theta = sin^{-1}(1/M)$. This is because in a given time, t, sound wave travels a distance of at while the source travels a distance of $V t$ and so $sin\ \theta = a/V$ (see Figure 2.8). The subject of gas dynamics treats the subject of how the flow behaves at super sonic conditions where the wave propagation behavior is central to this behavior discussed briefly below.

2.3.2. Gas dynamical features

A significant part of the physics is obtained using inviscid approximation. The supersonic to subsonic flow transition occurs via shocks that are treated as discontinuities on either side of which there will be significant differences in all flow properties - velocity, pressure and temperature (as well as composition in case of hypersonic flows) except for change that occurs close to M near unity. A condensed version of the principal features is set out below:

1. As different from incompressible flows where fluid velocity changes are coupled to changes in pressure only, in compressible flows, changes in temperature and density need to be accounted for.

2. Gas dynamics requires invoking stagnation conditions of all these quantities - T_{stag}, p_{stag} and ρ_{stag} in addition to static quantities - T, p and ρ.

3. Flow can accelerate from subsonic to supersonic conditions or decelerate from supersonic to subsonic conditions isentropically - without any stagnation pressure loss. The accuracy of capture of physics depends on whether the flow is external or internal - external flows are those over wing shapes and fuselage for aircraft, cone-cylinder or ogive shapes for missiles and launch vehicles; internal flows like those through ducts, engine components including nozzles. The isentropic relations along with the definition of the speed of sound, a defined as $a = \sqrt{\gamma R T}$ and $M = V/a$ can be obtained in terms of the ratio of specific heats at constant pressure and volume $(\gamma = c_p/c_v)$ as

$$T_{stag}/T = 1 + \frac{(\gamma - 1)}{2} M^2 \tag{2.3}$$

$$p_{stag}/p = [T_{stag}/T]^{\gamma/(\gamma-1)} \tag{2.4}$$

$$\rho_{stag}/\rho = [p_{stag}/p]^{1/\gamma} \tag{2.5}$$

4. Accelerating flows can be analyzed accurately under ideal assumptions without viscous effects to a first degree. Decelerating flows can also be analyzed similarly for some external flows. Internal decelerating flows are indeed more complex and viscous effects cannot be usually ignored. Supersonic air intakes for aircraft and missiles are an example of this class.

5. Supersonic flows decelerate to subsonic conditions usually through a local normal shock. Normal shocks are governed by relationships between downstream and upstream conditions derived simply from one-dimensional flow considerations of mass, momentum and energy as follows:

$$M_2^2 = \frac{M_1^2 + 2/(\gamma - 1)}{2\gamma M_1^2/(\gamma - 1) - 1} \tag{2.6}$$

$$\frac{p_2}{p_1} = 1 + \frac{2\gamma}{(\gamma + 1)}(M_1^2 - 1) \tag{2.7}$$

$$\frac{T_2}{T_1} = \frac{[2\gamma M_1^2 - (\gamma - 1)][(\gamma - 1)M_1^2 + 2]}{(\gamma + 1)^2 M_1^2} \tag{2.8}$$

$$\frac{p_{stag,2}}{p_{stag,1}} = \left[\frac{(\gamma + 1)}{[2\gamma M_1^2 - (\gamma - 1)]}\frac{(\gamma + 1)M_1^2}{(\gamma - 1)M_1^2 + 2}\right]^{\gamma/(\gamma-1)} \tag{2.9}$$

$$\frac{T_{stag,2}}{T_{stag,1}} = 1 \tag{2.10}$$

In a normal shock with M1 being supersonic, M2 is subsonic; the static pressure, temperature and density rise significantly through the shock. The stagnation temperature does not change indicating iso-enthalpy condition. The stagnation pressure decreases through the shock, stronger the shock, the decrease larger. This is an indication of rise in entropy across the shock.

6. Supersonic flows encounter objects such as wedges or cones in wings and air intakes. The flow may be required to turn inwards - for all changes in direction less than 180^0 or outward - more than 180^0 (see Figure 2.9). In these cases, the adjustment of the flow occurs through the formation of a shock in the first case and expansion waves in the second case. Figure 2.9 shows the emanating shock waves and expansion waves at inward and outward turning corners. In the case of an inward turning corner (inward implies a change in direction less than 180^0), it can be imagined that the turn will occur through a number of small changes, each change giving rise to a small increase in pressure. Each succeeding wave from the incremental change in direction coalesces with the previous wave making it stronger as shown in the figure at (a1). This process leads to a well developed shock. The behavior of the shock is analyzed through the velocity diagram. The oblique shock can be thought of as a normal shock with a tangential velocity imposed so that the change in direction is accounted for. The change in the direction of the flow bears an angle δ to the horizontal line and the angle of the shock is $\theta = 180^0 - \theta'$. Analysis of the flow to keep the normal velocity the same on both sides of the shock gives an implicit relationship between θ, the shock angle to the inlet Mach number M_1 and the wedge angle δ as

$$\tan \delta = 2 \cot \theta \left[\frac{M_1^2 \sin^2 \theta - 1}{M_1^2(\gamma + \cos 2\theta) + 2} \right]$$

(2.11)

Once θ is obtained, one can use the equations for normal shock introducing M_1 sin θ in place of M_1 to obtain downstream properties.

There is another interesting feature of the supersonic flow over two-dimensional and three-dimensional objects. If one considers the flow at a fixed supersonic speed ($M = 2$ here) over a wedge and cone (axisymmetric three-dimensional body), it can be seen from Figure 2.10 that the shock angle is much larger for
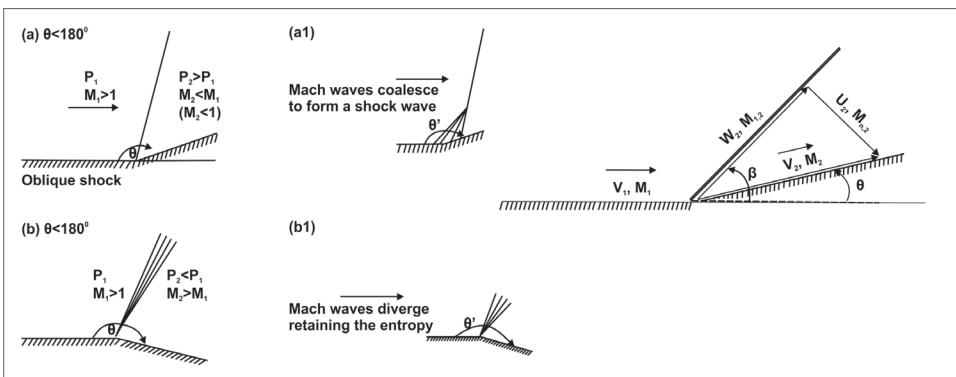
Figure 2.9.: (a) and (a1): The properties of an oblique shock at an inward turning corner and the explanation for the formation of the shock - waves coalescing into a strong wave; b and b1: The properties of expansion at a corner - the Prandtl-Meyer expansion fan and the flow behavior at the corner - waves diverging from each other preserving isentropicity of the flow; (c): The velocity diagram - note that the tangential velocity is the same at the shock
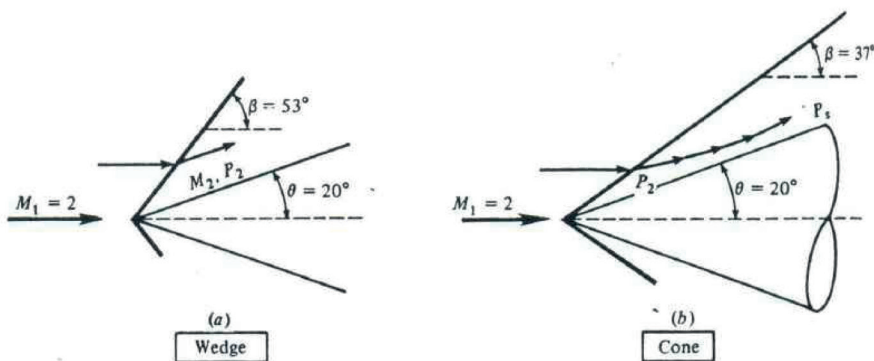
Figure 2.10.: The shock wave over a cone and wedge of the same angle. The shock wave over the wedge is much stronger than over the cone as the shock angles indicate. Cone has three-dimensional relief helping manage the supersonic flow with smaller deviation.

the wedge compared to cone. This is understood to be due to three-dimensional relief provided by the cone. This also leads to another flow difference. While the wedge flow after the shock is parallel to the wedge, the cone flow has a curvature. Curved shock flows produce additional entropy change.
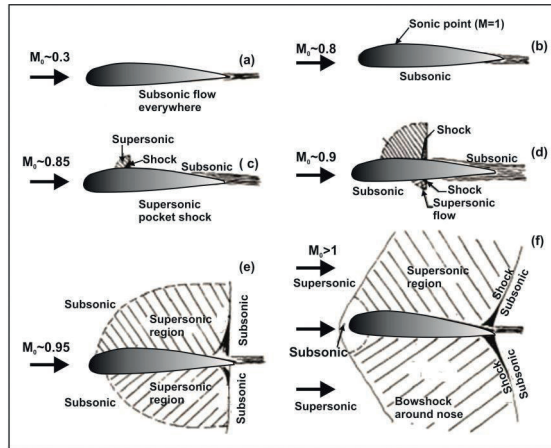
Figure 2.11.: Note the regions of subsonic and supersonic regimes with increased flight Mach numbers, adopted from open internet sources

2.3.3. Flow over the airfoil at increased speeds

In Figure 2.11 (a), it can be noted that the Mach number is subsonic ($M < 1$) throughout the flow field. Since the presence of the wing is felt ahead due to acoustic wave propagation (see Figure 2.8). As the speed increases, the flow acceleration over the wing leads to the attainment of $M = 1$ at some point on the wing [see (b)]. The free stream Mach number at which the peak speed over the wing just becomes sonic is called *critical Mach number*. With increase in Mach number beyond this value, the zone that has supersonic conditions over the wing will increase. At close to sonic flight condition [Figure 2.11 (e)], the flow accelerates to mildly supersonic flow over large regions of the flow and it becomes subsonic at the end of the airfoil because of flow turning at the trailing edge. Figure 2.11 (f) is one in which the entire flow is supersonic except a small subsonic region ahead of the wing. Rest of the flow behavior is the same as in the earlier case. The pressure changes that occur in cases where the flow is at high speeds due to shocks and expansion waves is so much larger compared to those in subsonic flow that the wave related forces dominate the force field.

Figure 2.12 shows pictures of shock waves in laboratory and flight conditions. These pictures are obtained through the use of schlieren or shadowgraph techniques. These techniques capture the density gradient and density change itself respectively. Both these are large in a shock system and hence either of the
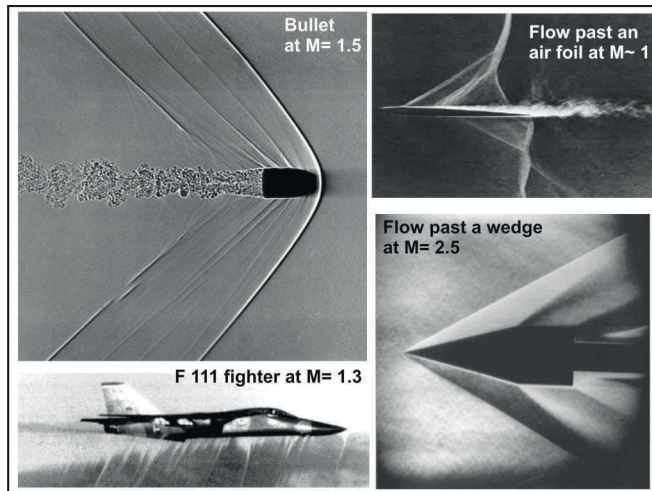
Figure 2.12.: Shock waves captured on a number of systems: Top left: Sharp shock waves on a bullet travelling at M = 1.5; Top right: Flow past an airfoil in a transonic wind tunnel at a Mach number slightly in excess of 1; Bottom left: General dynamics F111 fighter flying at M = 1.3; botton right: a sharp wedge in a supersonic tunnel at M = 2.5; drawn from Dimitriadis (2016) and other open internet sources

techniques can be adopted wherever possible. In laboratory situations, one can set up a schlieren system with suitable optics and capture the image(s) for steady conditions or in a dynamic situation. The top left part of Figure 2.12 shows the sharp shadowgraph picture of a bullet traveling through air at M = 1.5 (NASA, 2007). Since the bullet is a "blunt" object, the shock wave in front of the bullet appears bow shaped. The flow in the stagnation region in front of the bullet will be subsonic. The flow then accelerates over the bullet and the directional changes cause other waves which are all captured accurately. The flow behind the bullet constitutes a wake-flow and is subsonic and highly turbulent. The fine structures of turbulence are also captured well. The top right picture is the schlieren picture of a wing in a flow that has crossed sonic conditions. The flow accelerates over the wing and the complex flow structure including downstream flow separation are clear in the picture. The bottom left is that a General Dynamics F-111 fighter in transonic flight at low altitude with oblique shocks clearly seen against the background light/dark boundary of a mountain ridge. The jet exhaust is also seen though not sharply. This picture constitutes
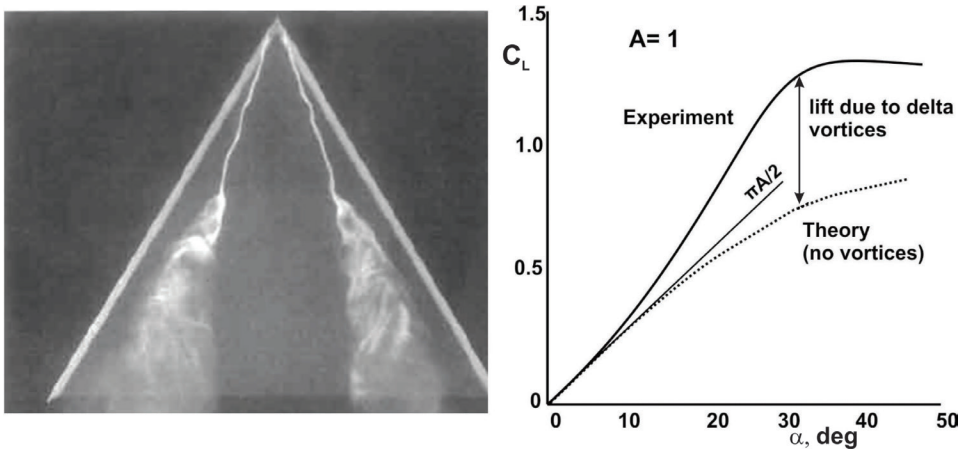
Figure 2.13.: Leading edge vortices on a delta wing and the lift characteristics

a shadowgraph. The bottom right is a schlieren picture is of a wedge in super-sonic flow at $M = 2.5$ in a wind tunnel.

Shock waves are observed in non-aeronautical applications like nuclear blast, racing cars moving at sonic speeds and are not limited to terrestrial phenomena, either. Apparently, "NASA's Galaxy Evolution Explorer" captured an image of a racing star, called Mira, that resembles the bullet photo. The ultraviolet image shows a gigantic shock wave, a bow shock, in front of the star, and an enormous, 13-light-year-long trail of turbulence in its wake. Nothing like this tail has ever been seen before" (see Wikipedia2, 2016).

2.4. High Speeds and Delta Wings

For high supersonic speeds ($M \sim 2$), deeply swept wings lead naturally to delta wings. The flow over such wings is dominated by the formation of leading edge vortices which make a substantial difference to the lift characteristics. The generation of these vortices leads to low pressures on the top surface, hence leading to increments in lift coefficient. The vortical structure and associated benefit in c_L are particularly important at high angles of attack, as illustrated in Figure 2.13.

2.4.1. Hypersonic flows

Hypersonic flows are supersonic flows at $M > 5$, typically. This Mach number defines the beginning of hypersonic flows because under these conditions, ma-
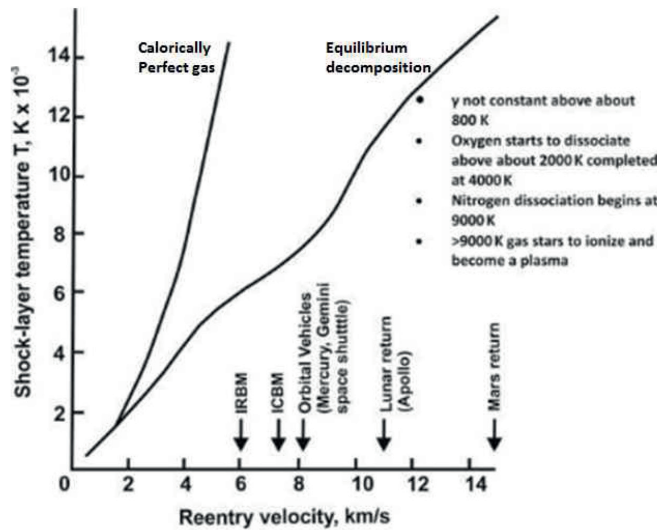
Figure 2.14.: Shock layer temperatures with re-entry speeds and the vehicles that make re-entry at the indicated speeds. Note that the calorically perfect gas assumption breaks down at about 2 km/s (*M* ~ 7); drawn from Mason (2016) and other internet sources

ny assumptions that are reasonable in supersonic flows become questionable. Principally, air, composed of many elements treated as a single fluid in supersonic flows addressed above, but will begin to dissociate to other gases.

Hypersonic flows acquire great importance in problems of vehicle re-entry into the atmosphere since these occur at M up to 30. The stagnation temperatures calculated from the simple equation (2.3) meant for a calorically perfect gas at M = 5, 15 and 30 are 1500 K, 8000 K and 34000 K (more than the surface temperature of the sun) respectively. In fact, these conditions are better characterized by *stagnation enthalpy rather than stagnation temperature*. Stagnation enthalpy is virtually the kinetic energy, $V^2/2$. At 5 and 10 km/s these are 12.5 and 50 MJ/kg. If we compare these with the energy of hydrocarbon - air mixture of 2.5 to 3 MJ/kg at which level, temperatures are only 2500 K, one can appreciate the energy involved with levels as large as 12 to 50 MJ/kg that need to be absorbed. The only way this occurs is by dissociation, excitation of vibrational energy and ionization. One of the most stable molecules that resists dissociation is nitrogen; nitrogen ions and electrons as well as oxides of nitrogen will be found in copious amounts in the high temperature zones of the vehicle
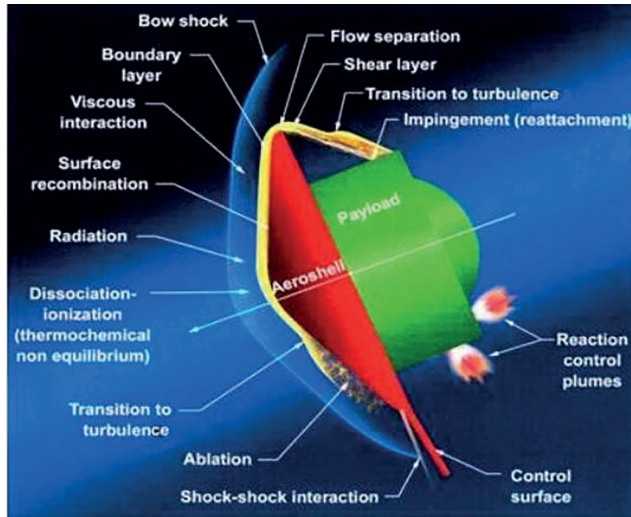
Figure 2.15.: Shock layer structure showing the importance of various aspects in a re-entry blunt vehicle like a lunar landing vehicle, drawn from Mason (2016) and other internet sources

engaged in re-entry. Figure 2.15 shows the peak temperatures achieved in the shock layer as a function of re-entry velocities. These high temperature of the ionized zone transfers heat to the surface in which the radiative component is as much as 30 to 80 % of the heat transferred. Also, the presence of ionized species and electrons is responsible for the classical communication black-out experienced during re-entry of space vehicles.

As M keeps increasing, the shock angle for fixed wedge angle for two-dimensional flows or cone angle for axisymmetric geometries reduces such that the region between the shock and the body surface reduces. Because of very high temperatures, the viscosity increases (as $\mu \sim T^{0.7}$) and hence contributes to viscous effects. The boundary layer thickness at high Mach numbers behaves as $\delta_{bl} \sim M^2/\sqrt{Re_x} \sim V^{3/2}\mu^{1/2}/\left(T\sqrt{\rho}\right)$ and is large because all the parameters in the last expression favor large values under the conditions of hypersonic flow. This implies that viscous effects *unlike supersonic flows* are so significant that the pressure changes through the shock wave and pressure over the body are affected by it.

Handling heat transfer issues in these conditions is important issue and invok-

es two complimentary aspects - aerodynamics and materials science. One of the key questions that arises is: Should one use a stream lined body or a blunt body treated as an axisymmetric geometry. The heat flux into the body is the highest at the stagnation zone and is given by

$$\dot{q}'' = 0.783 Pr^{-0.6} (\rho_0 \mu_0)^{1/2} \sqrt{du_e/dx} (h_0 - h_w) \sim \frac{\rho_0^{1/2} V^{5/2} (1 - h_w/h_0)}{r_c^{1/2}}$$

(2.12)

where $\dot{q}''$ is the heat flux (kW/m²), $\rho_0 \mu_0$ is the product of free stream density and viscosity (ρ in kg/m³, μ in kg/ms), du_e/dx (1/s) is the free stream velocity gradient related to the pressure profile over the body, h_0 and h_w are the free stream and wall sensible enthalpies (MJ/kg), and r_c is the radius of curvature of the stagnation zone (m), V is the free stream speed (m/s). The second expression is obtained by expressing the velocity gradient in terms of pressure gradient and using the Newtonian pressure distribution over the surface (p. 310, Anderson, 2006). The fact that the heat flux varies inversely with $r_c^{1/2}$ implies that a reduction in the heat flux can be achieved by increasing the nose radius of curvature. This leads to the conclusion that a *blunt body is better than a streamlined body* from heat transfer point of view.

A different approach has been chosen to get to the same conclusion. By equating the energy rate due to aerodynamic heating with that due deceleration be-cause of drag, the energy transferred into the vehicle is obtained as as Q_{total} = $(mV^2/2)$ $(c_f/2c_D)$ where m is the mass of the body, c_f is the skin friction coefficient and c_D is the drag coefficient of the body which is composed of profile drag and skin friction drag. The energy stored is considered as the kinetic energy of the vehicle, $mV^2/2$ is multiplied by the coefficient $c_f/2c_D$ that is the ratio of skin frictional drag with total drag coefficient. Since a sharp nosed slender body has less strong shock, the contribution to drag due to skin friction is quite significant making $c_f/c_D \sim 1$. On the other hand, in the case of blunt body skin friction will become a smaller fraction of the total drag which is because of a very strong shock in front of the body. Consequently, $c_f/c_D \rightarrow$ small values. This brings down the total heat accumulated in the body which is simply a consequence of the heat flux being much lower. Thus both the arguments suggest that a bluff body is better for a re-entry body. Even if the body is

not blunt, the manner in which it reenters the atmosphere will be arranged so that blunt body will be the front of the body. The re-entry of Space shuttle will be at an angle of attack of 40^0.

As indicated earlier, the re-entry systems need thermal protection systems (TPS). The approaches are different depending on whether the application is a one-shot affair like missiles or repeated use like with Space shuttle or other reusable launch vehicles. For one-shot applications, ablative compositions that are structurally stable are appropriate. Much work has been done in this area (Wikipedia1, 2012). Essentially, silica based phenolics, carbon-phenolics and carbon-carbon have been deployed as ablatives for applications involving high heat flux areas of solid propellant rocket nozzles. These materials have to be processed with care for use since the processing strategy impacts the quality of the performance. The ablative works on the basis of the polymeric resin pyrolizing - gasification with break-down of the large polymeric molecules to smaller fragments the process being endothermic. Using additives that absorb the enthalpy by dissociation is an important strategy in the design of ablatives. Since the actual performance of an ablative is crucial to the thermal environment of the vehicle and there are variations in the flux and the properties of the ablative, the thickness of the ablative is set with suitable margins. For reusable applications, silica tiles have been deployed even though they are brittle. Space shuttle used them and required inspection and repair after each flight.

2.5. Bird and Insect Aerodynamics vs. Aircraft Aerodynamics

The need for understanding bird and insect aerodynamics and applying the principles understood in aircraft aerodynamics is not simply one of joy that arises from understanding. Many new flying devices and micro-air vehicles are being built for military purposes and significant research & development effort has been going on from the last decade towards exploring the natural systems and the evolutionary optimization that has gone on in them to further benefit from them. And, of course, the human endeavour to fly has always received inspiration from bird and insect flight. Also, in the last twenty years much information has been accumulated on the flight behavior of birds and insects. Experiments on bird flying in wind tunnels have been extensively conducted. Birds in natural habitat have also been instrumented to determine the flying features.

The area has been made rich by contributions from zoologists, aeronautical engineers and scientists. Insects have been investigated substantially (Tennekes, 2009; Osborne, 1951; Ellington, 1999; Pennicuick, 2008). A very interesting and readable book by Tennekes (2009) has developed the relationships using simple and effective physical reasoning. Dhawan (1991) has addressed some questions of limiting speeds of flight of birds.

Here, only three representative examples, the arctic tern, albatross and a humming bird are presented for the purposes of understanding and illustration (see Figure 2.16). The Arctic Tern, known as the bird of the Sun is perhaps the only species that sees the sun the most in its life and is justly famous for its migration. Weighing about 100 g, it flies at speeds up to 40 km/h from its Arctic breeding grounds to the Antarctic and back each year. Data show that Arctic Terns that bred in Greenland or Iceland each covered 70,900 km on average in a year, with a maximum of 81,600 km. The average Arctic Tern lives about twenty years and travels about 2.4 million km!

The hummingbirds are among the smallest of birds measuring a maximum of 130 mm and weighing 2 to 5 g. They fly at speeds up to 50 km/h. Their normal flying habit, though, is akin to a helicopter. They can hover in mid-air by rapidly flapping their wings. The Giant hummingbird's wings beat up to 25 beats per second (600 flaps per minute), the wings of medium-sized hummingbirds beat up to 30 beats per second and the smallest can reach 100 beats per second during courtship displays. They are also the only group of birds being able to fly backwards. Studies by Douglas Warrick and coworkers (2005) in a wind tunnel using particle image velocimetry on one variety of hummingbirds has shown that the birds produced lift of 75 % of their weight support during the downstroke and 25 % during the upstroke. Most hummingbirds are given to migration. When migrating, they generally fly during the day and sleep at night. One variety, the Ruby-throated hummingbirds when flying over the Gulf of Mexico during migration continue to fly since there is no place to land and sleep. It is amazing to think that these little tiny birds travel over 700 km of water with a head wind of 30 km/h for over 20 hours to reach their favorite breeding grounds. There are other varieties of hummingbirds that travel tree-top over the land keeping in mind the availability of food sources.
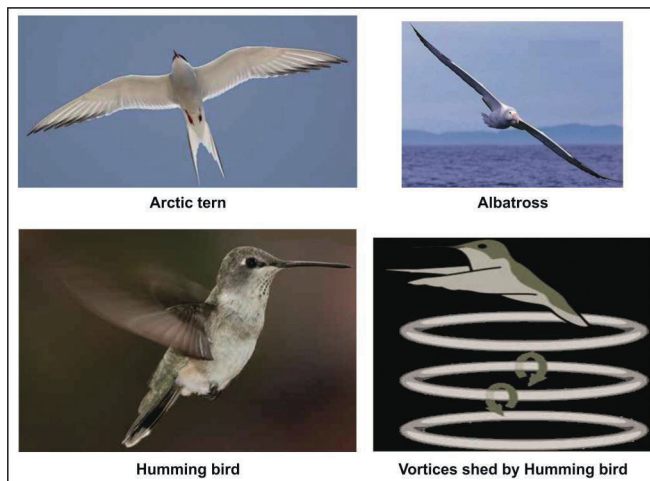
Figure 2.16.: The Birds - The Arctic tern, bird of the sun travels nearly 80000 km in one year; the Albatross with the largest wings glides most effectively; the hummingbird ex-tracts nector introducing its beak into the flower's base by hovering by flapping the wings vigorously. Notice the vortices shed by the bird during the flapping

Albatross is an excellent example of gliders in terms of flying capabilities. The wingspan of large albatross is about 3.5 m, the largest of any bird with a mass up to 10 kg. The wings are stiff and cambered, with thickened streamlined leading edges. Albatrosses travel huge distances with techniques used by many long-winged seabirds, dynamic soaring and slope soaring. The former technique involves repeatedly rising into wind and descending downwind thus gaining energy from the vertical wind gradient. The latter involves the use of rising air on the windward side of large waves. Albatross have high glide ratios close to 23. Interestingly, they are aided in soaring by a shoulder-lock, a sheet of tendon that locks the wing when fully extended allowing the wing to be kept outstretched without any muscle related energy expenditure. Take-off is the most energetically demanding part of a journey needing flapping. Some albatrosses use a flight style known as flap-gliding, where the bird progresses by bursts of flapping followed by gliding. When taking off, albatrosses do run much like aircraft, albeit using flapping to reduce the take-off run.

In the long distance journey, when faced with little helping wind, they rest on the ocean surface in calm seas until the wind picks up. They combine the soar-

ing techniques with predictable weather systems like those in the southern hemisphere flying north taking a clockwise route and those flying south taking counterclockwise route. Apparently, they are so well adapted to the lifestyle that their heart rates while flying are close to the heart rate when resting (it is thought they sleep on flights, a fact not demonstrated yet!).

Insects have a range of the mass (m_{in}) from 20 μg to a few grams. It appears that the wing area and flapping frequency vary as $m_{in}^{(2/3)}$) and $m_{in}^{(1/4)}$ even there is fair amount of scatter in the data. The power demanded for flying is largely proportional to the mass of the insect (bird) and the flying is characterized by minimum power demand. The flapping mode of generation of forces has significant geometric changes in both turn and twist of the wing as well as strong unsteady effects both of which are demonstrated experimentally in recent times. Warrick et al (2005) showed that hummingbirds move their wings in the shape of "8" during the hovering flight. In general, even though the way the lift and drag of an insect (bird) flying at speed V and flapping at speed w (taken at the wing mid-span) are expressed as

$$L = \rho A_w c_L(V^2 + w^2)/2; \quad D = \rho A_w c_D(V^2 + w^2)/2 \tag{2.13}$$

Thus, the lift and drag coefficients are intertwined in the dynamics of force gen-eration. For hovering by flapping, the expression for lift that equals the weight becomes $L = W = c_L \rho \omega^2 b^4/4AR$, where ω is the flapping frequency, b is the wing span and AR is the aspect ratio. This strong dependence on the wing span is ameliorated by the natural evolution of AR and the choice of the flapping frequency. A typical variation of the lift coefficient with drag coefficient and the lift as a function of flapping frequency from the work on flapping micro-air vehicle, RoboFly and DelFly (Lentink et al, 2009) are set out in Figure 2.17. It may be noted that the lift coefficients are large as also the drag coefficients. The L/D is typically about 1 to 1.5, and the lift variation with flapping ferquency is linear instead of quadratic, a feature related to the variation in geometry during the flapping action.

For the case of soaring or gliding flight, the relationships discussed earlier for the case of aircraft apply. It is useful to compare the broad parameters of the

insects, birds, civil and military aircraft to get an appreciation of commonalities and differences. Drawn from several sources, the data of flying systems segregated into insects, birds, human powered aircraft and hang gliders, civil aircraft and military aircraft are set out in Tables 2.1 and 2.2.

In Table 2.1, the weight of insects and birds varies between a few mN to about 100 N, whereas man made craft go up to 5.6 MN (560 tonnes); of course, insects and birds carry only their mass and food in their beak or mouth. Some birds like eagles carry fish that is a significant fraction of their mass. Their wing loading is much smaller than of aircraft due to largely the speed of flight. In a steady flight, the weight is balanced by the lift generated aerodynamically. This implies $W = c_L A_w (\rho V^2)/2$ that leads to $W/A_w = c_L (\rho V^2)/2$. The values of lift and drag coefficients for birds vary over a range. If c_L is chosen as 0.4 and 0.6 with ρ = 1.2 kg/m³, one gets W/A_w = (0.24–0.36)V^2 and for arctic tern and albatross, the speeds of flight work out to 9 to 7.7 and 18.5 to 13 m/s. The higher values are close to the observed values. There are issues on bird geometry, aerodynamics and metabolism that are being studied even as of now (see Pennicuick, 2008). Broadly, higher wing loading implies higher speed of flight.

The aircraft, Daedalus is an experimental aircraft built at MIT to test the limits of human powered aircraft. The performance of this is exemplary and obtained at considerable cost. This followed Gossamer Candor and several other experiments documented well by Roper (Intnet2, 2012). Hang gliders that are used largely for adventure sports have ideas that involve having a shaped thin wing and using height and wind condition with which any individual can run and get into air, maneuver to stay in the air by using the currents as long as atmospheric conditions permit. Civil aircraft presented here are long distance airliners. Their design is aimed at allowing the fastest movement of people with affordable cost. The prime driver here is the cost of the fuel. Given the externalities governing the cost of the fuel, aviation turbine fuel (ATF), the control that is available to the industry is one of improving the design of the engine to burn less fuel for the same power/thrust. This effort of improving the specific fuel consumption is compounded by the need to reduce the emissions of CO and unburnt hydrocarbons, that too with slow but continuous movement of the composition of kerosene towards lower H:C ratio. The primary characteristic common to all the above air vehicles is to obtain as a large a L/D as possible (subject to other constraints) so that one can minimise the demand of propul
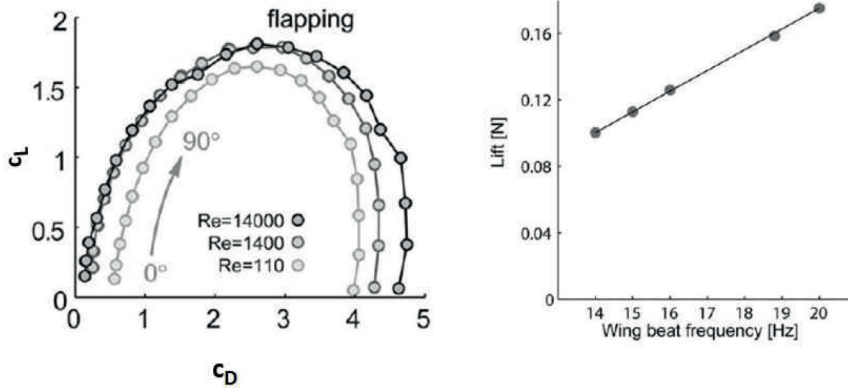
Figure 2.17.: Aerodynamic characteristics of RoboFly - c_L vs. c_D with amplitude variation up to 90^0 (left) and Lift vs. flapping frequency, ω (right)

Table 2.1.: Geometric and performance parameters of selected flight systems - 1, V = cruise speed or nominal speed, * for military aircraft, the performance data depend on operational conditions; E-4 = 10^{-4}

Flying Object	W	A_w m^2	W/A_w N/m^2	b m	AR -	L/D -	V m/s	Alt km	M -	Range km
Birds										
Diptera	2.5mN	2E-4	12	0.03	6		4	0.1	0.01	1
Arctic tern	1.2 N	0.06	20	0.8	11	14	11	0.1	0.03	40000
Albatross	85 N	0.62	140	3.4	19	25	19	0.5	0.08	10000
Human powered aircraft and Glider										
Daedalus	1 kN	30	33	34	37	38	7	0.01	0.11	30
Hang glider	1 kN	15	67	10	7	8	8	1.0	0.02	200
Civil aircraft										
Boeing 737	0.85 MN	125	6800	35	10	15	230	9.0	0.83	3000
Boeing 777	3.5 MN	435	8050	65	10	20	240	10.0	0.85	12000
Boeing 747	4.0 MN	524	7630	80	8.1	16	240	11.0	0.87	8000
AB A380	5.6 MN	845	6630	80	7.5	16	240	10.0	0.87	12000
Military aircraft										
F 16*	0.17 MN	27	6300	9.8	3.5		420	15.0	2.0	3900
LCA-Tejas*	0.13 MN	38.4	3390	8.2	1.8		390	15.0	1.8	3000
B 52*	2.2 MN	372	5910	56.4	8.6	16	245	16.0	0.86	16000
Sukhoi30MKI*	0.39 MN	62.0	6290	14.7	3.5		410	17.0	2.0	3000

sive force (thrust). This will inevitably reduce the fuel required on a per km basis. Passenger aircraft manage to achieve 50 to 70 g fuel per passenger-km of flight (3.5 to 5 kg fuel per km of flight distance). The demand for high speed combined with minimizing the drag with best practical design limits the maximum speed to about 0.86 of that of sound. At this speed, the only appropriate way is to fly at a height that balances the weight of the aircraft at the maximum speed possible (such that Mach number at the altitude is 0.85 to 0.86).

We first recognize that the distribution of the atmospheric pressure and temperature with altitude is such that temperature drops till tropopause (at around 10 km altitude) and remains constant beyond this altitude (see Chapter 1, section 1.1.1). Noting that $\rho V^2 = 2(W/A_w)(1/c_L)$ can be recast by recognizing that the $M = V/a$, where a is the local acoustic speed given by $a = \sqrt{\gamma RT}$ where the terms under the square root are the ratio of specific heats, the gas constant and the local static temperature respectively as $\gamma p M^2 = 2(W/A_w)(1/c_L)$ where p is the atmospheric pressure. The wing loading for most long range aircraft is between 6500 to 7000 N/m². The atmospheric pressure becomes $p = 13000$ to $14000/(c_L M^2)$(Pa). At a Mach number of 0.85 to 0.87, the static pressure becomes p = 17000 to $18000/c_L$. With typical value of c_L of 0.6, $p = 28$ to 30 kPa. This corresponds to 9 to 10 km, the typical altitude at which transport aircraft fly. Of course, in a long distance flight other issues crop up: variation of the weight of the aircraft due to fuel consumption, vertical and horizontal separation distances between flying aircraft due to safety reasons, and recommendation to avoid certain corridors due to clear air turbulence. All these require that the aircraft be flown at altitudes even up to 12 km over certain distances. These are managed by changing the c_L, increase of which will enable achieving higher altitudes at the same speed.

Military aircraft have evolved significantly and in an enormous variety for army, navy and air force segments of the defence services. Many a time, technological interventions are made first for these applications and these enter directly or in a moderated or modulated form into the civilian sector. The design of the vehicle depends on the mission - bombing, interdiction, ground attack, day and night strike, deep penetration, reconnaissance, refuelling, evacuation and transportation, and fighter escort missions. While some of the missions are fulfilled by design choices not different from civil aircraft, others require

Table 2.2.: Geometric and performance parameters of selected flight systems - 2, P = Power, F_{sl} = Thrust sea level

Bird or Aircraft	P	V m/s	V_{opt} m/s	F_{sl} MN	W/P N/W,	W/F -	Fuel rate
			Birds				
Arctic tern	1 W	11	7 - 9	2.7	1	L/D	0.1 g/h
Albatross	64 W	19	16 - 19	1.2	1.4	L/D	6.4 g/h
		Human powered aircraft and Glider					
Daedalus	180 W	7	10.5	-	5.5	L/D	19 g/h
Hang glider	-	8	-		-	L/D	-
	Civil aircraft, + = *at 10 km altitude; fuel rate at 10 km alt.*						
336 MW 737	57 MW	230+	238	0.25		3.4	2.5 t/h
Boeing 777	240 MW	240+	259	1.0		3.5	5.5 t/h
Boeing 747	240 MW	240+	252	1.0		4.0	8 t/h
AB A380	336 MW	240+	235	1.4		4.0	8 t/h
	Military aircraft,ᵃ= *Max. Speed at 12 km alt, * = with afterburner*						
F 16		420a		0.08/0.13*		2.1/1.3	3 t/h
LCA-Tejas		390a		0.05/0.09*		2.6/1.5	2 t/h
B 52		245a		0.61		3.6	10 t/h
Sukhoi 30MKI		410a		0.07/0.12*		5.6/3.3	3 t/h

that the aircraft be looked at very differently. These involve short action times, maneuverability and avoidance of missile hit by the choice of mission profile (like flying low on the order of 100 m and flying very high of the order of 15 km at high speeds) or by stealth features.

A single point optimization like cruise with civil aircraft will not be possible.

While fuel consumption optimization or first cost is kept in mind, they will not be the guiding criteria in the design. Due to these considerations, many designs have emerged from Russia, USA, France, Germany and United Kingdom over the last five decades. Table 2.1 gives a sample of four aircraft. Of these B 52 is a bomber with the largest endurance - 36 hours and very large range both of which are accomplished because of mid-air refuelling. Other strike aircraft - F16, LCA-Tejas and Sukhoi have maximum achievable Mach numbers of around 2, altitudes of 15 to 17 km. Achieving high speeds at the wing loading that they have (4 to 6.5 kN/m²) demands low AR due to structural considerations; the wing shape is changed from swept back to delta shape. This leads to

lower L/D and hence the need for higher thrust engines; the demand for even higher thrust is justified due to expectations of high maneuverability - high climb rate, turn rate, and acceleration, features typical of military aircraft. The range of these aircraft is modulated by allowing for in-flight refuelling. One of the ways of combining good low speed performance with that at high speed is to have variable geometry of the wing. This enables the aspect ratio to be kept at high value at low speed and reduce it at high speed. It is a challenge to mechanical engineering to design this system to operate reliably with minimal weight penalties. This class of aircraft has been built by a few countries: Russia has six types, USA two and Europe one. They are not favored these days because the weight penalties associated with variable geometry are considered too severe for the promised performance. Table 2.2 presents information on propulsion-related aspects of the systems described in Table 2.1.

Based on extensive measurements on the consumption of oxygen by birds in wind tunnels and other aspects of bird metabolism (Tennekes, 2005; Pennicuick, 2008), it is known that birds generate a power of about 100 W/kg of muscles that constitute about 20% of the bird mass. This implies that the power output is about 2 W/N of body weight. For arctic tern and albatross, the power available will be 2.4 W and 170 W, and with the L/D of 14 and 25 for these birds, the drag force is 0.09 N and 3.4 N respectively. These correspond to power needed for steady flight of 11 and 19 m/s for both the birds equal to drag × steady speed as 1 and 64 W in Table 2.2. Thus, birds have an excess power ratio of about 2 - 3 that can be used for climbing and dash to escape from predators. The maximum power from human beings is about 500 W and a steady value of 200 W for well trained professionals. Daedalus was piloted by a professional who trained specially for this purpose.

To estimate the power/thrust and fuel consumption of aircraft, we depend on the data of the engines used to power these aircraft. For estimating the "fuel consumption" of birds we need to get information on the metabolic rates of the birds and the energies involved. The unit energy (also called calorific value) is 39 MJ/kg for fats and vegetable oils, 14 MJ/kg for sugar and honey (42 MJ/kg for kerosene used in aircraft). Since the energy of fat is very much larger than for sugar, nature's design for long distance flight is around fat. For power levels of 1 and 64 W, taking the efficiency of conversion of "fuel" to mechanical energy
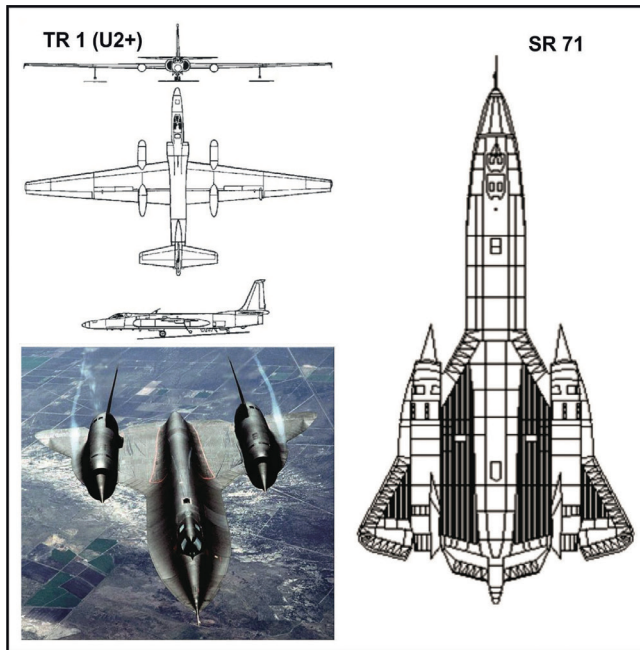
Figure 2.18.: Top left: TR1 is a variant of U2 reconnaissance aircraft; Bottom left and right: SR71 USA built aircraft. It established many records for altitude and speed not broken till now

of 10 %, the fuel consumption at 39 MJ/kg will be about 1 and 60 g/h. In a 10 hour flight, the consumption will be 10 and 600 g for covering 360 km and 630 km for Arctic tern and Albatross respectively. The amount consumed forms a significant part of the available fuel inside the body.

These migratory birds show extraordinary abilities in terms of non-stop range and a few others do look for stop-overs in between, on the passing ships or a calm sea looking for food (the equivalent of refuelling for aircraft).

Civil aircraft show flight power of the order of 100's of MWs as obtained from the product of thrust (at altitude) and speed. The optimum speed for flight is not vastly different from the actual speed. Considering the fact that aircraft move inside the atmosphere with tail and head winds of 20 to 100 km/h in specific sectors in different seasons and so the ground speeds will accordingly vary, the actual speeds at which the aircraft fly can be taken to be close to the optimum values. The thrust per unit weight is about 25 % for most civil air cr-

aft. Since military aircraft need maneuverability, they have a power plant with much higher thrust capability. Two special aircraft are now described to indicate the realization of the range in thinking on the concepts use for building actual aircraft. The aircraft considered are U2 and SR71 presented in Figure 2.18. U2 is a single seater reconnaissance aircraft flying subsonic (M = 0.58, 210 m/s) at more than 21 km altitude has a high AR (10.6) and relatively low wing loading (1900 N/m²) and is powered by a 85 kN turbofan and stays in the air for at least 6 hours with a range of over 4500 km. To optimize on the amount of fuel and active payload to be taken on board, the standard landing gear was sacrificed in favor of *a simpler design of single main landing gear and a small caster like wheel at the rear section both located on the fuselage center line*. Due to these reasons, landing was indeed difficult so that the ground crew was needed to chase in a car behind the aircraft to guide the pilot to a safe landing. Wing tips were fitted with titanium skid plates to avoid wing damages in case of the aircraft rolls to on one side. As soon as the aircraft is brought to halt after landing, wing supports called "POGOs" were hooked to the aircraft at the runway for safe taxiing. These supports remained on the aircraft during take-off run and were dropped at end of the runway before wheels left the ground (collected back by the ground crew later). The most remarkable feature is that this aircraft in its later versions (TR-1A is a later version - TR stands for technical reconnaissance) is still in service after nearly 55 years of service. Built by the famed "Kelly" Johnson in Lockheed Skunk works, one humorous story is of a U-2 pilot calling Air Traffic Control and requesting Flt. level 700 (meaning 70000 ft or 21.3 km). The Controller is supposed to have asked: "and what makes you think you can get up to 70,000?" The pilot reply was: "Oh, I don't want to go up to 70,000...I want to come down to 70,000!"

The two seater reconnaissance aircraft, SR71 overcame the low speed issue of U2 that caused the soviet missile hit to one of the flights piloted by Gary Powers (Internet3, 2012). The idea of SR 71 was to fly high and at very high speeds to overrun any missile terminal speed at that time. This was achieved by flying in the stratosphere at an altitude of over 25 km at a maximum M = 3.3 (900 m/s). This aircraft built of 93 % titanium in the early nineteen sixties was one of the most outstanding one built in early military aeronautical development times with little computational support that the designers of aircraft receive these days. The design of this aircraft was also spearheaded by Kelly

Johnson. With a total weight of 0.78 MN, a wing loading of 4.6 kN/m², a delta wing with $AR = 1.7$ powered by 2 engines with a total thrust of 0.3 MN, the design integrated ideas of stealth in aerodynamics and turbojet-ramjet ideas in the engine.

The stagnation temperatures at M = 3.3 would be as high as 430°C and the entire aircraft parts had to withstand these conditions in a steady mode. The inboard parts of the wing were corrugated since it was noticed that a smooth skin would distort due to large traverses in temperature. The corrugations helped changes in specific way that allowed increase the strength. The fuselage panels fitted loosely at near ambient temperature and sealed only at high speeds. The inner regions needed to be cooled because temperatures would reach 200°C. This was achieved by using the liquid fuel, JP7 as the coolant. This would lead to heating the fuel that was difficult to ignite at ambient conditions - a double benefit.

The stagnation pressure achieved at the highest speed is between 10 to 12 atm. The flow that gets into the air intake is at a pressure that would have been delivered by the compressor of the engine. As such, under these conditions, further compression is redundant. This implies that the turbojet becomes redundant and the propulsion system can operate in the ramjet mode. Thus, the propulsion system operated largely in turbojet mode at low speeds and as a ramjet at high speeds. In order to provide appropriate flow rate with as much of a stagnation pressure recovery as possible, the air was processed through a special intake that allows for variable geometry.

Stealth was expected to be provided by the use of "chines", a hemispherical horizontal sharp-edged surface to help reflect the electromagnetic waves. This aspect was not greatly effective to stealth since the aircraft was huge and its radar signature was not small despite these artifacts. On the other hand, it was discovered that the chines generated vortices that created additional lift leading to unanticipated aerodynamic performance improvements. The angle of incidence of the delta wings could then be reduced for greater stability and less drag at high speeds; more weight, such as fuel, could be carried to increase range. Landing speeds were also reduced, since the vortices from chines created turbulent flow over the wings at high angles of attack, postponing wing stall. However, high-alpha turns were limited by the internal airflow dynamics leading to flame out in the engine.

Most historical and technical aspects of the project have been documented (Internet, 2012). One feature not connected to the subject dealt with later concerns navigation. Navigation uses fixed stars to provide the location (we must remember that those were the days before the invention of the global positioning system, GPS). Also other aspects of ground photography and information record were the state-of-the-art at that time. Some of these became outmoded later and led finally to the closure of this project.

Amongst concepts that have been tried out is the variable sweep based wing. Some eight different aircraft were built by Russia, USA and Europe. While variable sweep has indeed many advantages, particularly in terms of shortened takeoff distance, load-carrying ability, and the fast, low-level penetration role, the penalty in weight and complexity imposed by the configuration made it unattract with the advent of relaxed stability flight control systems in the 1970s. No new variable-sweep wing aircraft have been built in the last twenty years and those which were in operation (like MiG 23 in India and several other countries) have been phased out.

2.6. Compressible Flow c_L and c_D

Compressibility correction to lift coefficient by Prandtl and Glauret gives

$$c_L = \frac{c_{L,incomp}}{\sqrt{(1 - M^2)}}$$

$$(2.14)$$

The above relationship assumes that the c_L - α relationship is linear, a feature that is true at moderate angles of attack. For supersonic flows, a simple theory gives for all $M > 1/cos\Lambda_{le}$, where Λ_{le} is the leading edge sweep angle,

$$c_L = \frac{4\alpha}{\sqrt{(M^2 - 1)}}$$

$$(2.15)$$

Subsonic and supersonic lift relations do not hold good at $M = 1$. This is a reflection of the fact that the behavior is vastly different from the assumptions made in the theory. The equations for the transonic regime have singularities that need to be dealt with specially. Further, in practice, there is considerable flow unsteadiness due to viscous effects like shock-boundary layer interaction

leading to separation that the efforts at making any simpler deductions inappropriate.

The drag coefficient has three components – the profile and viscous drag as well as wave drag. The subsonic regime is composed of the first two components. The drag coefficient associated with these two components is termed as parasite drag coefficient and remains about the same up to a critical Mach number defined as a free stream Mach number at which sonic condition is reached at some point on the airfoil. This usually happens at the maximum thickness point. Another quantity that is defined is called drag divergence Mach number. This Mach number is the value at which the drag coefficient is larger than the incompressible value by 2 points (that is 0.002).

The wave drag component begins its influence just beyond the drag divergence Mach number through supersonic flow conditions. Wave drag for two-dimensional configurations can be obtained by calculating the changes in the flow parameters over surfaces when they change directions. If one considers for simplicity a two-dimensional geometry, a sharp edged wedge at a positive angle of attack will have expansion waves on the top of the wing and shock wave over the bottom edge. This leads to the pressure in the bottom region being much larger thain the top region. Since the pressure acts normal to surface, the components of the force in directions along and normal to the stream direction give the lift and the drag.

In so far as aircraft drag is concerned, theoretical analyses and wind tunnel tests have shown that at supersonic speeds, slender, pointed bodies whose cross-sectional area varies smoothly along the fuselage with a possible peak area around the middle region has minimum wave drag for its size. These low wave drag shapes need one that reduces the fuselage cross section at the wing interface in such a manner that the cross sectional area does not have sharp changes. This has been known as *the area rule*.

The magnitude of the wave drag for these bodies varies as

$$c_{D,max} = \frac{4.5\pi}{A_w}[\frac{A_{max}}{l}]^2(0.74 + 0.37\cos\Lambda_{LE})\left[1 - 3\sqrt{(M - M_{c_Dmax})}\right]$$ (2.16)

where c_D, max is the drag coefficient A_w is the wing area, A_{max} is the maximum cross sectional area, l is the overall length and $Mc_{Dmax} = 1/\cos\Lambda_{LE}^{0.2}$. Figure 2.19
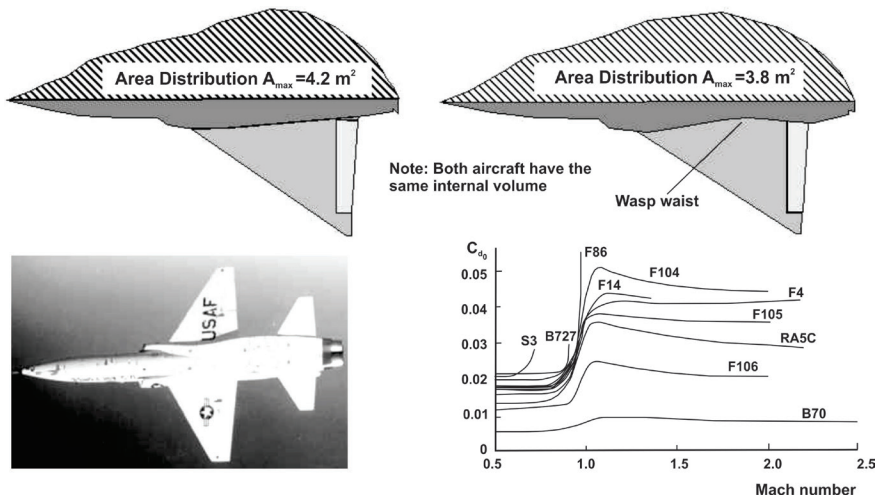
Figure 2.19.: The shapes of wings for supersonic aircraft designed with area rule; bottom left: The shape of cross section of an actual aircraft; bottom right: c_c with flight Mach number

presents two shapes of equal volume with one shaped such that the cross sectional area follows the area rule. The shape of the reduced fuselage section around the central area is indicative of the use of area ruling. The actual values of the drag coefficient are presented as a function of Mach number for a number of aircraft. The incompressible drag coefficient itself varies widely from 0.006 to 0.022. achieving values close to 0.006 requires considerable effort in making the surfaces smooth. Larger values result from missiles, bombs and other military equipment beneath the wings. The drag coefficient remains about the same till M about 0.8 to 0.85 and rises to larger values in the transonic regime and then drops off. The aerodynamic center moves back significantly as Mach number approaches 1; in the supersonic range it approaches $0.5\ \bar{c}$ from the incompressible value of $0.25\ \bar{c}$. The unsteadiness of the flow in the transonic regime causes downstream effects on tail plane that affect the stability. These are discussed in Chapter 5.

2.7. Other Aerodynamic Aspects

The basic aerodynamics of the wing depends on the geometric parameters: thickness variation over the chord, camber distribution, sweep, taper and twist,

dihedral or anhedral or the use of a canard wing. In addition, every aircraft has to have aerodynamic control surfaces. In most aircraft, these are elevator, aileron, and rudder for pitch, roll and yaw. There are also control surfaces like flaps, spoilers and slats for help in take-off and landing with drag chutes being added for some military aircraft. Winglets and riblets are also used for improving the aerodynamic performance.

In order to operate these surfaces, control lines are drawn to the cockpit to enable the pilot to execute suitable controls. In the early aircraft, the pilot had to be "strong" to provide the forces required for the movement of the control surfaces. It was then uncovered that geometric changes can be made at hinge or other locations to reduce the force exerted. These are called trim tabs. The control of these is brought into the cockpit. Many a time, making small changes in the trim tab may be adequate to bring the aircraft to the required balance. Over years, when developments in electronics, electrical and hydraulic devices became available, the force required to move the control surfaces was dealt with by hydraulic or electric or electro-hydraulic drives with the pilot having just to get the lever to the appropriate level. However, in order that the pilot has a feel of the magnitude of force caused, pilot-feel devices were introduced. Computerised data management and control became also a development in this period.

The function of many of the control surfaces *depends on the altitude and flight Mach number*. They have influence on equilibrium, stability, climb, turn, acceleration performance of the aircraft. In the following are detailed the features related to the aspects discussed above.

2.7.1. Wing geometric features

Figure 2.20 shows the variety of shapes used in aircraft. As presented earlier, the wing plan form changes its shape as speed increases from near-rectangular, untapered or tapered through sweep back into delta shape. On the third row are the canard wing shapes. Canard is a small wing ahead of the main wing. Its primary role is to provide a broader stall behavior. Stall, when it occurs will happen on the Canard wing. The main wing design coupled with the canard wing is performed such that the smaller area effect will minimise the effect of stall. There are other effects of the canard wing on the stability of the aircraft and these need to be accounted for. The canard wing can be used with the ma-
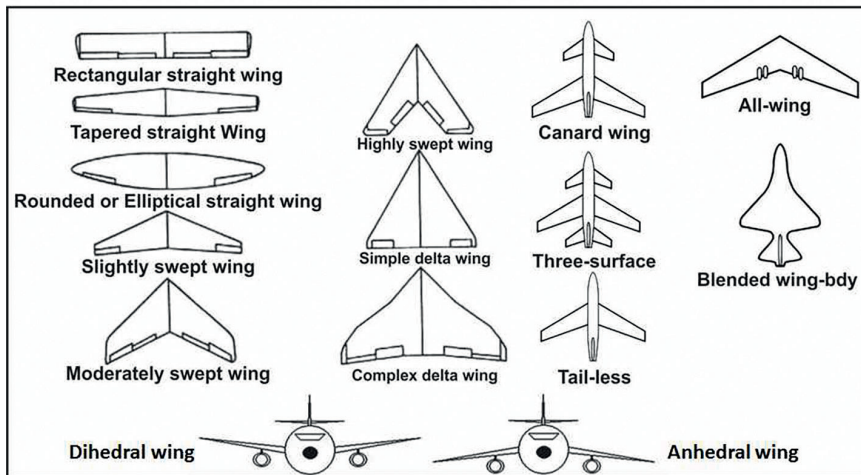
Figure 2.20.: The shapes of wings - from rectangular to tapered to sweep back to delta shapes as speed increases. Two-wing and three wing shapes are also termed Canard wings - the small wing in front is the canard. Tail-less wing plan form and Wing-fuselage inte-grated shapes are used in military aircraft; dihedral and anhedral wing forms in the lateral direction, drawn from open internet sources.

in wing and a tail plane so that it becomes a three-wing configuration. As different from all these, one can have an all-wing configuration as shown on the top right in Figure 2.20 and a wing-fuselage integrated configuration below that. In the bottom two figures, the dihedral and anhedral geometries of the wings are shown. Dihedral provides weathercock lateral stability and anhedral arrangement that is most suitable in high wing configuration (wing located towards the top of the fuselage).

It must be understood that any change in the wing geometry in some regions, even small ones can have a major effect on other aspects of the performance. Consequently, it is important that any contemplated change be evaluated for all its aerodynamic influences on the performance.

In respect of space vehicles discussed in Chapter 1, space shuttle has aircraft-like features that enable it to land like a glider. The orbiter has double-delta wings swept back 81^0 at the inner leading edge and 45^0 at the outer leading edge. The leading edge of its vertical stabilizer is swept back at 50^0 angle. The four elevons (elevator + ailerons) mounted at the trailing edge of

the wings, and the rudder/speed brake attached at the trailing edge of the stabilizer, with the body flap controlled the orbiter during descent and landing.

High lift devices

It is perhaps useful to understand why one needs high lift devices in an aircraft. It is to be noted first that every aircraft should be able to take-off and land. It is expected that the aircraft takes off (or lands) at as low a speed as possible and accelerate suitably to the appropriate cruise or operational altitude at the appropriate speed. If the aircraft has to take-off, the lift force must exceed the weight of the aircraft. This implies that

$$(1/2)\rho V^2 c_L A_w > W \ \text{ leading to } \ V_{to} > \sqrt{(W/A_w)(2/\rho)(1/c_L)} \quad (2.17)$$

Since W/A_w is fixed, the ambient density and c_L control the take-off speed. It is useful to compare the take off (or landing) conditions to steady cruise conditions. We can take that the wing loading remains the same to get

$$V_{to} \sim V_{crs}\sqrt{\frac{\rho_{crs}}{\rho_{to}}\frac{c_{L,crs}}{c_{L,to}}}$$

$$(2.18)$$

where the subscripts *crs* and *to* refer to cruise and take off conditions. For typical values of V_{to} = 60 m/s, V_{crs} = 240 m/s, ρ_{crs} = 0.4 kg/m³, ρ_{to} = 1.2 kg/m³, we get $c_{L,crs}/c_{L,to}$ = 0.19. For $c_{L,crs}$ = 0.6, the needed $c_{L,to}$ = 3.2. The maximum value of c_L that the wing shape meant for cruise can give is less than 1.2 and even that at high angles of attack, unacceptable in any passenger aircraft. Therefore, one needs to change the geometry to obtain large values of c_L at take-off. This is done by any of the devices described in Figure 2.21. It should be noted that there are several options for enhancing the lift coefficient. Devices like slat and flap are arranged such that both the wing camber and area are altered; the local pressures on the top surface become much lower than in a cruising flight. Slat is a device on the leading edge and flap near the trailing edge. In addition, active flow arrangements like suction and blowing are also practiced. As should be noted from Figure 2.21, c_L value as high level as 3.6 seems possible. It is also to be noted that the effective wing area also increases significantly (by as much as 20 %) and the actual demand for c_L may be only up to 2.6. This is accomplished by double slotted flap or with slat and this configuration is widely adopted.
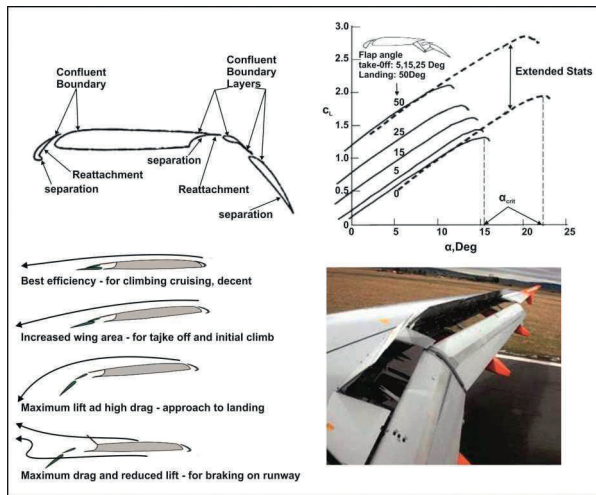
Figure 2.22.: Top left: Relative locations of the high lift devices with important fluid flow behavior; Top right: Variation of c_L with angle of attack; Bottom left: the flow behavior in different conditions of flap and slat; Bottom right: the aircraft wing after landing, with flaps and spoiler on

Figure 2.22 shows several aspects related to high lift devices. The way in which slat and the multi-element flaps are located on the airfoil shape are shown at the top left. The variation of c_L with angle of attack, α is shown at the top right. Enhanced c_L with the same level of $dc_L/d\alpha$ and a larger stall angle of attack are the result. The way fluid flow behaves when it passes over the modified wing surface at various conditions is shown at the left bottom. The bottom-most figure shows the case where the full flap and a "spoiler" are deployed. Spoiler is a surface which faces the oncoming flow on the top of the wing surface causing such a disruption to the flow that the lift comes down significantly when it is operated. This happens always at landing condition.

Just at the point of touch down, it is necessary to eliminate the residual lift to cause the aircraft to be on the ground and rolling. The spoiler continues to be in position till the speed of the aircraft is brought down significantly for brakes to be applied to reach the taxiing speed level. The figure on the bottom right shows the section of an aircraft on the runway with both flaps and spoilers in the "On" position.

Winglets

It has been brought out that three dimensional wing shapes have the problem of wing tip vortices leading to reduction in lift coefficient. To reduce the influ-
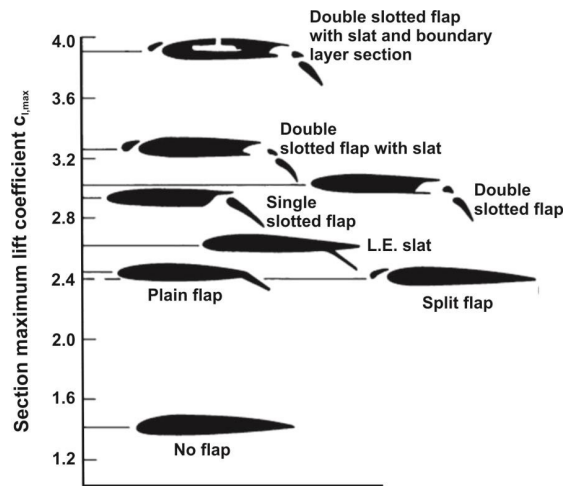
Figure 2.21.: Options for high lift devices. From bottom up: 1. No flap, 2. Plain flap, 3. Split flap with leading edge slat (L.E slat) 4. non-slotted flap, 5. Single slotted flap, 6. Double-slotted flap, 7. Double-slotted flap with slat and 8. Double-slotted flap with slat and boundary layer suction; the right part of the figure shows the possible lift coeff cients attainable with these devices, composed from open internet sources and Bertin and Cummings, 2013, Torenbeek and Wittenberg, 2009

ence of the wing tip vortices, wing tip management is done so that the intensity of these vortices comes down. The use of the wing tip management device called "winglet" has other concomitant issues - slightly enhanced drag, some positive and not-so positive influences on stability. It is brought into picture towards the late stage of development in many instances. There are several types of winglet designs in practice. These are shown in Figure 2.23.

Trim tabs

Trim tabs (see Figure 2.24) are devices that are located on major control surfaces like elevator or fin to enable small corrections to the position can be performed. These are so located that their center of gravity matches with the hinge and hence the loads required to deflect them will be small, their location towards the aft end provides sufficient moment around the elevator hinge to cause the motion by small deflections. They are particularly useful when the aircraft has reached the cruise altitude and has to perform a long steady flight. The parameters are adjusted so that small changes that the aircraft experiences due to fuel consumption or gusts can be taken care with the use of the trim tabs.
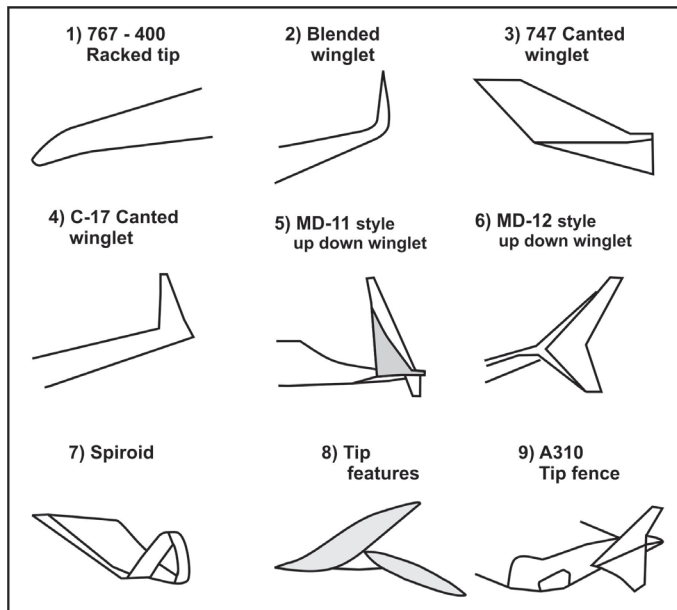
Figure 2.23.: Winglet designs on different aircraft

2.8. Role of Computational Fluid Dynamics (CFD)

The basic idea of CFD is that one solves the fundamental equations of motion, which for fluids are termed Navier-Stokes equations. These equations represent the conservation of mass, momentum, energy and species mass fractions. The solution of these equations along with appropriate boundary conditions and initial conditions (in case of unsteady flow) provides the description of the flow field for all quantities - pressure, density, temperature, velocity and species mass fractions. For laminar flows, the solution of these equations provides an accurate result for the flow.

For turbulent flows that are more practically relevant, there are several approaches. If the equations in primitive variables, ρ, p, V, T, Yi (where these are density, pressure, the velocity vector, temperature and mass fractions) are split into steady and a fluctuating parts. Averaging the equations over time, one gets a set of equations for the average quantities called Reynolds averaged
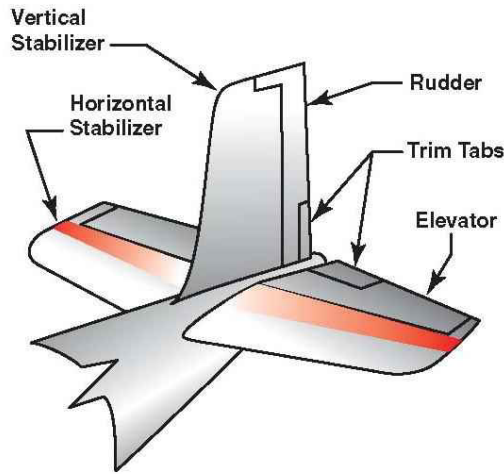
Figure 2.24.: Trim tabs on the tail section of an aircraft

Navier-Stokes equations (RANS equations) that contain terms that are the averages of products of fluctuations that are not known *apriori*. These need modeling. The models vary from zero-equation, one-equation, and two-equation models and even in two equation models there are variations depending on whether one solves turbulent kinetic energy and dissipation (the famous k-ε model) or turbulent kinetic energy - vorticity (k - ω model) or several others. In compressible flows, the averaging is performed in density weighted variables and these averaged equations are called Favre-averaged equations.

There are several methods of discretizing these equations like the classical finite difference method and the most common method is called the finite volume method. In this method, volume integrals of a partial differential equation that contain divergence terms are converted to surface integrals using the divergence theorem. These terms are then evaluated as fluxes at the surfaces of each finite volume with scalars like pressure, temperature and species concentrations at the center of the volume. Since the flux balance is maintained across the adjacent surfaces these methods are conservative. Another advantage of the finite volume method is that it is easily formulated to allow for unstructured meshes somewhat like the finite element method used widely in structural mechanics. Several commercial codes have been made available in

the last two decades with continuous software upgrading with newer models to deal with turbulence and other yet-to-be-modeled phenomena. Technical support has added to greater responsible use in education and design teams in the last fifteen years.

In the nineteen fifties and sixties, design of flight vehicles was performed using large amount of testing, analysis with simple correlations, and intuitive understanding of the flow behavior. These approaches were indeed successful. While experiments on scaled models and in some instances full scale models were helpful in achieving the objectives, the time scales were large and the cost was significant (can even be termed prohibitive from current approaches of design and realization). Computational approaches to understand the fluid behavior were developed in the late sixties with accompanying advances in computers that have scaled down the computational time and scaled up the problem size by a factor of hundred thousand! While the early calculations with low order algorithms, approximate models for turbulence, and crude grids were considered a significant breakthrough that presentations were largely composed of colored contours of the flow field. These were humorously referred to as colorful dynamics presentations. It was indeed difficult to develop confidence in the results of calculations. Slowly, but surely, algorithms were refined, models of Reynolds averaged Navier-Stokes (RANS) calculations with zero-equation, one-equation and two-equation models with finite volume approach to discretization and adoption of fine grid resolution led to results that could be relied upon.

In fact, a critical comparison of results of computations with experimental results showed on occasions anomalies in experimental results needing review of the experimental approach and harmonization of the results with computational results. The maturity of CFD has been so high that calculations are performed at several levels to clarify the flow features and select calculations are made on the full scale geometry. This approach has resulted in reduced testing and an overall reduction of the time between conceptualization and realization of a new vehicle or a subsystem. An important point to note is that all advanced developments have the basis of earlier developments and the knowledge base. As such, any new development is looked upon as an incremental effort and gets completed with much reduced time and cost.

A remarkable outreach of CFD in recent times concerns the faith of fighter pilots in CFD. In a defense laboratory where the tests of a missile launch from a military aircraft were contemplated, the strategy for conducting these with aircraft safety in mind was discussed. There were programmatic time considerations for carrying out the development tests. After much consideration, CFD was thought of as an alternative to raise the confidence of the pilots before the conduct of the flight test. Many simulations of the launch process and the relative movement of the missile vis-a-vis aircraft-in-flight were performed and discussed with the team in which final decision was left to the pilots. It was clearly noted that pilots had to depend on no other supporting evidence for safe operations except those obtained from CFD. They agreed to fly with the evidence from CFD and associated physics based justification; indeed flights were carried out successfully and the match between the flight information and the results from CFD was considered excellent. This incident helped to raise the trust in this tool for a large community of scientists.

From mid nineties, the focus of interest in CFD related activity has shifted to solving complex engineering problems through the use of parallel machines. The measure of speed is the achievement of sustained floating point operations per second (FLOPS). Current value of computational speed is about 100 peta flops at this time (2016) (100×10^{15} flops) where as it was 100 GFLOPS (100×10^{9} flops) in 1990!

2.9. Summary

This chapter is concerned with the aerodynamic principles that govern the design of flight vehicles from very low speed to very high speeds - from incompressible flow to hypersonic flows covering a Mach number range of 0 to 30. Viscosity creates conditions for forces to be developed on bodies with the lift nearly independent of viscous influence (high Reynolds numbers) but drag strongly dependent on it. Flight Mach number (M) less than about 0.3 covering a large range of low atmospheric flights can be treated as incompressible. Three aspects of importance connected to aerodynamics are the center of pressure, aerodynamic center and neutral point. Center of pressure of a wing or an aircraft is the point where the lift acts. Aerodynamic center is the point in the wing where the pitching moment of the wing does not vary with angle of attack. Neutral point it the location of center of gravity where the aircraft is neutrally stable.

Compressibility effects need corrections to lift and drag coefficients that appear in the form of $\sqrt{(1 - M^2)}$ and so, these become important only at higher subsonic speeds. Significant departures occur at M close to 1. An important parameter called critical Mach number that signifies the attainment of sonic condition at the maximum thickness point. An associated engineering parameter is the drag divergence Mach number which signifies increase in drag by a small amount (0.002). The flight in the transonic regime (M between 0.9 to 1.1) is beset with unsteadiness because the appearance of shocks over part of the wing body causes separated flows due to shock-boundary layer interaction. Flow becomes steady soon after the transonic regime is crossed. Supersonic flight regime is characterized by shock waves across which sharp changes in fluid flow parameters occur. Even though the lift generation process is due to pressure differences between the top and the bottom of an airfoil, the mechanisms responsible for this pressure difference are different in subsonic and supersonic regimes. In the subsonic regime, the pressure distribution governed by the condition that allows the flow to smoothly exit from the trailing edge leads to the lift and drag forces. It is the shock waves (caused by the coalescing of non-linear propagation acoustic waves) that is predominantly responsible for the forces in the supersonic regime.

Increase in speeds beyond Mach number of 5 qualifies for hypersonic flows. Here, unlike subsonic and supersonic flows where viscosity affects lift aerodynamics very weakly, it causes first order differences to hypersonic lift aerodynamics.

The commonality between bird aerodynamics and flight vehicles has two principal features - birds like hummingbirds are similar to helicopters and seagulls, albatrosses and arctic tern are similar to cruising wing based vehicles. The data of the flying characteristics of many insects and birds have been examined on the basis of principles of aerodynamics. Aerodynamic principles have been exploited to build aircraft of extraordinary and sometimes extreme capabilities. U2 and SR71 are identified as examples of the excellence in designs, as are F117 or F22.

Excellence in aerodynamics meant for economic "high speed" air transport implies flying at a speed close to but lower than the sonic speed ($M = 0.85$ to 0.87) and optimizing the airfoil to obtain as high an L/D as possible and deploy a swept wing shape on occasions using wing tip arrangement to reduce the lift induced drag. Such designs carry 250, 500, 800 people in a single aircraft,

2000, 5000, 10000 km across the globe with extremely high reliability. This performance using modern science and technology has far exceeded bird flights on many performance indices, notwithstanding a variety of spectacular flight capabilities of the avian species.

Bibliography

[1]   Anderson, J. D (1984) Fundamentals of Aerodynamics, McGraw-Hill Book Co.

[2]   Anderson, J. D (2006) Hypersonic and high temperature gas dynamics, second edition, AIAA Education series.

[3]   Anderson, D. F and Eberhardt, S (2010) Understanding flight, second edition, McGraw-Hill Book Co.

[4]   Bertin, J. J., and Cummings, R. M., 2013, Aerodynamics for engineers, 6th edition, Pearson-Prentice Hall publishers.

[5]   Dhawan, S., Bird flight, 1991, Sadhana, v. 16, pp. 275 - 352.

[6]   Dimitriadis, G, 2016 (accessed) http://www.ltas-aea.ulg.ac.be/cms/uploads/Aerodynamics01.pdf

[7]   Warrick, D. R., (2005) Tobalske, B.W. and Powers, D.R., Aerodynamics of the hovering hummingbird, Nature v. 435, pp. 1094-1097

[8]   Ellington, C. P., 1999, The novel aerodynamics of insect flight: applications to micro-air vehicles, J. Experimental Biology, v. 202, pp 3439 –3448,

[9]   Internet, 2012 http://www.globalsecurity.org/military/systems/aircraft/rotary-op.htm

[10] Internet2, 2012, Human powered flight http://www.humanpoweredflying.propdesigner.co.uk/

[11] Internet3, 2012, http://en.wikipedia.org/wiki/Lockheed_SR-71_Blackbird

[12] Lentink, D., Jongerius, S. R., Bradshaw, N. L., The scalable design of flapping micro-air vehicles inspired by insect flight, in Flying Insects and robots, D. Floreano et al (eds), Springer verlag, 2009

[13] Mason, W. H., 2016 (accessed) http://www.dept.aoe.vt.edu/ mason/Mason_f/HypersonicPres.pdf

[14] NASA, 2007, http://www.nasa.gov/mission_pages/galex/20070815/f.html

[16] Osborne (1951), Aerodynamics of flapping flight with application to insects, J. Experimental Biology, v. 28, p 221 - 245, http://www.ece.ucsb.edu/courses/ECE594/594D_W10Byl/papers/Osborne51.pdf

[17] Shyy, W., Lian, Y., Tang, J., Viieru, D., and Lio, H., (2008) Aerodynamics of Low Reynolds number fliers, Cambridge University Press

[18] Tennekes, H. (2009), The simple science of flight, from insects to jumbo-jets, The MIT Press

[19] Torenbeek, E and Wittenberg, H., (2009) Flight physics (essentials of aeronau-tical disciplines and technology with historical notes), Springer

[20] Wikipedia1 (2012) http://en.wikipedia.org/wiki/Atmospheric_entry; see also http://en.wikipedia.org/wiki/Space_Shuttle_thermal_protection_system

[21] Wikipedia2 (2016) https://en.wikipedia.org/wiki/GALEX; also see https://en.wikipedia.org/wiki/Bow_shocks_in_astrophysics

[15] Pennicuick, C. J., (2008), Modeling the flying bird, Academic Press.

3
Propulsion Systems

3.1. Introduction

Aerospace propulsion has been achieved by a range of propulsive devices based on several principles. In this book we are concerned largely with chemical propulsion. This implies that the energy for propulsion is derived from the energy in the bonds of chemical structure of species. There are other devices like electrical rockets, plasma jet, nuclear rockets which are relevant to space missions and are discussed very briefly towards the end.

The discussion is largely devoted to the principles involved, a description of the system elements, their performance and the relevant segments of applications. Discussion also includes the role of computational tools, called RCFD (Reacting Computational Fluid Dynamics) in the design and realization of these vehicles. RCFD differs from CFD discussed in the earlier chapter because of the need to account for the chemical heat release due to exothermic reactions between the fuel and oxidizer. In civil air propulsion, there is serious concern for emissions of incomplete products of combustion that can affect the near earth atmosphere with climate change effects.

The propulsion systems are composed of the following engines: reciprocating engines (or piston engines), gas turbines and their variants, solid and liquid fuel ramjets, solid, liquid and hybrid rocket engines as well as scramjets. The propulsive devices based on chemical energy evolved over the last century can be classified as shown in Table 3.1. In the first set, the air from the atmosphere is taken in and used as the oxidizer. In the second set, there is no restriction on the kind of chemical compounds that need to be used as an oxidizer. As such, solid or liquid oxidizers and fuels can be used. In the third set, the best elements of operation of both non-air breathing and air breathing engines are used to evolve efficient propulsion systems for specific applications.

Table 3.1.: The various propulsion systems

Airbreathing engines	Non-airbreathing engines	Hybrid engines
✻ Piston engine- Propeller	+ Liquid rockets	✻ Integral ram-rockets
✻ Turbojet	+ Solid rockets	✻ Ducted rockets
✻ Turbojet-Propeller	+ Hybrid rockets	✻ Air-turbo rockets
✻ Turbo fan		
✻ Pulse jet		
✻ Ramjet		
✻ Scramjet		

3.2. Fuels, Operating Conditions and Principles

All these engines work by a general principle, namely that a working fluid raised to high pressure and temperature expands through a turbine to generate power and/or expands through a convergent or convergent-divergent nozzle to generate a net force called thrust.

(a) In the case of air breathing engines, the pressure of air is raised first and heat added at high pressure through a combustion process with fuels (like kerosene). It is possible to expand the gases through the turbine nearly completely and deliver power in excess of what is needed for the compressor to a propeller to generate thrust. Alternately, the high pressure hot gases at the end of the turbine pass through a nozzle to generate thrust.

(b) In the case of solid rocket engines, a solid propellant composed of oxidizer and fuel elements stored in a chamber with suitable geometry is ignited to generate high pressure hot gases. The high pressure is maintained because of a throat (lowest cross section region) set in a convergent-divergent nozzle shape.

(b) In the case of liquid rocket engines, fuel and oxidizer (called propellants) are stored in tanks at moderate pressures and get pumped at high pressure into a chamber through injectors into fine sprays that are ignited to release hot gases. High pressure here again is maintained by connection to a convergent-divergent nozzle with a defined throat.

Air breathing engines for military applications are expected to have life of components in terms of several hundred to thousand hours and for civilian applications, several thousand hours. In the case of missile applications rocket engines have a life of a few seconds to about hundred seconds. These distinguish the demand on performance as well.

Thermodynamic analysis indicates that the use of higher pressures at which heat is added gives higher efficiency. This is reflected in terms of a quantity called specific impulse. This term is used mostly in the field of rockets. The term used in air breathing engines is called specific fuel consumption (sfc). Specific impulse is the inverse of sfc. Higher efficiency implies higher specific impulse of 2 to 4.65 kN.s/kg for rocket based systems and 18.0 to 50.0 kN.s/kg (0.7 to 2 kg/kgfh) for thrust producing air breathing engines. What this implies is that to generate a certain thrust demanded by the vehicle, if the specific impulse is high, one needs to use a smaller kg/s of the fuel (for air breathing engines) or propellants (for rocket engines). The amount of fuel or propellants to be carried on board to achieve the mission is smaller. This reduced demand for expendables for the same output helps make the system more compact in addition to the direct benefit of having to lift lower mass. And compactness is the hall mark of aerospace systems, because it implies reduction in drag as the vehicle travels through the atmosphere and hence better flight performance.

Deploying higher pressures has its engineering related issues. High pressures imply higher chemical reaction rates and hence higher heat release rates. While this provides for the benefit in terms of greater compactness, the hot fluids flowing at high pressure cause higher heat transfer to surfaces over which they are passing. Thermal protection systems have therefore to be in place in all propulsion systems. High heat release rates also lead to a coupling between acoustics and heat release that cause difficult-to-solve high frequency instabilities.

Since performance benefits ultimately form the key driver, other associated problems are solved by appropriate techniques. Early designs adopted low pressure ratios for gas turbines and low chamber pressures for rocket engines. As time progressed, as a response to demand for higher performance, high pressures were deployed both in air breathing and rocket engines. Modern day gas turbines and turbofans have a compressor pressure ratio of 40 while five decades ago it was 10 and four decades ago it was brought up to 20. Rocket engines like the PSLV rocket motors or Russian engines with storable propellants (that means non-cryogenic propellants) use chamber pressures of 60 to 100 atm while Space Shuttle Main Engine (SSME) used on space shuttle that used liquid oxygen and liquid hydrogen as the propellants had a chamber pressure of 200 atm.

Table 3.2.: Features of various engines, Ox. = Oxidizer, T_{ini}, T_{fl} = Initial and flame temperatures, RE = reciprocating engine, GT = gas turbine, GTA = gas turbine afterburner, TP = Turboprop, TF = Turbo fan, LPR = liquid propellant rocket, SPR = solid propellant rocket, HRE = hybrid rocket engine, SJE = scramjet, UDMH = unsymmetrical dimethyl hydrazine (l), NTO = nitrogen tetroxide (l), Al = aluminum (s), HTPB = hydroxy terminated poly butadiene (s), NC = nitrocellulose (s), NG = nitroglycerine (l), AP = ammonimum perchlorate (s), HMX, RDX = complex nitramines (s), V.air = vitiated air, LH_2 = liquid hydrogen, LOX = liquid oxygen, HC = Hydrocarbon

Engine	Fuel	Ox.	Comb. Pr, atm	T_{ini} K	T_{fl} K	sfc / I_{sp}
Air breathing engines, sfc in kg/kWh, kg/kgh (power or thrust delivered)						
RE	Gasoline	Air	50	250 - 300	2200	0.3 kg/kWh
GT	Kerosene	Air	10	350 - 450	1500	1 kg/kgh
GTA	Kerosene	V. air	~3	800 - 800	2100	2 kg/kgh
TP	Kerosene	Air	15	350 - 450	1400	0.3 kg/kWh
TF	Kerosene	Air	20 - 40	350 - 450	1900	0.6 kg/kgh
SJE	Kerosene, HC	Air	0.5 - 1	~ 1200	2700	1.5 kg/kgh
Rocket engines, Specific impulse, I_{sp} in kNs/kg						
LPR	Amines	RFNA	100	20 - 320	3500	2.2
LPR	UDMH	NTO	100	20 - 320	3500	2.6
LPR	Kerosene	LOX	100	300/100	3000	2.6
LPR	LH_2	LOX	200	20/100	3600	4.65
SPR	NC	NG	100	220 - 340	2500	2.2
SPR	HTPB, Al	AP	100	220 - 340	3600	2.55
SPR	HTPB, Al	HMX/RDX	100	220 - 340	3600	2.6
SPR	NC	NG, AP	100	220 - 340	2500	2.65
HRE	Polymer	NTO, LOX	50	220 - 340	3500	2.5

High pressures in gas turbine engines also imply higher combustion temperatures arising out of optimizing the performance. Systems designed and produced earlier at lower compressor pressure ratios and small gas turbines even today have a turbine inlet temperature (TIT) - the same as combustor outlet temperature, typically of 1200 K and the current day TIT's have reached 1900 K with the aim of reaching 2100 K in the coming decade. If we note that the

peak adiabatic flame temperature of kerosene - air system is about 2400 K (for the gas turbine combustor entry conditions of 450 K for air and 300 K for kerosene at air-to-fuel ratio near stoichiometry), we recognize that the theoretical limits are being approached in practice. In all these engines, one has to use turbine blade cooling along with thermal barrier coating approaches to handle the severe thermal problems.

In rocket engines, the use of reactive propellants leads to adiabatic flame temperatures of 2600 to 3600 K. Raising pressures from 30 to 100 atm raises the flame temperature of a given fuel-oxidizer system at the same stoichiometry by 150 to 200 K due to reduced dissociation at higher pressures.

The broad features described above are condensed in Table 3.2 that has a range of information of value. All the values presented in the table should be interpreted as indicative. The fuels used for air breathing engines are always hydrocarbons. Reciprocating engines generally use gasoline or some mix of lower petroleum fractions. The combustion in a reciprocating engine occurs cyclically and reaches a peak pressure of 40 to 50 atm and temperatures of 2000 K+. The specific fuel consumption (sfc) of these engines as well as turboprop (and turbo-shaft engines used on helicopters) is expressed in terms of kg/kWh since what is delivered by the engine is power and not thrust. In contrast, in the case of all thrust producing systems, the sfc is expressed in terms of kg/kgh. In the case of rocket engines, the fuel consumption is stated in terms of specific impulse which is the inverse of specific fuel consumption. Thus I_{sp} (Ns/kg) = 36000/sfc (kg/kgh). Thus a turbine engine with an sfc of 1 kg/kgh has a specific impulse of 36000 Ns/kg (36 kNs/kg). This enormous number in contrast to rocket engines is simply because the oxidizer is not carried aboard in air-breathing engines.

Kerosene refined to eliminate sulfur and to restrict other components like the aromatics, called aviation turbine fuel (ATF) is used for all gas turbines; a high boiling variety is used in supersonic aircraft. While air is the oxidizer for all air-breathing engines, the afterburner of the gas turbine engine, however, works with vitiated air coming from the main engine combustor at higher temperatures (800 to 900 K) and combustion occurs at much lower pressures (2 to 4 atm). As can be observed, gas turbine combustors work over a wide range of pressures and temperatures. Engines designed and developed in the nine-

teen sixties had a lower compressor pressure ratio and over a time the pressure ratios have increased dramatically to as high as 40, improving the overall efficiency substantially. An interesting feature of gas turbines as well as other air breathing engines is that when they operate over a range of altitudes - from sea level to 15 km, say, the pressures in the system vary by a factor of four. This is also the reason for the lowest combustor pressure to be as low as 3 atm even when it is operating at about 10 atm during take-off or landing of vehicles. This is not so with rocket engines whose operation is independent of the ambient conditions in so far as combustion process is concerned.

The choice of fuels in the case of rocket engines is freed from the need to restrict to air that has 79 % inert in the form of nitrogen. Exotic chemicals that are highly energetic both in terms of fuel and oxidizer are used. In fact most of chemicals used have fuel and oxidizer elements in them and are bound in a manner that the energy release is significant; one therefore talks of oxidizer or fuel richness in these cases. NC (Nitrocellulose) is fuel rich and NG (Nitroglycerine) is oxidizer rich; so is AP (Ammonium perchlorate). HMX and RDX, the tetracyclo tetranitramine and tricyclo trinitramine are nearly stoichiometrically balanced.

The combustor inlet temperature in the case of gas turbines is dependent on the compressor pressure ratio. The compression process is close to adiabatic process and hence higher compression ratio implies higher temperature at the end of compression. The adiabatic flame temperature is a consequence of the combustion process at the appropriate oxidizer-to-fuel ratio. For gas turbines, the temperature limits posed by the turbine determine the air-to-fuel ratio. For rocket engines, the choice of oxidizer-to-fuel ratio is dependent on optimizing the performance of the rocket engine in conjunction with the vehicle. The choice of combustion chamber pressure in the case of rocket engines is usually much larger and the performance derived from the engine is dependent on this pressure. Even the engine compactness is dependent on this aspect (see Mukunda, 2004). Solid rocket engines used for tactical applications operate over a wide ambient temperature range and this poses serious developmental problems in terms of meeting the required mechanical properties at low tem peratures (-40^0C) for propellant designers. The choice of HTPB as a polymer has been guided by this requirement.
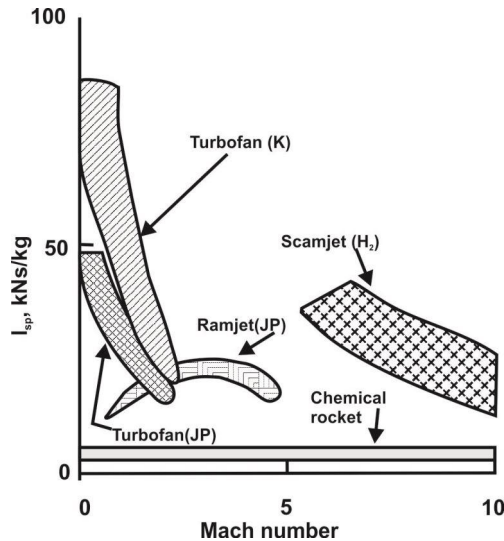
Figure 3.1.: The performance of all the propulsion systems set on a specific impulse (I_{sp}) vs. flight Mach number plot. For air breathing engines, I_{sp} kNs/kg = 36000/sfc (kg/kgh)

The reduction in sfc between turbojet and turbofan is related to the fact that the fan handles large mass flow flow rate and accelerates it much less in comparison to the turbojet that handles lower flow rate and accelerates it to much larger speeds (this fact is related to propulsive efficiency. see for instance, Mukunda, 2004). The larger levels of specific impulse in rocket engines is related to energetics. A peculiar feature balances this behavior. The mean density of the fuel-oxidizer combination comes down as specific impulse increases. This demands the use of larger volume; this feature is measured by density impulse which is the product of specific impulse and density. Consequently, the choice of propellants is made depending on the mission. Figure 3.1 shows the specific impulse as a function of flight Mach number for various propulsion systems. This figure also depicts the regime of flight Mach number over which the propulsion system is appropriate for use.
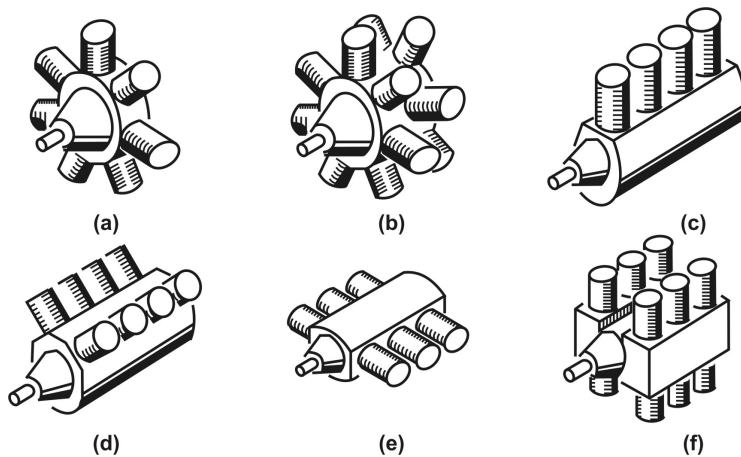
Figure 3.2.: Various configurations of piston engine - propeller system (a) refers to single row radial arrangement, (b) refers to two-row arrangement allowing for more power with the same frontal area, (c) a typical four – cylinder in-line arrangement liquid or air cooled,(d) V – configuration usually liquid cooled, (e) a horizontally-opposed configuration, both air and liquid cooled alternatives used extensively, and (f) a H – configuration is effectively used for high power levels, drawn from [?]

3.3. Piston Engine - Propeller

Figure 3.2 shows the elements of a piston engine - propeller system. Several arrangements in a multi-cylinder configuration are shown in this figure – radial, V, inline and H. Others including X and Y arrangements are also possible. While the reciprocating engine is similar to the engines used in automobiles on the road, the flight version will need to be much lighter for the same power. During the early part of twentieth century, the water cooled engines developed by the Wright Brothers that powered the first heavier-than-air craft flights produced about 9 kW shaft power with engine mass of 90 kg (0.1 kW/kg). Subsequently, Manly developed an engine suitable for aircraft at a record of 0.57 kW/kg producing 40 kW of power with a water cooled radial design. While typically, the power to engine mass ratios were in the range of 0.4 to 0.6 kW/kg during the early forties, they have evolved to levels of 0.9 to 1.2 kW/kg in recent times. Apart from the measure of power-to-engine mass ratio, one should also consider the power-to-volume ratio, because at large power levels, the recipro-

cating systems can turn out to be voluminous and this would affect the choice of the systems. Typical power-to-volume ratio of most reciprocating engines lie between 0.3 to 0.5 kW/m^3.

The power output (P) from the reciprocating engine can be written as,

$$P = K N V_c \; \rho air \; (1 + f) \; Q_m \; (f) \; \eta_{ov} \qquad (3.1)$$

where, K = constant = 1 or 0.5 depending on whether the engine is two stroke or four stroke, N = rpm of the engine, V_c = volume of the cylinder, ρair = density of air, f = fuel/air ratio of operation – typically stoichiometric, Q_m = heat released per unit mass of the mixture, η_{ov} = overall efficiency.

The above expression is otherwise described in words: The engine power is proportional to the product of air mass flow rate ingested modified to include the fuel burnt in the engine, the heat released per unit mass of the mixture and the overall efficiency of conversion from heat to work. Typically overall efficiency of the engines varies between 20 – 25 %.

From the above expression it is clear that the power output is proportional to the ambient density. Since the ambient density decreases with increase in altitude, power output of the engine decreases with altitude. The power reduction rate can be offset by deploying a turbo-super-charger that compresses the incoming air flow with the power obtained from the exhaust gases of the engine. The expression also indicates that power output increases with rpm. For fixed power, one can make the engine more compact by increasing the rpm.

The power generated by the engine is transmitted to the propeller whose rotation causes increase in the speed of the stream passing through the blades. This increased momentum flux generates the force. Thus, the thrust producing element is the propeller. While this device was the main stay of propulsion till the end of 1940's, subsequently, jet propulsion became a dominating system and the development of piston-engine propeller systems took a low profile. Even so, newer applications of piston engine-propeller are continuously being identified and these engines still continue to be developed. For example, in recent times, low power, low mass, high efficiency engines are used in small single seater aircraft and unmanned aerial vehicles. Advanced propeller concepts have been revitalized in the use of propeller driven devices primarily for reducing specific fuel consumption (sfc).
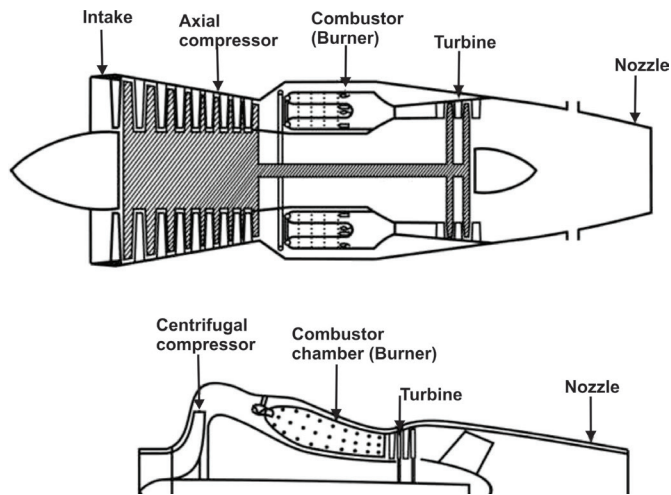
Figure 3.3.: A simple Turbojet with axial (top) and centrifugal (bottom) compressor

3.4. Turbojet

Though turbojets were conceived a long time ago, practically realizable concepts were put together in Italy (1936), in Germany (1939), and United Kingdom (1941) towards a working turbojet. Since then, the growth of turbojets or their variants for application to flight systems in aircrafts and missiles – has never been a matter of doubt. The last forty years have seen several significant performance improvements in terms of specific fuel consumption, compactness, engine mass, life of components, modularity of elements, reduced pollution levels both in terms of noise and chemicals in the exhaust stream.

Turbojet aims at generating hot gases at pressures much higher than the ambient for expansion in a nozzle. The ambient air taken in (i) through a simple or complex air intake depending on the flight speed and the geometry of the aircraft is (ii) compressed in an axial (top part of Figure 3.3) or radial compressor, (iii) heat put in through combustion of a liquid fuel in the combustor, (iv) with a part of the energy used to run a turbine that provides power for running the compressor, and (v) the remaining energy of the fluid stream is extracted by expansion in a nozzle to produce thrust.

Thus, *the intake – compressor – combustor – turbine forms a gas generating system and the nozzle is the thrust generating element*. The thrust generation from a turbojet is the integration of the pressures acting on the surfaces and

all components contribute to it in differing proportions (see Mukunda, 2004). Figure 3.3 shows the typical elements of a turbojet. In the bottom of Figure 3.3, the compressor is of centrifugal type, the type developed by Sir Frank Whittle in the early forties. The top part of the Figure 3.3 shows the engine with an axial compressor, the original idea cedited to German engineers as well as Griffith (also famous for initiating fracture mechanics described in Chapter 6) in the United Kingdom.

Typical pressure ratios in the case of centrifugal compressors vary up to 4 in a single stage. In recent times, single stage pressure ratios of 8 have been achieved in some compressors using supersonic compression. Axial compressors use many stages, each stage consisting of a stator and a rotor. The first stator is called inlet guide vane. In the rotor, the fluid is accelerated and in the stator the kinetic momentum is recovered in the form of enhanced pressure. Typical pressure ratios across a single stage vary from 1.4 – 1.6. But as a part of a multistage compressor, the pressure ratio across a single stage exceeded unity slightly up to nineteen fifties. A six stage axial compressor produced pressure ratios of 4 – 5.5. In recent times, fluid flow aspects of turbo-machinery have been better understood and current designs achieve single stage pressure ratios of 1.1 – 1.3 in a multistage system. One of the features responsible for this situation is the use of multi-spool systems that leads to a better organization of the fluid flow and higher pressure ratios. Advanced engines develop a pressure ratio of 30 in 16 – 18 stages constituting sequentially the fan, low, intermediate and high pressure stages.

The gases entering the combustion chamber usually have temperatures varying between 400 – 750 K depending on the compressor pressure ratio. Fuel, which is typically kerosene of suitable grade, is burned in the combustor to raise the temperature to about 950 – 1700 K (this is also the turbine inlet temperature, TIT) depending on the design and technology used for the turbine blades. Managing higher temperatures requires efficient combustion chamber liner and turbine blade cooling techniques.

The hot gases pass through the stator and rotor stages of the turbine. In most modern turbines, the flow gets choked in the turbine blades (i.e. the pressure ratio across the turbine section is more than about 1.8). The gases at reduced pressure (1.5 to 2.5 atm) and temperature (550 – 850 K) flow through the jet

pipe and are expanded in the nozzle which is usually of the convergent type. In most cases, the flow at the exit section gets choked; i.e., flow attains a speed equal to acoustic speed in the fluid (M = u/a = 1) at the appropriate static temperature. Following Newton's second law, the thrust developed in a turbojet can be written down as

$$F \;=\; \dot{m}_a[(1+f)\,V_e \;-\; V_a] \;+\; A_e\,(p_e \;-\; p_a) \tag{3.2}$$

where $\dot{m}_a$ = mass flow rate of air, f = fuel air ratio, V_e = exit speed of the fluid, V_a = aircraft forward speed, A_e = nozzle exit area, p_e = exit pressure, and p_a = ambient pressure.

In the above equation the first term on the right hand side constitutes the difference in convective momentum flux between the exit and the inflow. The second term constitutes the pressure thrust arising out of the difference in pressure between the exit plane and the ambient. It can be derived by integrating the pressures exerted on the inner wall throughout the propulsion unit (see for instance, Barrere et. al, 1960). It can also be reconciled by looking upon the propulsion unit as a black box with appropriate inlet and exit plane fluxes.

An analysis of eqn. 3.2 leads to an interesting result that the thrust depends weakly on the flight speed because while mass flow rate of the air increases, the difference in the exit and inflow velocities decreases and it is the product of the two that gives thrust. The dependence on altitude that occurs very significantly through the ambient pressure (or density) occurs such that the thrust comes down with increase in altitude. This feature limits the height the aircraft can fly.

There are conditions of the nozzle flow where $p_e = p_a$. In such cases the flow would have been completely expanded and this condition is called optimum expansion. It occurs if the stagnation pressure at the entry to the nozzle bears a definite ratio with the ambient static pressure (typically of the order of 1.8). For all pressure ratios larger than this value, the exit plane pressure (p_e) is larger than the ambient pressure (a condition called under-expansion) and so the second term called pressure thrust term makes a non-zero contribution. One can show that the thrust is maximized when jet is expanded optimally.

Table 3.3.: The variants of the simple turbojet (F. = Fixed, V. = Variable, AB = Afterburner, C. = Convergent, TPC = Two position convergent, VGC = Variable geometry convergent, Geom = Geometry, CD = Convergent-Divergent.)

Air intake	Compressor	Combustor	Turbine Jet	Pipe	Nozzle
Subsonic	Centrifugal	Can	Axial	No AB	F. Geom.
Supersonic	Axial	Annular	Radial	AB	TPC
F. Geom.	Mixed	Can-annular			VGC
V. Geom.	1/2/3 spool	Reverse flow			CD

If the engine is taking off or is on a fixed test bed on ground, the velocity V_a = 0 and we have

$$F = \dot{m}_a\,(1 + f)\,V_e + A_e\,(p_e - p_a) \tag{3.3}$$

As discussed earlier, the fuel consumed in generating the thrust is expressed in terms of specific fuel consumption (sfc) or specific Impulse (I_{sp}). In the case of air breathing engines, the propellant is only fuel. Thus,

$$\text{sfc} = \dot{m}\text{fg/F [kg(fuel)/hr kg (thrust)]} \tag{3.4}$$

$$= \dot{m}\text{fg/F [kg/N s] in SI Units.} \tag{3.5}$$

Conventionally, sfc is denoted in terms of kg/hr kg. The more appropriate way of stating it is kg/N s. Recent literature (for instance, Janes All the World Aircraft Series) expresses it in both ways.

As discussed earlier, specific impulse is the thrust per unit mass flow rate of the propellant. Hence, I_{sp} = F/$\dot{m}_f$, N s/kg. The conversion from one to the other is, sfc in kg/kgf hr = 36000/I_{sp}. Typical values of sfc for turbojets is 1.1 – 1.3 kg/hr kg (31 – 36 mg/N s) or in terms of I_{sp} ~ 32.1 – 27.15 kN s/kg in the early periods of development and in recent times the sfc has dropped to about 0.9 – 1.0 kg/kgf hr (or specific impulse raised to 39.2 – 35.3 kN s/kg).

The performance characteristics of turbojet engine are just not thrust and specific fuel consumption. They also include the compactness of the engine given by the thrust per unit air flow rate, (larger quantity implies smaller cross section for a given thrust and so smaller drag), thrust per unit dry mass (larger quantity implies lighter engine), life of components, modularity of design (im-

plying quick change of elements and hence, a better turn around time), and exhaust pollution concentration etc.

The various alternatives for the elements of a turbojet are presented in the Table 3.3. Air intakes are an important part of the system. The aim of the air intake is to receive the free stream air flow and deliver it to compressor face at low enough speeds (M ~ 0.3) with minimum stagnation pressure loss. Those aircraft that fly at subsonic speeds equipped with gas turbines have relatively simple smooth curved convergent geometry. Those that fly at supersonic speeds must have well designed air intakes that decelerate the free stream across one or two oblique shocks and a final normal shock in a manner that suitable adjustments can be made while the aircraft is accelerating or decelerating and flying with angles of attack. These are met with a variable geometry intake (see Mukunda, 2004).

The choice of the compressor between centrifugal or axial type is governed by the pressure ratio needed as discussed earlier. For pressure ratios up to 4, a single stage centrifugal compressor is satisfactory. For reduced frontal area, axial type is preferred. One uses a single shaft or single spool engine for pressure ratios of 4 or thereabouts. For higher pressure ratios, usually one uses a two spool axial compressor system. Occasionally a three spool system has been used for high efficiency over the entire thrust range.

The combustion chamber can be of the four types as listed in Table 3.3. The nozzles are usually of fixed geometry, convergent type. The engines with after-burning sometimes use a two position nozzle. In recent times, the engines use variable geometry nozzle. Till recently, exhausts had only circular cross section. Now engines with rectangular exhaust have been developed (YF 22). The more significant reason for rectangular shapes is the possibility of achieving stealth. By using these shapes and faster mixing of the hot gas with co-flowing air stream, the thermal signature of the exhaust is brought down.

Table 3.4 lists some turbojet engines. Mamba is a small engine used in small unmanned air vehicles. The other engines have thrust as high as 50 kN without after burning and about 70 kN with after burning. Small engines run at high rpm – as much as 50000. Larger engines run at lower rpm – like 8400 rpm for ATAR SNECMA. This is because of the limits of peripheral speeds due to compressibility. The specific fuel consumption indicated are similar to the

Table 3.4.: Turbojet engines (* = kg/kgf.hr, π_c = compressor pressure ratio, TIT = Turbine inlet temperature, $\dot{m}$ a = air mass flow rate, AB = Afterburner)

Name	Mass	F	sfc	πc	TIT	$\dot{m}$ a
	M, kg	kN	*		K	kg/s
Mamba	0.15	0.42	6.4	0.25		2.8
TRI-60	45.0	3.43	1.25	3.9	1023	5.6
Teledyne 402	45.0	2.94	1.2	5.8		4.35
RR-Viper	790	16.7	0.94	5.8		26.5
J 3-IHI-7C	430	13.5	1.05	4.5		26.4
J85-4,USA	188	13.1	0.98	7.0	1180	20.0
J85-21	310	15.6	1.0	8.3	1250	20
(AB)		22.2	2.13			
J79-7A,11A	1685	44.5	0.84	12.4	930	74.4
(AB)		70.3	2.07		1985	
Atar 9K-50	1582	49.2	0.97	6.1		70.7
(AB)		70.6				
Orpheus 703	400	22.0	1.05			
Olympus 593	3175	139.4	1.0	15.5	1560	186.0
		169.2	1.4			

values described earlier. The compressor pressure ratio of small engines is less than 4 and for large engines which use axial compressors goes up to 12. The turbine inlet temperatures are typically in the range of 1000 – 1300 K. The thrust per unit mass flow rate in the non-dimensional form indicated is about 1.5 – 2.0, the latter value being valid for large engines. It is almost directly related to the choice of pressure ratio. The thrust per unit dry engine mass is low for small thrust engines and about 71 (N/kg) or 7 (kgf/kg) for large engines. These are the typical values valid even in recent times. Jet engines are generally sleek, particularly with axial compressors. Typical thrust-to-volume values are 15 to 30 N/m³, with the entire engine periphery taken into account.

3.5. Thrust Augmentation in Turbojets

While the turbojets are designed to produce a certain level of thrust for large range of operating conditions, there is need for excess thrust for short durations. These may arise (i) for turbojets or turboprop engines during take-off at high altitude and/or at unusually large ambient temperatures, (ii) when the pilot of

an aircraft involved in a combat decides to get away from the scene of combat in a short duration, or (iii) when enemy strike aircraft needs to be intercepted by quick climb at short notice. Though the scenario of combat is continuously changing with the advent of long distance radars, pilot-less target aircraft and other related advances, the need for short duration excess thrust/power from the power plant remains. Two devices which have been used extensively are the afterburner or reheat system and injection of water or water-methanol into the compressor or combustor.

3.5.1. The Afterburner

Afterburner is essentially a long pipe between the turbine exit and the nozzle entry as in Figure 3.4. It is firstly to be recognized that because of limitations of turbine, the main combustor does not utilize the full combustion capabilities of the air taken in. Whereas typically, one needs a fuel to air ratio (*f*) of 0.067 for obtaining peak temperature of 2300 K, one limits the fuel air ratio in the main combustor to 0.01 – 0.03 to restrict the temperatures to 1200 – 1600 K. This means that only about 20 – 45 % of the oxidizing capability would have been used.

The rest can be put to use by burning the fuel in the afterburner at *f* up to 0.067 raising the temperature to 2300 K. The nozzle continues to be choked because the pressure ratio across the nozzle is not reduced. Since the inlet temperatures are higher, the nozzle exit temperatures also will be higher. The choking at higher temperatures implies higher exit velocity (equal to acoustic speed). This causes the enhanced thrust. Another important feature is that the density of the gas stream goes down because of enhanced temperature; this causes the mass flux ρu to decrease like $1/\sqrt{T}$ because $u = a$ (acoustic speed) varies like $\sqrt{T}$ and $\rho \sim 1/T$. Thus, to accommodate the same mass flow (only slightly enhanced by additional fuel), the exit area has to be increased so as to keep the conditions ahead of the afterburner unaffected. Most after-burning turbojets use variable area nozzle. Only some use a two position system. The operation of the after burner also calls for care since inadvertent operation involving fixed nozzle area causes jet pipe pressures to shoot up. These cause pressure waves back into the compressor and compressor stall or surge occurs, destabilizing the engine operating point. Examination of Table 3.4 shows several large thrust engines like J 79 have afterburners. Others like J 85, Orpheus 703 also have versions involving afterburners. As can be noted, the thrust augmentat-
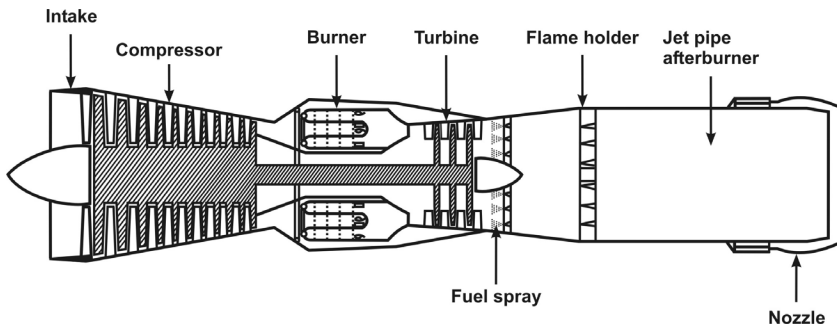
Figure 3.4.: A Simple turbojet with afterburner (or reheat)

ion is by as much as 40 – 60 % and specific fuel consumption goes up by more than 100 %.

Thus, the sfc increase is much larger than of thrust. This is the reason why this operational mode is used only under certain circumstances described earlier. It is also interesting to reason why combustion occurring in the main combustor leads to lower fuel consumption than after burner to produce the same thrust. The behavior is due to the fact that energy addition to fluid at high pressure is more efficient than that at lower pressure.

3.5.2. Water – Methanol Injection

The second method of thrust augmentation is by using water or water-methanol mixture. Water can be used in the combustion chamber or at the entry to the compressor. The injection of water into the combustion chamber causes an enhanced flow rate of hot gases. This enhancement is significant particularly because the turbine inlet temperature is a control variable and held constant. This calls for the increase in fuel flow rate, albeit a small fraction of the water flow rate. This is primarily because the evaporation of water calls for about 2.5 MJ/kg whereas the heat of combustion of kerosene is 42 MJ/kg. Use of methanol in water-methanol mixture is essentially to prevent water from freezing at the low temperatures which the liquid is subject to in flight conditions. If we note the fact that the flow across the turbine is usually choked, the enhanced mass injection upstream of turbine blades causes increase in combustor operating pressure. This implies compressor pressure ratio is increased. The pressure ratio gets set at a value which is determined by the compressor – turbine power balance. The use of the mixture of water and methanol partially offsets

the loss of energy due to the use of water alone. Again, the sfc increases (not as much as with water alone) when the mixture is used.

3.6. Two – Three Spool Engines

Amongst the engines designed in the last twenty years, many high thrust engines have two or three spools and variable stators. There are good reasons for such a development. To understand this, we must examine as to what happens in various regions of an axial compressor. As the fluid moves through the compressor pressure increases. The static temperature also increases. These are such that the density increases through the compressor (because, temperature rise is much smaller than pressure rise due to the isentropic relationship); acoustic speed increases as well. In order to account for these changes and maintain good performance at each stage, the cross section is decreased as we move towards the high pressure stages. One can do this by reducing the tip radius or increasing the hub radius or both.

While the the first feature was indeed the characteristic feature of some early designs, there is no special advantage in it. Increasing the hub radius alone can cause enhanced tip clearance losses in later stages, decreasing the tip radius implies reduction in blade tip Mach number and thus lowering the pressure ratio across the stage. It is possible to look for an optimum and make the above scheme satisfactory at one design point. At off-design conditions, because of the non-linear dependence between pressure, velocity and temperature across the stages, the front stages and rear stages are affected differently; at lower speeds, the axial speeds in the front stages will be relatively lower than the tangential speed and so higher effective angles of attack. This causes greater tendencies of flow separation over the blades and so towards 'stall' exactly like in external flows discussed in the earlier chapters. The rear axial stages will be poorly loaded and they would be "wind-milling" implying that the pressure through these stages will come down rather than increasing. These problems are indeed serious for all compressors beyond a pressure ratio of about 4. One of the classical methods of overcoming the problem is to use two or three spools. Figure 3.5 shows the schematic of a two spool turbo-jet. The low pressure compressor is run by a low pressure turbine both being fixed on the same shaft. The intermediate pressure compressor is run by an intermediate pressure turbine, if such a stage is used. The high pressure stage running at higher speeds is run

Intake   Compressor   Burner   Turbine   Nozzle
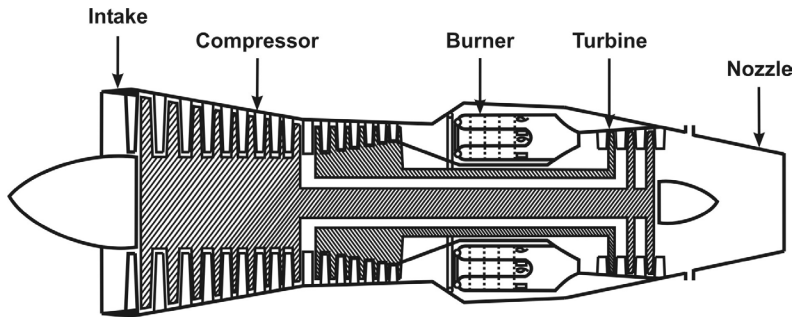
Figure 3.5.: A two shaft axial compressor based turbojet

by the high pressure turbine, both mounted on the outer (or outermost) shaft. The high pressure stage is run at higher speeds to take advantage of the higher static temperature in this region. It is this stage that is involved in the control circuit of the gas turbine. Depending on the strategy used for control, one needs to consider the turbine inlet temperature (TIT) and speed of the H.P. compressor along with fuel flow rate and nozzle exit area. Some engines run with fixed high pressure compressor rpm or corrected rpm, while not exceeding a fixed TIT.

It is the high pressure spool that is cranked up during the start-up of the engine. Because of the smaller overall moment of inertia, the starting systems turn out to be smaller and lighter.

3.7. Turboprops

We have already discussed piston engine-propeller combination and turbojets. In the first case, the thrust producing element is the propeller. In the second case, it is the jet. If one uses a gas turbine and couples propeller to a turbine such that most of the expansion takes place across the turbine with little left to the nozzle, one gets a turboprop. Of course, one has the freedom of splitting the power delivered partially to the propeller and partially through the jet.

The performance of turboprop is between that of a piston engine-propeller system and turbojet. It is far more fuel efficient compared to a turbojet and has a
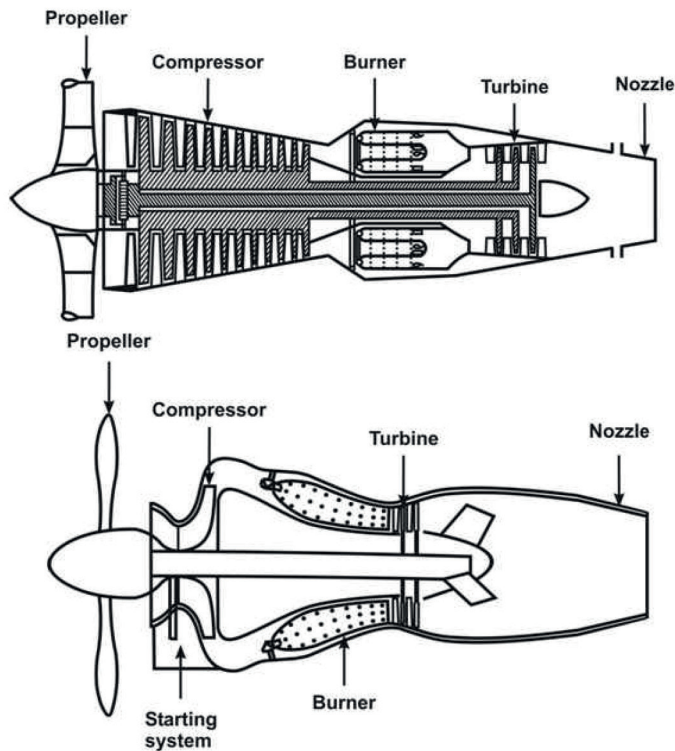
Figure 3.6.: Turbo Prop Engines based on axial (top) and centrifugal (bottom) compressors

larger range of altitude – speed envelope for its operation compared to piston engine. Its better fuel efficiency in comparison to a turbojet emanates from the fact that it moves a larger mass of air through a smaller velocity increment to give the same thrust. This increases propulsive efficiency and so leads to reduced specific fuel consumption.

Turboprops are used for aircrafts and in one form as turboshaft units for helicopters. They fill in a range of speeds up to 500 km/hr and altitudes up to 8 km. The flight Mach numbers are restricted to about 0.7 because at this Mach number and beyond, shock waves are formed on the surface of the rotating propeller reducing the efficiency of the power conversion to useful propulsive power.

There are several variations in turboprops. These are the conventional turbo
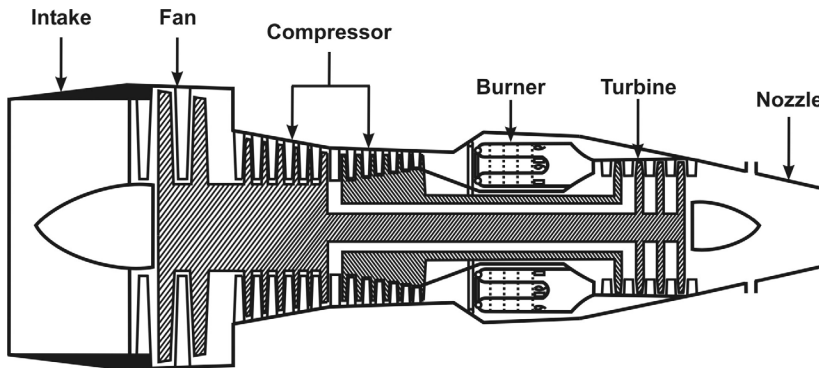
Figure 3.7.: A two shaft (spool) Turbofan

-props, the free turbine systems and turboshaft engines. Figure 3.6 shows the elements of these engines with axial and centrifugal compressors. In these systems, the propeller is connected through gearing to the shaft which drives the compressor.

In free turbine concept, the compressor – turbine system is decoupled from the shaft which connects the propeller to a turbine mounted on the same axis. This gives flexibility in the rotational speed of the compressor – turbine system governed by certain considerations and those of propeller – turbine system which are governed by other aspects. This feature is somewhat like the multi-spool system in turbojets/turbofans. In both of the above concepts, the power sharing between the propeller and jet can be different.

A turboshaft engine is one in which the expansion work of the hot, high pressure gas is entirely taken through a turbine so that all the energy is available in terms of shaft power (helicopter power for the rotating blades is derived from engines of this category). All that this means is that the expansion in the turbine must result in comparatively lower pressures and so the turbine blades for these stages have to be indeed large. Even so, they are lighter than the piston engine propeller system for the same power.

Single engine power level is as much as 5000 kW with sfc of 0.4 – 0.6 kg/kW hr. The pressure ratios of engines vary from about 6 – 14. Some of the engines

like Turbomeca Boston and Dart use water-methanol injection for obtaining enhanced power for short durations, like during take-off. The power-to-engine mass ratio varies from 4 to 10 kW/kg, about two to ten times that of reciprocating engines and the power-to-volume ratio is 1 to 8 MW/m^3, the maximum being eight to ten times that of reciprocating engines. It is for these reasons that larger aircrafts use turboprops rather than reciprocating engine-propeller combinations.

3.8. Turbofans

Turbofans (see Figures 3.7 and 3.8) are a further evolution over the turboprops in terms of permitting extended range of flight speeds. If, in front of the propeller and over it, one adds a duct which acts as a diffuser, then it is possible to reduce the speeds in front of the propeller for a given flight speed and thus extend the range compared to turboprop. Further, if one shapes the annular space between the outer profile of the core engine and the outer duct such as to generate a convergent nozzle, one can expect to generate thrust from the system. These are the prominent differences between the two systems. Thus, once one has a duct, the propeller becomes a fan which compresses the air. The compressed air is expanded and one obtains an enhanced velocity and so, thrust. Obviously the efficiency depends on the amount of air handled via fan and its pressure ratio. The ratio of the air handled by the fan to that going through the core engine is called the bypass ratio, α. A straight turbojet has $\alpha = 0$. Table 3.5 shows the details for several engines, civil and military.

There are some basic features that govern the choice of the bypass ratios. The single most important performance criterion for a civil aircraft engine is the specific fuel consumption. Increase of α will help achieving the thrust demand by keeping the velocity increment (between the exhaust and intake) low. Typical bypass ratios of engines for civil aircraft go up to 6; there have been arguments about increasing it further. Inordinate increase will lead to a large frontal area. This leads to enhanced nacelle drag. It is argued that even though this large size is reasonable in large aircraft where the the contribution of the drag from the engine is a small fraction of the total drag, it begins to have avoidable drag increase amongst other features –enhanced diameter of the engine and an increased separation of the engine from the ground implies larger and heavier landing gear. Even so, General Electric company has developed the GE 90 engine with a bypass ratio of 9.

Intake duct

Starter-generator
Engine oil pump
Accessory gear box

LP compressor

Booster
compressor

Hydraulic oil pump

Fuel pump

Engine
electrical control

Centrifugal
compressor

Oil-to-fuel heat
exchanger

Igniter

Diffuser

Burner

HP turbine

Fine Injector

Annular bypass duct

LP turbine

Exhaust duct
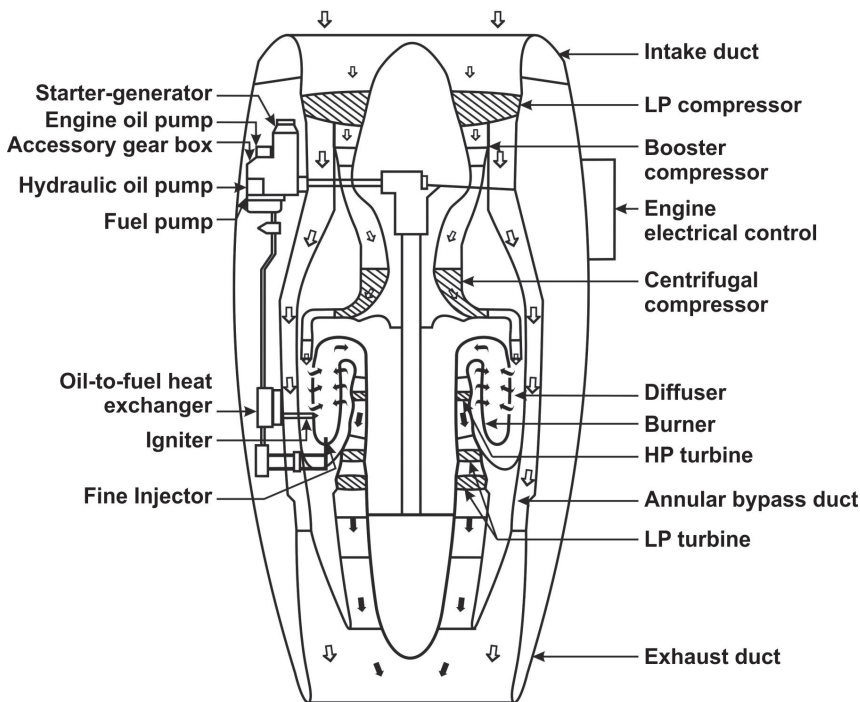
Figure 3.8.: A Turbofan in section using a fan, a two stage axial-centrifugal compressor, a reversed flow combustor, and an axial turbine

Engines of military aircraft that operate in supersonic range are usually buried in the fuselage. They need to be compact. They need also an afterburner to obtain burst of thrust for short durations. Low specific fuel consumption is not an important criterion. Hence, afterburning turbojets are one good choice. If the engines have a high enough turbine inlet temperature, there will not be enough of oxidizing ability available for obtaining desired enhancement of thrust. In such a case a low bypass ratio turbofan would provide enough bypass air for obtaining desired enhancement of thrust. Hence, military aircrafts use bypass ratios, typically between 0.3 to 1.0. Many western engines use single stage fan with pressure ratio of 1.4 –1.6 with bypass ratios close to 1. It is also possible to design for very low bypass ratios, but higher pressure ratios with multi-stage arrangement. Russian engines use relatively low bypass ratios but a number of stages leading to pressure ratio of 2.5 – 3. This arrangement can

Table 3.5.: Turbofans (* = kg/kgh, π_c = Compressor pressure ratio, π_f = Fan pressure ratio, $\dot{m}_{core}$ = Core mass flow rate, $\dot{m}_{fan}$ = Mass flow rate through the fan, α = Bypass ratio, to = Take off, ab = Afterburner

Engine	Mass M, kg	F kN	sfc *	π_c	$\dot{m}_{core}$ kg/s	πf	$\dot{m}_{fan}$ α kg/s, -	TIT K
Ivchenko	290	to, 15	0.56	8		1.7	- , 2.0	
(6 km, M = 0.6)		3.5	0.84					
GE F404	908	52.0	0.85	27.1	54.2	-	18.5, 0.34	1560
		ab, 81	1.9					
P&W F100	1371	64	0.68	23		2.57	- , 0.6	
		ab, 106						
P&W JT9D-70A	4153	to, 236	0.37	24.0	116.0	1.6	568.0, 4.9	1520
11km, M = 0.85		53.2						
GE CF 6 50M	5000	to, 247	0.38	32.4	121.0	1.6	532.0, 4.4	1563
10 km, M = 0.85		52.4	0.65					
RR RB 211 524	5980	to, 227	0.37	25.0	121.6		535.4, 4.4	
11 km, M = 0,85		50.0	0.66					
P&W TF30-P-100	1807	ab, 112	2.45			2.14	118.9, 0.34	1589

provide for higher thrust-to-area ratio. The thrust-to-engine mass ratio is typically 30 to 40 N/kg and the thrust-to-volume is 30 to 50 N/m³. These values are slightly lower than pure jet. For an afterburning turbofan however, the values will be much larger.

The power absorbed by the fan can be substantial as compression of large flow rates is involved. In order to provide for this, the compressor pressure ratio of the core engine usually has to be large – 8 to 30. By the arguments made earlier, to handle these pressure ratios, one needs multi-spool designs for compressor-turbine system. Thus, the evolution of a modern turbofan from the turbojet and turboprop seems natural in extending the flight envelope without sacrificing the desirable low specific fuel consumption. The fan can be ahead of the core engine like in most engines or in the aft portion like in the general electric CF 700 engine in which the fan blades are an extension of aft turbine blades.

An examination of Table 3.5 along with Table 3.4 shows that the sfc of turbofans is about 55 – 65 % of turbojets. The thrust-to-engine mass ratio goes up to 60 (N/kg) and the turbine inlet temperature goes as high as 1550 K. These
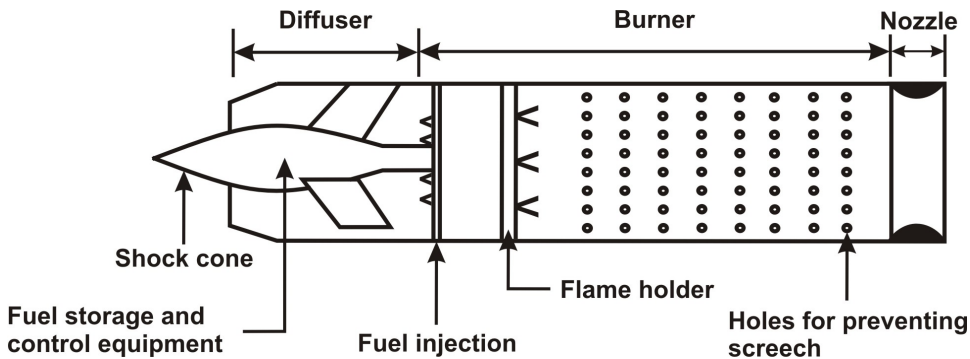
Figure 3.9.: Schematic of a Ramjet

have been achieved through the use of better materials and turbine cooling techniques.

3.9. Ramjets

Ramjets can be thought of as propulsive devices evolved out of turbojets. As flight Mach number increases say up to 2, the stagnation pressure of the stream is 12 times the free stream static pressure. Taking the recovery of the stream stagnation pressure as 60 – 70 % as is usually the case in fixed geometry intakes, the free stream diffuser end pressure is seven times the static pressure. This pressure, as may be recognized, is comparable to what one obtains at the end of a compressor of a turbojet. Thus, one can dispense with the compressor. Once the compressor is dispensed with, the turbine can also be dispensed with, since power need not be generated to run the compressor. One, therefore, has a diffuser, combustor and an exit nozzle. The stagnation pressures available at the end of the combustor will be several times the ambient pressure (at least 5 – 7 times). In order to extract the expansion work, one uses a convergent-divergent nozzle. Figure 3.9 shows the schematic details of a ramjet.

By the arguments made earlier, it is clear that ramjets operate well only at high speeds, typically M = 2 – 4. The combustion mode being not very different from that of an afterburner, the specific fuel consumption is comparable to an afterburner, namely 2 – 3 kg/ hr kgf (specific impulse of 12000 - 14000 Ns/kg). Because of the high speed at which they are efficient and yet simple in construction, they are used for missiles extensively.
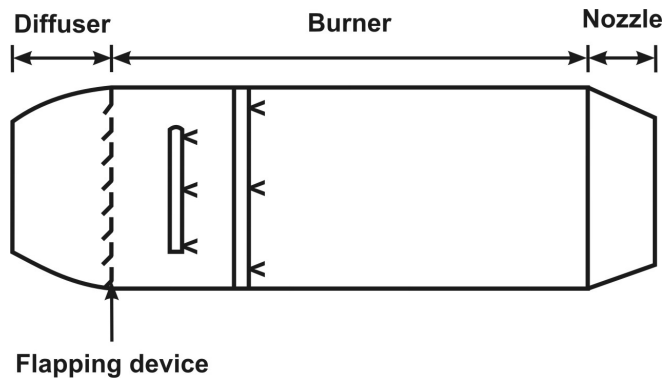
Figure 3.10.: Schematic of a Pulsejet

The ramjet, unlike turbojet and turbofan does not produce any thrust at zero flight speed. Therefore, ramjets need an auxiliary system to propel the vehicle to a speed (or Mach number) range where ramjets can work. In most missile systems, rocket engines boost the vehicle to a range where ramjets can begin functioning. Two of the applications correspond to solid fuel ramjet (SFRJ) and Integral ram rockets (IRR). In the case of solid fuel ramjets, as the name indicates, the fuel is a solid block. Air flows through the port of the fuel block, combustion takes place at higher pressures created by the ram effect, and the hot gases pass through the nozzle producing thrust. In the case of integral ram rockets, the chamber which contains the rocket propellant is used as the ramjet combustion chamber after the rocket propellant is burnt up in the boost phase.

3.10. Pulsejet

Pulsejet is a constant volume combustion device (unlike ramjet which is a constant pressure device) which is quite efficient only at low speeds and uses unsteady combustion for its operation. Once the system is started, it works by taking in air and fuel and combusting them during a part of the cycle and exhausting it during the next part of the cycle (Figure 3.10). In order to promote and sustain the operation, a flapper device of metal or plastic, in recent times, is used in the front end. During the exhaust of the gases through the nozzle, the pressure falls down and it causes the flapper valve to open. This causes air to come in. At the same time fuel is injected and igniter spark is put on. This initiates combustion and pressure rises in the combustor.

Table 3.6.: Properties of air at stagnation conditions at high Mach numbers calculated for ambient conditions of 243 K and 0.0058 atm (Note that all the composition is in terms of mole fraction. 3E-04 implies 3.0 ×10⁻⁴)

$M\infty$	T_{stag} K	N_2	O_2	NO	O	CO_2	Ar
4.0	980	0.7808	0.2095	4E-05	-	3E-04	0.00932
5.0	1355	0.7803	0.2087	0.001	-	3E-04	0.00932
6.0	1788	0.7780	0.2070	0.004	3E-04	3E-04	0.00932
7.0	2265	0.7730	0.2015	0.015	3E-04	3E-04	0.00932
8.0	2777	0.7630	0.1910	0.034	0.002	2.9E-04	0.00930
9.0	3293	0.7450	0.1700	0.072	0.010	2.5E-04	0.00930
10.0	3878	0.7275	0.1518	0.092	0.018	2.1E-04	0.00920

Due to this pressure rise, the flapper valve closes. This whole operation repeats by itself and there will be net thrust developed during the cycle. In modern times, several new devices which work without valve (called valve-less pulse-jets have been developed). These use acoustic behavior of ducts for their operation. In these cases, the organ pipe longitudinal mode frequency is given by a_c /4L, where a_c is the speed of sound in the combustion chamber. For temperature of 1800 K, the acoustic speed is about 840 m/s and for L~ 1 m, f ~ 210 Hz. At this frequency, combustion interacts with acoustics in such a manner that the fluctuations in the chemical heat release are in phase with that of the acoustic fluctuations and an oscillatory combustion operation is set up. The fluctuations generate pressure waves so as to enable continuous self-induction of the air and the subsequent combustion. The hot gases exhausting through the nozzle produce thrust.

3.11. Scramjet

Flights at high Mach numbers are characterized by large stagnation temperatures and pressures. At the high temperatures experienced under stagnation conditions or even behind oblique shocks, it is possible that air will dissociate. As Mach number increases, the stagnation temperature rises sharply and air normally thought as a single fluid (even if composed of nitrogen and oxygen) for most gas dynamic applications below a Mach number of 4, begins to generate other species like NO and O. The fraction of oxygen in the dissociated stream

comes down. At M = 10, oxygen fraction (including atomic oxygen) is about 16 % compared to 21 % at M = 4. Argon (Ar) is monotonic and inert. Its marginal change reflects changes in other species.

At M = 7, the stagnation temperature is 2265 K, comparable to fuel-air combustion temperatures at ambient conditions. This implies that adding heat to fluids brought to rest from high Mach number conditions becomes marginal. This happens largely because, most of the energy at high enthalpies goes into dissociating the species and thrust generation potential becomes small. Also, at M = 9, the stagnation temperature is 3293 K that is close to the maximum temperature that a chemical system can provide because beyond this value, dissociation prevents energy input into translational mode. Hence, in a scramjet the flow is not decelerated to subsonic conditions like in the case of a ramjet, but is decelerated to about a third of the flight Mach number. Thus, at a flight Mach number of 6, the combustor Mach number is about 2. In this process, the static temperature in the combustor is maintained at about 1200 to 1400 K to enable smoother ignition of the fuel (hydrogen or a hydrocarbon fuel). The static pressure becomes as low as 0.5 to 1.0 atm. Since chemical reaction rates vary as the square of the static pressure, the reduction in static pressure reduces the reaction rates significantly.

3.11.1. Scramjets vs. other vehicles

Turbojet based aircrafts have been built to fly at Mach numbers close to 3 (MiG. 25 flies at M = 2.8, TR1 flies at M = 3). Ramjet based missiles fly at M = 2 to 3. These are generally cylindrically shaped and boosted to the required speed by a rocket, and subsequently, the ramjet works in a sustain or weak–acceleration mode. Scramjets have been conceived for meeting a part of the propulsion needs of a space launch vehicle – between Mach numbers of 4 to 10. The only well argued case for a scramjet has been a cruise missile to fly at Mach numbers between 6.5 to 8. In this case the missile needs to be boosted to the required Mach number and allowed to function in cruise mode for long time, typically 10 to 20 minutes. The ostensible reason for this mission is to have a "very fast" missile that cannot be chased and shot down by other missiles of the current generation that operate at a maximum Mach number of about 4. Since the missile has to function for a reasonable duration with some minimal pay-
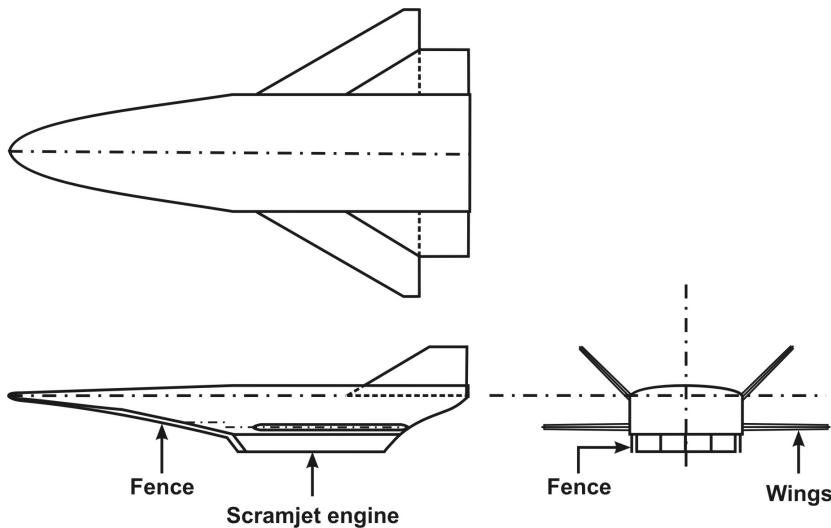
Figure 3.11.: The schematic of a hypersonic vehicle

load, it has to carry substantive amount of fuel. It is optimal to consider a winged vehicle so that the demand on the propulsion can be brought down by-numbers is a delta wing. This is aimed at reducing the drag penalties common to nearly all of the supersonic aircraft. Because of the deep delta configuration, the aspect ratio (the ratio of the square of span to the wing area) of the wing will be so small ($\sim 1.5 - 2$) that one cannot expect a lift-to-drag ratio of more than 4. The engines are usually located at the bottom of the wing as shown in Figure 3.11.

Another feature of hypersonic flight is the very significant interaction between the engine and the rest of the vehicle. This is true even for other flying vehicles, but takes on increasingly important role as Mach number increases. Normally discussed under the title airframe-engine integration, the design of interfaces can be tuned if there is demand for say, change of the engine profile within limits for most aircraft. In the case of hyperplane, the entire plane has to be looked at together since the engine fore and aft-body are very closely connected. For instance, it should be understood that the 'air intake' starts from the nose of the vehicle with external compression in the entire bottom section ahead of the engine framework with possible additional compression inside the engine

portion. Hence, any change that occurs in the geometry far ahead of the engine can affect the pressure recovery and mass flow characteristics of the engine.

Further, the drag D written as $D = (\gamma p_o M_o^2/2)c_D A_w$, where c_D is the drag coefficient and A_w is the wing area that rises sharply with Mach number. Hence, the thrust produced must equal the large drag values for steady flight. The engine must have the ability to produce some excess thrust to enable control of the vehicle. Since this excess happens to be the difference between two large quantities, it is important to ensure that other geometric or flow features do not affect the availability of this excess force. One fluid dynamic feature in hypersonic flow regime that remains inadequately understood is the flow transition process. Hypersonic boundary layer over a non-smooth heated surface with curvature is known to have extended transition regime that can affect the drag experienced by the vehicle and this uncertainty must be covered in the design margin. The above features are special to hypersonic vehicle in comparison to supersonic aircrafts and ramjet based missiles.

The design of the combustion system is usually contemplated along the lines of can combustor in gas turbine engines. The basic idea is to build a module and use as many modules as needed to enable reduction in development costs. One of the classical modules contemplated is not a circular geometry, but a rectangular one. This is because, circular geometry does not provide any benefits due to complex shock structure in the flow field with struts, injectors and such other protrusions. Scramjets have been successfully demonstrated in the USA flying at M = 10 for about 10 seconds autonomously as projects named X-43 and X-43A. Other countries have also put in efforts into the development. Recently (in 2016), flight tests to demonstrate autonomous hypersonic flight at M = 6 with supersonic combustion have been successfully completed by Indian Space Research Organization.

3.12. Start-up Systems

Most of the air breathing engines are not self-starting (as discussed earlier in the case of turbojet). The starting devices for turbojets, turboprops and turbofans spin the rotating machinery up to a certain minimum speed (15 – 20 % rated speed). During this period, the air flow is taken in, pressurized and then passed through the combustor and turbine. When a minimum air flow rate is a achieved, fuel is injected, and ignited. The gases flow through the turbine and

generate power to accelerate the compressor. Typical time required to achieve steady state varies be-tween $30 - 80$ s depending on the size of the engine, smaller engines taking smaller time to accelerate. All starting systems automatically disengage once the main system starts functioning.

Engine start-up is done by using (i) ground based compressed air, (ii) electric motor, and (iii) pyrotechnic operated systems. In the first type, the compressed air jets impinge on the main turbine or an auxiliary turbine connected through the gearing to the main system until the speed crosses a minimum value. At this stage, the fuel injection sequence under the action of the control system begins to take over. The igniter is a high energy continuous spark source with an energy of about 2 J. This level of high ignition energy is not needed in the more benign circumstances of ground starting. However, it is provided so as to account for a far more critical condition that arises during an in-flight blow-out of the flame in the combustor during adverse conditions of high altitude, high angle of attack of flight, and heavy rain. Some engines have more than one spark source so that redundancy of ignition is provided for. In the second type, the auxiliary power source on board the aircraft is used to run the electric motor which runs the rotating machinery through a gearing system.

In the third type, an auxiliary turbine is started by using a small rocket motor fitted with a propellant which burns for $3 - 4$ s. At the end of the combustion, the main rotating machinery would have accelerated. Some aircraft like Canberra fitted with Avon engines use such cartridge starters. Each engine has a maximum of three cartridges which can be used during a flight. The discharged cartridges are recharged at the end of each flight.

Ramjets and scramjets are not self-starting and begin to produce positive thrust only at relatively high speeds ($M = 0.8 - 1.2$) and ($M = 4 - 5$) respectively. Therefore, they need to be accelerated to their optimum speeds (of the order of $M = 2 - 2.5$ for Ramjets and around $M = 7$ for scramjets) before being allowed to operate. The acceleration is performed using rocket engines (mostly solid rockets operating for a short burn time of the order of tens of seconds).

Pulse jets are not popular devices in many applications. The starting of pulse jets with flapper valves is initiated by causing combustion in an interrupted manner for a few operating cycles. For valveless pulse jets, the operation is automatic after the system has been heated up.

Table 3.7.: Propulsion performance on vehicles

Vehicle	Total	Fuel mass, t	Engine mass, t	Output sea level	Speed M
Metro	7.5	2.6	2 x TPE331	0.82 MW	0.46
ATP	22	5.1	2 x FW126A	2.0 MW	0.44
AN 32	27	5.4	2 x Ai20D	3.8 MW	0.42
A320-200	74	24.0	4 x CFM56	139 kN	0.78
B757-200	100	42.3	2 x RB211	178 kN	0.80

3.13. Engine-aircraft Integration and Operation

Aircraft engines are developed independently, and there is usually no specification of the aircraft on which it is installed. The same engine can go into several aircraft or the same aircraft may use different engines of the same class (thrust and overall features being similar). The aircraft designer may plan to locate the engines in a variety of ways. Several of these are shown in Figure 3.12. Engines are located on the nose, in the sides, in front or at the back. When the number of propeller engines is large, they are placed behind the wing in what is known as pusher propeller configuration. Such an arrangement reduces the distortion of the flow over the wings. Turbine engines are usually pod mounted. The thrust derived from an engine as inferred from isolated engine tests is different from those obtained when installed in an aircraft. The influences caused by the engine in an aircraft are evaluated experimentally. With the advent of CFD, advance estimates of the influence under various flying conditions are available. In fact, optimization of the precise locations of the engines viewed from aerodynamic considerations can be performed. These locations need to be examined with regard to static and dynamic structural aspects before acceptance.

Military aircraft are designed to have the single or twin engines inside the fuselage itself. The wing is invariably used for armament fitments. The choice of three engines is somewhat limited and outmoded. The choice of four turbine engines was necessitated due to the availability of peak thrust per engine. There is a general shift to pod mounted twin engine configuration with the availability of higher thrust engines. Table 3.7 provides a view of the features of several propulsion systems.

Reciprocating or turbo-engine propellors

Jet engine

Single engine — Spitfire / Starfighter F-104

Twin engine — P-38 / F-4 Phantom

Three engine — SM=79 / HS Trident

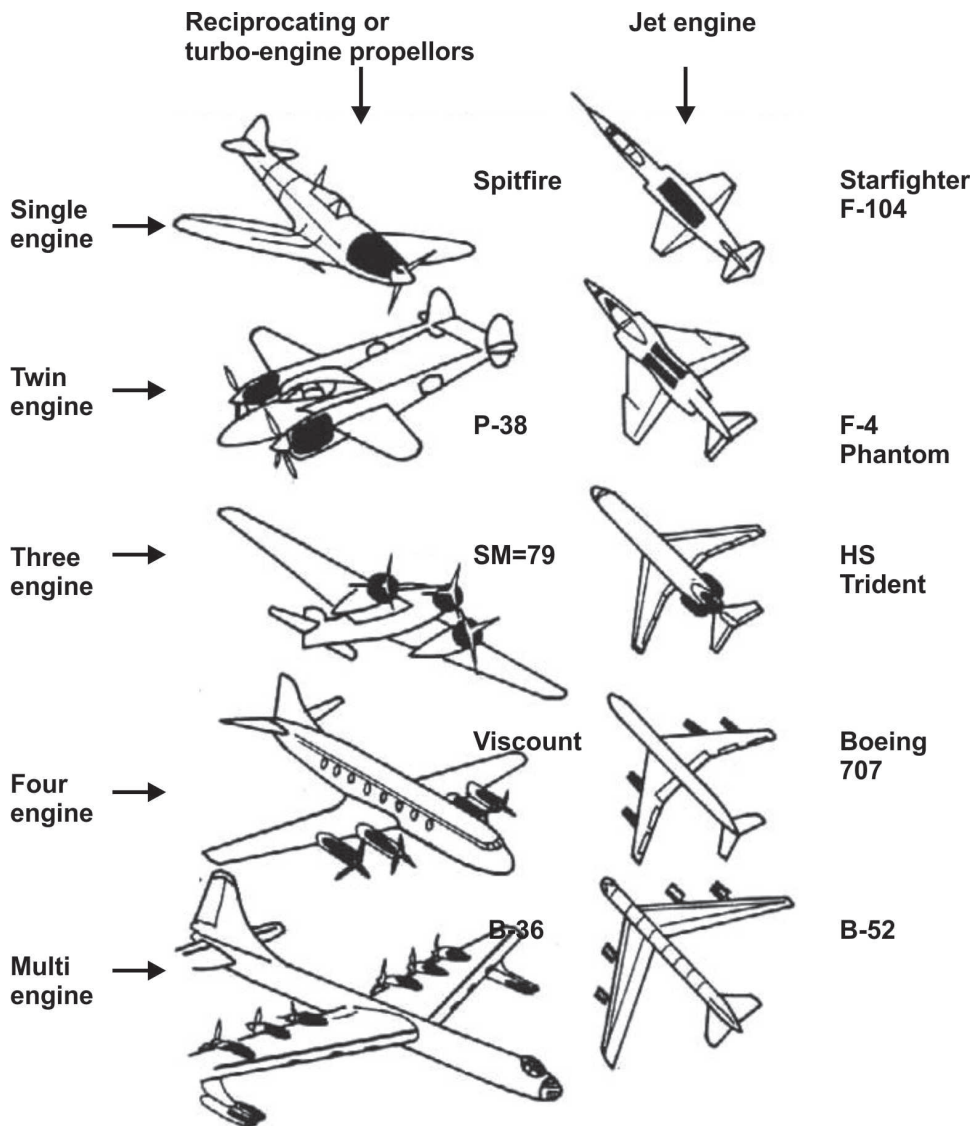**Four engine** — Viscount / Boeing 707

Multi engine — B-36 / B-52

Figure 3.12.: Possible engine locations on an aircraft: left - propeller engines, right: turbine engines

3.14. The Non-airbreathing Engines

Non-air breathing engines came into being in an effort to provide flight outside the atmosphere or large thrust for short or ultra short durations (like fractions of a second) for missile applications and precede air breathing engines. The only way of achieving these was to avoid dependence on the ambient air for the purposes of exothermic oxidation and use more exotic oxidizers of high density to facilitate obtaining high energy density. Rocket engines do this precisely. They dispense with air of the ambient atmosphere. As a result of this, they can provide thrust even in outer space devoid of air. They carry their own oxidizer and fuel. The argument that air compressed to say a thousand atmospheres to achieve densities comparable to solids or liquids in favor of air is dispensed with by the consideration of two features. First, compressed air needs to be stored in a vessel. The weight of the vessel will indeed be significant because of the high pressures. Instead, one can use a solid or liquid so that storage does not call for a vessel with high pressure and hence, lesser weight. Second, Nitrogen in air does not contribute to energy, but absorbs whatever energy is released because of the reaction of oxidizer with fuel. Hence, one can eliminate the molecular nitrogen in the oxidizer and use in this case, for instance, liquid oxygen. Indeed, it was the oxidizer thought of by early rocket pioneers; it has since been used extensively for boosters based on liquid rockets. Another feature with rocket propellants is that many of them are compounds composed of both fuel and oxidizer elements. Depending on the relative weightage of the fuel and oxidizer, the compound will express itself as fuel or oxidizer.

All rocket motors generate thrust by expanding hot gases through a nozzle. The thrust of a rocket motor is given by

$$F = \dot{m}V_e + Ae\,(p_e - p_a) \qquad (3.6)$$

where $\dot{m}$ is the mass flow rate of gases (kg/s). V_e is the exit gas velocity (m/s), Ae is the exit cross sectional area (m²) and $(p_e - p_a)$ is the pressure difference between the exit and the ambient (N/m²). The above equation is different from the one for air-breathing engines in the sense that there is no inflow of air-stream and hence, the contribution of inflow momentum is zero here. The magnitude of the second term in equation (3.6) constitutes no more than a few percent of the first term in most well designed situations.
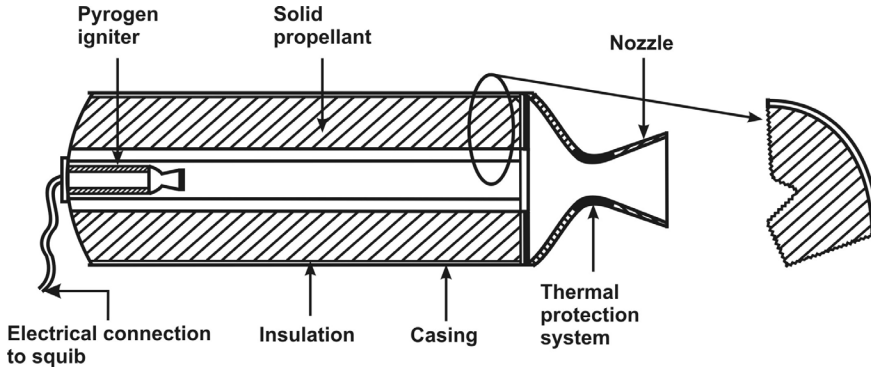
Figure 3.13.: Elements of a solid rocket engine

Typical exit speeds are about 2 – 4 km/s, being more close to 2.5 km/s in solid rockets and about 4 km/s for full cryogenic liquid rocket engine. This implies that one kg/s of flow rate gives a thrust of 2 – 4 kN. The single most important parameter characterizing the performance of rocket engines is the thrust per unit propellant mass flow rate or impulse per unit mass of the propellant, denoted as the specific impulse (I_{sp}). The exit speed is in itself a measure of the performance.

The specific impulse depends on two features: The energy of propellants as expressed through what is termed the characteristic velocity ($c*$, m/s) and a quantity called thrust coefficient (c_F) describing the nozzle expansion process. The relationship between the three quantities is described by

$$I_{sp} = c* \, c_F \tag{3.7}$$

where $c* = \sqrt{RT_c/\mathcal{M}}$ / $\Gamma(\gamma)$, R = Universal gas constant = 8314 m²/s²K (also J/kg-mole K), T_c = Temperature of gases in the combustion chamber (K), $\mathcal{M}$ = Molecular weight of the gases. $\Gamma(\gamma)$ = 0.62 to 0.6 for γ between 1.15 to 1.25 covering most rocket engine operating conditions. The thrust coefficient, c_F is expressed as

$$c_F = f(p_c/p_a, \, A_e/A_t, \, \gamma) \tag{3.8}$$

Where p_c and p_a are the chamber and ambient pressures. A_e/A_t is the nozzle exit to throat area ratio.

As I_{sp} depends on nozzle expansion process, any statement of its magnitude in a specific case must involve the explicit indication of the chamber and ambient pressure as well as A_e/A_t. If, however, the nozzle expands the gas to the ambient pressure, the area ratio need not be indicated as it gets fixed by the condition of complete (or optimum) expansion. For solid rocket motors and liquid rocket engines in many instances, p_c = 1000 psi or 70 atm or 7.1 MPa is taken as a reference pressure, $p_e = p_a$ = 0.1 MPa for the case of optimum expansion. In many cases where the engine operates in near–vacuum conditions at very high altitudes, a term known as vacuum specific impulse is used. In the case p_a = 0, one needs to know p_c as well as area ratio A_e/A_t for the interpretation of actual values.

3.15. Solid Propellant Rockets

Solid rocket engines are traditionally called solid rocket motors. The rocket motors are classified based on the physical state of the constituents of the solid propellant used in these motors. A homogeneous combination like nitrocellulose (fuel) and nitroglycerin (oxidizer) has been used as a solid propellant for a long time for military applications. As different from this kind, heterogeneous propellant (also, a composite propellant) that uses a solid oxidizer like ammonium percholorate (AP) and a polymeric fuel like hydroxy terminated polybutadiene (HTPB) has been developed and extensively used in the last four decades because of much higher performance. The typical elements of a solid rocket engine are shown in Figure 3.13. The outer shell can be of metal or fibre reinforced composite material. Between the propellant and the wall is the insulation. The face towards the nozzle end may have an inhibitor. Inhibitor is a polymeric material which is chemically bonded to the propellant so that the exposed surface does not burn. If the surface is covered with a 'fuel', then no combustion can take place in this zone. The nozzle, as indicated earlier, is the element of convergent-divergent construction which expands the hot and high pressure gases to low pressures nearly equal to the ambient pressure. In this process gases acquire high velocity at the exit so that thrust is generated.

Most solid rocket motors are single start systems. No controllability or re-startability is possible. However, some systems do have restartability and different levels of thrust in pulse mode (see Janes All World Aircraft, 1977-78).

Another important element of a solid rocket motor is the igniter. Igniter can be a bag of pellets of a composition, usually, having higher metal loading (40 – 60 %). It has also an initiator and a squib which is essentially a nichrome or similar wire coated with a heat sensitive composition. On the application of a current of about one ampere, the wire becomes hot and the heat sensitive composition bursts into a flame. This then causes the main igniter composition to burst into a much larger flame. The products consisting of hot gaseous products as well as hot metal oxide particles impinge on the surface of the propellant and cause ignition of the main propellant. While small rockets work with igniters of the kind noted above, large rockets have smaller rockets with igniter composition to cause ignition. These are called Pyrogen igniters.

The ignition systems of modern boost motors have safe arm devices and protection against electromagnetic interference (EMI). In some designs, the ignition current is not initiated until the current exceeds several hundred amperes essentially to protect against EMI.

Solid propellants have high density and reasonable specific impulse. Double base or homogeneous propellants have a density of 1500 kg/m^3 and specific impulse of 2000 – 2250 N-s/kg and are used in tactical military arsenal. Composite propellants have a density of 1700 – 1790 kg/m^3 and a specific impulse of 2400 – 2500 N s/kg. They are largely used in strategic military vehicles or launch vehicles for space applications.

Solid rockets have been built to produce thrust of no more than a few Newtons to as much as several hundred kilo-Newtons. The burn time varies from a few milliseconds to as much as thousand seconds. The applications of solid propellant rockets vary from those required to cause impulse for structural response analysis (systems called Bonkers) through auxiliary power generating units in missiles to missile and launch vehicle propulsion systems.

A good historical account of the development of solid propellant rockets in India can be gleaned from Rajaram Nagappa (2014).

3.16. Liquid Propulsion Systems

There are many types of liquid propulsion systems. They can be based on a single liquid which decomposes in the presence of a catalyst to hot gases which expand through a covergent-divergent nozzle to produce thrust. These are called mono-propellant thrusters. They are usually limited to low thrust and relatively small durations during each firing.

As different from them, there are bipropellant thrusters which use two liquids in which one is a fuel and the other oxidizer. These rockets vary in size from small to very large, many can be restarted and some are of variable thrust. The bipropellant thrusters are further classified in two different ways depending on whether (i) they form a self-igniting (called hypergolic) combination or otherwise and (ii) they storable at ambient conditions or they need special facilities for storage.

Many fuels like amines–aniline, xylidine, triethylamine and hydrazine and its derivatives like unsymmetrical dimethyl hydrazine and monomethyl–hydrazine are all hypergolic with white fuming nitric acid (having 4 – 6 % nitrogen tetroxide), red fuming nitric acid (having 10 – 14 % nitrogen tetroxide) or nitrogen tetroxide which are the oxidizers. All the above propellants are earth storable (storable under normal earth conditions without any special equipment). The fuel-oxidizer combination like liquid oxygen-liquid hydrogen is non–hypergolic and cryogenic, i.e. they need carefully insulated low temperature storage vessels. The combination liquid oxygen–kerosene is non-hypergolic and semi–cryogenic in which liquid oxygen alone needs low temperature storage. Some unusual combinations like ammonia–liquid oxygen have also been used in some rocket engines (X-15 Research Aircraft).

Every propulsion system has two elements – a feed system and a thrust chamber. The feed system in relatively small impulse rockets are fed by using a high pressure inert gas source on board. Large impulse rockets are turbo pump fed. Most monopropellant rocket engines are pressure fed due to the additional need for reliability. Figure 3.14 shows the elements of a monopropellant rocket. The feed system consists firstly of high pressure inert gas storage. The inert gas can be either nitrogen or helium (to reduce the weight of the gas). The pressure at which the gas is stored is 300 – 350 atm essentially to reduce the total weight of the feed system. The pressure is dropped to levels of 20 – 40 atm
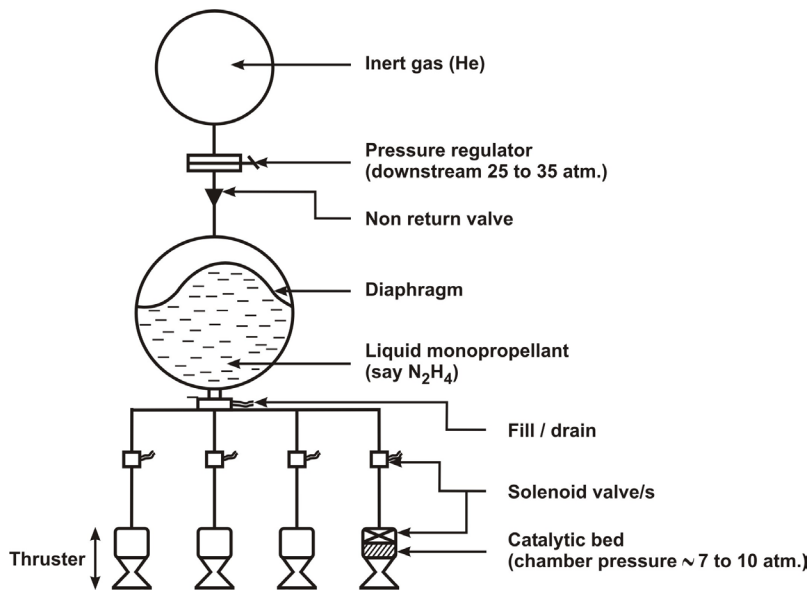
Figure 3.14.: A Liquid Monopropellent Thruster System

(depending on the design) through a pressure regulator and the gas pressure is applied on the surface of the liquids in the container of the liquid propellant.

Since many monopropellant thrusters are used for space applications involving zero gravity, the feed systems involve positive expulsion devices. Bladders made of teflon or EPDM (Ethylene-Propylene Diene Monomer) over which gas pressure is imposed was a conventional technique. The liquid is expelled independent of the orientation of the vehicle or space craft. A more recently developed device is the surface tension acquisition device having high expulsion efficiency (~ 99 % or better).

The thrust chamber receives the liquid from the tank through a solenoid valve which serves the purpose of being set on or off. The thrust chamber has an injector which atomizes the liquid to fine droplets which impinge on a catalytic bed. The catalytic material is porous alumina pellets of 2 to 6 mm dia with a coating of noble metals like Iridium. The catalytic bed is packed between meshed screens. The exit of the screen becomes the entry to the convergent-divergent nozzle. The mono-propellant thrusters have a thrust as low as 0.1 N
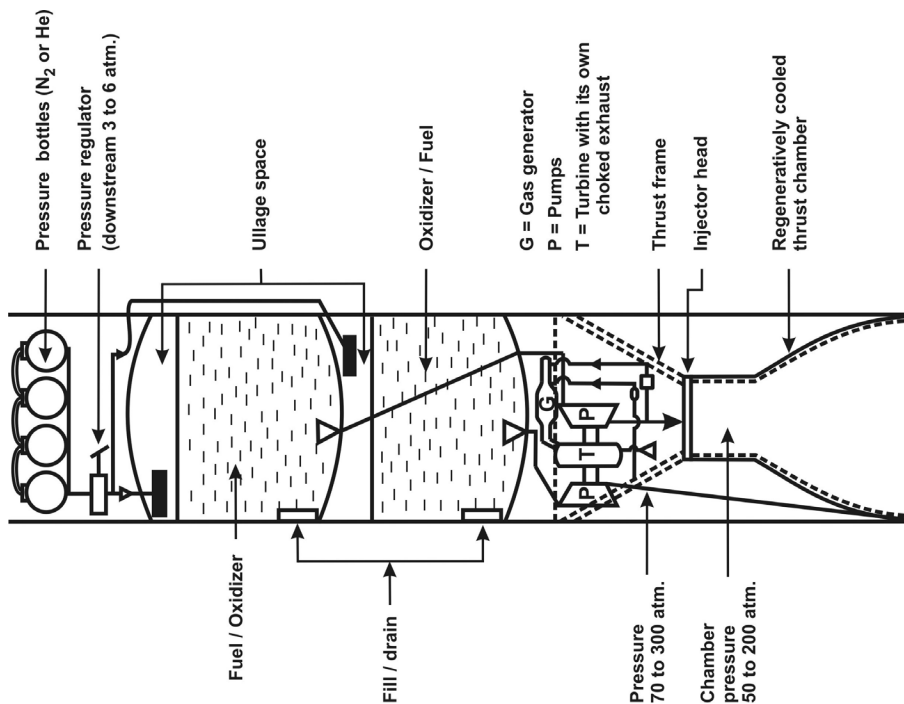
Figure 3.15.: Schematic of a bipropellant turbo-pump fed liquid rocket engine

to as much as 20 N. The duct carrying the liquid monopropellant in a 0.1 N thruster has a diameter of 200 μm. The diameter of the thruster is about 1.5 mm. The thruster is maintained at temperatures up to 300^0C to ensure smooth start-up and long life.

To start the system all that one does is to open the solenoid valve which allows the liquid monopropellant to flow into the thrust chamber, decompose and pass through the nozzle to produce thrust. Shutting off the solenoid valve automatically cuts off the flow and causes thrust to decay to zero. For high thrust engines, the fact that the tanks need to have high pressure in pressure fed engines, will imply excessive weight of the feed system. For dealing with this, the tanks are maintained at relatively low pressure (5 to 6 atm) and the fluids pass though pumps which raise the pressure to as much as $80 - 450$ atm.

The high pressure fluids pass on then to the thrust chamber through valves operated hydraulically or pneumatically. Figure 3.15 shows the various elements of a turbo pump fed system. While the pressure fed system can start with the opening of valves, without any other system element entering into picture, in the case of turbo-pump fed system, the pumps have to be spun by running the turbine. The source of power for running the turbine can be several. One of these is a separate monopropellant gas generator; a separately pressure fed tank supplies the liquid at the predesigned rate to a combustion chamber; the gases from the combustor at temperatures not exceeding 1200 – 1400 K at reasonably high pressures (30 – 40 atm) are led into the turbine for extraction of work. In another scheme that is more extensively used, the fluids from the outlet of the pumps are drawn-off in predesigned amounts and delivered to a combustion chamber usually termed gas generator. The oxidizer-to-fuel ratio used here is far off-stoichiometry to limit the temperatures to no more than 1400 K keeping the operation of the high speed turbine in view. The second system is called boot–strap system as it draws off the fluids from the main system itself.

There are two methods of starting of the turbo pump system. The conventional system is to spin the turbine with hot gases from a separate small solid propellant cartridge that burns up in a few seconds. Once the turbine has reached enough speed, a separate liquid monopropellant stream injected into the gas generator decomposes exothermically and maintains the condition for steady operation. Alternately, one could derive a part of the fluids that are delivered by the pumps and introduce them into the gas generator for ignition and combustion leading to steady operation.

A second strategy is to allow the fluids to flow under the pressure of the storage vessel (maintained at 3 – 6 atm in the tanks) rotate the pumps as they flow into the combustion chamber. Subsequently a control system will keep metering amounts of fuel and oxidizer from the outlet of the pumps into a gas generator, the gases from which keep feeding power through the turbine into the pumps. In large thrust engines, this operation usually takes 2 – 4 s till the steady full thrust is achieved.

Liquid engine combustion chambers and nozzles experience high temperatures and high flow rates and added to this, the high pressures of the combustion chamber contribute to high heat fluxes. The walls of the thrust chamber are

therefore to be thermally protected. There are several techniques for keeping the walls of the thrust chamber relatively cool. By design, the mixture ratio near the outer periphery is arranged somewhat fuel rich so that temperatures are lower. In addition, fuel jets may be directed towards the wall to allow vaporization processes to occur to keep the wall zone cool. In some designs, one might have an ablative layer. In others, the internal portions of the nozzle may be coated with ceramic. In most high thrust engines one adopts what is known as regenerative cooling. In this technique, the fuel or the oxidizer with better cooling capacity is passed around the chamber at relatively high velocities with heat transfer occurring across thin walls. The liquid extracts the heat and later enters the combustion chamber. This technique is used in very long duration and high thrust engines and provides excellent performance.

Typical single chamber thrusts can go up 6.8 MN as in the case of F 1 engine used on the Apollo mission to moon. In the case of high pressure engines the chamber pressure goes up to 200 atm as in Space Shuttle Main Engine (SSME). The burn times of the booster rockets go up to 120 – 160 s. In special cases, they can be extended up to several minutes mostly limited by the volume of the propellants in the tankage. Table 3.8 summarizes details of some of the liquid rocket engines of the world. The thrust to engine weight is about 50 to 90 for regeneratively cooled engines, but is about 15 for Vikas engine. This low thrust-to-weight ratio is due to the use of ablatively cooled thrust chamber.

3.17. Hybrid Rocket Engines

Hybrid rocket engines are those which use liquid oxidizer and a solid fuel. The other possibility namely, solid oxidizer and liquid fuel is not common because the solid oxidizer, usually is a crystalline powder and cannot be produced in a mechanically acceptable form. The liquid oxidizers used are nitric acid in the white fuming or red fuming variety, nitrogen tetroxide, hydrogen perox ide or liquid oxygen. The solid fuels which are hypergolic with nitric acid or nitrogen tetroxide are not easy to make and not well known. Liquid oxygen with polymeric fuels have been used to develop semi-cryogenic hybrid rocket engines. Figure 3.16 shows the typical elements. The liquid oxidizer is atomized and sprayed over the fuel block. The oxidizer content of the hot product gases decreases along the port and the length of the grain. Two issues in this comb-
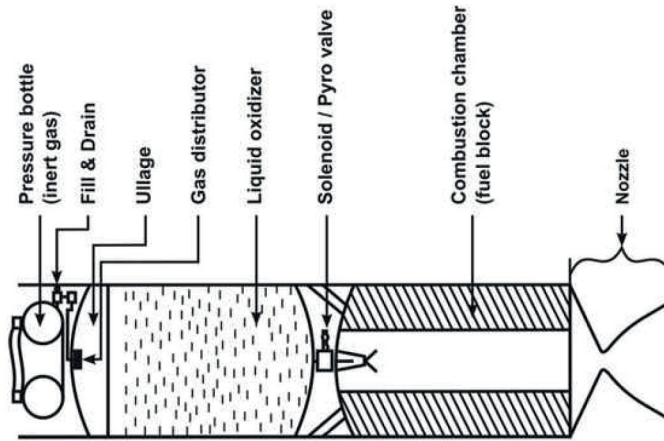
Figure 3.16.: Schematic of Hybrid rocket with a solid fuel and a liquid oxidizer

Table 3.8.: Liquid Rocket Engines; M_{eng} = engine mass, LOX = liquid
oxygen, LH_2 = liquid hydrogen, RP1 = Kerosene, U-NTO = UDMH-N_2O_4

Engine	Vehicle	Country	Thrust	Prope-	I_{sp}	p_c	M_{eng}
			MN	llants	kNs/kg	atm.	t
HM7	Ariane	France	0.07	LOX/LH$_2$	4.25	35.0	0.15
J 2	Apollo	USA	1.04	LOX/LH$_2$	4.20	55.0	1.58
F 1	Apollo	USA	6.86	LOX/RP1	2.61	76.3	8.35
SSME	Space shuttle	USA	1.87	LOX/LH$_2$	4.65	299.0	3.53
Vikas	PSLV, GSLV	India	0.73	U-NTO	2.95	54.0	5.10

ustion process are: (i) mixing of the oxidizer rich and fuel rich gases across the diffusion flame occurs much later than the length of the fuel grain and (ii) small fuel regression rate. The first issue is resolved by adding mixing devices and the second issue by adding a certain amount of oxidizer into the fuel. Hybrid rocket engines retain the advantage of controllability like liquid rockets because of the fluid line and are simpler compared to liquid rockets because of a single fluid line. Specific impulse comparable to liquid and solid rocket engines have been achieved.

While most of the current developments have been devoted to sounding rockets, ideas about their benefits for launch vehicle applications keep appearing

in literature. It has been used in the first space vehicle developed by Space-ShipOne industry (see section 1.4 in Chapter 1). The development of hybrid rocket engines has not attracted the attention of major propulsion system designers essentially because both solid and liquid rockets were in an advanced stage of development by the time the combustion behavior in hybrid rocket engines that affects the performance was understood. The higher safety of the hybrid rocket engine in comparison to solid or liquid rocket engine is due to the fact that the fuel is solid and the oxidizer is held separated from the fuel. The most powerful oxidizer, liquid oxygen that may be contemplated for use due to performance benefits is handled in many commonly known industrial uses and hence, is understood much better for safe handling. The added safety is an attraction for use of hybrid rockets in situations calling for safety similar to civil aircraft operations. There may be possibilities for their use in single stage-to-orbit vehicles providing low cost access to space.

3.18. Thrust Vector Control

Thrust vector control is a principal demand of military aircraft, missile and satellite launch vehicles. It is needed because the flight path of a military aircraft or missile is determined by the military operational scenario - a moving target, usually. Satellite launch vehicles and even larger size missiles launched from ground (IRBM and ICBM class) move at very small speeds during the time they leave the launcher. At these speeds, due to possible thrust axis differences and wind effects there will be flight path instabilities. Aerodynamic control is ineffective at these speeds necessitating an on-board thrust vector control of the propulsion system.

3.18.1. Rocket engines

The very first such thrust vector control system was developed and implemented on V-2 missile. Figure 3.17 shows the system deployed on V-2 rocket on the left most figure and it is schematically represented in the middle figure. Jet vane is a standard thrust vector control system for many tactical missiles even today. It consists of four fin-like control surfaces attached at the base to a high torque motor that moves on command from the guidance system. When the control surface rotates around the base, the flow is intersected asymmetrically and so a lateral force is created.
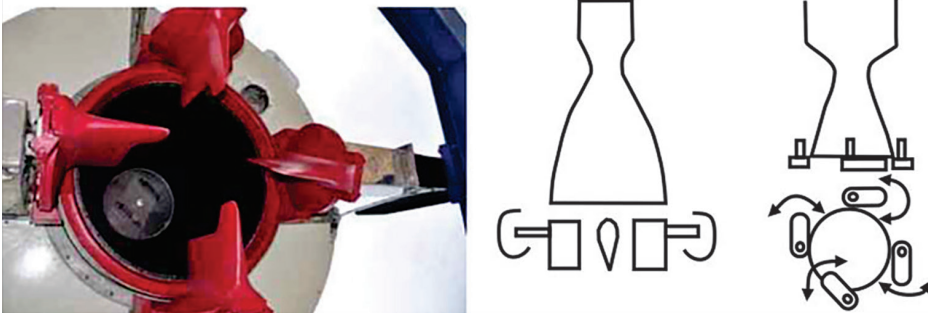
Figure 3.17.: Jet vane system on V-2 rocket and its schematic; the last figure is Jet tab

By moving two control surfaces 180 degrees apart in the same manner, one gets control force that can be used for pitch-up or down and the other two to provide lateral movements. By operating the surfaces 180 degrees apart asymmetrically, one can get rolling moment. Thus all possible control forces can be derived from this approach. The negative aspect of this device is that it has to be in the flow field all through even when no control is demanded leading to a performance degradation due to shock losses. Also, the high temperature, high velocity condition demands a suitable material. Typically, high density graphite is used. The right most sketch is of Jet tabs. In this approach, there are four surfaces located outside of the nozzle and will be brought into the flow field whenever control force is demanded. Thus, there will be no performance loss when control force is not demanded. There are variations in the geometry of the tabs conceived and implemented.

Larger rockets use flexible nozzles to enable directing the thrust vector. Normally, this approach is deployed for rockets in upper stages of launch vehicles and are used for flight path correction. Figure 3.18 shows the details of the flexible nozzle used on upper stages of solid rockets. The flexible assembly consists of alternate layers of special rubber and metal segments bolted together in a manner that any rotation at one end can compress or expand the other end. In order to protect it from the severe thermal environment, a flexible "thermal boot" is located just around the flexible segment. This ensures that the flowing hot gases are kept away from this flexible segment and there is a reduction in
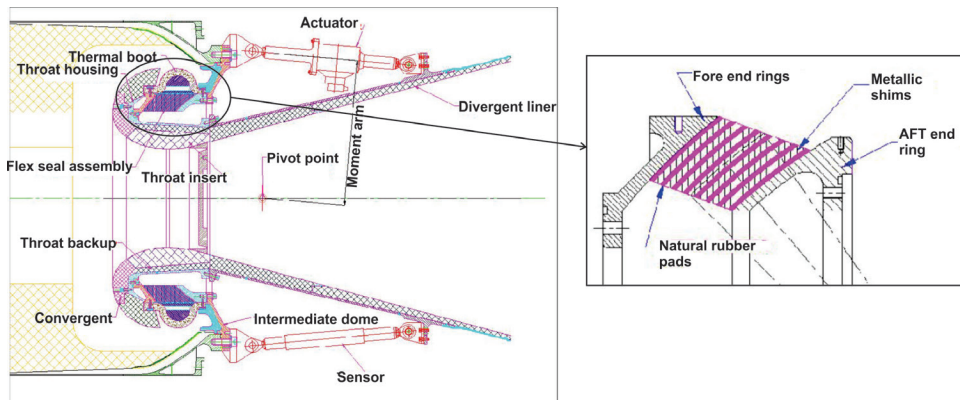
Figure 3.18.: The flexible nozzle on a typical upper stage solid rocket motor; the inset shows the details of the flexible assembly

the radiation received from the high temperature of the gases (~ 3500 K). The flexible seal material should have low spring torque, high shear strength and small axial compression. Typical vectoring capability is about ± 8⁰. Such systems have been built and successfully used for space and defense applications in many countries including India (third stage of PSLV vehicle).

Very large rocket motors using (liquid) side injection thrust vector control (SITVC) inject the liquid at some angle to the flow into the divergent section of the nozzle as in Figure 3.19. The demand on the control forces is limited to a duration when aerodynamic fin control on the vehicle is yet to become effective because of insufficient flight speeds (or equivalently, wind speeds with respect to the vehicle).

A reactive liquid oxidizer (strontium perchlorate is one option used on SLV and PSLV vehicles) is stored in a high pressure vessel that receives regulated high pressure inert gas (nitrogen). This liquid is discharged through one or more of the orifices into the divergent section of the operating rocket nozzle. The injection causes shock wave structure to be formed ahead of the liquid jet as shown in Fig. 3.19. This causes the pressure to become higher than that ahead of the shock region in a curved segment on the nozzle. The asymmetric distribution of the pressure leads to the generation of a side force towards the injection region. The number of injection holes is four or more, typically eight. By injecting at
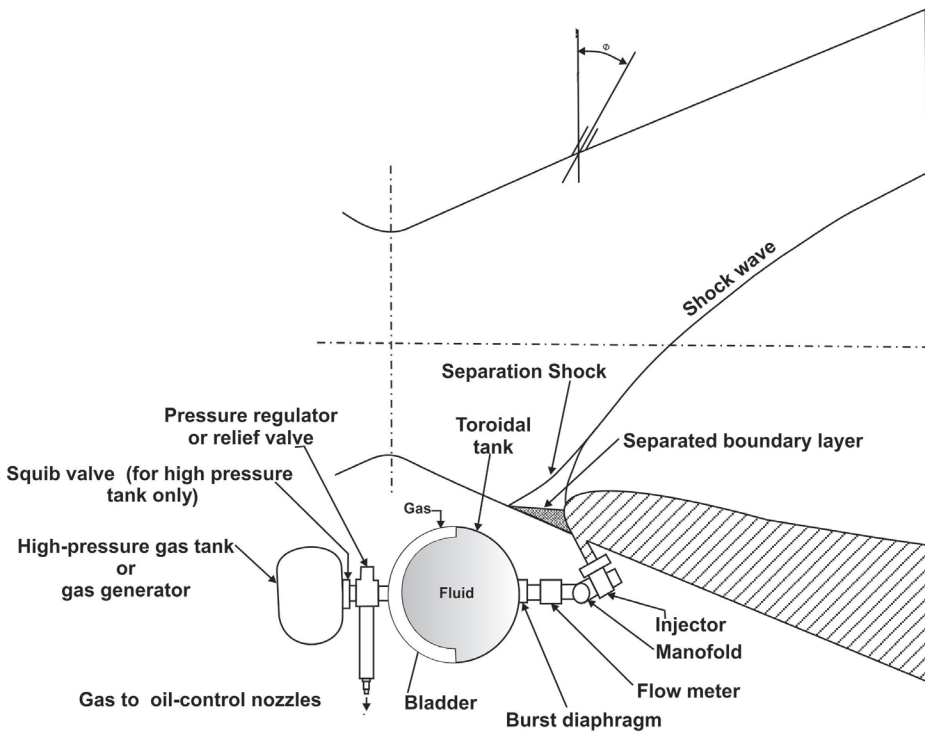
Figure 3.19.: The schematic of liquid injection thrust vector control and the fluid flow features

points next to each other the side force can be aligned to a zone in between. Since the hardware associated with SITVC adds to the lift off mass, optimization requires the estimation of disturbances. Most usually, optimization occurs with experience over several flights.

For liquid engines, the control arrangement is different. While in solid rockets, the propellant is inside the combustion chamber and the nozzle is attached to it, in the case of liquid rocket engines, the propellants are stored separately in tanks and the thrust chamber (consisting of an injection head, combustion chamber and the nozzle) is a separate unit connected to the propellant supply tanks through high pressure plumbing. Thus, for thrust vector control, jet vanes can be used in smaller thrust systems or the entire thrust chamber can

be gimballed around a pivot joint using hydraulic servo systems. In the case of large rocket engines, one can have separate small thrusters around the main engine outside the main engine and they can be controlled using a gimballed arrangement. They may use a separate set of propellants or draw from the main system. If the propellant combination is hypergolic, no additional ignition strategy is needed.

3.18.2. Aircraft engines

Aircraft depend on aerodynamic surfaces for control, civil aircraft being the example. Military aircraft needing vertical take-off and landing (VTOL) or short take-off and landing (STOL) can benefit from thrust vector control. One early aircraft, the British Harrier built in the late nineteen seventies (see Wikipedia, 2016), has a thrust vectoring system shown in Figure 3.20. A single Pegasus turbofan engine mounted in the fuselage is fitted with two air intakes and four vectoring nozzles for directing the thrust generated: two for the bypass flow and two for the jet exhaust. In order to balance the moments during vertical flight, small reaction nozzle systems are fitted in the nose, tail and wingtips these being brought into operation by the control system.

For other military aircraft whose combat performance is continuously being improved by many nations, use of thrust vectoring is considered unavoidable. It alows the aircraft to enter and recover from a controlled flat spin, yaw being executed even if rudder is ineffective as it usually happens at high angles of attack. Even for aircraft with canard wings use of thrust vectoring reduces drag during level flight, thus improving the operational effectiveness. The more recent developments both in the USA and Europe applied to F119, F22, F16, Rafale and Typhoon benefit from ideas of geometry controlled two-dimensional and axisymmetric nozzles. Typical strategies are set out in Figure 3.21.

Since military aircraft always have an afterburner to provide for short-duration bursts of thrust for take-off or get-away, nozzle throat control will be an essential part of the engine. This is arranged such that the operation of the after burner does not affect the core engine operating point. The system arrangement for nozzle exit area-to-throat area optimization is carried out in a very limited way. As different from this, arrangements with "three rings" to control the throat and exit area along with swivelling the entire nozzle around
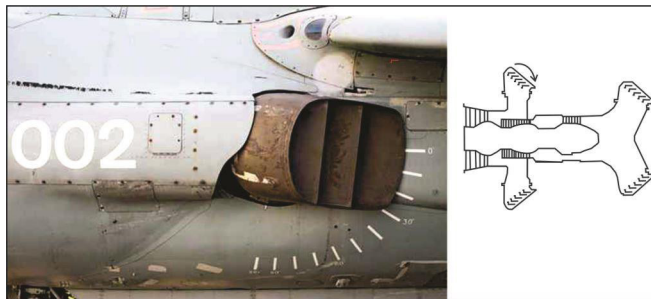
Figure 3.20.: Thrust vector control system of Hawker Siddley Harrier aircraft built in the sixties - the left shows the picture of the actual system and the right is a schematic, adapted from wikipedia (2016)

to provide complete three-dimensional thrust vector control are also conceived.

The availability of optimal and reliable thrust vector control can be conceived as an opportunity to reduce the control surface areas aiding the reduced total mass of the aircraft. The three-dimensional control strategy shown on Fig. 3.21 (d) has a large number of petals put together in a manner that through articulation of rings and hydraulic powered plungers, one gets the direction, the nozzle throat area and expansion. There could be some loss of expansion through petal spacings which need to be accepted. While F22 uses rectangular nozzle shapes with divergence control of two surfaces, Typhoon depends on three-dimensional control.

While undoubtedly, the low speed high angle-of-attack as well as high speed high altitude performance are improved significantly by the use of thrust vectoring (Smolka et al, 1996), the extent of thrust vector control required vis-a-vis aerodynamic surface control is being debated and future military aircraft may evolve through these debates and considerations (see Cenciotti, 2013; Picard578, 2013). One of the arguments being made is that aircraft doing exotic maneuvers with thrust vector control like the Cobra maneuver (as with Sukhoi 30 aircraft, see Fig.1.15, something that has been accomplished later by F22 and other aircraft as well) is that subsequent to this, the energy loss in this process makes the aircraft more vulnerable in a combat situation when the opponent is aware of this possibility.
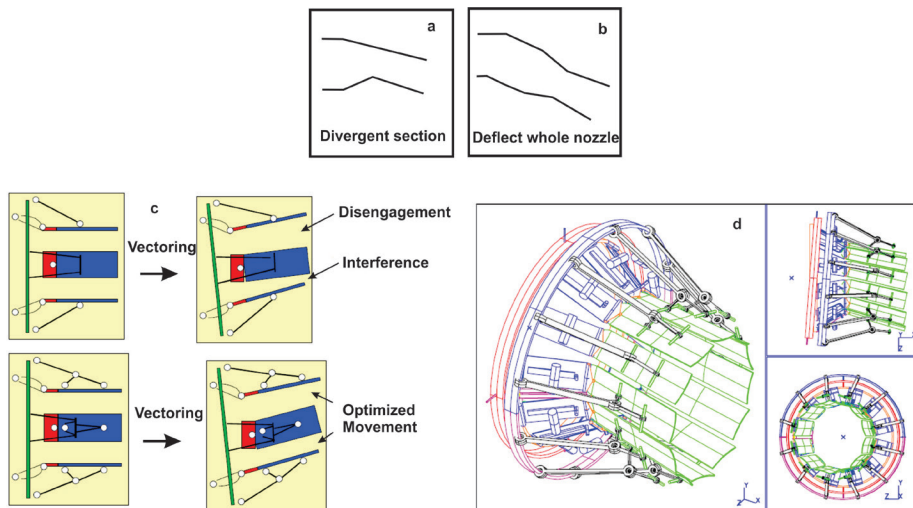
Figure 3.21.: Thrust vector control system strategies: (a) divergent section control, (b) all nozzle control, (c) geometric details of divergent section control and (d) geometric details of all nozzle control

3.19. Modes of Combustion

Most of the combustion process occurs in gaseous phase. When liquids or solids are used, vaporization or pyrolysis is the first step. In the gas phase, there are essentially two modes of combustion - diffusive and premixed. In the diffusive mode, mixing between fuel and oxidizer vapors will be the limiting feature for the combustion process. Reaction rates and hence heat release rates are comparatively large and hence, the rates of conversion will be dependent on mixing. In several instances, the vaporization process itself will be the limiting feature. Kerosene combustion in gas turbines is vaporization limited as also for bipropellant liquid rocket combustion, both of which can be analyzed as a diffusion limited process. Composite propellant combustion in which fuel and oxidizer are separate constitutes classical diffusive mode of combustion. But fine particles of ammonium perchlorate decompose and mix with the binder and this leads to premixed class of behavior over some pressure range. Hence AP-Polymer propellants show up a behavior that is a mix of diffusion and pre-mixed controlled aspects.

On the other hand, the combustion process in a DB solid propellant is of pre-mixed nature, because fuel and oxidizer elements are mixed on a molecular

scale and the mixing process is not rate limiting. In this case, it is the rate of chemical reactions that controls the burn rate. Burn rate controlled by diffusive process shows weak pressure dependence and that controlled by premixed process have stronger pressure dependence.

Reactions do not proceed in one step from reactants to products as one may presume. The pathways are complex and even a simple chemistry like H_2 - air reaction scheme has seven reversible reactions and seven species - H_2, O_2, OH, HO_2, H_2O, N_2, NO. One can simplify these to six species if NO formation is dropped. If C-H-N-O system is adopted as is necessary for most applications, one needs a minimum reaction set of about 30 reactions and eleven species. Computation of flows with complex chemistry is beset with accounting for rates that vary over an order of magnitude and therefore, demands very small time steps and so, is very expensive. When one is interested in heat release distribution, it may be adequate to make a choice of fast chemistry option or in some instances, simplified chemistry models.

3.20. Computing Combusting Flows

Computing reacting flows is more complex and time consuming compared to non-reacting flows. This is because (a) the number of variables to be computed is enhanced by the number of species to be accounted and (b) the non-linear chemistry term that has sharp gradients - the zones of combustion are very thin because the operating conditions lead to high heat release rates. Precisely because of this, in some approximations, one uses a thin-flame approach in which an ideal thin flame zone separates reactants on one side and products on the other. It is not that computation offers any great simplicity; but the time it takes to compute specific problems is made simpler. The next step is to treat a single step chemistry. The choice of the pre-exponential factor and the activation energy are very important and care needs to be exercised in this choice. While literature provides many guidelines, one sure approach would be to validate the choice against some standard relevant cases before using the data for practical prediction. Different levels of accuracies need to be aimed at in different cases. We will examine these in the case of each of the engines.

3.20.1. Ramjets and after-burners

In analyzing the performance of a ramjet, it is adequate to use a cycle analysis treating the property (pressure, Mach number, and Temperature) at each point -inlet, exit of the diffuser and inlet to the combustion chamber, exit of the combustion chamber and inlet to the nozzle and the exit of the nozzle as a variable for performance evaluation. Ground tests will help determine any lacunae in performance - usually reduction of combustion efficiency, or a local hot spot. Usually, an examination by the design team and some intuitive analysis allows corrections to be made to the hardware and next test follows. A couple of tests may be adequate to obtain the features of the hardware that is acceptable to the project team from the point of view of combustion. Many successful designs were built this way over the last fifty years.

In the recent past, several investigators have done a computational fluid dynamic study on this system. The non-uniformity that arises at the section where the air flow is introduced into the combustion chamber usually in a part-symmetric manner comes down in a distance of 3 d_c (combustor diameter) without combustion and about 5 d_c with combustion. The non-uniformity is not deemed as a major problem. The reduction in performance is usually due to spray being coarse or distribution inadequate. Both are amenable to intuitive understanding which is deployed with ease. Even when the problem is not resolved in the first few tests, doing a few more is usually not expensive or difficult and hence is done. In ramjets, therefore reactive flow computational fluid dynamics may be considered a luxury by the development team and is usually only of academic interest.

After-burners are combustion chambers similar to ramjets. The inflow is a hot vitiated air stream from the turbine exit at temperatures of about 600 to 700 K with the flow having non-uniformities including swirl. Here again, fuel is injected from struts and a separate set of struts are provided for flame holding. The exit of the gases is through a convergent or a convergent-divergent nozzle. Issues of development are similar to those of ramjets. The range of conditions over which an after-burner operates is much wider and expectations of performance more stringent. Hence, RCFD is performed as a tool to determine if decisions made on intuitive understanding are correct and as a prelude to more complex problems of instability. One problem that affects both

the devices is the high frequency instability - also called screech. The problem is far less severe compared to liquid rocket engines. A standard way of solving the problem is to provide a perforated sheet all through the combustion chamber, with the holes on the sheet tuned to absorb the energy in the frequency range around which the instability is experienced. This frequency can also be estimated relatively easily from the acoustics of the combustion chamber. This problem is also amenable to modern day CFD analysis of acoustics and CFD may become a valuable tool in shortening the development cycle.

3.20.2. Gas turbine main combustion chamber

Gas turbine main combustor is an incredibly complex device that burns mixtures outside the flammability limit producing a not-too peaky temperature profile at the exit of the combustor, a feature characterized by the smallness of a quantity called temperature quality factor. It reflects the difference between the peak and low temperatures in the gas. Ensuring Building such a device to function effectively over a range of mixture ratios constitutes a tall order. Predictions of emissions relevant only in the case of engines for civilian applications need a more careful accounting for chemistry. There are also simpler procedures for obtaining fuel rich and fuel lean zones using mixture fraction approach that does not involve chemistry and these are helpful in the improvement to the design of the gas turbine combustor.

The geometry of the combustor is also complex, some times with little space between the compressor and turbine to accommodate an in-line combustor (in which case, one uses a reverse flow combustor). Typical cycle time for the development of a satisfactory combustor used to be 60 months thirty years ago and it has become 18 months in the last three years. This incredible change has occurred largely because of RCFD and computational speed. Thirty years ago, there used to be rig tests on part combustion chambers with at least ten major modifications over several cycles. In recent times, there have been changes. The design starts a RCFD investigation for a new design in the back drop of a historical record of problems and solutions for several engines documented well. After some months of RCFD runs and discussions and modifications, a single hardware is built and test run. Only in one out of three cases would one need to create a different model for a rig and test run the system. It is being anticipated that the cycle time from specification to realization will be brought

down to 12 months. This remarkable achievement is one of the primary motivations for all to exploit RCFD.

3.20.3. Scramjet

There are issues in the design of a hypersonic vehicle using scramjets beyond those discussed in section 3.11. Fuel needs to be injected into the combustor that has supersonic flow inside with large enough static temperatures, and much larger stagnation temperatures. Avoidance of hot pockets near the walls implies that the fuel be injected from centrally located struts. The usual circular configuration for combustors is sacrificed in favor of a rectangular configuration. Typical velocities in the combustion chamber are about 1 to 1.5 km/s and the Mach numbers 1.4 to 2.3 for a typical combustor entry Mach number of 2.5. Local heat release leads to enhanced temperatures. This causes increased acoustic velocity $\sqrt{\gamma RT}$ and reduction in Mach number even if the local speed is unaltered. One can expect a non-uniform temperature distribution since the fuel sprays are introduced over parts of the cross section. This leads to non-uniformity in other quantities as well.

Even the pressures are not uniform since local shocks can create the mechanism for sustaining the pressure changes. The last feature is unlike subsonic flows where non-uniformity in temperature does not mean non-uniformity in pressure. To this we must add the feature that the inflow into the combustion system comes from an air intake that begins from the nose of the vehicle and decelerates through a series of shocks from the changes in the surface at the bottom of the vehicle that would be inherently non-uniform. In view of these features, the flow through the rectangular intake will be three-dimensional. Many geometric features like a step or a protrusion, wanted or unwanted will all make a significant difference to the flow field. The flow field over the vehicle at $M = 10$ would be reactive – significant dissociation of the air stream would take place. Enthalpy turns out to be more relevant parameter; at lower Mach numbers, enthalpies and temperatures have synonymous meanings. At the high enthalpies, significant dissociation occurs with addition of heat or passage of the fluid through a shock. Hence RCFD is very critical to the understanding and the design of the system. Whatever subsidiary aerodynamic or thermodynamic data that would be required for design on the computer could be obtained from separate experiments in hypersonic tunnels and shock

tunnels. RCFD is so critical that contemplating the design without CFD tools would be just impossible. One would want to fly the vehicle on a computer before the design is considered acceptable. Hypersonic propulsion could not have been built in an era where RCFD tools were not available.

3.21. Non-chemical Propulsion Systems

While the main stay of propulsion remains chemical, there are specific applications that make non-chemical propulsion systems advantageous when very low thrust is needed; if this can be delivered with high I_{sp}, it appears even better. Many applications such as station keeping of small satellites (the satellites are subject to random forces due to minor changes in gravity, solar activity generated pressure, random meteorite hits that need to be managed to maintain the orientation of the spacecraft) and planetary travel belong to this category. The propulsion systems are (a) nuclear rockets, (b) resistojets, (c) arcjets, (d) various types of ion thrusters and (e) plasma thrusters. Each of these is briefly described below.

(a) In the case of nuclear rockets, just as in the case of nuclear power generators, one can use radioactive decay, or nuclear fission (or fusion) energy, to heat a propellant medium like hydrogen (as the propellant) without combustion at high pressure which passes through a nozzle generating thrust. Solid-core nuclear fission rocket engines like NERVA deliver an I_{sp} around 9000 Ns/kg. The problem with nuclear rockets is related to perceived issues on nuclear safety on both technical and political fronts.

(b) Resistojet heats up a high electrical resistance metal coil based on tungsten that transfers heat to the propellant that flows over the metal coil. The hot gases then pass through the nozzle producing thrust. It is conceived that these can be used in conjunction with monopropellant thrusters so that heating the product gases to a higher temperature provides better specific impulse (from 2 kNs/kg nom-inal to 3 kNs/kg with resistojet). International space station uses this thruster for station keeping purposes.

(c) Arc-jets use a high voltage spark to break up the propellant to fine fragments reducing the mean molecular weight of the gases with effective temperatures about the same as in chemical rockets to produce thrust at I_{sp} of the order of 15 kNs/kg.
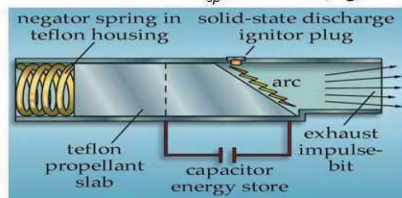
Resisto-jet propulsion system on international space station
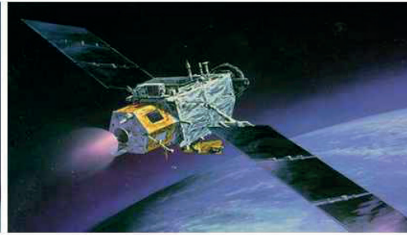
The Argos spacecraft, shown above, tested a 26 kW NH_3 based arcjet in orbit. 2 N thrust was delivered with I_{sp} of 8000 Ns/kg,

NASA's Deep Space 1 mission used an ion thruster for its primary propulsion. The engine operated at 2.3 kW producing a thrust of 0.09 N with I_{sp} of 3100 Ns/kg.

PPTs create a plasma by pulsing an electric arc over the surface of teflon slab . The induced magnetic field accelerates the plasma. As the teflon shrinks, the spring feeds it into the arc.

Figure 3.22.: Four types of non-chemical propulsion systems. Top left: Resisto-jet used on the international space station, Top right: The arc jet being used on a spacecraft (Ar-gos); Bottom left: Ion thruster used on NASA's deep space 1 mission; Bottom right: Pulsed plasma thruster in development

(d) Ion thrusters are characterized by the use of heavier positive ions of mercury, indium or cesium stripped of electrons, accelerate them in an electric field to produce the desired thrust. Electron bombardment thruster uses electron bombardment of propellant in storage to produce the needed ions. Ion contact thruster uses a hot ionizer to generate ions and colloid thrusters pass a colloid (small droplet) mixture through an intense electric field. These devices need to maintain a neutral charge on the surrounding spacecraft. For this purpose, a negatively-charged neutralizing cathode seeding electrons in the exiting ion stream to remove the positive charge from the ion beam is used. This leads to reduced performance.

(e) Plasma thrusters are characterized by use of neutrally charged plasma (mix of electrons, positive ions, neutral atoms) produced from electrically heating a propellant in storage accelerated by techniques exploiting electric and magnetic fields. Inert gases like xenon and krypton are a common propellant choice. One technique uses the Hall effect to accelerate the plasma. Hall effect is a force resulting from an axial electric field in the presence of a radial magnetic field, with a spiral movement of electrons (Hall current) aiding the force development, in addition to keeping the plasma beam neutrally charged at the exit. There are also pulsed plasma thrusters (PPT) that use the plasma to vaporise and breakdown molecules of a material like teflon and accelerate them using the induced magnetic field to generate thrust. The advantage of these thrusters is that the energy required can be obtained by charging capacitors over a long time with low power generators and then discharging the energy over a brief period during which the corrective force is generated. Though their electrical efficiency is low (~ 20 %), they produce thrust in the range of 0.01 - 1 mN with I_{sp} of 7 to 15 kNs/kg. Figure 3.22 shows four of the types discussed above.

Many more details of these propulsion systems can be found in Humble et al (1995) as well as Wertz and Wiley (1999).

3.22. Summary

In this chapter, the various propulsive devices in current existence are described. Their evolution, from devices first built – namely propeller driven devices has been brought out. Piston engine-propeller systems were the first set of propulsion systems built and they met the needs of flying at low altitudes at speeds less than about 400 km/hr. The requirement to fly at higher speeds and altitudes has been fulfilled by turbojets. The speeds of M = 3 and altitudes of 20 km can be reached by using turbojets. Fuel efficiency for low subsonic transport compelled the adoption of the more compact turboprops (compared to piston engines). Achieving speeds as high as possible under subsonic conditions, typically M = 0.85 has been met with by the development of turbofans. Obtaining higher fuel efficiency in turbofans has driven the design to the choice of bypass ratios as high as 9 for civil transport. Turbofans with small bypass ratios (less than 1) have been developed to combine the need for compactness with higher thrust augmentation for military applications. Flying for short durations at

speeds of M = 2 − 3 has resulted in the development of ramjets (for missiles). Flying at higher speeds (M > 6) has resulted in the quest for propulsion systems where the combustion process has to be handled under supersonic conditions because deceleration to subsonic conditions prevents additional heat being put in from the fuel and no net thrust can be generated. This technology has crossed the demonstration stage with a system being flown at M = 7 for about 10 s in an autonomous mode. The important feature of this technology is that the process is highly sensitive to geometry and flow conditions. Flying within the at-mosphere for short durations with high accelerations as demanded from military defense systems calls for the use of rocket engines. Those of such systems designed for tactical operations (like anti-tank missile, air-to-air and surface-to-air missiles of short range – up to 50 km, say) demand that the principal propulsion system be as compact as possible. These are fulfilled by the option of solid rockets better. Control demands are taken care of by aerodynamic means where ever possible. If these are inadequate, liquid propellant based control thrusters are deployed.

Flying outside the atmosphere (> 25 km, say) calls for the use of rocket engines for all vehicles. Space vehicles depend only on rocket engines that need to carry their own fuel and oxidizer. Solid rocket motors are largely used for single burn applications. Solid propellants have very high density and reasonable specific impulse. Compared to solid propulsion systems, liquid propulsion systems have a range of specific impulse from about 60 % to 180 %, but much lower density –from 60 % to as low as 20 %. Hence, the choice between solid rockets and liquid rockets needs additional features to be considered. Generally, for upper stages, the choice is more dependent on specific impulse and liquid oxygen-liquid hydrogen is the propellant combination of choice. Liquid rocket engines are capable of restart, variable thrust (that can be decided during the flight) and pulsing, features that are beyond the realm of solid rockets. Different class of liquid propellants and systems are used for these applications. Monopropellant systems are used in satellites for station keeping and related operations using some times, the pulse mode of firing the thrusters. Getting a satellite from transfer orbit to the designated orbit (that is typically a geo-synchronous orbit) is usually performed by a bipropellant liquid rocket engine that allows multiple burns and adopts hypergolic storable combinations. Booster propulsion is performed by solid rockets as well as liquid rockets and the choice

is many times on the consideration of costs. Semi-cryogenic liquid propellants are perhaps the cheapest of the propellant combinations and provide specific impulse comparable to solid rockets but lower density impulse. Since the density impulse is not an important criterion for the choice of propellants for large boosters (though it is an important criterion for tactical propulsion systems), semi-cryo systems are very good candidates for booster propulsion systems. The fact that liquid bipropellants are carried in tanks maintained at lower pressures compared to solid propellants that require to be in the combustion chamber that functions at very high pressure allows the inert weight fraction of large liquid propulsion systems to be much smaller than of solids. Satellite launch vehicles are sized for a predesignated trajectory to the orbit.

Control of the thrust vector is a demand for military aircraft (most usually with after burner) and moderate-to-large rocket engine based vehicles. For aircraft, thrust vector control is exercised by (a) moving the top and the bottom surfaces of the divergent section of the nozzle, (b) geometric change of the divergent with changes of the throat section or (c) by full control of the nozzle. For launch vehicles, in the first stage with solid rocket, one uses liquid side injection thrust vector control and for upper stages with solid rockets, flexible nozzles are used. In the case of large liquid rockets, separate control rockets are deployed. For smaller size systems, gimballing the thrust chamber around a central pivot with side hydraulic servo controlled plungers is adopted. Finer attitude control is also possible by mounting liquid bipropellant thrusters on the vehicle and operating them depending on the need. Thrust modulation as a part of launch sequence is not demanded. Strategic missile propulsion needs thrust termination scheme to be available to enable a single missile capable of being used on targets with different ranges.

A number of non-chemical based propulsion systems have been built over the last thirty years. These distinguish themselves from chemical propulsion systems in covering a range of thrusts that are much lower, specific impulses higher and propulsion system weights higher. They have considerable value for use in station keeping and long distance space travel. There are a few other systems (like solar based systems) not discussed here. The books by Humble et al (1995) as well as Wertz and Larson cover these and other non-chemical propulsion systems in greater detail.

The variety of propulsion systems built over the last hundred years (particularly in the last fifty years) has met most of the needs. The familiarity with the various kinds of engines in this chapter provides the back drop for further analysis and discussion of the performance of the engines. Several parts of the subject covered in this chapter are found in text books on propulsion (see for instance Kerrebrock, 1992; Sutton, 1992; Hill and Peterson, 1999; Mukunda, 2004).

Bibliography

[1] Barrere, M„ Jaumotte, A., Veubeke, B. J., and Vanderkerchkove, J., (1960) Rocket Propulsion, Elsevier.

[2] Cenciotti, D (2013) https://theaviationist.com/2013/02/21/raptor-vs-typhoon-us/

[3] Hill, P. G., and Peterson, C. R., (1999) Mechanics and Thermodynamics of Propulsion. Addison Wesley Longman, second edition.

[4] Humble, R., Henry, G. N., Larson, W. J. (1995) Space propulsion analysis and design, McGraw Hill Inc., NY

[5] J. L. Kerrebrock. (1992) Aircraft Engines and Gas Turbines. The MIT Press, second edition.

[6] Marguet, R., Ecary, C., and Carzin, P., (1979) Studies and tests on rocket-ramjets for missile propulsion, Proc. ISABE IV. pp 297 –306

[7] Mukunda, H. S. (2004) Understanding aero and space chemical propulsion systems, Interline publishers.

[8] Picard578, (2013) https://defenseissues.wordpress.com/2013/04/13/usefulness-of-thrust-vectoring/

[9] Rajaram Nagappa, (2014) Evolution of solid propellant rockets in India, DRDO monographs/special publication series, DRDO, New Delhi 110011

[10] Smolka, J. W., Walker, L. A., Johnson, G. H., Schkolnik, G. S., Berger, C. W., Conners, T. R., Orne, J. S., Shy, K. S, Wood, C. B., (1996) F15 ACTIVE flight research program, http://www.nasa.gov/centers/dryden/history/pastprojects/Active/pub_online/setp_d6_prt.htm

[11] Sutton, G. P., (1992) Rocket Propulsion Elements. John Wiley and Sons, Inc., New York, sixth edition.

[12] Wertz, J. R and Larson, W. J (1999) Space mission analysis and design, 3rd edition, Kluwer Academic Publishers, Netherlands

[13] Wikipedia (2016) https://en.wikipedia.org/wiki/Hawker_Siddeley_Harrier#/media/File:Vector-nozzle-sea-harrier-jet-common.jpg

[14] Ikaza, D (2000) Thrust vectoring nozzle for military aircraft engines, http://www.icas.org/ICAS_ARCHIVE/ICAS2000/PAPERS/RESERVED/ICA0534.PDF, 2000

4

Performance
of Aircraft and Rocket
Based Vehicles

Propulsion Systems

4.1. Introduction

This chapter is devoted to discussion of performance of aeronautical and rocket based vehicles. The first part is devoted to the discussion of the performance of aeronautical vehicles. In the case of aircraft, the central issues related to performance are take-off and landing, range and endurance, climb and coordinated turn. Range and endurance are steady performance features and others involve acceleration characteristics. Hence, it is simpler to analyze and understand the factors that impact range and endurance. All the performance features are related to aerodynamic data on lift and drag characteristics of the aircraft, propulsion data on engine power or thrust with altitude and speed as well as structural mass ratio from the view point of carrying inert mass. These data are drawn from the three features discussed in the earlier chapters. Many aspects of performance particularly in relation to birds vs. aircraft are already discussed in Chapter 1. The second part is devoted to rocket based vehicles. The discussion begins with the statement of mission profiles because the expected performance is intimately dependent on them. The mission profile refers to a nominal trajectory or flight path that is considered in the design of a vehicle. It is an important specification to be fulfilled before a vehicle is considered for acceptance. In addition, one might have other constraints imposed for the vehicle to be acceptable. We will briefly examine the considerations involved in the mission profiles for civil and military aircraft.

4.2. Mission Profile – Civil Aircraft

The mission profile is decided by examining the travel requirements. The primary parameters are: the distances to be flown, the number of passengers, the frequency of the most common trips, if non-stop trips are needed or desired, and the number of stops for refueling. While design exercise is performed, one looks at several possible scenarios keeping the above parameters in mind and use the largest occurrences of the profile as a possible mean profiles. Typically, one comes across (a) short haul limited passenger transport (50 to 90 passengers), a requirement fulfilled by the use of turbo-prop based aircraft that provides fuel economy with cruise at an altitude of 5 ± 1 km, (b) short haul medium passenger transport (150 to 200 passengers) fulfilled by narrow body jet aircraft with cruise at an altitude of 8 to 10 km, and (c) long range large pas-

senger transport (400 to 800 passengers) dealt with by wide-body large bypass turbofan based aircraft that cruise at 10 to 12 km and fly over 6000 to 10000 km. Some times, the requirement of enhanced speed overrides fuel economy in the case of short haul applications and aircraft using turbo-fan engines have become more popular, particularly because, the noise in the passenger cabin is much less for aircraft with turbo-fan engines than turbo-prop engines.

All civil transport are subject to traffic regulations that stipulate a vertical and horizontal separation between flying aircraft. The instructions for any change in flight path are relayed by local air traffic controllers to the pilots. These also depend on avoidance of regions of clear air turbulence to ensure smooth flight. Further, the non-availability of landing clearance due to atmospheric conditions or other non-technical reasons (like the landing of a very important person) for varying durations is possible. For these reasons, the fuel consumed by an aircraft has a segment of unpredictable aspects that will need to be factored into the design.

4.3. Mission Profile - Military Flight Vehicles

The current status of military vehicles is consequent upon the development and field experience over several decades. Normally, the special roles define the nature of the aircraft. However, in recent times, there are a number of aircraft designed as multi-role aircraft, or designed to change roles during the execution of a mission; these are termed swing-role type. The long developmental time of complex military aircraft has led to some aircraft continuing to remain in service long after their introduction; such aircraft have adopted new roles as a result of new weapons being mounted or updates. The flexibility of weapons and methods of carrying weapons and the adaptability of sensors and avionic systems has caused this situation aided further by the lower cost of modifications vis-a-vis new procurements. The largest contributor to such a philosophy has been due to advances in the technology of sensors and avionics.

The different roles of military aircraft are air superiority, ground attack, interdiction, deep penetration and bombing and transport. The primary aim of the role of air superiority is to deny to an enemy the airspace over the battlefield, thus allowing ground attack aircraft the flexibility to destroy ground targets (also to prevent enemy aircraft access to destroy host's infrastructure) and assist ground forces without concern for enemy airborne threat. Such an aircraft
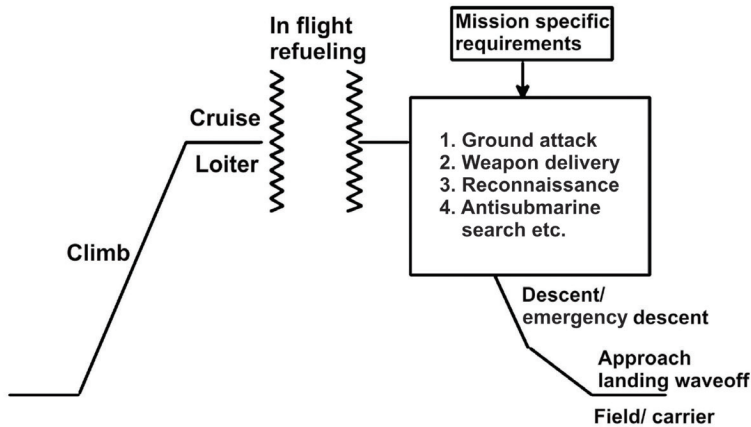
Figure 4.1.: Typical military mission profiles

is designed for rapid pilot response to a deployment call that may involve climb to intercept or loiter on combat air patrol and then to engage enemy targets, generally beyond visual range.

The aircraft should also have the capability to engage in close combat, or dogfight with enemy aircraft if needed. For this to be successful, an extremely agile system is necessary with "care-free handling" capability. The systems must facilitate accurate navigation, identification and prioritisation of targets, and the features that enable joining tactical communications network. The aircraft LCA, F 16, F 18, Euro-fighter Typhoon, MiG 21, MiG 23, MiG 29 and F 117 all belong to this category.

The ground attack role involves the tactical situation on the battlefield. Systems to identify the right target - stationary or moving - among the ground clutter and multiplicity of targets and friendly units on the battlefield must help a prepared pilot. The ability to designate targets by laser has been the development in the last decade to perform precision laser-guide bombing to reduce uncalled-for casualties. This role also includes one called close air support (CAS), where support is given to ground forces (most often under their direction) with weapons being deployed close to friendly forces. Interestingly, the ground attack role may be fulfilled by either fixed-wing or rotary-wing

aircraft. While fixed-wing aircraft needs are in terms of very fast, low-level performance with agility to perform attack maneuvers and take evasive action, rotary-wing aircraft provide benefits for attack in terms of extreme low-level movement with the ability to loiter in natural ground cover showing up when required. Sepecat Jaguar, Sukhoi Su 24, Tornado belong to this aircraft category, Apache helicopter belongs to the second category. Military aircraft are used to airlift troops and weapons to forwrad bases outside the control of commercial airspace. They are a vital part of any defense services. These aircraft are built as variants of civil aircraft or in several cases specially for the purpose. Illushin-76, Antonov An-32, Boeing C-77 are some of the well known military transport aircraft.

Bombing with deep penetration is another of the missions carried out by high flying high speed aircraft with inbuilt stealth characteristics. F 111 and B-2 belong to this category. It is also possible that this is accomplished by cruise missiles that fly low (to take advantage of radar clutter and reduce detection possibilities) and at moderate speeds using turbojets for propulsion.

Maritime operations with a wide range of applications need aircraft and rotor-craft. The mission profile has to account for reconnaissance, shadowing, tactical support to strike aircraft, intelligence collection and transmission and in some instances, early warning capability. Several of these demand large endurance. Figure 4.1 depicts some of the mission profiles. There are many other missions like search and rescue operations that have complex mission profiles that are met with existing aircraft or helicopters with appropriate avionics.

4.4. Aircraft Lift and Drag Versus Speed and Altitude

The lift and drag equations for low speed flows described in Chapter 2 (equations 2.1) are

$$c_L = \frac{2\pi}{(1 + 2/eAR)}; \quad c_D = c_{D0} + \frac{c_L^2}{\pi eAR}$$

(4.1)

where c_{D0} is the zero-lift drag coefficient, c_L is the lift coefficient both of which are functions of angle of attack. The compressibility corrections for subsonic flows are accounted for by dividing the values obtained as above by $\sqrt{(1 - M^2)}$ as already shown in equation 2.15. The lift and drag coefficients (c_L and c_D)

Table 4.1.: Typical values of c_{D0} and k for several classes of aircraft

Type of aircraft	c_{D0}	k
Sail plane or glider	0.012 - 0.015	0.017 - 0.02
Jet transport	0.015 - 0.02	0.03 - 0.04
Supersonic fighter	0.02 - 0.03	0.08 - 0.12
Turbo-prop transport	0.02 - 0.025	0.03 - 0.04
Twin-engine piston-prop	0.022 - 0.03	0.03 - 0.04
Agricultural	0.04 - 0.07	0.05 - 0.08
Microlight	0.02 - 0.035	0.03 - 0.05

are evaluated experimentally for the aircraft through several means - combining the theoretical and experimental information for individual elements and tests on scale models of aircraft and in some cases, tests on full size aircraft. These data are harmonized by careful examination of experimental errors and influence of various aspects like surface roughness and the presence of protruding components. These data are central to the performance of aircraft. The experimental data are set out for any aircraft in the form

$$c_D = c_{D0} + k\ c_L^2$$

(4.2)

where $k = 1/\pi e AR$. Typical values for various classes of aircraft are set out in Table 4.1. Those vehicles which have a clean configuration and the outer surfaces smooth have the lowest c_{D0} and those with high AR have lower k.

Optimization of performance for range and endurance of propeller and jet based aircraft requires maximizing (a) c_L/c_D, (b) $c_L^{0.5}/c_D$ and (c) $c_L^{1.5}/c_D$ as will be seen in section 4.7. We can simply determine the optimum value of c_L for these conditions by treating the expression $c_L^m/c_D = c_L^m/(c_{D0} + kc_L^2)$ and obtain the optimum value as occurring at

$$c_L = \sqrt{\frac{m\ c_{D0}}{(2-m)k}}$$

(4.3)

These give the optimum values of c_L for cases (a), (b) and (c) noted just above as $\sqrt{c_{D0}/k}$, $\sqrt{c_{D0}/3k}$, and $\sqrt{3c_{D0}/k}$ respectively. The cruise speeds at which these are realized will be the lowest for case (c), medium for case (a) and the highest

for case (b). The lowest and the highest may be impractical in some situations. The highest speeds for jet transport will be limited by drag rise considerations, typically M less than 0.86.

The equations for L and D can be written as

$$L \;=\; c_L(\rho V^2/2)A_w \tag{4.4}$$

$$D \;=\; \left[c_{D0} + \frac{kL^2}{(\rho V^2/2)^2 A_w^2} \right](\rho V^2/2)A_w \tag{4.5}$$

For cruise flight we can write $L = W$ where W is the weight of the aircraft and rewrite the equation for drag as

$$D = \left[c_{D0}(\rho V^2/2)A_w + \frac{kW^2}{(\rho V^2/2)A_w} \right] \tag{4.6}$$

This equation for drag has a well known important behavior. The first term related to basic drag (friction and form drag components) increases as the square of the flight speed. The second term related to induced drag decreases as the square of the flight speed. Thus, the sum may be expected to have a minimum at some speed as shown in Figure 4.2 where the components of drag and total drag are set against flight speed.

Another important feature of equation (4.6) is that if altitude varies such that ρV^2 is constant, drag is the same. Thus as one flies higher, velocity can be increased without the concern of increasing the drag provided ρV^2 is maintained constant. By a simple analysis of seeking for the minimum, the speed for minimum drag is obtained as

$$V_{D,min} = \left[\frac{2W}{\rho A_w} \right]^{1/2} \left[\frac{k}{c_{D0}} \right]^{1/4} \tag{4.7}$$
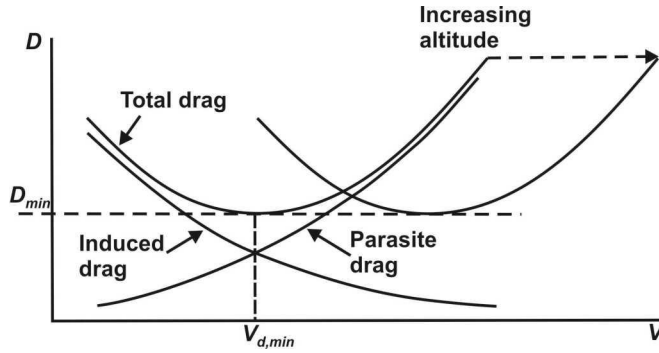
Figure 4.2.: Total drag and the drag components. Parasite drag increases with speed and lift induced drag decreases with speed leading to an it optimum speed for minimum total drag

Minimizing the drag reduces the thrust demanded for propulsion and is an important operational feature in aircraft design. Increasing the altitude reduces the density and hence increases the optimal speed. This is taken advantage of by aircraft to fly high to operate at the optimal speed.

This is taken advantage of by aircraft to fly high to operate at the optimal speed. The minimum drag can be obtained by substituting the expression for $V_{D,min}$ as above to get

$$D_{min} = 2W \sqrt{k c_{D,0}}$$

(4.8)

This equation can be recast in terms of $(L/D)_{opt}$ as

$$(L/D)_{opt} = \sqrt{k c_{D,0}}/2$$

(4.9)

It is clear from this equation that the two principal driving factors for enhancing the lift-to-drag ratio lie in reducing the basic drag coefficient and increasing the aspect ratio. Aspect ratio cannot be increased beyond a limit because of structural mass optimization considerations. Typical values of $e = 0.8$, $AR = 10$, $c_{D0} = 0.02$ lead to $L/D = 17.7$ which is close to the value for Boeing B747 aircraft.

Equation (4.5) points to dependence of drag on altitude through the dynamic pressure ($\rho V^2/2$). It can be displayed in an interesting manner by factoring out the ambient pressure effects. We can write (ρV^2) = $\gamma p_a M^2$ where γ is ratio of specific heats, p_a the ambient pressure, and M the free stream Mach number. A quantity $\delta = p_a/p_0$ where p_0 is the ambient pressure at sea level is defined and the quantities $\bar{L} = L/\delta$ and $\bar{D} = D/\delta$ to express the scaled lift and drag as

$$\bar{L} = L/\delta = c_L(\gamma p_0 M^2/2)A_w \tag{4.10}$$

$$\bar{D} = D/\delta = \left[c_{D0} + kc_L^2\right](\gamma p_0 M^2/2)A_w \tag{4.11}$$

Thus, when the results of lift and drag are plotted in terms $\bar{L}$ and $\bar{D}$ vs. M, altitude effects are included.

There is a further aspect with respect to the flight speeds. There are two terms used in this connection - true flight speed and equivalent flight speed. Since the flight measurement of speed is done using a pitot-static device, one gets the dynamic pressure directly. One can define the equivalent air speed, V_{eq} as $\rho_0 V_{eq}^2/2 = \rho V^2/2$, where ρ_0 is the ambient density at sea level and V is the true flight speed. In this case, $V = \sqrt{V_{eq}}/\sigma$ where σ is the ratio of density at any altitude (ρ) to the density at sea level (ρ_0). Drag when plotted with V_{eq} will be independent of altitude.

4.5. Power vs. Flight Speed and Altitude

There are aircraft that use power delivering engines - propeller-running power plants whose flight performance optimization requires thrust power to be optimized. Thrust power is estimated for cruise conditions by examining drag power (P) which is the product of drag and flight speed, DV. Expressing DV as the sum of frictional and induced drag terms, we have

$$DV = \left[c_{D0}(\rho V^3/2)A_w + \frac{kW^2}{(\rho V/2)A_w}\right] \tag{4.12}$$

Due to proportionality to V^3 and $1/V$ in the first and the second terms on the right hand side, the curve is skewed in relation to drag-velocity curve. The minimum power does not occur at the velocity for maximum L/D, and it shows a strong altitude effect. Treatment on optimal speed for minimizing power leads to

$$V_{P,min} = [W/(\rho A_w)]^{1/2} \, [k/(3c_{D,0})]^{1/4}$$

(4.13)

The actual minimum power, P_{min} is obtained as

$$P_{min} = 4[W^3/\rho A_w)]^{1/2} \; c_{D,0}^{1/4} \; (k/3)^{3/4}$$

(4.14)

The behavior of the components of drag power and the flight speed for minimum power are presented in Figure 4.3. The minimum drag power increases with altitude unlike the minimum drag that remains the same with altitude. It can be noticed that the figure includes a line of tangency - line tangent to both the curves and passing through the origin. The point of contact of the line of tangency with the curves represents the speed for maximum L/D.

4.6. Propulsive Thrust vs. Speed and Altitude

We turn our attention to propulsion as it is central to determine the maximum possible flight altitude. There are two terms associated with altitude that can be reached by the aircraft. These are service ceiling and absolute ceiling. These refer to flight altitudes at which the climb rate of the aircraft reaches about 0.5 m/s (100 ft/min) and 0 respectively. There are also other acceleration features of the flight that are possible if only there is excess thrust or power. To further elucidate these aspects, it is important to restate equation 3.2.

$$F = \dot{m}_a[(1+f)\,V_e \, - V_a] \, + \, A_e\,(p_e \, - \, p_a)$$

(4.15)

The air mass flow rate, $\dot{m}_a$ a and exhaust velocity, V_e are dependent on the cycle parameters like compressor pressure ratio (π_c) and turbine inlet temperature (TIT) as well as ambient temperature and the geometric parameter namely, A_e,
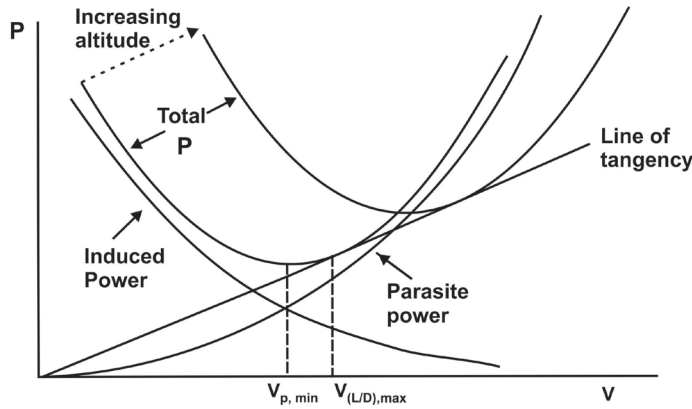
Figure 4.3.: Total drag-power and the components. Parasite drag power increases with speed and lift induced drag power decreases with speed leading to an it optimum speed for minimum total drag power

the exhaust nozzle area. This equation can be subject to further analysis based on the cycle of choice (see for instance, Mukunda, 2004). This leads to

$$\frac{F}{p_a A_e} = f\left(\pi_c,\ M,\ TIT/T_{amb}\right)$$

(4.16)

In the above equation, the dependence of thrust on altitude comes from ambient pressure, p_a and temperature, T_{amb}. The compressor pressure ratio itself is dependent on the rotational speed of the turbomachinery and the efficiencies of all the elements. In this sense, the dependence is more complex and the results from static test beds or better, flight test beds are the basis of actual performance calculations. Even so the broad behavior is captured by simple relations of the above kind as well as equation (3.1) for reciprocating engines.

As can be noticed from the above equation, higher the altitude, lower is the pressure and lower is the thrust. Thrust will not vary much with flight speed because of near-compensation between increasing air mass flow rates and decreasing difference between exit and inlet air velocities. In the case of drag, however, since the speed is intentionally increased as one climbs to altitude, say, keeping the dynamic pressure nearly constant, the drag vs. equivalent air
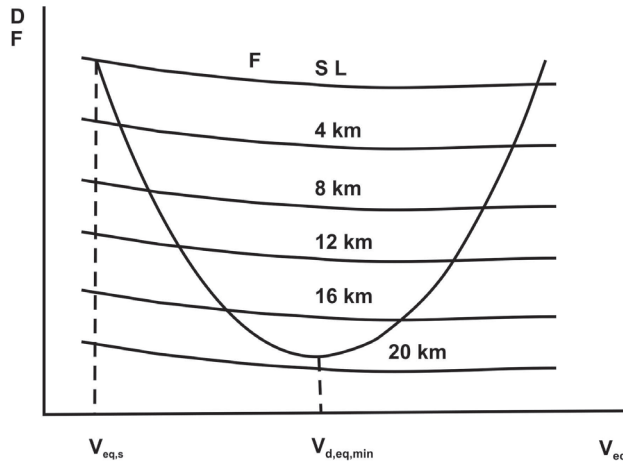
Figure 4.4.: Engine thrust and drag as a function of equivalent flight speed; note that at about 20 km altitude thrust is just below the drag. This constitutes the absolute ceiling

speed will show a minimum like in Figure 4.2. Thus when thrust at any altitude falls below the drag, *that altitude will be the absolute ceiling*. Keeping the ability to have some climb rate in reserve, the (thrust - drag) that permits a climb rate of 100 ft/min (30.5 m/min) is used to describe *what is known as service ceiling*. Most aircraft are expected to stay much below the service ceiling in actual operations. Figure 4.4 shows the variation of the thrust and drag as a function of the equivalent flight speed. As can be noticed, with increase in altitude, thrust remains about the same for varying V_e and decreases significantly with altitude. Equipped with aerodynamic and propulsion characteristics described above we can begin to examine various other performance aspects.

4.7. Range and Endurance

The starting point for the analysis of range and endurance for cruise conditions is that the mass loss rate of the aircraft arises from fuel consumption rate. This fuel consumption rate is related to the specific fuel consumption multiplied by power or thrust depending on the source of energy - propeller driven or a hot jet exhaust. Power from the engine passes on to a propeller which creates the momentum required for generating thrust. Then onwards, linking the thrust

to drag and lift to weight leads to simple equations that on integration give the desired results. Thus

$$-\frac{dm_a}{dt} = \dot{m}_f = (sfc)_P(DV/\eta_{prop}) \tag{4.17}$$

$$= \dot{m}_f = (sfc)_F F = (sfc)_F D \tag{4.18}$$

where the negative sign on dm_a/dt on the left hand side is related to the fact that the term refers to fuel consumption rate, m_a is the mass of the aircraft, and $(sfc)_P$ refers to the specific fuel consumption (kg/kW-h) for a propeller driven system and the power delivered by the power plant is expressed in terms of the flight power divided by the conversion efficiency.

The flight power needed is thrust times the flight speed; thrust itself is equal to drag for cruise conditions. The second equation refers to thrust producing systems and that is why the terminology $(sfc)_F$ (kg/h kg) is adopted. The above equations on integration lead to endurance. For obtaining the result for range, dt is expressed as ds/V where ds is the increment in distance. We can rearrange the above equations by expressing D as $(D/L)\,m_a g$ that is also the same as $(c_D/c_L)m_a g$ and $V = \sqrt{2gm_a/\rho A_w c_L}$. For obtaining range and endurance, we write

$$-\frac{dm_a}{m_a^{3/2}} = dt\left[\frac{(sfc)_P}{\eta_{prop}}\frac{c_D}{c_L^{3/2}}\sqrt{\frac{2g}{\rho A_w}}\right] \tag{4.18}$$

$$-\frac{dm_a}{m_a} = ds\,\frac{(sfc)_P}{\eta_{prop}}\frac{c_D}{c_L} \tag{4.20}$$

$$-\frac{dm_a}{m_a} = dt\,(sfc)_F\frac{c_D}{c_L} \tag{4.21}$$

$$-\frac{dm_a}{m_a^{1/2}} = ds\left[(sfc)_F\frac{c_D}{c_L^{1/2}}\sqrt{\frac{\rho A_w}{2g}}\right] \tag{4.22}$$

These are now integrated with limits as follows: on m_a, the initial mass, $m_{a,i}$ and final mass, $m_{a,f}$; on $t,$ 0 to E (endurance); and on s, 0 to R (range). These lead to the results presented below. Specifically, E_p and E_F , denote the endurance of propeller and thrust based aircraft, R_p and R_F , the range of propeller

Table 4.2.: Results for specific aircraft on the range and endurance;
* = kg/kWh, + = kg/h kg

Aircraft	$m_{a,i}$	$m_{a,f}$	A_w	AR	L/D	sfc	c_L	ρ	V	E	R
	t	t	m^2					kg/m³	km/h	hr	km
Anatonov An32	27	21	75	11.3	15	0.5*	0.5	0.6	470	1.3	2200
Boeing 747	375	240	511	6.9	17	0.87+	0.5	0.4	965	11	12000

and thrust based aircraft. Thus,

$$E_p = 98 \sqrt{\frac{2\rho A_w c_L}{g m_{a,i}}} \frac{c_L}{c_D} \frac{\eta_{prop}}{(sfc)_P} \left[\sqrt{\frac{m_{a,i}}{m_{a,f}}} - 1 \right] \qquad (h) \qquad (4.23)$$

$$R_p = 367 \frac{c_L}{c_D} \frac{\eta_{prop}}{(sfc)_P} \ln \frac{m_{a,i}}{m_{a,f}} \qquad (km) \qquad (4.24)$$

$$E_F = \frac{c_L}{c_D} \frac{1}{(sfc)_F} \ln \frac{m_{a,i}}{m_{a,f}} \qquad (h) \qquad (4.25)$$

$$R_F = \frac{2}{(sfc)_F} \frac{c_L}{c_D} \sqrt{\frac{2 m_{a,i} g}{\rho A_w c_L}} \left[1 - \sqrt{\frac{m_{a,f}}{m_{a,i}}} \right] \qquad (km) \qquad (4.26)$$

In the above equations, c_L^n/c_D with $n = 3/2$, 1 and 1/2 are written by absorbing $c_L^{1/2}$ into the terms outside of the brackets. The term $\sqrt{2\rho A_w c_L/(g m_{a,i})}$ is a flight speed with $m_{a,i}$ as the mass which is about 2 to 2.5 % lower than the initial loaded mass because this amount is what is used up as the fuel in take-off and climb to altitude. In these expressions, *speed must be set in terms of km/h to be consistent with the expected units.*

A few important features are immediately clear from these expressions – aerodynamics, propulsion and structures control the performance. The aerodynamic part comes in through c_L^n/c_D, or really c_L/c_D. Larger this value, greater is the range and endurance. Propulsion performance comes through *(sfc)$_P$* and *(sfc)$_F$* both being lower is always desirable; these being lower has other environmental advantages. The role of engine improvements that have occurred over a time along with aerodynamics and structures have all gone into reducing the specific fuel consumption. For instance, the Boeing 707 of the earlier era carrying about 140 passengers used to burn up 600 liters/min in cruise, and

the modern day Boeing 777 carrying about 300 passengers consumes only 160 liters/min. One can get an idea of the enormity of differences in efficiencies that have occurred because of all round system developments with time, more particularly in propulsion.

The key reason for the difference in performance between Boeing 707 and 777 is that Boeing 707 built in 1955 could use only turbojets that really gurgle up the fuel, but the Boeing 777 uses turbofan engines with a very high bypass ratio of 8 to 10 (different families) and compressor pressure ratios of 40 to 60. This has had also significant positive environmental effects. The amount of CO_2 put into the atmosphere consequent upon the aircraft flights will be reduced; this is expressed as aviation carbon footprint being lower and is taken advantage of in the current environmentally conscious world. The initial and final masses of the aircraft controlled by the inerts consisting of structural mass and some residual fuel preserved due to operational safety considerations. Lowered structural mass using advanced tools of design and materials (a subject of Chapter 6) will contribute to enhanced range and endurance.

It is useful to get an idea of the values predicted using the above equations. Table 4.2 provides the details. The results presented in Table 4.2 for a turbo-prop based aircraft and a long distance airliner are approximate and consistent with the published data on the performance of these aircraft.

One might ask if the flight duration between different points on the earth follows the results given above - that is, would one reach the destination within the time given by R/V calculated as above? The answer is: not quite. The reason lies with the presence of jet streams in the upper atmosphere. The jet stream is a strong stream of air that flows around our planet high up in the atmosphere, at around the level of the tropopause at speeds of up to 200 km/h. This is caused by a combination of factors that includes the rotation of the earth (the Coriolis effect) and steep temperature gradients in the atmosphere.

The region situated between the troposphere and the stratosphere begins at a height of 11 km at the poles and 17 km at the equator. Both the subtropical jet and the polar jet travel from west to east and both would travel relatively uniformly affected by various local factors including the absorption of solar radiation. Figure 4.5 shows the schematic picture of the jet streams in the polar region as well as sub-tropical zones.
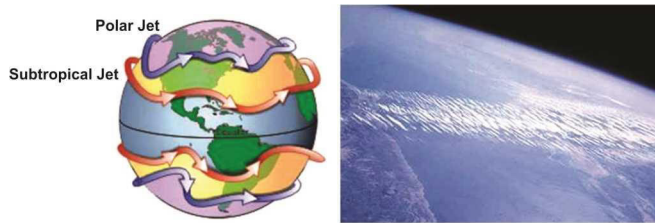
Figure 4.5.: The left figure shows the schematic of the jet stream in in the polar region as well as sub-tropical region. The right side figure is the photograph taken from space shuttle at 320 km altitude.

On the right is included a picture of the jet stream taken from the space shuttle. The jet stream appears in rolls of thin clouds and appears well bounded. While this feature is largely true, it also meanders around the edges both along the height and the width. Because of this feature, the flight path of transatlantic flights that use the upper latitudes is usually altered by using local advisory coupled with information from on board detection systems. Due to these reasons, the transatlantic flights in the northern hemisphere will take much longer one way and shorter the opposite way, In the equatorial region, the presence of the jet stream does not affect the flights since they are several kilometers higher than the flight path.

4.8. Influence of Center of Gravity (*cg*)

The role of the center of gravity of the aircraft (*cg*) on the fuel performance in intertwined with design and operational aspects of an aircraft. To begin to appreciate the role of center of gravity on the performance, we can re-examine Figure 4.6. The center of gravity is ahead of the aerodynamic center assuring a stable flight operation (see section 1.2.4). If the *cg* is far ahead, implying nose heavy, one will need to apply more elevator (or horizontal tail) angle to generate larger amount of force to counteract the moment due to wing lift to get to the trim condition. Since $L_w = W + L_t$, where L_t is the tail lift, W is the weight of the aircraft, the wing lift, L_w will be larger due to the need for higher L_t with more forward *cg*.

This also means higher drag and so larger thrust and larger fuel consumption. Higher lift also means higher angle of attack and so higher lift coefficient.
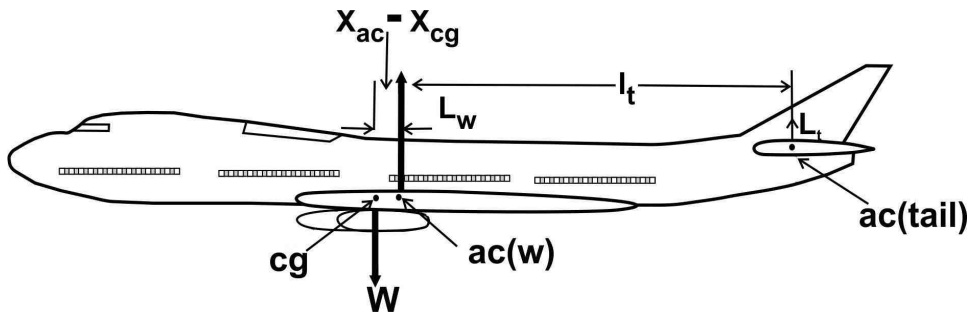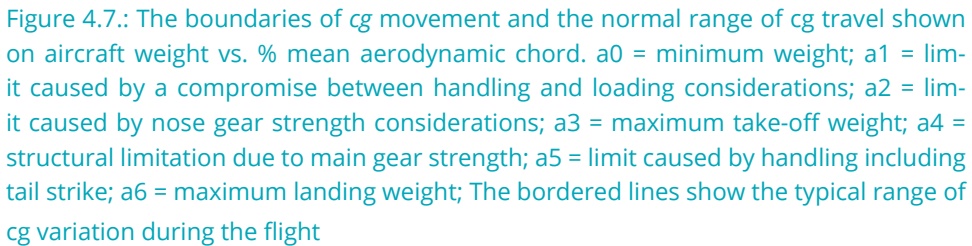
Figure 4.6.: The forces on the aircraft under steady stable flight

Hence the operating flight speed will become slightly lower. Similarly if the operating *cg* is moved aft, the speeds will be higher, reduction in fuel consumption better achieved with the margin of stability coming down. During the flight, fuel is continuously consumed. Depending on the locations where the fuel is stored, typically different parts of the wing and in the tail and in a few cases close to the fuselage, the center of gravity will shift. Amongst other factors that affect the center of gravity are the position of the loading of cargo, movement of passengers and service carts in the aisle, toilet water and flushing. Also during the taxiing phase before take-off, climb and the descent phases, the parameters of fuel loading, thrust demanded and the fuel consumed could all be different for each flight. In all phases of flight, the flight path is controlled by air traffic regulations. Thus the flight dynamics, implying speed -altitude relationship will vary. Thus there is need to manage the *cg* travel during the different phases, the prime attempt being to minimize the fuel consumed in the flight, particularly for passenger aircraft.

In many aircraft including the large ones, an automatic fuel management system moves the fuel stored in parts of the wing - outboard and inboard, and the tail region to ensure appropriate *cg* location during the flight. Therefore, the region for *cg* location from the point of view of performance and stability is carefully arranged. Different aircraft have different arrangements of various components and hence different ranges of *cg* movement. The permissible range is used during ground operations and the actual range is used during take-off and landing phases. The limits of the *cg* variation and the causes for them are set out in Figure 4.7. The figure caption details the causes for various segments

Figure 4.7.: The boundaries of *cg* movement and the normal range of cg travel shown on aircraft weight vs. % mean aerodynamic chord. a0 = minimum weight; a1 = limit caused by a compromise between handling and loading considerations; a2 = limit caused by nose gear strength considerations; a3 = maximum take-off weight; a4 = structural limitation due to main gear strength; a5 = limit caused by handling including tail strike; a6 = maximum landing weight; The bordered lines show the typical range of cg variation during the flight

of the *cg* travel zone. This diagram is typically used to perform what is known as weight and balance planning for each aircraft. If the ambient temperature is high and payload high, the amount of excess fuel loaded is optimized to ensure meeting the flight regulations and a safe flight, for, it is said: "One needs fuel to carry fuel". It is also the responsibility of the flight crew to seek and choose pathways to optimize the flight fuel use.

Those aircraft that have fly-by-wire system and automated *cg* control, something most modern aircraft have, do possess the ability to change the position of the fuel and reduce the *cg* movements to the desired position to the extent the situation demands. There are manuals that each manufacturer produces in great detail on all aspects of each aircraft type on the position of *cg* and how to manage it under different flight conditions (see Wikipedia4, 2015 and others that can be searched on the internet).

4.9. Influence of Flight Parameter Deviations

The flight speed and altitude (and so, the flight path) of commercial aircraft deviates from what may be optimal from the viewpoint of fuel optimization due to a variety of factors including atmospheric conditions and flight delays on the tarmac because of air traffic controller instructions. The flight path is also regulated due to air-safety considerations in terms of separation and an-apriori knowledge of the weather. On occasions, flights are operated at speeds slightly higher than originally intended to compensate for possible delays in take-off. Tail-wind and head-wind on flight are known issues with positive and negative effects. It is therefore useful to understand the influence of these parameters on fleet performance in terms of fuel burn. Lovegren and Hansen (2011) have conducted a study of a large number of flights and several airlines in the USA and have concluded that fuel burn is most sensitive to speed and altitude with the possibility of up to 3.5 % reduction. A typical sensitivity plot drawn from their work is set out in Fig. 4.8. As can be seen from Fig. 4.8, in this specific case, there is flight corridor with M_0 - 0.74 to 0.79 and altitude - 345 to 380 kft (10.5 to 11.6 km) where near-optimum conditions prevail; any deviations in terms of higher altitudes cause much greater consumption of fuel compared to lower altitudes. Similarly, increase in M_0 beyond the optimum is more unforgiving than lower M_0. These calculations need to be performed for each aircraft over a number of flights to obtain a mean behavior and derive benefit in terms of operational guidelines, one of which could be to restrain from exceeding the optimum M_0 despite the possible desire to let passengers reach their destination earlier.

4.10. Take-off

Take-off is more crucial and difficult to deal with than cruise or climb in a civil airliner; while cruise is also handled by an autopilot, the take-off segment requires the intervention of the pilot (landing, a subject discussed in the nex-section is even more difficult than take-off since there is a greater option for aborting a taking-off under adverse weather conditions).

It is only in unmanned air vehicles that the take-off and landing actions are partly automated; even here, ground based controls are relayed to the aircraft. Every airport has a windsock and all take-offs and landings occur in a direction opposite of the wind as this reduces the effective ground speed and ground run.
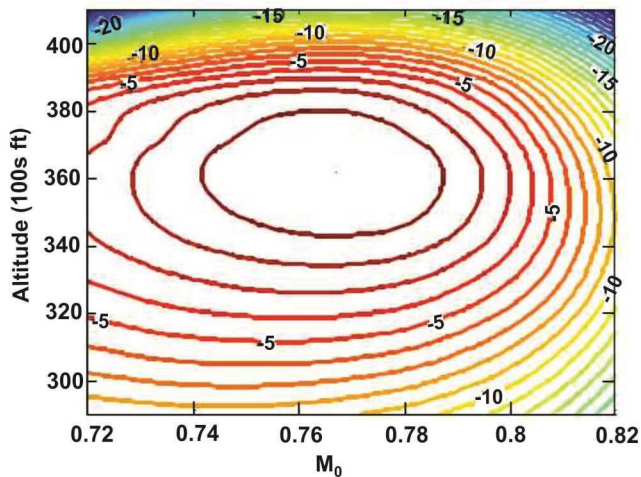
Figure 4.8.: Contours representing reduction in standard air range on altitude-flight Mach number (M_0) with the optimal being at the center of the contours - drawn from Lovegren and Hansen (2011)
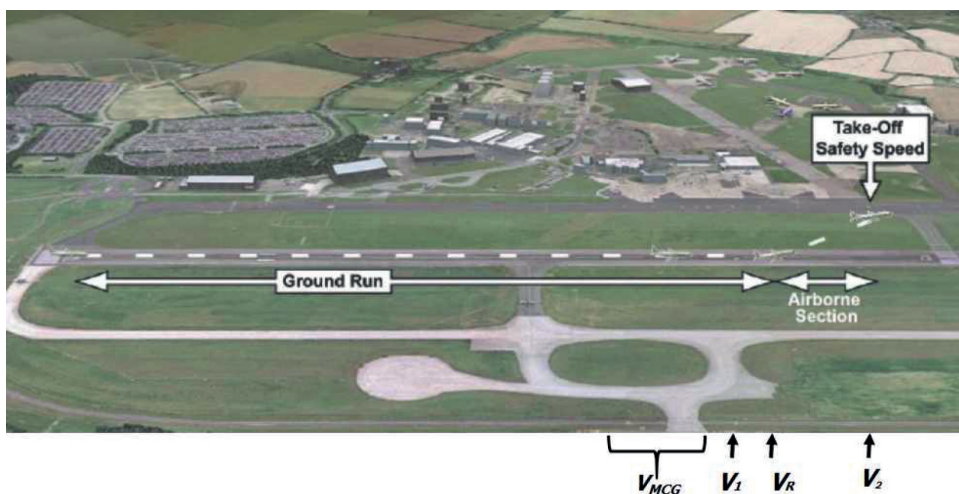

Figure 4.9.: Figure shows a typical air strip. It has a ground run and an airborne segment. It is classified into four parts as also the speeds of the aircraft for operational and safety reasons; V_{MCG} = Minimum ground control speed, V_1 = Decision go, no-go speed, V_R = Speed at which rotation is initiated, and V_2 = One-engine inoperative climb speed for take-off

Most long range aircraft need runway lengths of up to 3 km, other medium range aircraft and several military aircraft need much lower runway lengths (of 0.5 to 2 km).

Take-off run is defined as the distance between take-off starting point to the location of standard height above the airstrip that the aircraft must acquire. Hence take-off includes ground run plus an airborne section as indicated in Figure 4.9.

The ground run is typically 65 to 75 % of the take-off distance on the runway. The runways have several features: (a) stopways, an area beyond the end of runway where the aircraft can be safely brought to a stop in an emergency. The stopway should be clear of obstructions that could damage the aircraft, (b) clearway ia an area that includes the stopway and any additional surface cleared of obstacles. This is an area under the control of the appropriate authority, selected or prepared as a suitable area over which an aircraft may make a portion of its initial climb to a specified height, (c) TODA (takeoff distance available) is the length of the take-off run available and a length of the clearway, (d) TORA (takeoff run available) is defined as the length of runway available for the ground run of an aeroplane taking off, (e) ASDA or EMDA (Accelerate-Stop distance available or Emergency distance available) defined as the length of the take-off run available plus the length of any stopway, and (d) LDA defined as the length of runway available for the ground run of a landing aeroplane. These features are illustrated in Figure 4.10.

The take-off operation is associated with several relevant speeds as already shown in Figure 4.9. These are described below.

1. Minimum control speed, V_{MCG} is the speed on ground that gives directional control with one engine failure

2. Decision speed, V_1 is the speed which dictates whether a malfunction during the take-off roll results in rejecting the take-off or continuing (go or no-go speed)

3. Rotation speed, V_R is the speed at which the aircraft nose is lifted from the ground for take-off

4. Lift-off speed, V_{LO} is the speed at which the entire aircraft is airborne.
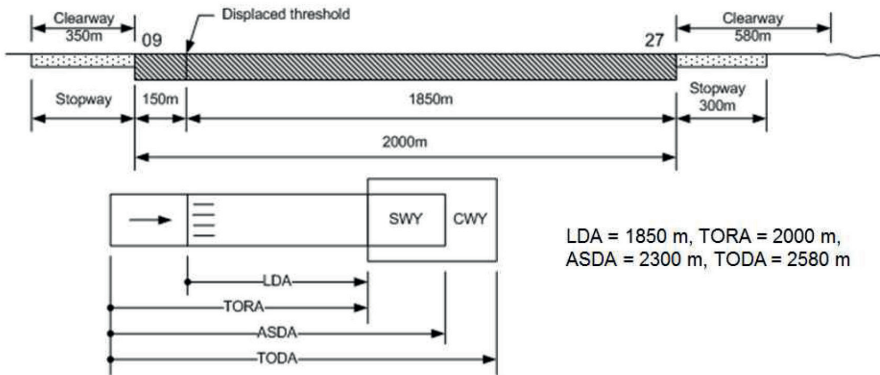
Figure 4.10.: Various terms used with regard to runway - TODA, TORA, ASDA (or EMDA) and LDA, with values for a typical runway

5. Take-off safety speed, V_2 is the minimum safety speed to be attained at a height of 11.5 m (35 ft)

These speeds are arranged such that $V_1 < V_R < V_{LO} < V_2$ even though there is a range of minimum and maximum values for each of these speeds for every flight depending on aircraft configuration, the weight at take-off, weather and runway conditions. The rotation at the speed V_R is performed typically at 2 to 3⁰/s. It should not be larger than this value since otherwise, the tail may brush against the airstrip. This is technically called a tail-strike that long aircraft are more prone to if correct rotational operation is not adopted. The various speeds are called by the co-pilot (V_1 completed, etc) and recorded on the black box as a routine flight operation.

The most crucial speed associated with the aircraft is the stall speed. The stall-speed is given by

$$V_{stall} = \sqrt{\frac{2m_{a,i}}{\rho A_w c_{L,to}}}$$

(4.27)

where $c_{L,to}$ is the take-off lift coefficient. Typical values of these are described in section 2.7.1. This lift coefficient (as well as drag coefficient) is dependent on the aircraft geometry that will have flaps down, perhaps, slats opened (see section 2.7) and another effect called ground effect. The ground effect that is caused by the fact that on the upper side of the wing the stream extends to un-

limited height while on the bottom it is limited by the ground. These both lead to increased lift and decreased drag. When landing, ground effect can give the pilot the feeling that the aircraft is "floating". When taking off, ground effect reduces the stall speed. The pilot can then fly level just above the runway while the aircraft accelerates in ground effect until a safe climb speed is reached. This is particularly important in the case of aborted landing on aircraft carrier. When a wing is flying very close to the ground, wingtip vortices are unable to form effectively due to the obstruction of the ground. The result is enhanced lift coefficient and lower induced drag component.

In aircraft operations, the V_{LO} is set at 10 to 20 % higher than V_{stall} (10 % for military aircraft and 20 % for civil aircraft).

Amongst the various segments of the take-off, namely, ground run, rotation distance, and transition distance to 10.5 m height, the first segment, "ground run" amounting to 60 to 65 % of the take-off distance can be analyzed simply. The forces on the aircraft during the ground run are shown in Figure 4.11. Lift and drag increase because of increase in speeds during the ground run. As lift increases, the force exerted on the ground becomes lower as it is the difference between wight and lift that is felt by the ground. For this reason, the frictional force also decreases during the ground run. As can also be seen in the figure, engine thrust does not vary much with speed. The acceleration of the aircraft is thus caused by the difference between the thrust and a combination of drag and frictional force. Therefore,

$$m_{a,i}\frac{dV}{dt} = \text{net force} = F - D - \mu(m_{a,i}g - L)$$

(4.28)

Here F is the engine thrust, D and L are aircraft drag and lift, μ is the frictional coefficient between the tyres and the surface of the runway. As the aircraft gains momentum because of engine thrust, the lift force will unload the weight of the aircraft in reducing the frictional component; when lift-off occurs, this term goes to 0. This equation can be cast into a form bringing distance covered by noting $V = ds/dt$. Thus,

$$m_{a,i}\frac{dV}{dt} = m_{a,i}V\frac{dV}{ds} = F - D - \mu(m_{a,i}g - L)$$

(4.29)
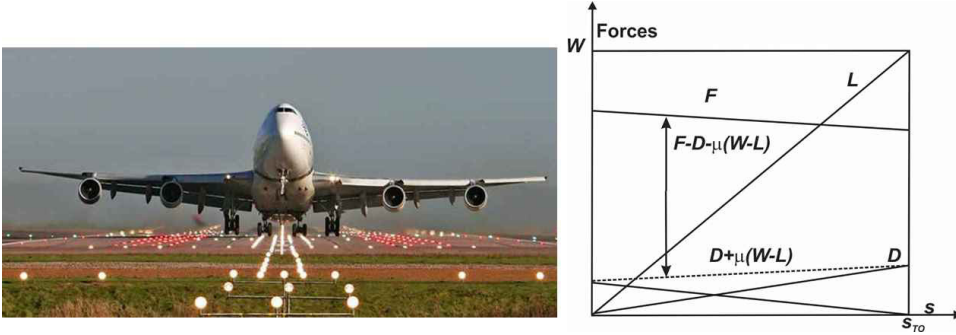
Figure 4.11.: The takeoff process and the variation of forces during a take-off. Lift (*L*) and drag (*D*) increase, the surface frictional force (*μ(W − L)*) decreases, the engine thrust, *F* , changes mildly and the net accelerating force, *F − D − μ(W − L)* changes moderately

Integrating it gives s_{TO} the take-off distance as

$$s_{TO} = \int_0^{V_{LO}} \frac{m_{a,i} V \, dV}{F - D - \mu(m_{a,i} g - L)} \tag{4.30}$$

The quantity μ is dependent on the surface quality. It is about 0.02 to 0.05 without brakes and 0.4 to 0.6 with brakes fully on. There are various values for different surfaces (see for instance Sariaas, 2007 for additional data). The dynamics of the aircraft when it takes off or lands in slush has complex frictional behavior that needs to be dealt with by the pilot when such a takeoff or landing is called for.

In the above integral, the quantities L and D vary with distance and hence stepwise integration is required. Since the net force does not vary much during this period as seen from Figure 4.11 (for jet aircraft), it is possible to make a simple approximation of taking the force as an average at an intermediate speed. The suggestion is that this calculation can be done at 0.707 V_{LO} (Sariaas, 2007).

The result for ground run can be expressed by taking an average value is

$$s_{TO} = \frac{2m_{a,i}}{\rho A_w c_{L,to}} \; \frac{m_{a,i} g}{[F - D - \mu(m_{a,i} g - L)]_{avg}} \tag{4.31}$$

In the equation 4.31, the subscript *avg* is used to indicate the value calculated at the mean speed. Some interesting conclusions follow from the above result. The ground run increases as the square of the aircraft mass and inverse of ambient density. These have serious implications. Military aircraft flying out of airstrips at high altitudes with heavy payload have indeed to be very careful about the length available for take-off. Design of heavy wide-bodied large passenger aircraft have to factor in the runway lengths in airports they intend operating from.

The distance covered during rotation is calculated as $V_{LO}t_R$ taking a value of 3 s for t_R. This will constitute about 10 to 15 % of the ground run. Calculation of the distance from this location to the position at 10.5 m altitude involves pilot technique involving the point of landing gear retraction. This segment will constitute additional 10 to 20 % of the ground run. The runway lengths at the major airports in India vary between 3.5 to 4.3 km. Airports operating in cities for a long time have difficulty in extending the airstrip length demanded by the heavier jets like airbus A 380 or Boeing 787 both of which need a take-off length of 3 km.

4.11. Landing

Landing most usually occurs with a mass much smaller than at take-off, because of which the landing distance can be accommodated within the take-off distance. However, landing an airplane is always known to be far more difficult than take-off, as discussed earlier. It is not possible to decide against landing under weather conditions similar to take-off for there may be no simple alternative. Figure 4.12 shows some aspects related to landing. Like take-off, landing has three phases -steady approach, flare or floating phase and a ground run. Pilots when approaching the runway have to align the aircraft with the runway utilizing the automatic landing system [or instrument landing system (ILS), see Chapter 7] that provides inputs to the cockpit on whether they are on the glide line towards the airstrip and whether they are online laterally as well. This segment is called steady approach.

The flare or the transition phase is the one in which attempt is made to reduce the rate of sink to zero and the forward speed to a minimum, which must be larger than V_{stall}. To ensure sufficient margin, regulations demand that the velocity at identified height (10.5 m) must be at least 1.3 V_{stall} and 1.15 V_{stall} at

Figure 4.12.: The approach, the landing process and the air strip required for landing

touchdown. There is a short floating phase where the flare creates conditions just ready for touch down in which aircraft flies horizontally just above the airstrip. At this stage stalling the aircraft by reducing the speed and/or increasing the angle of attack by allowing the hind wheels to touchdown the runway will ensure that the aircraft moves from airborne condition to on-ground condition. Sometimes, this phase is eliminated for aircraft with nose wheel type of landing gear, which, due to a relatively low ground angle of attack, can perform a touchdown at speeds above V_{stall}.

The last phase is the ground run. The ground run in many cases should be calculated in two sections. First, right after touchdown, the free rolling distance needs to be calculated while the pilot gets the nose wheel on the ground and starts to apply reverse thrust and brakes. Second, the relatively longer deceleration distance that is required for the aircraft to come to rest or to reach a speed sufficiently low to be able to move away from the runway must be determined. It is important to recognize that landing is affected by local wind conditions. The direction of landing is usually opposite of the wind direction. This results in the shortest landing run as much as take-off as it creates the lowest ground speed. In addition to this, problems may arise from cross-wind. Very quick corrections need to be made to ensure balanced wing positions. Quite often these are better achieved with higher landing speeds and pilots may choose to be on the higher side of the speeds. Consequently large margins are provided for landing distances. Safe landing distance has 70 % extra allowance and an additional 15 % is added on wet runways.

Sometimes when the air-traffic controller decides to delay the landing of specific aircraft because of traffic problems or local bad weather like fog or emergency

arrival of other aircraft, the aircraft may need to remain loitering over the airport. Further, if the cross-winds are large (typically more than 50 km/h), pilot needs to use a technique for causing the touchdown with the ailerons and rudder to keep the direction of movement on the runway within bounds. The decision to abort landing and loiter for more time or divert the plane to another city airport may also be made. In any case, even if all the corrections required for landing are made, the aircraft must be stabilized by 150 m above ground level on a clear day. If not, as per flight regulations, a mandatory go-around or aborting the landing will be needed to be adopted.

The ground run constitutes about 60 % of the landing distance and can be estimated by procedures similar to take-off. The primary differences, however, are that (a) most airplanes land with the engines at idle – F ~ 0, (b) the aircraft lands with an initial touchdown velocity, V_{TD}, and decelerates to rest and (c) the resistance forces, namely, drag, reverse thrust and ground friction are intentionally increased in this segment. These aspects are illustrated in Figure 4.13. Drag may be increased by using spoilers on the wings of the aircraft as it happens with most transport aircraft or adding a parachute as it happens with many military aircraft (it was also adopted in space shuttle). Reverse thrust is applied in all transport aircraft. It is obtained in propeller driven aircraft by reversing the pitch of the propeller and in jet aircraft by closing the exit nozzle with suitable petals and opening a side exit that directs most of the bypass flow and reduces the thrust. A typical example of thrust reverser in a jet engine is shown in Figure 4.14.

At a suitable stage in the landing run when the speeds have come down, brakes are applied in most cases. In aircraft that land on aircraft carriers, an arresting gear latches on to aircraft to reduce its speed on landing.

Because of these uncertainties, it is only the ground run that can be estimated accurately. Such an attempt will help understand the influence of various parameters on the landing distance. We follow the approach described for take-off to get

$$s_{land} = Const + V_{TD}^2 \ \frac{m_{a,TD}}{2\left[D + \mu(m_{a,TD}g - L)\right]_{avg} - F}$$

$$(4.32)$$
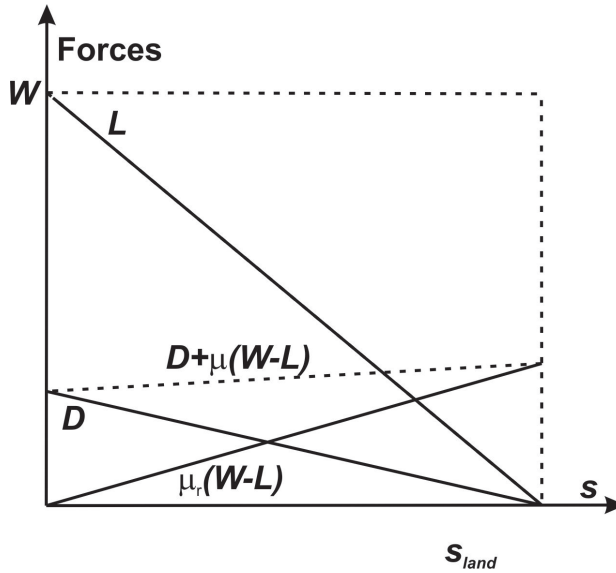
Figure 4.13.: Various forces on an aircraft during the landing process. Both Lift (*L*) and drag (*D*) decrease and the surface frictional force, $\mu(W - L)$ increases during the landing run. The net force, $D+\mu(W-L)$ mildly changes till the aircraft slows down to taxiing speed

where the subscript *TD* refers to touch down conditions. The term *Const* refers to components not dependent on flight speeds significantly. If the engine is brought to idle conditions, the approach speed of aircraft is 30 % higher than the stall speed calculated for the approach conditions of low fuel. If emergency landing conditions arise much before the normal landing conditions, the fuel will usually be dumped into the atmosphere to reduce the weight of the aircraft at landing. The touchdown speeds of most aircraft is about 15 % higher than the stall speed, V_{stall}. Thus,

$$V_{TD} = 1.15 \sqrt{\frac{2 \, g \, m_{a,TD}}{\rho_{TD} A_w c_{L,max}}}$$

(4.33)

Figure 4.14.: The thrust reverser arrangement on a typical turbo-fan based engine. On the application of the reverser, the four flap doors open up covering a part of the exit area and directing most of the bypass flow laterally and in part in the forward direction; drawn from Wikipedia5, 2016

Using the expression for V_{TD} we can write the equation for the landing distance as

$$s_{land} = Const + \frac{g(1.15m_{a,TD})^2}{\rho_{TD}A_w c_{L,max}\left[D + \mu(m_{a,TD}g - L)\right]_{avg} - F} \quad (4.34)$$

Torenbeek and Wittenberg (2002) make some simple arguments breaking up the landing path into two parts - inclined flight path along the glide angle and a landing run. This leads to

$$s_{land} = \frac{h_{land}}{tan\gamma_{land}} + 1.69\frac{m_{a,TD}}{\rho_{TD}A_w c_{L,max}\bar{d}} \quad (4.35)$$

where the subscript l_{and} refers to landing condition, h_{land} is the landing height taken as 15 m, γ_{land} is the landing angle typically 3^0 (and so $tan\gamma_{land}$ = 0.05), $\bar{d}$ is the ratio of average deceleration to the acceleration due to gravity ~ 0.3 to 0.5 for dry concrete runway. The equivalence between the two expressions can be

established by an approximate treatment that involves D and L being taken proportional to V_{TD}^2.

Like in the case of take-off, landing is also strongly controlled by the mass of the aircraft. Heavier aircraft and landing at higher altitudes require higher landing speeds and therefore, longer landing runs. Whenever the aircraft has to execute an emergency landing with larger fuel loading, it needs to dump the fuel to near-normal-landing conditions before attempting the landing.

4.12. Issues of Ice and Water on the Runway

While heavy rainfall can occur in all seasons, winter in latitudes both deep north and south brings forth problems of snow and slush. During take off, pilots need to decide whether to initiate actions towards take-off and so there are detailed guidelines provided on water, slush and wet snow depths beyond which take-offs are not permitted; typically water layers of 13 mm or dry snow depths more than 100 mm are the limits. There are also detailed procedures for deicing with time indicated for hold-over-time (HOT), the results which are subject to judgment by the pilots.

When it comes to landing, wetness on the runway reduces the braking effectiveness. With a combination of higher landing speeds and a minimum water layer, there is an effect called "hydroplaning" in which a sheet of water is created between the tire and the runway. To minimize hydroplaning problems, some runways are grooved to help drain off water, a facility not available in most airports. Use of higher tire pressure maintains the geometry such that there is less supportable area over water layer. This enables the tire to have much higher contact with the runway surface and so, friction to reduce the speed of the aircraft. Such a situation also arises when runways are covered with ice. For landing in such situations, reduction in speed is considered important for smooth operation and this is achieved by using reverse thrusters on the engine.

4.13. Climb Performance

The climb phase of any aircraft follows the take-off and ends when flight altitude (denoted by FT, FT 350 implying 35000 ft - 10.7 km) is reached. Continuing with take-off, the lift is larger than the weight. With increasing altitude, at the same attitude and speed, the lift reduces due to reduced ambient density till lift equals weight when aircraft levels off for a steady flight. Usually, the

flight path is controlled by increasing the angle of attack and thrust in multiple phases which on a segment may also include lift lower than the weight and so load factor less than unity (giving a slight weightless impression).

Civil aircraft take 10 to 30 minutes to reach the cruise altitude and military aircraft may take a minute or two reach desired altitude; typical specification of climb segment is climb rate (R/C). Typical values of the climb rates for passenger aircraft are 150 to 300 m/min and military aircraft have climb rates up to 10 km/min depending on the payload. The climb rate is dependent on the excess power that the aircraft has and how much it weighs. Figure 4.15 shows the features related to the climb segment. If we make a force balance along and normal to the flight path, we get

$$m_a g sin\theta = F - D; \quad m_a g cos\theta = L \tag{4.36}$$

We note that the climb rate is essentially $V sin\theta$ and therefore,

$$\text{R/C} = V sin\theta = \frac{V(F - D)}{m_a g} \tag{4.37}$$

The numerator on the right hand side is the difference between the engine flight power and power due to drag. The middle part of Fig. 4.15 shows that this difference increases from take-off to a maximum and reduces as flight speed increases. This is because the engine flight power increases at a slower rate (between V and V^2) compared to that due to drag power (that varies as V^3). The two intersect necessarily and there is a maximum speed at which climb rate becomes zero. This is what is depicted in the last part of Fig 4.15. If we draw the engine power and drag power as a function of altitude, we find that beyond a certain altitude, the available power becomes lower than the drag power (see Figure 4.4). This then becomes the ceiling of the aircraft flight. There are two terms associated with the ceiling - absolute ceiling (rate of climb = 0) and service ceiling which is the maximum usable altitude of flight (rate of climb is normally set at 30 m/min). Typical absolute ceiling for commercial airliners is 12.8 km and some business jets, it is 15.5 km. Some military aircraft have a service ceiling upwards of 25 km.
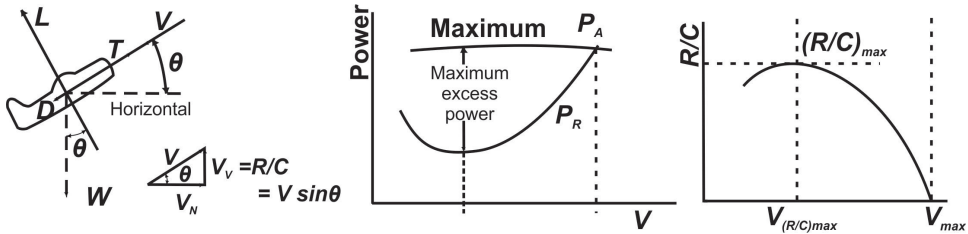
Figure 4.15.: Schematic of aircraft during climb and the force diagram (left); the power available from the engine and the power needed for maintaining a certain flight speed (middle); the rate of climb vs flight speed; θ is the flight path angle

The maximum climb angle can be simply derived from the above equations if first write

$$sin\theta = \frac{F}{m_a g} - \frac{D}{m_a g} = \frac{F}{m_a g} - \frac{Dcos\theta}{L} = \frac{F}{m_a g} - \frac{cos\theta}{L/D} \tag{4.38}$$

If we take the maximum of $cos\ \theta$ as 1, we immediately get maximum climb angle given by $sin\theta = F/(m_{ag}) - c_D/c_L$. More analysis can be performed for jet and propeller driven aircraft on the speed at maximum climb angle and maximum climb rate using certain models of thrust or power of the engine variation with speed and altitude [see Saarlas (2007) and Tornbeek and Wittenberg (2009)].

4.14. Turn Performance

Civil aircraft execute mild turns when moving from one corridor to another as per the ground control instructions and on occasions, loitering over an airfield waiting for landing permission from the air traffic control. The change in flight path is executed in what is known as coordinated turn that implies that the passengers feel mild push-down in their seats without lateral movement.

If there is a force imbalance, it may lead to side-slip or yaw and a definite lateral acceleration will be caused. Military aircraft will need to execute more maneuvers – deep turn, loop, deep climb, and others aimed at evading enemy gun fire or missile attack. A common feature of these maneuvers is the availability of substantial engine power/thrust that characterizes the difference between a transport and a military aircraft. It is possible to understand the behavior of the aircraft in turn near-horizontal or loop using simple dynamical relations.

Figure 4.16.: Forces on an aircraft executing a coordinated turn

Figure 4.16 shows the forces on an aircraft while executing a coordinated turn. The lift (L) is an angle ϕ with respect to the vertical. The vertical component balances the weight of the aircraft and the horizontal component of the lift balances the centrifugal force, F_r. These lead to

$$L\ cos\phi = W = m_a g; \quad L\ sin\phi = F_r = m_a V^2/R \tag{4.39}$$

where m_a is the mass of the aircraft, V is its velocity and R is the radius of turn. The value of ϕ is between 0 and 90^0. For steady flight ϕ = 0, L/W = 1 and for all turns, ϕ > 0. For these cases, $L > W$. The ratio L/W denoted by n is called the load factor and represents the load experienced beyond normal gravity by the pilot and the aircraft. For steady normal flight, n = 1 and for maneuvering flights n > or < 1, implying that one experiences more or much lesser loads than normal gravity. It is well known that n = 0 refers to zero-g conditions experienced in space flights and n as high as 6 is experienced by fighter pilots for short durations in deep turns and acceleration. Larger n (also described by saying pulling larger *g's*) is unsafe except for short durations. In fact, for safe operations, there is a map of n vs. duration for which the pilot experiences the acceleration within which he/she is expected to operate.

The features of turning are connected deeply with the load factor and hence it is useful to express the relations in terms of n. Now, simple algebra leads to

$$n = \frac{L}{m_a g} = \frac{1}{cos\phi} = \sqrt{1 + \left[\frac{V^2}{gR}\right]^2} \tag{4.40}$$

$$tan\phi = \frac{V^2}{gR} = \sqrt{(n^2 - 1)}$$

(4.41)

$$R = \frac{V^2}{g\sqrt{(n^2 - 1)}}$$

(4.42)

For a fixed flight velocity, sharper turn (reduced R) implies larger n. This calls for larger ϕ. At $\phi = 90^0$, n → ∞; The limit for n is set by safe-pilot operations, structural integrity factor and the engine power/thrust availability. The thrust-drag balance gives

$$F = D = \frac{D}{L}\frac{L}{W}W = \frac{c_D}{c_L}nW$$

(4.43)

This equation shows that the engine thrust increases with the load factor modulated by c_D / c_L which varies with the angle of attack. Thus, for change from steady flight to a coordinated turn, the pilot has to increase the lift by increasing the angle of attack and also increase the engine thrust. If we use $n = L/W = c_L \rho V^2 A_w / W$ we get $V = V(n = 1)\sqrt{n}$ that tells us how the speed increases as we move towards larger load factor in this manner. The time for turn which is a performance index can be obtained from $t_{turn} = 2\pi R / V$.

For passenger transport, during loiter, n = 1.05 to 1.15. For these cases, a bank angle of 17 to 30^0 and passengers experience an apparent increase in their weight by 5 to 15 %. For a typical flight speed of 250 km/h (69.5 m/s), the radius of turn is 4.8 km (n = 1.05) and 1.5 km (n = 1.15). The speed increase for these values of n is 2% and 7.5%. But if we consider a coordinated turn of 60^0, we experience n = 2 and the speed increase is as much as 41 % compared to steady flight.

There are other performance parameters like minimum time for turn, minimum turn radius and load factor and related features can be explored using similar anaysis (Saarlas, 2007).

4.15. Pull-up and Pull-Down Maneuvers

Pull-up maneuver is often performed in dog-fight conditions and a combination of pull-up and pull-down resulting in a loop is also a part of dog-fight strategy.

Escaping missile hit needs sharp changes of flight path executed with turn, pull-up and pull-down maneuvers. The pull-up maneuver is executed by accelerating the aircraft using engine power/thrust and also increasing the angle of attack by operating the elevator. The pull-down maneuver is the one that results from a loop, the first step of which is the pull-up maneuver. Both these maneuvers can be simply analyzed by examining the force balance in the vertical direction. It leads to

$$\frac{m_a V^2}{R} = L \pm W = W(n \pm 1)$$

(4.44)

It leads to

$$R = \frac{V^2}{g(n \pm 1)}$$

(4.45)

In the above equation, the negative sign refers to pull-up maneuver and positive sign to the pull-down maneuver. Other aspects of the performance can further be derived along the lines indicated earlier.

There are several maneuvers that a fighter may need to execute in close combat. Wikipedia (wikipedia2, 2014) describes many varieties of maneuvers used in close combat, some of which are (i) Combat spread, (ii) Defensive split, (iii) Sandwich,(iv) Break, (v) Barrel roll attack, (vi) High-side guns pass, (vii) Split-s, (viii) Pitch-back, (ix) Wing-over, (x) Low Yo-Yo, (xi) High Yo-Yo, (xii) Lag displacement roll,(xiii) High Yo-Yo defense, (xiv) Unloaded extension, (xv) Scissors, (xvi) Flat scissors,(xvii) Rolling scissors, (xviii) Guns defense, (xix) High-g barrel roll, (xx) Defensive spiral. Further, the cobra maneuver named after Pugachev (Russia) who performed it on Sukhoi 30 in Paris air show in 1989 is one in which an airplane flying at a moderate speed suddenly raises the nose momentarily to the vertical position and slightly beyond (120^0) and drops back to normal flight. It uses large engine thrust to maintain approximately constant altitude through the entire move (see Fig. 1.15 and wikipedia3, 2014). It was also subsequently demonstrated on F-22 aircraft. It demonstrates the aircraft's pitch control superiority, high angle-of-attack stability and engine-inlet compatibility and of course, the pilot's skill. Achieving it is considered an accomplishment of super-maneuverability in military aircraft. The strengths and limitations of the ability to perform these maneuvers vis-a-vis overall aircraft acceptability for military operations are discussed in Chapter 7.
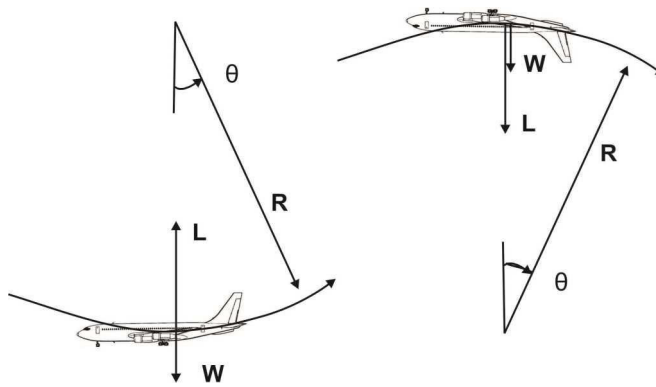
Figure 4.17.: The force diagrams for pull-up and pull-down maneuvers

4.16. Performance of Rocket Based Vehicles

Rocket based vehicles are: tactical missiles, IRBMs and ICBMs (intermediate range and intercontinental ballistic missiles) and satellite launch vehicles. We will address them now.

4.16.1. Tactical missiles

Tactical missiles have requirements of being sleek with small reaction times; they must pack as much of propulsion within a small volume - diameter and length. This demands high density impulse of the propulsion system. Using high chamber pressures (100 to 150 atms) inside the combustion chamber primarily to obtain a high nozzle efficiency and so higher specific impulse is a normal practice. Added to this using higher density propellants is considered important. These combined with prepackaging requirements implies that solid propellants are the better choice. Most operations are of boost-sustain variety. A short burn time of 2 to 5 s with longitudinal acceleration up to 10, lateral accelerations up to 20 are considered reasonable in the boost phase. Once the missile has achieved a high speed (Mach numbers up to 4), the longer sustain operation up to 30 s maintains the speed and allows the control and guidance systems time to maneuver the missile to the target, aerial for air-to-air missiles and terrestrial for air-to-surface missiles. The missiles based on rockets can be heavier for some missions. In such situations, a combination of air-breathing

and non-air breathing engines is adopted. For the boost phase one uses rock-ets. For the sustain phase of the flight within the atmosphere, one can use a ramjet or a turbojet depending on the application. Use of ramjets and rockets separately is not uncommon (like in Blood Hound missile of United Kingdom). Use of turbojets for cruise missiles which fly long distances (1000–1500 km) at tree top heights carrying nuclear warheads is another common feature (like Tomohawk of USA). Ducted rockets, ejector rocket-ramjets and integral ram rockets are concepts considered for use in missiles with liquid fuels or solid fuel rich propellant for the ramjet phase. Figure 4.18 shows the sizes of dif-ferent vehicles to achieve a fixed mission (drawn from the interesting work of Marguet et al, 1979). For relatively short duration missions (~ 50 s or less), the vehicle performance will be affected by the volume required to store the propellant. The specific impulse of liquid propellants will be higher (~ 10 kN s/kg) and the density lower (kerosene – 800 kg/m^3) compared to those of fuel rich solid propellant based ramjets with values of I_{sp} = 6 kN s/kg and a density of 1700 kg/m^3. In terms of comparison of weights of the systems at launch, the ratio of fully solid propellant : rocket-liquid ramjet: rocket-solid fuel ramjet sys-tems is 1 : 0.6 : 0.5 for the operational duration of 50 s or less.

4.16.2. IRBMs and ICBMs

The mission of IRBMs and ICBMs is to deliver a nuclear payload to a distant target - more than a few thousand km away. This is achieved by a rocket based launch vehicle which positions the payload at a specific location with a specific velocity in the atmosphere for the launch of the ballistic payload (warhead) because the accuracies on both position and velocity affect the accuracy of the payload reaching a specified target location. The trajectory of the payload with a warhead is ballistic (much like the pathway of a stone thrown physically). The key to the trajectory is specific point of release of the payload in its ballistic tra-jectory and the velocity at the point of release. Essentially, the launch vehicle can be thought of as providing velocity increment to the payload. The velocity increment is composed of three parts - the velocity increment to reach that al-titude and the velocity required for the ballistic path of a missile. The last part is the terminal segment that ensures that the warhead reaches the intended target with desired accuracy. Following the completion of the propulsive

10m

Rocket engine

6m

Integral rocket ramjet

Kerosene

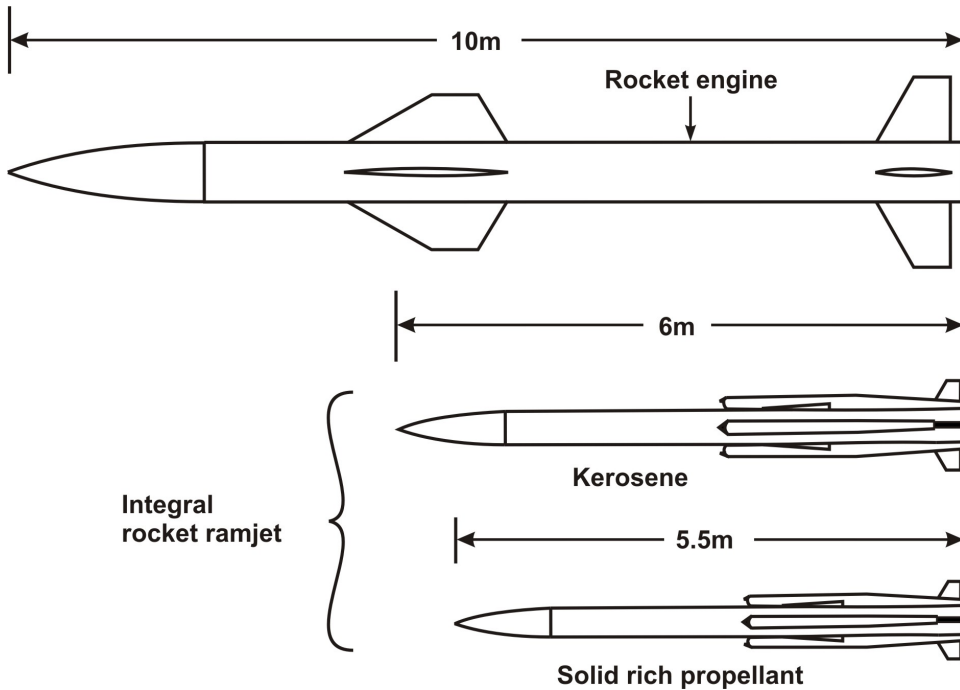**5.5m**

Solid rich propellant

Figure 4.18.: Options for a missile to achieve a mission drawn from Marguet et al, 1979

phase of the mission, the missile will get aligned, inertially stabilized allowing the payload to go on a ballistic trajectory to re-enter the atmosphere toward a pre-selected target. During atmospheric re-entry, the exterior of the pay-load needs thermal protection due to extensive aerodynamic heating (discussed in section 2.4.1 of Chapter 2). Usually, for the payload, a non-lifting configuration has been the choice for its simplicity. Accuracy in reaching a ground target is ensured by the choice of injection parameters which are calculated to reach a specific re-entry point. If multiple targets are to be reached as in MIRV (multiple independently targetable re-entry vehicle) reaching specific targets not too far from each other, it is done by separation and injection at the time of re-entry. Figure 4.19 presents the details of a typical flight path of Minuteman II drawn from Wikipedia7 (2016). It must be noted that each ICBM can be assigned any of the targets within the overall range between a minimum and a maximum that the ICBM is designed for.
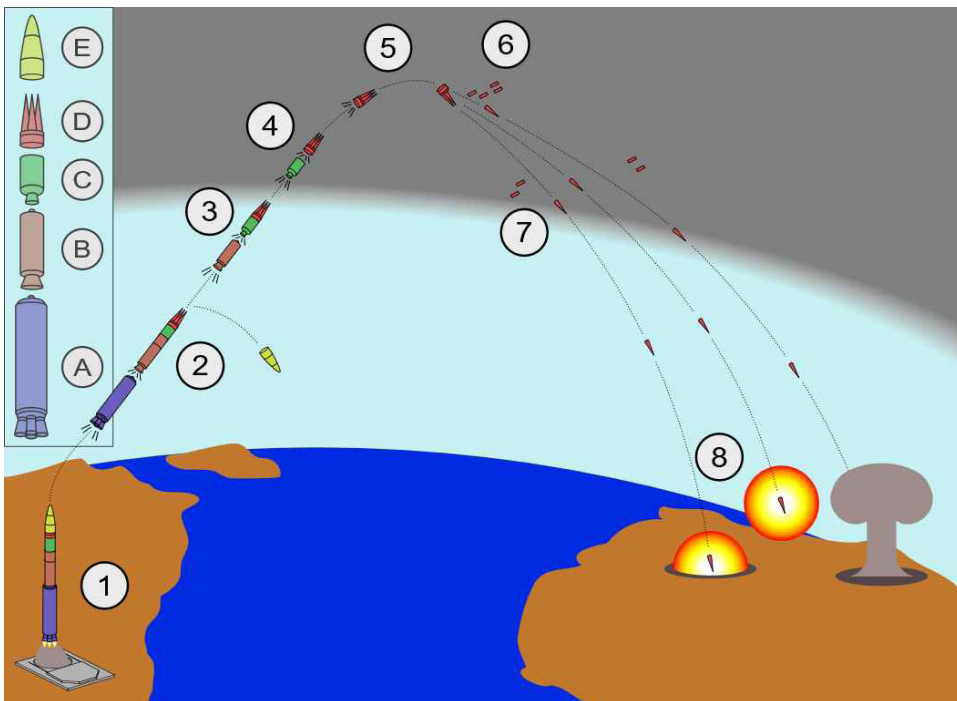
Figure 4.19.: The Minuteman II flight sequence: The missile launches out of its silo by firing its first-stage boost motor (A). 2. About 60 seconds after launch, the 1st stage drops off and the second-stage motor (B) ignites. The missile shroud (E) is ejected. 3. About 120 seconds after launch, the third-stage motor (C) ignites and separates from the 2nd stage. 4. About 180 seconds after launch, third-stage thrust terminates and the post-boost vehicle (D) separates from the rocket. 5. The post-boost vehicle maneuvers itself and prepares for the payload (the reentry vehicle) deployment. 6. While the post-boost vehicle backs away, the payload, decoys, and chaff are deployed (this may occur during ascent). 7. The reentry vehicles and chaff reenter the atmosphere at high speeds and are armed in flight. 8. The nuclear warheads detonate, either as air bursts or ground bursts; drawn from Wikipedia7 (2016)

Some of the re-entry vehicles are designed with wings so that they can be aerodynamically controlled along with suitable guidance and control systems to ensure reaching a specific target. The principal advantage of the use of lifting body approaches is that the re-entry loads can be minimized with flexibility in landing site selection. There is another class of systems called the ASBM's (anti-ship ballistic missile) to deal with enemy warships at sea. These are called quasi-ballistic missiles because the ballistic segment is a small fraction of its

trajectory and/or the missile is capable of being maneuvered during the ballistic phase. Many of the guidance systems that are crucial for deployment have a global positioning system or can be steered directly into a target with TV guidance during the terminal phase.

The development of ballistic missile has created the need for ballistic missile defense systems. These are designed in a manner similar to the offense systems. The demand for guidance and control with MIRV offense systems will be even more involved in these cases.

The accuracy of reaching targets in the case of IRBMs/ICBMs is about 0.3 km and of quasi-ballistic missiles about 10 m.

The trajectory after lift-off lasts for 180 to 300 s with a vehicle velocity increment of 4 to 8 km/s and altitude of 150 to 400 km. The second phase that lasts 900 to 1400 s follows an elliptic flight path with apogee of 500 to 1200 km. The final re-entry phase lasts about 120 s starting at an altitude of about 80 to 100 km with impact speed up to several km/s. Indian developments of the AGNI series of ICBMs with MIRV capability are being developed to achieve target reaching accuracies of less than 10 m (Wikipedia8, 2016). One of the key elements in trajectory calculations is an accurate description of earth's gravity that decreases with altitude. At one level of accuracy, it decreases as $g(h) = g_0[1/[1 + h/Re]^2$ where $g(h)$ is the gravitational acceleration at an altitude h, g_0 is the gravitational acceleration at the surface of earth = 9.81 m/s² and R_e is the radius of the earth at equator (6371 km). When finer accuracies of the trajectory are demanded, it is important to know that g_0 is influenced by the actual shape of earth which is different from that of a sphere with the polar radius being shorter by 21 km (0.33 %) compared to the equator because of centrifugal forces causing the deformation. The local gravity is also affected by the presence of mountains and can change due to movement of masses inside the earth. For this reason the gravitational model has to be updated periodically for the target reaching accuracies to be maintained.

The velocity increment indicated in the previous paragraph is composed of several aspects. Firstly, overcoming the gravity to get to an altitude in a vertical direction that depends on the time taken to reach the altitude. This depends largely on the initial thrust to weight ratio of the vehicle. This is accompanied by drag losses due to atmospheric friction. Steering loss is another factor that needs to be factored due to instantaneous thrust vector not being parallel to

the current velocity vector, the magnitude depending on the mission profile. These are discussed below.

4.16.3. Satellite launch vehicles

Orbital vehicles need a net velocity increment, ΔV typically of 9 to 12 km/s (as with ICBMS). It is possible to perform simple analyses to obtain these values. Space dynamic considerations will be used to obtain the energies in the orbits and energy required to transfer the payload from earth to the orbit and also discussed are the associated aspects of gravity loss and drag loss.

4.16.4. Orbit energies and Velocity increments

One simple minded approach to getting to the orbit would be to lift the payload by the thrust from the engines, reach an altitude where its vertical velocity is nearly zero and then create thrust vector change to enable circularizing the orbit. In the determination of the velocity increments required, the acceleration due to gravity, g plays the principal role which as indicated earlier, decreases with altitude. Because of this, it is more appropriate to obtain the velocity component required to reach the altitude by equating the energy at the earth with the value at altitude as given by

$$\frac{-GM}{R_e + h} = \frac{-GM}{R_e} + \frac{V_1^2}{2}$$

(4.46)

where GM is the product of gravitational constant and the mass of the earth = 3.93 x 10^5 km³/s², and V_1 is the projection velocity required to achieve an altitude of h above earth. The above equation can be expressed as

$$V_1 = \sqrt{\frac{GM}{R_e}} \sqrt{\frac{2x}{1+x}}$$

(4.47)

where $x = h/R_e$. The velocity required to be provided to a payload of ICBM (V_2) is calculated by solving the dynamical equations to reach a specific target location on the earth. This is typically 7 to 8 km/s. For the case of satellite, the velocity required (V_2) is the same as the orbital velocity. For a circular orbit, this

Table 4.3.: The kick velocity required for reaching an altitude and the orbital velocities

Altitude	$x\ (h/R_e)$	V_1	V_2	$V_1 + V_2$
km	-	km/s	km/s	km/s
200	0.031	1.92	7.7	9.67
1000	0.156	4.07	7.3	11.37
36000	5.64	10.2	3.0	13.2

is obtained by equating the centrifugal forces with gravitational pull. We get

$$\frac{V_2^2}{R_e + h} = \frac{GM}{(R_e + h)^2} \tag{4.48}$$

and this leads to $V_2 = \sqrt{GM/R_e}\ (1/(\sqrt{1+x})$. If we sum up V_1 and V_2 we get

$$V_1 + V_2 = \sqrt{\frac{GM}{R_e}} \left[\sqrt{\frac{2x}{1+x}} + \frac{1}{\sqrt{1+x}} \right] \tag{4.49}$$

$$= 7.85 \left[\sqrt{\frac{2x}{1+x}} + \frac{1}{\sqrt{1+x}} \right] \tag{4.50}$$

If we make calculations using the above relationships, we get the results as in Table 4.3. As can be noticed from the table, the kick velocity increases as altitude increases, but the velocity required to keep the satellite in orbit decreases. However, the combined velocity increases.

The sum of velocities calculated for the geosynchronous orbit is reduced by using the idea of elliptic orbit transfer (Hohmann) discussed earlier. To get the vehicle into the orbit, one has to account for losses due to gravity, drag and steering. There will be conflicts in the choice of the trajectory and the optimum solution depends on the parameters of the mission. These issues are discussed below.

4.16.5. Launch phase behavior

While the design of the mission involves the calculation of the flight path in 3-d accounting for aerodynamic and gravitational effects, much insight can be gained from a simple one-dimensional analysis. This is particularly so for the

launch phase where both of the above effects play an important role; beyond the atmosphere, space dynamics takes over.

The equation of the flight path is described by

$$m\frac{dV_z}{dt} = F\,sin\theta - mg - D \implies \frac{dV_z}{dt} = \frac{F\,sin\theta}{m} - g - \frac{D}{m} \tag{4.51}$$

$$m\frac{dV_x}{dt} = F\,cos\theta \implies \frac{dV_x}{dt} = \frac{F}{m}cos\theta \tag{4.52}$$

where V_z and V_x are the vertical and horizontal vehicle velocities, F is the rocket thrust that can be represented by $F = \dot{m}_p I_{sp}$ with $\dot{m}_p$ being the propellant mass burn rate (is also equal to m˙ , the mass loss rate of the vehicle) and I_{sp}, is the specific impulse characterizing the propellant and the nozzle expansion ratio (see for more discussion Chapter 3 section 3.14), D is the drag due to aerodynamic effects and θ is the thrust vector angle with horizontal also called pitch angle. For vertical launch, θ is 90^0. The flight path is governed by the relationship between vertical and horizontal velocities. The angle between the horizontal and vertical velocities given by $\gamma = tan^{-1}[V_z/V_x]$, the flight path angle. This angle is also 90^0 for vertical launch. The prime reason for the difference between θ and γ is the presence of gravity term which gets aligned with the thrust vector only for vertical path. The difference $\theta - \gamma$ is the angle of attack and is never zero for this reason. Some interesting conclusions can be derived from an analysis of the equations that are discussed well in Turner (2006). The advantage with vertical pathway through the atmosphere allows drag losses to be brought down. To understand the way gravity loss is influenced, it is useful to treat the simpler case of vertical flight without drag (it can be added separately). The equation becomes

$$\frac{dV_z}{dt} = \frac{F}{m} - g \tag{4.53}$$

By expressing the terms as

$$\frac{dV_z}{dt} = I_{sp}\frac{\dot{m}_p}{m} - g = I_{sp}\frac{\dot{m}}{m} - g = \frac{dm}{mdt} - g \tag{4.54}$$

we can recast the equation as

$$dV_z = I_{sp}\frac{dm}{m} - gdt$$

(4.55)

Integrating which we get

$$\Delta V_z = I_{sp}ln\left[\frac{m_{ini}}{m_f}\right] - gt_b$$

(4.56)

where ΔV_z is the velocity increment provided by the propulsion system. It can be interpreted as V, the final velocity of the vehicle with initial velocity 0. The quantities m_{ini} and m_f are the initial and final masses of the launch vehicle the difference $(m_{ini} - m_f)$ constitutes the propellant mass. The burn time t_b can be expressed as $(m_{ini} - m_f)/\dot{m}_p$ and therefore the gravity loss expression (the second term on the right hand side) can be written as

$$\text{Gravity loss} = gt_b = g\frac{(m_{ini} - m_f)}{\dot{m}_p} = I_{sp}\frac{m_{ini}g}{F}\left[1 - \frac{m_f}{m_{ini}}\right]$$

(4.57)

where the ratio m_{ini}/m_f is called the mass ratio of the vehicle and $F/m_{ini}g$ constitutes the thrust-to-initial weight of the vehicle. How do we interpret the above expression for gravity loss? If a certain ΔV_z is to be achieved, one should have larger values for both thrust-to-initial weight ratio and mass ratio. Enhanced specific impulse implies lower propellant mass for the same total performance and this also leads to lower total mass. Since thrust acts against gravity for a time to meet the velocity increment, smaller the duration over which it completes the function, smaller will be the loss. Thrust-to-initial vehicle weight is a direct indication of acceleration of the vehicle. Use of a larger thrust-to-weight ratio implies larger acceleration which is limited by payload - sensitive instruments and astronauts. Typical values are between 1.3 to 2. Increasing the mass ratio is affected by reducing the structural mass for the same function and is limited by materials and technology. Thus there are limits to reducing the gravity loss. One approach in which one can launch nearly horizontally to reach the trajectory that has little gravity loss has the issue of enormous drag loss because the greater depth of the atmosphere to be crossed. Therefore, the best strategy comes out as a combination of a vertical trajectory to cross thicker

part of the atmosphere first and then initiate a curved transition to a trajectory that is nearly horizontal with a segment of final entry into the orbit.

The curved transition requires the use of thrust vector control to enable the vehicle to move away from the vertical path. This process will lead to angle of attack on the wing surfaces and asymmetric pressure build up on the vehicle both of which leading to additional aerodynamic loads. This feature is directly quantified by the dynamic pressure denoted by $q = \rho V^2/2$. Keeping the q loads within limits of structural integrity is an important constraint in the flight path design. To get at optimum parameters, full scale simulations are undertaken. Even though the typical range of q is 20 to 50 kPa, in specific missions, it could go up to 100 kPa or more. Larger dynamic pressure implies the need for more robust structure contributing to higher structural factor. One important way to reduce the dynamic pressure is to do reduce the thrust during the initiation of gravity turn. This is more easily accomplished in liquid rocket engines with variable thrust capability. In solid rockets the thrust programming is integrated into the propellant grain geometry to provide a shaped pressure-time curve (see Chapter 3) and also use parallel staging like in most launch vehicles in which one can ignite some or all of the strap-on boosters at ground or at some desired altitude as is practiced in PSLV and GSLV and other launch vehicles.

The way the trajectory is managed is to have a vertical segment for 4 to 10 km, initiate then, a roll stabilized arrangement for stability of the vehicle motion and provide a vectoring of the thrust vector by one of the approaches discussed in Chapter 3 and section 3.18. This will cause the pitch angle, θ to become less than 90^0. Once the vehicle is moving along a non-vertical trajectory, gravity will come in and tilt the trajectory downwards. This part is the well known gravity turn - gravity assisted trajectory. It is possible that thrust vector can continue to be modulated later towards the desired mission pathway; this is called pitch programming.

Typical gravity losses can be 1 to 2 km/s. The drag losses integrated over the trajectory, $\int [D/m] dt$ varies from 0.3 to 0.6 km/s.

4.16.6. Further consideration on staging of vehicles

Equation 4.56 (changing $Vz\ to\ V$) for the case without gravity and drag losses is

$$\Delta V = I_{sp} ln \left[\frac{m_{ini}}{m_f} \right]$$

(4.58)

where ΔV is the velocity increment provided by the propulsion system. The quantities m_{ini} and m_f are the initial and final masses of the launch vehicle and the difference $(m_{ini} - m_f)$ constitutes the propellant mass. The burn time t_b can be expressed as $(m_{ini} - m_f)/\dot{m}_p$. Typical value of I_{sp} can be taken as 2700 Ns/kg or 2.7 km/s. For ΔV of 8 km/s, the mass ratio becomes 19.3 implying that the structural fraction is 1.7 %. This is unattainable since the achievable structural fractions rarely go below 10 % (see Table 1.5). The most favorable choices of ΔV = 7.5 km/s and I_{sp} = 3000 Ns/kg lead to a structural fraction of 8 % that is still unattainable. Hence, a single stage rocket to orbit is currently beyond realization. For structural factors currently achievable multi-stage rockets are the only solution. Typically 3 or 4 stages are used. This conclusion is unaffected by the gravity and drag losses that constitute about 15 to 20 % of the total drag loss.

One can conceive of serial staging or combine with parallel staging. In AGNI vehicle, it is serial staging and in PSLV and GSLV vehicles (see Figure 1.19), it is parallel for the lower most stage and serial for upper stages. The optimum number of stages as a function of individual stage performance and structural factors can be obtained from an analysis based on Lagrangian multipliers (see Chapter 11 of Curtis, 2005). If individual stage structural factors are brought down, the number of stages can also come down. While in early development of launch vehicles, 4 stages were used, later designs that combined liquid and solid propulsion systems appropriately and the use of better materials have led to the choice of 3 stages.

A typical mission profile with event marked operations for the Indian GSLV vehicle is shown in Figure 4.20. The important events on the vehicle flight path, the altitudes and vehicle velocities are also set out in this figure. The final vehicle velocity to reach the geo-transfer orbit (GTO) is 9.8 km/s. Beyond this point, circularising the orbit, possible orbit rising and satellite positioning operations will be conducted with thrusters on the satellite.

India has two vehicles - PSLV for sunsynchronous missions (SSO) and GSLV for geosynchronous missions (GTO orbit). Soyuz is capable of all the missions
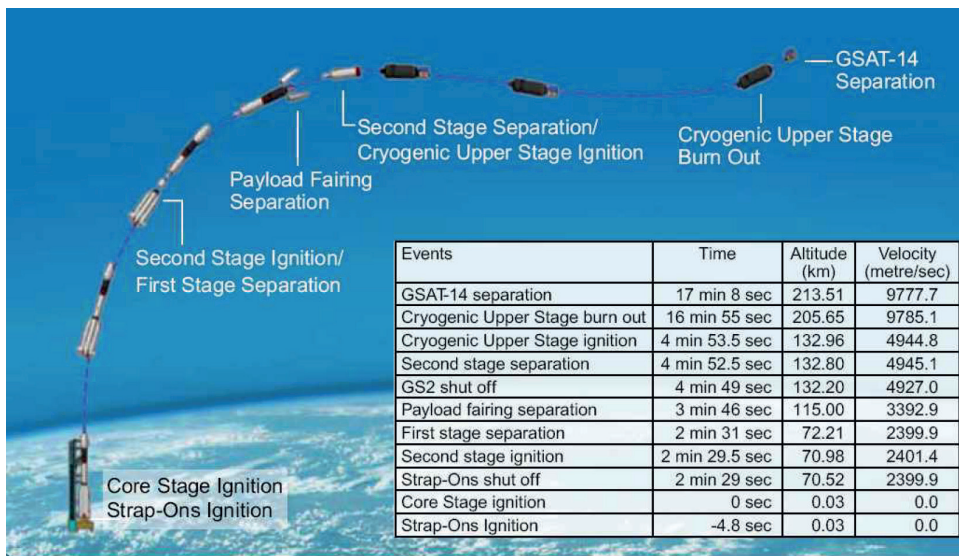
Events	Time	Altitude (km)	Velocity (metre/sec)
GSAT-14 separation	17 min 8 sec	213.51	9777.7
Cryogenic Upper Stage burn out	16 min 55 sec	205.65	9785.1
Cryogenic Upper Stage ignition	4 min 53.5 sec	132.96	4944.8
Second stage separation	4 min 52.5 sec	132.80	4945.1
GS2 shut off	4 min 49 sec	132.20	4927.0
Payload fairing separation	3 min 46 sec	115.00	3392.9
First stage separation	2 min 31 sec	72.21	2399.9
Second stage ignition	2 min 29.5 sec	70.98	2401.4
Strap-Ons shut off	2 min 29 sec	70.52	2399.9
Core Stage ignition	0 sec	0.03	0.0
Strap-Ons Ignition	-4.8 sec	0.03	0.0

Figure 4.20.: Typical flight path of the geosynchronous satellite launched from Shriharikota range, India along with altitudes and velocities at various vehicle staging operations

Table 4.4 shows the details of the stage performance of four launch vehicles. The vehicles, PSLV, GSLV (Indian), Soyuz (Russian flown from French Guyana) and Ariane 5 (French flown from French Guyana) are in the increasing order of lift-off masses, payload capability and efficiency. This table was constructed from open source information from ISRO (2016) and Arianespace (2016) that contain details of PSLV, GSLV, Soyuz and Ariane 5 vehicles. Some information was also obtained from several launch videos posted on the internet. While the timings, height and velocity information is available on these vehicles, some aspects on weights were to be interpolated from several sources. This table is very instructive.

India has two vehicles - PSLV for sunsynchronous missions (SSO) and GSLV for geosynchronous missions (GTO orbit). Soyuz is capable of all the missions - SSO, GTO, MEO and LEO (see section 1.2.12 in Chapter 1) and is launched from Kourou in French Guyana in cooperation with Arianespace. Ariane 5 is a very heavy launch vehicle and is capable of all the missions with heavy payload. The demand for satellite utility for various societal applications is increasing, the satellite mass is continuing to increase and the demand for heavy launchers. Of course, smaller payloads are also in demand and these

require vehicles with lower lift-off weight and these are served by vehicles like PSLV and GSLV. It must be noted that when satellites are launched, the final segment delivered to the orbit will carry the inert mass of the last stage that will get separated from the satellite and in addition, the satellite itself carries many elements apart from the relevant active payload like the propulsion system for orbit management purposes.

As can be noted from Table 4.4, the payload delivered per unit lift-off mass is 0.004 for PSLV, 0.0052 for GSLV, 0.01 for Soyuz and 0.013 for Ariane 5. If PSLV is configured for the GTO mission, the payload fraction will be even lower. The primary cause of this is in the choice of propulsion system for the stages. For large impulse applications (meaning thrust-burn time product) of the kind demanded from these missions, solid propulsion systems are inherently heavier than liquid systems as can be noted from the data on "stft". The reason for this is as follows. The combustion chamber in a rocket engine has to be at high pressure - 50 to 200 atms to deliver the needed performance (specific impulse). In a solid propulsion system, the combustion chamber carries the solid propellant. Hence the entire volume is at very high pressure needing a heavier casing. In the case of liquid propulsion system, the liquids are carried in tankages that are maintained at low pressures (about 4 to 6 atms). This is independent of the choice of combustion chamber pressure and so, the high pressure is restricted to the turbo pump exit, the plumbing and the combustion chamber-nozzle combination (also called thrust chamber) the mass of all of which constitute a small fraction.

Therefore, the dry structural mass of liquid propulsion system stages will be much lower than for solids. This is evident in Table 4.4 (see the column "stft"). Further, for large rocket systems, volume limitation is not significant. Therefore, even lower mean density systems like LOX-LH$_2$ can perform very well. Figure 4.21 shows the Soyuz and Ariane vehicles with high performance. The fact that Soyuz vehicle was conceived in the mid sixties was based on the same class of propellants as Saturn vehicle (USA). Even though its performance was intermediate in terms of specific impulse, the scale of the vehicle allowed for higher performance than solids with its much lower structural factor. Ariane 5 benefited from long duration burning high performance LOX-LH$_2$ with an unusual staging scheme - making it the core engine along with solid propulsion strap-ons. From these developments, it appears that the limitations arising from conflicts in the variation of specific impulse and density impulse

Table 4.4.: Stage mass (mst), propellant mass (mprop), thrust (F), Stagem = stage mass, structural fraction (stft) = (structural mass + inerts)/stage mass), stage mass ratio (MR), Thrust (F), burn time (tb), Specific impulse (Isp, ΔV = stage velocity increment, and altitude (h), 0 stage = strap-on; S = Solid - AP-HTPB-Al, * vacuum performance can be taken 10 -12 % more than sea level performance; L1 = UDMH, N2O4; L2 = Hydrazine, Mixed oxides of nitrogen; L3 = LH2, LOX; L4 = Kerosene - LOX

Vehicle Stage	m_{prop} t	m_{st} t	Stagem t	stft	MR	F kN	tb s	I_{sp} Ns/kg	ΔV km/s	h km
PSLV - SSO; SHAR launch; Inertial velocity at start = 0.45 km/s										
0 (S, 6)	72.0	18.0	90.0	0.20		2780*	45	2300*		41.4
1 (S)	138.6	29.0	167.6	0.17	2.9	4470*	100	2370*	1.71	66.0
2 (L1)	40.6	5.4	46.0	0.12	2.8	810	147	2890	1.96	216.0
3 (S)	7.6	0.5	8.1	0.06	1.7	335	109	2650	1.81	423.8
4 (L2)	2.5	0.4	2.9	0.14	2.0	14	516	2950	1.68	514.3
Extra-Str		4.1	4.1							
Payload+		1.3	1.3							
Total	259.3	58.7	320.0	0.18				917	7.16	
GSLV-GTO; SHAR launch; Inertial velocity at start = 0.45 km/s										
0 (L1, 4)	162.8	22.4	185.2	0.12	2816*	148	2400*			
1 (S)	138.2	28.3	166.5	0.17	3.6	4470	100	2370*	2.4	72.3
2 (L1)	39.5	5.5	45.0	0.12	2.7	810	150	2900	2.54	132.8
3 (L3)	12.8	2.5	15.3	0.16	3.7	74	720	4540	4.84	213.4
Extra-Str		1.0	1.0							
Payload+		2.2	2.2							
Total	353.3	61.9	415.2	0.14				1118	9.78	
Soyuz - GTO; Kourou launch; Inertial velocity at start = 0.45 km/s										
0 (L4, 4)	156.8	15.1	171.9	0.08		3350	118	2620	1.75	45.0
1 (L4)	90.1	9.6	99.7	0.10	4.7	792	286	2550	1.95	110.0
2 (L4)	25.4	2.3	27.7	0.09	2.7	298	270	3590	3.25	175.0
3 (L3)	6.6	0.9	7.5	0.12	2.1	19	1100	3320	2.35	656.0
Extra-Str		2.1	2.1							
Payload		3.3	3.3							
Total	278.5	32.6	312.2	0.10					9.30	
Ariane-5 - GTO; Kourou launch; Inertial velocity at start = 0.45 km/s										
0 (S, 2)	474.0	66.0	540.0	0.12	5.7	14160	140	2800	1.80	99.0
1 (L3)	170.0	14.7	184.7	0.08	3.1	1200	650	4540	5.20	154.0
2 (L3)	14.3	4.5	18.8	0.09		63	270	4540	9.30	702.0
Extra-Str		23.0	23.0							
Payload		10.5	10.5							
Total	658.3	118.7	777.0	0.15					9.30	

SOYUZ

Ariane 5 ECA

Satellite 1
← Payload fairing
← Syida 5
Satellite 2
← ESC-A H 14,4 Upper stage

Booster EAP P241

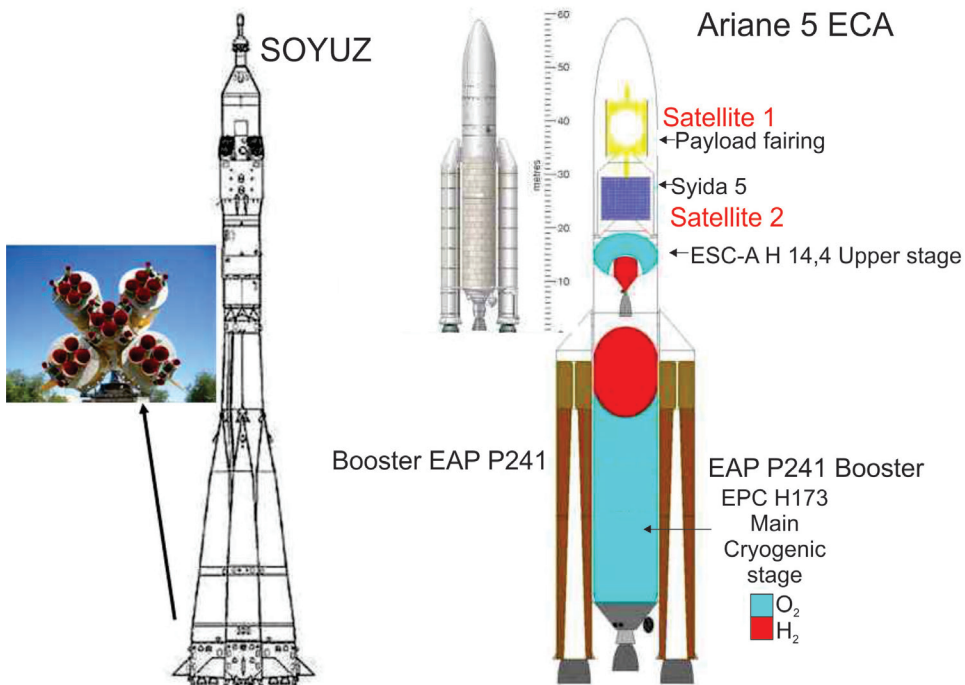EAP P241 Booster
EPC H173
Main
Cryogenic
stage
O_2
H_2

Figure 4.21.: Russian-Soyuz has Kerosene-LOX propellants in the lower stages and French-Ariane-5 launch vehicle has LOX-LH2 propulsion in the core and solid propulsion as strap-ons

with propellant combinations can be overcome with seemingly unusual concepts such as these.

An important observation of the table refers to the inertial velocity that the vehicle will receive (0.45 km/s for PSLV launch). Because earth is rotating around the north-south axis, any eastward launch benefits from the velocity provided by earth itself. It will add directly to the orbital velocity of GSTO and GSYO missions. For other missions, it has to be factored into appropriately. It can be seen from the table that the final vehicle velocity is about 7.6 km/s for SSO orbit and 10+ km for other orbits. The argument that a single stage vehicle cannot meet the demands of the mission can be derived by applying equation 4.58. For PSLV, $m_{ini} = 320$ t, $m_f = 60$ t (for a single stage system), mean I_{sp} of 2.7 kNs/kg, we get ΔV as 4.52 km/s. If we subtract the gravity and drag losses of 2 km/s, we get realised ΔV as about 2.52 km/s which is far below the demand of 7.6 km/s. This is the reason why staging is an essential aspect of vehicle design.

4.17. Summary

This chapter is concerned with performance of aircraft - civil and military. The demands of performance between the two classes are different. The most demanding aspect of civil aircraft is to reduce the fuel consumed on flights as it is directly linked to commercial operability of the fleet. The dependence of this feature is on the engine, aerodynamics and structures apart from the external impact of fuel prices. The specific fuel consumption of the engine (lower), the lift to drag ratio of the wing (higher) and the structural ratio of the aircraft (lower) control the expectation of reduced fuel consumption, naturally allowing for better range and endurance. Take-off and landing of aircraft - dependences on parameters show that heavier aircraft and higher altitudes as well as higher ambient temperatures demand longer take-off distances. Landing distance constitutes generally about 75 % of the take off distance. Therefore, the airstrip length is designed for take-off including possible aborted take-off. The climb and turn performances are strongly dependent on the thrust/power of the engine over the drag/drag power. Military aircraft are capable of much higher performances on maneuverability, even though civil aircraft need to possess a certain minimum of these.

Performance of tactical missiles is optimized by demanding high density impulse propulsion systems. The performance of strategic vehicles, namely ICBMs and satellite launch vehicles is enhanced by staging principles - dropping off a part of the hardware after the vehicle has acquired a certain velocity. The next propulsion system is ignited immediately or after some coasting depending on the mission design. The propulsion systems can be either solid based or liquid based. Both classes of systems are deployed. The choice is not always based on technical considerations; the available technological strength in the design and realization of the propulsion system also comes into play. Indian launch vehicles can launch satellites up to 2 tonnes into various orbits. Further development of semi-cryogenic engines (LOX - Kerosene) of larger total impulse will pave the way for launching heavier satellites.

Satellites function in several orbits and constitute a major feature of modern technological society. They are used to probe the surface of the earth for minerals, weather - both sea and wind, provide communication telephone and television, and for military purposes for both offence and defense. That there

are more than a few thousand satellites functioning in various orbits is an indication of the relevance of the technology for human life today. This area is undergoing vast investments in technological intervention.

Bibliography

[1]   Arianspace, 2016 www.arianespace.com/publication/soyuz-users-manu-al/; www.arianespace.com/publication/ariane-5-users-manual/

[2]   Curtis, H., (2005) Orbital mechanics for engineering students, Elsevier Butterworth-Heinemann

[3]   Fastfission, (2016) http://www.nukestrat.com/us/afn/Minuteman.pdf

[4]   ISRO, 2016 www.isro.gov.in/launcher/pslv-c35-scatsat-1; www.isro.gov.in/gslv-mk-iii- d1-gsat-19; also see other sites for launch vehicle descriptions

[5]   Kunhikrishnan, P, Sowmianarayanan, L., and Nampoothiri, M. V., PSLV-C19/RISAT -1 mission: the launcher aspects, Current Science, v. 104, pp 472 - 476, 2013

[6]   Lovegren, J. A and Hansman, R. J., (2011) Estimation of potential aircraft fuel burn reduction in cruise via speed and altitude optimization strategies, Report No. ICAT-2011-03, MIT international center for air transportation, MIT, http://dspace.mit.edu/bitstream/handle/1721.1/62196/Lovegren_ICAT- 2011.pdf?sequence=1.

[7]   Marguet, R., Ecary, C., and Cazin, P., (1979) Studies and tests on rockets ram- jets for missile propulsion, Proceedings of ISABE, pp 297 – 306

[8]   Perumal, R. V., Suresh, B. N., Narayana Moorthi, D., and Madhavan Nair, G., First developmental flight of geosynchronous satellite launch vehicle (GSLV -D1), Current Science, v. 81, pp. 167 -174, 2001

[9]   Sadraey M., (2009) Aircraft Performance Analysis, VDM Verlag Dr. Müller, also see http://faculty.dwc.edu/sadraey/Chapter%204.%20Preliminary%20Design.pdf

[10]   Saarlas., M. (2007) Aircraft performance, John Wiley & sons, USA

[11]   Torenbeek, E and Wittenberg, H., (2009) Flight physics (essentials of aeronau- tical disciplines and technology with historical notes), Springer

[12]   Wikipedia1 (2012), http://en.wikipedia.org/wiki/Jet_stream

5
Stability and
Control

5.1. Introduction

This chapter is devoted to stability and control of air and space vehicles. This subject has been brought up in the first chapter in section 1.2.4 in the context of its importance to flying systems. The word stability means the ability to return to the equilibrium state from a disturbance caused to its original state of equilibrium. There are two aspects to the study of stability - static and dynamic. The static aspect will enable us to know how much it is stable or unstable. The dynamic part will tell us how long does it take to get back to equilibrium or move away from it. This corresponds to asking for time it takes for the amplitude to halve or double from its initial value. Consistent with the motions of the aircraft, various aspects of stability are: pitching stability, lateral stability that includes rolling and yawing stability. There is coupling between these motions and their stability, rolling and yawing motions are deeply coupled, but the pitching motion is relatively independent; it is also a dominant mode because large part of the motions of aircraft are symmetric about the dominant axis (axis through the fuselage).

Control is related to changing the state of the flight vehicle from its current condition to a desired new one. Greater stability implies greater difficulty in control because the forces needed to change would be larger. Thus military vehicles that need to be agile have much reduced stability margins. In recent times, most military aircraft are basically unstable and receive stability through control system, this arrangement being managed by fly-by-wire systems.

We will first examine the static stability aspects at some depth. At any degree of stability, control for moving from one steady flying condition to another one demands that a certain amount of force be applied - push or pull to bring it to the position. This force is dependent on the gain/stiffness provided by the mechanism linking the control stick to the control surface and the hinge arrangement for the control surface. The latter is relevant because the force applied rotates the control surface around the hinge and the force to overcome the resisted moment about the hinge due to the pressure distribution over the control surface. It is possible to minimize the control forces by minimizing the net moment around the hinge. For every steady mode, if the control stick is left free, the control surface will take a position to produce zero moment around a hinge (perhaps, near-zero because frictional forces generate a band so that

small deviations of position of the control surface leave the control stick in the same position). Beyond such a situation, it is possible to fix the control surface or leave it free. The former is stick-fixed and the latter, stick-free stability.

The next part considers the longitudinal dynamic behavior - if the disturbance like gust hits a trimmed flying aircraft, how long does it take for this disturbance to die down. The aircraft behaves largely as a 2-degree of freedom system and so, there are two modes - short duration and long duration. The short mode is considered more bothersome and long duration mode, called "Phugoid" has such a long period of oscillation that the pilot has time to correct for it. Next, the lateral modes of instability are also briefly discussed.

A consideration of the aspects on stability leads naturally to an aspect called handling quality. The pilot when handling the control stick to alter the direction or modify the speed should pull back the stick when climbing, push it forward when going down, should experience a force in proportion to what he/she considers ap-propriate - small movements for small changes and larger for larger movements. Smaller aircraft are designed around manual pilot handling. Larger civil aircraft with positive stability margins and military aircraft operating with greater agility designed around negative margins of stability all demand larger forces for operating the controls and finely tuned times for response. These require powered controls; electrical systems coupled with hydraulic actuators are a standard feature of these designs. Acquisition of flight data, acceptance of valid data and rejection of suspect data, and processing them to be used for control purposes are other crucial features of these control systems. Modern developments in these will be briefly touched upon. The subject of stability and control in the modern context is very complex with significant emphasis on mathematics of control theory. What will be brought out here are the leading aspects and benefits that have accrued due to use of modern control theory in comparison to classical concepts.

Bird/insect related flight aspects with similarities and differences with aircraft have been touched upon in earlier chapters. Here too, the control strategies adopted by insects have inspired recent developments in micro- and nano-flight vehicles to maneuver through difficult uncharted terrain between buildings and inside habitat. These developments that have been successful have depended heavily on modern control system theory which will be discussed briefly. Fi-
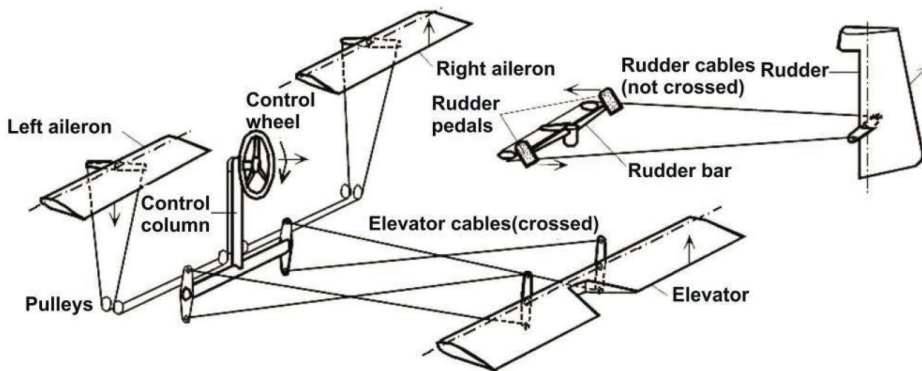
Figure 5.1.: The elements of a mechanically coupled control system in an early generation aircraft; column for pitch control connected to the elevator, wheel control connected to ailerons and pedals to the rudder, both wheel and pedals to be used appropriately for coordinated turn, adopted from Torenbeek and Wittenberg, 2009

nally, the ideas of controls in launch and space vehicles will be discussed. The connecting link of fly-by-wire ideas that originated from lunar module landing into aircraft control systems will be brought out to establish the commonality in pursuit of high technology between aircraft and space flight areas.

5.2. Control System Arrangements

It is useful to visualize the arrangements for control systems before examining the stability issues in some detail. The most elementary form of mechanical controls is described in Figure 5.1. When the column or control stick is pulled back, the elevator moves up (elevator angle β negative) to reduce the speed and when the column is pushed forward, the elevator moves down and the speed increases. In the case of reversible controls (implying both-way coupling between control stick and elevator), if the elevator is pushed down, the column moves forward. Thus for some reason, if the pilot takes the hand away from the control stick, it is possible that the control stick fluctuates because of random disturbances to the elevator. It is expected that the airplane maintains the stability even in such conditions described as stick-free. Thus the study of stability

occurs in two modes - stick-fixed and stick-free. The stick-free mode has another significance. If the pilot wishes to move from one flight condition to another, say speed or altitude or a combination, he/she will inevitably move the elevator from one trimmed operating condition to another. At the first trimmed condition, since the aircraft is considered stable, any minor random disturbances will maintain the same trim, implying the stick force to maintain this condition is zero. If the trim condition is moved to a different speed, one needs to move the elevator up or down to reduce or increase the speed. The force required to do this is from the zero force condition to another one needing the new position. In the new position, the tail plane stays trimmed; in larger aircrafts, this is achieved by attaching a trim tab to the elevator already discussed in Chapter 2 (see Figure 2.24). The mechanical arrangement for the trim tabs is shown in Figure 5.2. The way it functions is by ensuring that the net moment around the elevator hinge is zero (in this instance, $N_e l_e = N_t l_t$). Any aerodynamic disturbance is countered to bring the force to zero.

5.3. Stick-fixed and Stick-free Stability

The forces to be set out in a simplified mode are the same as described in Chapter 1, Figure 4.6. By balancing the moments of the aerodynamic forces and weight of the aircraft around an axis trough the center of gravity and non-dimensionalizing the terms in terms of coefficients of lift and moment, it was shown that we get (same as eqn. 1.12),

$$c_{Mcg} = c_{M0} - c_L \frac{(x_{ac} - x_{cg})}{\bar{c}} - c_{Lt} V_t - c_{Lt} \frac{A_t}{A_w} \frac{(x_{ac} - x_{cg})}{\bar{c}}$$

(5.1)

where c_{M0} is the moment coefficient of the aircraft at zero angle of attack, A_w and A_t are the areas of wing and tail, $Vt = A_t l_t / A_w \bar{c}$ is tail volume ratio, x_{ac} and x_{cg} are the distances of the aerodynamic center of the wing and the center of gravity from the nose of the aircraft (say) and $\bar{c}$ is the mean chord of the wing. If we separate the contributions of the moment coefficient of different parts of the aircraft - wing, wing and fuselage, tail and the entire aircraft, we get the results broadly as in Figure 5.3. This figure indicates that wing and fuselage could be mildly stabilizing/destabilizing and major contribution to stability comes from the tail. The variation of c_{Mcg} has two aspects; $c_{Mcg} = 0$ gives the trim condition and $\partial c_{Mcg}/\partial c_L$ gives an idea of stability. If this quantity is less than 0, then the equilibrium is stable.
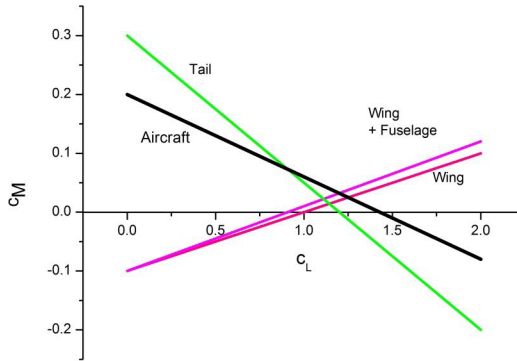
Figure 5.3.: The variation of the moment coefficient around the center of gravity for the wing, wing + fuselage, tail and the entire aircraft

For determining stability the term $\partial c_{Mcg}/\partial c_{L,} = \partial c_{Mcg}/\partial c_{L,}$ is to be obtained. This is the same as was obtained in Chapter 1, section 1.2.4:

$$c_{Mcg,cL} = \frac{\partial c_{Mcg}}{\partial c_L} = -\left[1 + c_{Lt,cL}\frac{A_t}{A_w}\right]\frac{(x_{ac} - x_{cg})}{\bar{c}} + c_{Lt,cL}V_t \tag{5.2}$$

where $c_{Lt,cL} = \partial c_{L,}t/\partial c_{L,}$. From this equation, the neutral point was obtained by setting $c_{Mcg,}c_L = 0$ as

$$\frac{x_{NP}}{\bar{c}} = \frac{x_{cg}}{\bar{c}} + \frac{c_{Lt,cL}V_t}{(1 + c_{Lt,cL}A_t/A_w)} \tag{5.3}$$

It is useful to reiterate that neutral point is a location such that moments about it (or axis) do not change with the angle of attack even when the forces change with angle of attack. We can express this in terms of stability margin as

$$\text{Stability margin} = \frac{x_{NP}}{\bar{c}} - \frac{x_{cg}}{\bar{c}} = \frac{c_{Lt,cL}V_t}{(1 + c_{Lt,cL}A_t/A_w)} \tag{5.4}$$

Using this relationship, the expression for $c_{Mcg,}c_L$ can be set out as

$$c_{Mcg,cL} = \frac{\partial c_{M,cg}}{\partial c_L} = \frac{(x_{NP} - x_{ac})}{\bar{c}} \left[1 + c_{Lt,cL} \frac{A_t}{A_w} \right] \qquad (5.5)$$

This stability margin can be interpreted in terms of stick-fixed conditions with the tail or elevator operated in a "fixed" mode or elevator "free" mode. In the latter mode, the elevator is allowed to rotate around its hinge such that the net torque around the hinge is zero. Under this condition, the stick also may move freely as it is connected to the control surface, and in this case, the elevator. If, now, the aircraft experiences a sharp gust, one would expect the aircraft to return to its original flight condition if the motion is stable with elevator "free". Such a stability mode is named stick-free stability. Both the neutral point and so, the stability margin are affected by the condition - stick-fixed or stick-free. As can be seen from equation 5.4, the parameter that controls this behavior is $c_{Lt,cL} = \partial c_{Lt}/\partial c_L$. It can be expressed as

$$c_{Lt,cL} = \frac{\partial c_{Lt}}{\partial c_L} = \frac{\partial c_{Lt}}{\partial \alpha_T} \frac{\partial \alpha_T}{\partial \alpha} \frac{\partial \alpha}{\partial c_L} = \frac{a_1}{a_0}(1 - \epsilon, \alpha) \qquad (5.6)$$

where $a_1 = \partial c_{Lt}/\partial \alpha_T$, $a_0 = \partial c_L/\partial \alpha$ and ϵ is the correction to the wing angle of attack to get the tail angle of attack because of downwash as $\alpha_T = \alpha - \epsilon$ from which we get $\partial \alpha_T/\partial \alpha = 1 - \partial \varepsilon/\partial \alpha$. And with ε, $\alpha = \partial \varepsilon/\partial \alpha$ we have the last term as indicated.

For understanding the difference between stick-fixed and stick-free modes it is sufficient to consider tail-elevator configuration as in Figure 5.4. The hinge on the elevator is so located that the net hinge moment is very small at reasonable deflections of the elevator (β). This reduces the forces to be applied at the pilot end to reasonable levels. By demanding stability under the stick free conditions, one is assured of the intrinsic stability of the aircraft even if the pilot has been inattentive for whatever reason. This situation is valid with reversible controls -this term implying that when the elevator moves the stick/wheel at the pilot end also moves; any other form of control (to be discussed later) will not be affected by this situation. The tail lift coefficient can be expressed as

$$c_{Lt} = \frac{\partial c_{Lt}}{\partial \alpha_T} \alpha_T + \frac{\partial c_{Lt}}{\partial \beta} \beta = a_1 \alpha_T + a_2 \beta \qquad (5.7)$$
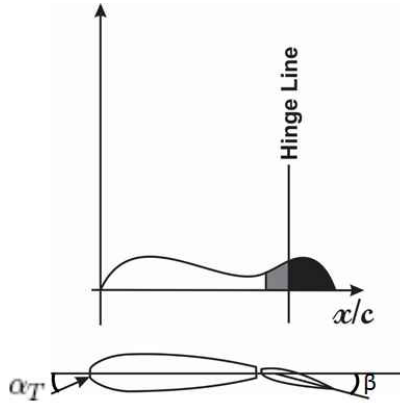
Figure 5.4.: The tail-elevator at an angle of attack controlled by the main wing and the pressure distribution over the tail-elevator combination

where α_T is the angle of attack of the tail and β is the elevator deflection angle. The above equation takes note of the fact that that the tail lift coefficient (c_{Lt}) is a function of tail angle of attack (α_T) and the elevator deflection angle (β) and assumes a linear behavior of the variation of the tail lift coefficient with the two angles. The moment coefficient around the hinge denoted by c_H can be expressed similarly as

$$c_H = c_{H0} + \frac{\partial c_H}{\partial \alpha_T}\alpha_T + \frac{\partial c_H}{\partial \beta}\beta = b_1\alpha_T + b_2\beta \tag{5.8}$$

where c_{H0} is the moment coefficient at zero αT and β. For simplicity the derivatives have been symbolized as

$$a_1 = \frac{\partial c_{Lt}}{\partial \alpha_T}; \quad a_2 = \frac{\partial c_{Lt}}{\partial \beta}; \quad b_1 = \frac{\partial c_H}{\partial \alpha_T}; \quad b_2 = \frac{\partial c_H}{\partial \beta} \tag{5.9}$$

The difference between stick-fixed and stick-free cases arises in the choice of β. If it is chosen such that $c_H = 0$ we have stick-free stability. We will examine this

option presently, we determine the value of β for $c_H = 0$ and substitute it in the expression for c_{Lt}. We get,

$$\beta = -(c_{H0} - b_1\alpha_T)/b_2; \quad c_{Lt} = a_1\left[1 - \frac{a_2 b_1}{a_1 b_2}\right]\alpha_T - \frac{c_{H0}}{b_2}$$

(5.10)

We can determine $c_{Lt,cL}$ as

$$c_{Lt,cL} = \frac{\partial c_{Lt}}{\partial c_L} = a_1\left[1 - \frac{a_2 b_1}{a_1 b_2}\right]\frac{\partial \alpha_T}{\partial \alpha}\frac{\partial \alpha}{\partial c_L}$$

(5.11)

It can be expressed as

$$c_{Lt,cL} = \left[1 - \frac{a_2 b_1}{a_1 b_2}\right]\frac{a_1}{a_0}(1 - \epsilon_{,\alpha})$$

(5.12)

We now introduce this into equation 5.4 to get

$$\text{Stability margin} = \frac{x_{NP} - x_{cg}}{\bar{c}} = \frac{\frac{a_1}{a_0}(1 - \frac{a_2 b_1}{a_1 b_2})(1 - \epsilon_{,\alpha})V_t}{1 + a_1(1 - \frac{a_2 b_1}{a_1 b_2})\frac{(1-\epsilon_\alpha)}{c_{L,\alpha}}\frac{A_t}{A_w}}$$

(5.13)

Since $A_t/A_w \sim 0.2$ and other associated terms are also generally small, a simpler expression is obtained by ignoring the second term in the denominator. We therefore get,

$$\text{Stability margin} = \frac{x_{NP} - x_{cg}}{\bar{c}} = \frac{a_1}{a_0}(1 - \frac{a_2 b_1}{a_1 b_2})(1 - \epsilon_{,\alpha})V_t$$

(5.14)

In the above expression, if $(a_2 b_1)/(a_1 b_2) = 0$, we get the result for stick fixed condition. We will calculate $(a_2 b_1)/(a_1 b_2)$ using realistic values for various quantities. Typically, we choose a0 = 5/rad (0.09/degree), ϵ_α = 0.4, a_1 = 2/rad, a_2 = 3/rad, b_1 = -0.2, b_2 = -0.4, V_t = 0.5, A_t/A_w = 0.1. The coefficients *b1* and *b2* are negative as chosen here; they depend on the location of the hinge location on the control surface. From these we obtain $(a_2 b_1)/(a_1 b_2)$ = 0.75. In this case, the aircraft is less stable stick-free compared to stick-fixed. The difference between the stick-fixed and stick-free neutral point is then obtained as

$$\frac{x_{NP,fix} - x_{NP,free}}{\bar{c}} = \frac{a_2 b_1}{a_0 b_2}(1 - \epsilon_{,\alpha})V_t \tag{5.15}$$

With the values of various parameters as earlier, this difference works out to 0.175. This means that the stick-free neutral point is ahead of the stick-fixed neutral point by 0.175 $\bar{c}$. Both stick-fixed and stick-free neutral points can be obtained by determining from flight tests by determining location of center of gravity at which the rate of change of elevator angle as well as stick force with angle of attack go to 0.

5.4. Trim Condition and Stick Forces

For this condition we set $c_{Mcg} = 0$ to get,

$$c_{Lt} = \frac{c_{M0} - c_L \frac{(x_{ac} - x_{cg})}{\bar{c}}}{V_t + \frac{A_t}{A_w}\frac{(x_{ac} - x_{cg})}{\bar{c}}} \tag{5.16}$$

For simplification we ignore the term involving A_t/A_w because it is small (as discussed earlier).

$$c_{Lt} = \frac{c_{M0} - c_L \frac{(x_{ac} - x_{cg})}{\bar{c}}}{V_t} \tag{5.17}$$

Further, we now use $c_{Lt} = a_1\alpha_T + a_2\beta$ as in eqn. 5.7 to write for β as

$$\beta = \frac{[c_{M0} - c_L \frac{(x_{ac} - x_{cg})}{\bar{c}}]}{a_2 V_t} - \frac{a_1\alpha_T}{a_2} \tag{5.18}$$

We can express α_T as $\alpha_T = \alpha(1 - \epsilon, \alpha) = c_L(1 - \epsilon, \alpha)/a_0$ and obtain

$$\beta = \frac{c_{M0}}{a_2 V_t} - c_L\left[\frac{(x_{ac} - x_{cg})}{\bar{c}a_2 V_t} + \frac{a_1(1 - \epsilon, \alpha)}{a_0 a_2}\right] \tag{5.19}$$

If we set $c_L = m_a g/[\rho V^2 A_w/2]$, we can express the condition for trim as,

$$\beta = \frac{c_{M0}}{a_2 V_t} - \frac{m_a g}{(\rho V^2/2)A_w}\left[\frac{(x_{ac} - x_{cg})}{\bar{c}a_2 V_t} + \frac{a_1(1 - \epsilon, \alpha)}{a_0 a_2}\right] \tag{5.20}$$
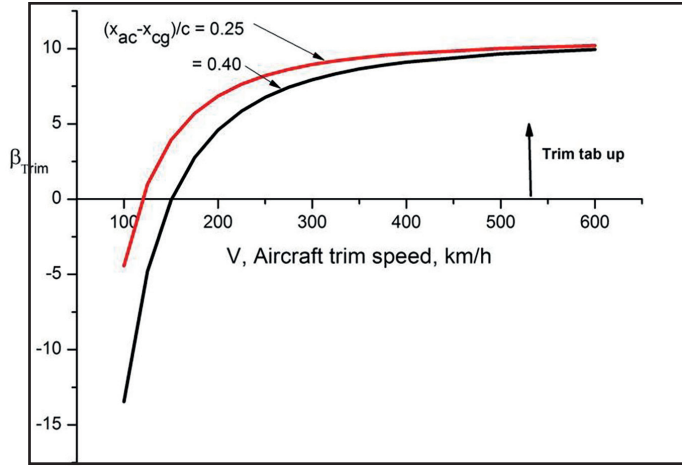
Figure 5.5.: The variation of trim tab angle, β with trim flight speed. β positive implies tail turn is downwards

This gives the relationship between trim tab angle and flight speed for steady flight; a typical variation is set out in Figure 5.5. As expected, the trim tab is pulled up with high c_L at low speeds and it is lowered to get lower c_L at higher speeds. In order to move from one speed to another, from one altitude to another, one needs to operate the control forces to generate the needed torque to move the control surface into a new position. It has already been pointed out that the pilot must experience a force neither too small nor too large and in some perceived proportion to the intended task. For this purpose, it is useful to know the magnitude of forces that can be applied under various circumstances. Since the stick force causes the movement of a lever to rotate the trim tab (or elevator in cases where it is used for control), this force can be expressed as

$$F_{pilot} = G_r(\rho V^2/2)A_{ttab}(c_H) = -G_r(\rho V^2/2)A_{ttb}[c_{H0} + b_1\alpha_T + b_2\beta] \tag{5.21}$$

In the above equation, G_r represents the gearing ratio between the stick and the trim tab or elevator and A_{ttab} is the area of the trim tab. If we introduce the expression for trim β from eqn. 5.20 and perform algebra we get

$$F_{pilot} = A + BV^2 \tag{5.22}$$

Table 5.1.: Typical forces (N) on the aircraft control sticks or wheels (Carley, 2011)

Effort	Elevator		Aileron		Rudder	With
	Stick	Wheel	Stick	Wheel	Push	1/2 hand(s)
Super-max, N	800	980	400	530	1780	2
Maximum, N	440	440	-	360	890	2
	310	310	220	220	-	1
Comfortable, N	-	180	-	130	270	2
	130	130	90	90	-	1

where

$$A = G_r A_{ttab} \frac{m_a}{A_w} \left[\frac{b_2}{a_2 V_t} \frac{x_{ac} - x_{cg}}{\bar{c}} - \frac{b_1(1 - \epsilon, \alpha)}{a_0} \left\{ 1 - \frac{a_1 b_2}{b_1 a_0} \right\} \right] \quad (5.23)$$

$$B = G_r A_{tbb} \left[c_{H0} + \frac{c_{M0} b_2}{a_2 V_t} \right] \quad (5.24)$$

The term B is negative since b_2/a_2 is negative. If we set $F_{pilot} = 0$ as required at trim condition, we get $V^2_{trim} = -A/B$. We can therefore write

$$F_{pilot} = (-B)(V^2_{trim} - V^2) \quad (5.25)$$

In order to get an appreciation of the forces that a pilot can exert on the control column (and the wheel and pedal meant for lateral control), it is useful to examine Table 5.1 drawn from Carley (2011) that provides the maximum control forces expected to be applied by the pilot under various circumstances. These values go from 90 N to as large as 1000 N, the values being different whether one uses a stick or a wheel, with the wheel allowing greater exertion of force with one hand or two hands. The demand on the control system design is to stay within these limits as far as the demand on the pilot is concerned. A typical plot of the force vs. speed is shown in Figure 5.6 indicating the variation of the stick force with speed. As can be noted, there is a change in the direction of the force at the trim condition. Bringing to lower speeds calls for pulling back and increasing the speed beyond trim calls for pushing the stick.
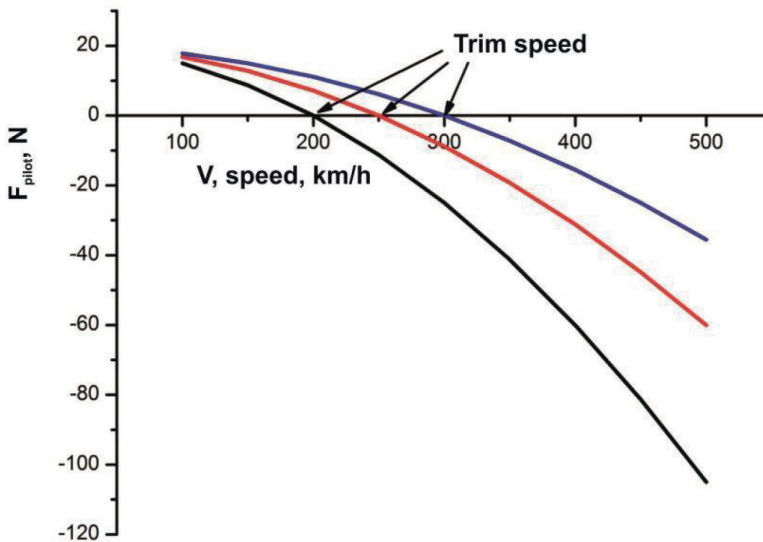
Figure 5.6.: The variation of the stick force (N) with speed (km/h). The trim speed also has a corresponding trim tab angle

5.5. Lateral Stability

While the mean motion of most airplane flight occurs along the symmetric axis, the motion due to a random gust from a side or during turn initiated intentionally leads to the asymmetric flight modes. One would need that these be stable. When there is a gust from a side, the incremental forces and moments are such that fuselage causes a moment that is destabilizing (the aircraft tends to move away from the side wind), but the effect of vertical tail plane – fin and rudder is stabilizing because the force developed due to this change leads to a moment that turns the airplane into the stream.

Because of the distance of the tail plane along the fuselage is sufficiently large, the moment due to tail plane is more than due to fuselage and so the motion becomes stable. This feature of the ability of the aircraft to align itself to the direction of the oncoming wind is called weathercock stability. It is a desirable feature but excessive stability implies frequent change of orientation if the oncoming wind changes the direction. Thus, there is need to limit this stability.

The vertical tail plane is not sized by this criterion. It is sized by the consideration of a single-engine failure in a twin-engine aircraft. The asymmetry caused by the loss of thrust on one side is combated through the use of rudder. This arrangement is adequate to take care of the stability as well.

If the pilot initiates a yaw maneuver, say moving the rudder to the right side (as seen by the pilot in the cockpit), the force will tend to yaw the aircraft to the right side. This causes the right wing to turn horizontally back while the left wing moves forward. This causes effective speed of the right wing to be lower than the left wing which is moving into the wind. This causes a higher lift on the left wing compared to the right wing and hence the aircraft rotates around the principal axis in the clockwise direction. This is the yaw-turn coupling.

As different from the above, let us say, the pilot wishes to induce a rotation of the aircraft around the principal longitudinal axis (rolling). This is initiated with ailerons. Such a rotation, say, clockwise as seen by the pilot causes the right wing to drop and the left wing to move up. This induces a vertical velocity that is proportional to the distance from the principal axis. The right side wing which is dropping experiences higher angle of attack compared to the left side wing, again, with varying amounts along the wings. This leads to differential lift – higher for the right wing compared to left and hence acts against the initiated aileron movement. Thus if the initiated action is random, the response of the aerodynamics of the wings is stabilizing. The effect of the aileron movement is not limited to this aspect. The vertical tail plane also rotates to the right and this leads to a force that causes a rotation around the vertical axis through the center of gravity towards right side. This leads to side slip. Operating the pedal to counter this effect is essential. This is the rotation – yaw coupling; this is why the lateral motion is deeply coupled between the aileron and rudder. If the motion is due to a random roll disturbance, then this yaw tends to cause a motion that was argued in the previous paragraph as being stable. Hence, on an average, the deeply coupled motions are stable. Ensuring greater lateral stability with enhanced area of the fin can cause dynamic stability problems (spiral and dutch roll) discussed later.

While most motions are transitional, the issue of stability becomes relevant only for coordinated turn. Several times, aircrafts have to loiter around the air
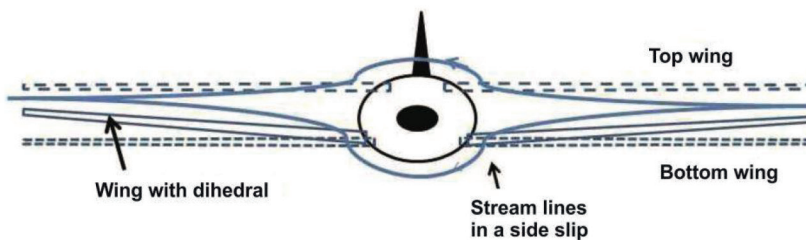
Figure 5.7.: Schematic of an aircraft in side slip with top wing, bottom wing and wing with dihedral; note the fluid flow lines with the top wing experiencing postive angle of attack compared to low wing configuration.

ports for reasonable times due to air traffic control demands because of traffic congestion or other considerations. The question of the aircraft stability in a co-ordinated turn with gust affecting the angle of attack or the speed is controlled by the features described above.

A connected aspect that controls the stability is the position of the wing on the fuselage – top, middle or low and whether there is dihedral or anhedral. Figure 5.7 shows the features of an aircraft with some of these possibilities. The flow over the wings with the top wing is such that with a side-slip as shown, the top wing produces additional lift on one wing and reduced lift on the other. This causes a moment around the principal axis that is stabilizing. For the bottom located wing it is destabilizing. To overcome this problem, dihedral is employed typically at 4 to 6 degrees. This produces an effect similar to the top wing but with reduced magnitude. This adaptation is almost universal for small and large transport aircraft; military aircraft desiring agility do adopt anhedral; such aircraft demand fly-by-wire control approach.

5.6. Dynamic Stability - Longitudinal and Lateral

As was explained earlier, the study of dynamic stability allows us to determine the time taken for return to equilibrium to say, half the amplitude or time for disturbance to grow to double the amplitude from the time disturbance hits the

aircraft. The study of a linear behavior of the disturbance provides valuable results and is what is most usually done first. This study calls for the solution of the equations of motion in three dimensions because there will be couplings between various motions. The equations of motion involve three velocities in the three directions, force system involving, lift, thrust and drag as well aerodynamic forces and the moments on the control surfaces. Linearization brings in derivatives of various force and moment coefficients with respect to the angles of attack, pitch, yaw or roll angles and flight speed. The most important dynamical behaviors experienced by aircraft can be classified into (a) phugoid oscillation, (b) short-period oscillation, (c) spiral mode and (d) dutch-roll. What will follow is a short description of the observed behaviors followed by brief analysis of these modes without involving mathematical details so that the scaling behavior is understood.

Phugoid mode involves a symmetric motion of the aircraft due to horizontal gust or such a disturbance that can get initiated by a short, sharp deflection followed by return to the centered position of the elevator; this results in a pitch increase (say) with no change in trim from the cruise condition that leads to a decrease in speed and the drop of the nose below the horizon. Because of inertial effects, the reduction in pitch causes increase in speed beyond the equilibrium value and the nose will climb above the horizon. The entire oscillatory motion occurs at near-constant angle of attack, with speed - altitude variation largely affected by energy exchanges between kinetic and potential energy with speed variation affecting the damping due to pitch variation. The oscillatory period depends primarily on the aircraft speed as will be discussed later, typically about one to two minutes. Damping of this mode is weak particularly for clean aircraft with large aspect ratio that directly impinges on the lift-to-drag ratio. While phugoid oscillations are more usually stable, divergent phugoid oscillations can be caused by a large difference between the incidence angles of the wing and tail that are generally rare.

The short-period oscillation is known to have a very small period of a few seconds with damping to half amplitude occurring in about a second or less. It occurs at near constant speed and is largely due to angle-of-attack fluctuations around the center of gravity. Consequently, the frequency is related to the static stability features namely, the static margin and $c_{Mcg,\alpha}$.

The spiral stability refers to the ability of the aircraft to return to straight level flight when ailerons are released in a turning flight, specially a coordinated turn. If this mode is unstable, it turns out that the release of ailerons during a coordinated turn causes inward side-slip motion so that the turn radius keeps decreasing. This also causes a dive that can be fatal if things go out of control. It is observed usually at lower speeds and is strongly dependent on the moment coefficients for side-slip and yaw; other features like sweep, also with gradually decreasing wing chord towards the wing tip have both positive and negative influences. The use of dihedral with bottom wings or just a top wing helps obtain the stability. This mode of stability is given special attention during development. The period of oscillation of this mode is in terms of tens to hundreds of seconds depending on the parameters described above.

Dutch roll mode is a combined mode between roll, yaw and side slip. These motions occur in a quick sequence (a few to several seconds each) that passengers feel considerable discomfort; this is specially an issue at higher altitudes when damping is weaker. This mode can be avoided by providing larger vertical tail that causes, however, greater tendency to spiral mode. Hence a compromise is required. It has to be dealt with by the pilot by being attentive to the controls in smaller aircraft. In larger aircraft, a yaw damper that is brought into the operation after yaw rate is measured to help overcome the problem.

5.6.1. Analytical approach

The dynamical equations of motion are to be solved for obtaining quantitative assessment of the behaviors described above. Some of this insight has been in the literature for a long time - Lanchester (1868 - 1946) and Bryan (1864 - 1928) are credited with elucidating principal aspects of stability. The principal procedures are covered in a useful set of lectures at MIT, Cornell and Stanford accessible on the internet (internet1 - internet3, 2015).

As can be expected, the analysis is separated between longitudinal and lateral modes. Even in the case of longitudinal modes, the observed phugoid and short-period oscillatory modes are distinct in terms of frequencies and damping and can also be dealt with separately. The equations are linearized around a steady equilibrium state and the perturbations are expressed as (amplitude) $\exp(\lambda t)$ where λ is a complex quantity $= \lambda_r + i_{\lambda im}$. The real part λ_r when evaluated can be positive or negative. If it is positive, it can be inferred that the

disturbance will amplify and the motion is unstable. If it is negative, then it implies that the disturbance dies and so, the motion is stable. The imaginary part λ_{im} provides the frequency of the oscillations. Such an analysis for phugoid mode gives the following equation for λ.

$$\lambda^2 + \frac{2g}{V}\frac{c_D}{c_L}\lambda + \frac{2g^2}{V^2} = 0$$

(5.26)

where V is the flight speed, g is the acceleration due to gravity, c_D/c_L is the inverse of the lift-to-drag ratio of the wing. This form is obtained from the more elabo-rate equations set out in references: internet1, internet2, internet3 (2015). The frequency or the period of oscillations from the imaginary part and the damping coefficient from the real part are obtained as

$$\text{Period} = \frac{\sqrt{2}\pi V}{g}; \quad \text{Damping coefficient} = \frac{1}{\sqrt{2}}\frac{D}{L}$$

(5.27)

These results are revealing. They indicate that for phugoid oscillations, the period is dependent on the speed of the aircraft. Thus larger jets which fly at much higher speeds than very small aircraft experience larger periods providing adequate time for correction by the pilot. The damping is directly related to L/D. Hence, high aspect ratio wing based aircraft experience very small damping. It is perhaps instructive at this stage to examine the very simple analysis by Lanchester in 1911 since it is based on energy exchanges between potential and kinetic modes and is insightful. It is first noted that

$$\text{Total energy} = \rho V^2/2 + gZ = \text{constant}$$

(5.28)

where Z refers to the height of the horizontal path. If we set

$$V = \bar{V} + v; \quad \text{and} Z = \bar{Z} + z$$

(5.29)

where $\bar{V}$ and $\bar{Z}$ refer to steady values and v and z refer to perturbational values. If we introduce these into the energy equation and retain first order terms we get

$$v = -gz/V$$

(5.30)

Now we invoke the force balance during the oscillatory motion and at equilibrium, $L = mg = (\rho V^2/2)A_w c_L$

$$m\frac{d^2z}{dt^2} = L - mg = \frac{1}{2}\rho A_w c_L (V^2 - \bar{V}^2) = -\rho A_w c_L g z$$

(5.31)

The last equality is obtained by invoking the relationship between v and z obtained above. The above equation is simplified as

$$\frac{d^2z}{dt^2} + 2\left[\frac{g}{\bar{V}}\right]^2 z = 0$$

(5.32)

This equation is similar to the equations of structural vibration discussed in the next chapter. The solutions of this equation are harmonic functions and the coefficient of z is the eigen value of the problem constituting the square of the frequency of oscillations. The resulting period is exactly as in eqn. 5.27 (the minor difference is that the speed in eqn. 5.27 should be treated as the mean value).

For short period oscillations, the equation is

$$\frac{I_y}{(\rho V^2)/2A_w \bar{c}}\lambda^2 - \frac{\bar{c}c_{Mcg,q}}{2V}\lambda - c_{Mcg,\alpha} = 0$$

(5.33)

where I_y is the moment of inertia around the lateral axis, $c_{Mcg,q}$ is the partial derivative of the moment coefficient about the center of gravity with respect to the dynamic pressure, $q = (\rho V^2/2)$ and $c_{Mcg,\alpha}$ is the partial derivative of the moment coefficient with respect to the angle of attack. From this we get

$$\text{Period} = \sqrt{\frac{I_y}{(\rho V^2/2)A_w \bar{c}(-c_{Mcg,\alpha})}}; \quad \text{Damping} = -\frac{c_{m,q}}{\sqrt{-c_{m,\alpha}}}\frac{\bar{c}}{4V}\sqrt{\frac{(\rho V^2/2)A_w \bar{c}}{I_y}}$$

(5.34)

The quantity $c_{Mcg,\alpha}$ is related to the difference between the neutral point and the aerodynamic center as in equation 5.5 and hence is related to the static stability as brought out earlier.

The analysis procedures for lateral modes are similar. But no general conclusions beyond the qualitative aspects discussed earlier seem possible. Perhaps it is useful to get some order of magnitude values for various quantities involved

in dynamic stability. For this purpose, the data presented in internet2 (2015) have chosen. The aircraft considered is Boeing 747 during landing at M = 0.25 as an example to illustrate the results of the analysis. The parameters are as follows:

Aircraft mass = 256 tonnes, A_w = 511 m², $\bar{c}$ = 8.32 m, wing span = b = 59.6 m, V = 306 km/h = 85 m/s, moment of inertia around the lateral axis, I_y = 44.8 ×10⁶ kg-m², moment of inertia around the principal axis = I_x = 24.4 ×10⁶ kg-m².

The aerodynamic data are: c_L = 1.11, c_D = 0.102, $c_{L,\alpha}$ = 5.7, $c_{D,\alpha}$ = 0.66, $c_{Mcg,\alpha}$ = - 1.26, $c_{Mcg,q}$ = - 20.8, $c_{Mcg,\beta}$ = - 1.34

Calculations of longitudinal modes reveal that the short period is 6 s, damping = 0.62, phugoid oscillation period = 38 s, phugoid damping = 0.06, time to half-amplitude for rolling mode = 0.6 s, time to half-amplitude spiral mode damping = 15.0 s, dutch roll mode period = 6 s and dutch roll mode damping = - 0.08. These results are sufficiently indicative of observations.

5.7. Flight Testing

Flight testing is an inescapable part of aircraft development. Qualified test pilots fly the aircraft after briefing sessions before the flight and provide their observations after the flight during de-briefing sessions. Data obtained from a large number of ground tests that first involve aircraft weight, center-of-gravity measurements are combined with with the analysis of wind tunnel tests on c_L, c_D, c_M characteristics of aircraft models. These are performed with different combinations of control surfaces and attachments along with estimates of stability derivatives by several methods, data sheets as well as flow calculations. These are all assimilated to get a coherent picture of the flight-worthiness of the aircraft. These are presented to groups involving the test pilot to evaluate the data to ensure pilot safety in later test flights. Initial flights are aimed at smooth take-off and landing, steady runs at various speeds and altitudes as well climb and descent trying to determine engine and drag performance under various conditions. Operation of various control surfaces by small amounts and relaxing them allows the determination of stability derivatives. Most data acquisition at high signal-to-noise ratio data analysis involves combining different approaches to determine the crucial quantities with known

accuracy. The flight test regime is slowly expanded to include critical parts of the flight envelope so that all the envelope is covered.

5.8. Fly-by-wire Control and Control Laws

Flight controls have moved from direct coupled mechanical wires and push rod arrangements through hydraulic systems that carry high pressure fluids through tubing to cause control action to computer controlled arrangements called fly-by-wire system. The transition to hydraulic systems occurred naturally when the aircraft size became larger and the control force demand became higher. Fly-by-wire system came into aeronautics through space related efforts. The first active control system system was deployed on A-4 (or V-2) missile built in Germany during Word War II using analog electronic simulators demonstrating the dynamic stability on ground. The space missions in the USA used early ideas from A-4 for Mercury, Gemini and Apollo missions with important milestones of 1961, 1965 and 1969. Admittedly, the Apollo mission with lunar landing was the most complex (can be stated so even to-day) and one segment, namely, lunar landing was considered most critical. It had to depend on fly-by-wire approach because, human responses to changing scenario were considered too-slow for reliable operation (Tomayko, 2000).

In a crucial maneuver, "As Niel Armstrong and Buzz Aldrin descended to the surface, the computer received so many requests for interrupts from the sensors that it began to get behind in its critical processing. This situation resulted in restarts that caused both crew and ground controllers considerable concern, so much so that there was nearly an abort.." (see p. 19 of Tomayko, 2000). With only a few seconds of fuel remaining, the mission was accomplished. This was the basis for research efforts in aeronautics starting with F-8 aircraft that was later adopted in F-16 and F-117 (Tomayko, 2000). Not all this adoption was smooth and the struggle to get across digital fly-by-wire control was significant in the years of development. In civilian sector it was the French aircraft, Airbus 320 that deployed fly-by-wire system and it was only later that Boeing company adopted it in 777 air-craft. The full details of fault tolerant designs of the control system architecture are provided in Briere et al (2001) and Bartley (2001).

There is a fundamental philosophical difference between the architectures of Boeing 777/787 and Airbus 320. Boeing 777 and 787 have conventional control

column and yoke. Artificial forces and electromechanical systems are added to retain the traditional feel of flying and airplane. In the airbus, pilot no longer applies a force on the controls to achieve maneuvering, but the side-stick displacement is a rate command; it controls the altitude and speed. In this approach, the pilot does not get a feedback force or stick shaker as the plane will always fly within its structural and aerodynamic limits managed by the control law. The airbus system depends on the computer to deal with all criticalities with no override option to the pilot and the Boeing architecture allows for pilot takeover at conditions decided by him/her appropriately. Airbus chose to introduce a flight control law known as c^* on the aircraft family. This particular control law uses pitch rate as the control variable at lower speeds (< 360 km/h) and acceleration based control variable at higher speeds. It aims at satisfying a commanded flight path through control of speed, configuration, and engine parameters. From the point of view of the pilot, this apparently provided the aircraft excellent control of flight path during all flight phases and especially during landing with only one defect namely, poor-average speed control. When pilots operating mechanical and hydraulic control systems on all earlier aircraft would not find the "feel" system and would find it a grumbling point. But many after having experienced both systems have apparently endorsed the airbus strategy as it relieves them of additional features not important to achieving the objective of flying.

5.8.1. Role of mathematical tools in control law design

The central issue of a controller design is to ensure that the demand of the pilot to get to a certain velocity at a certain position from a previous one happens in a smooth way. Sometimes, the entire path of the aircraft is set out at the start and is to be followed by the controller. The inputs for control will be the engine power/thrust and the control surface positions. The operation of control stick or a speed level position is to be interpreted in terms of values of these over time with feed back to determine if the command has been obeyed. By and large, changes in velocity or altitude will get linearly related to changes in the control surface movements with suitable coefficients. These coefficients are obtained from the flight test data analysis as touched upon earlier. But ensuring dynamic stability calls for treating multiple inputs to multiple outputs in an environment that may have gusts on occasions and/or turbulence by a robust procedure. This calls for mathematical treatment of relationships.

For a long time classical control system ideas prevailed. This consists of the treatment of linear system that can be handled in the spectral domain (frequency domain) or time domain. The former uses Laplace transform, Fourier transform or Z-transform and provides insight into issues of gain vs. frequency. The time-domain approach can be handled with linear systems and is equivalent to the spectral approach, but is easily capable of assimilating non-linearities. This is particularly important for high speed aircraft (with delta-wings) flying at high angles of attack because the aerodynamic behavior is not only non-linear, but could also have hysteresis; what more, with demand on efficient structural design, flexibility effects need to be factored in.

Modern control system approaches (Gangsaas et al, 1986) use ideas of linear *quadratic regulator* (LQR) and *linear quadratic Gaussian control* (LQG). The difference between the two lies in the inclusion of noise in seeking the optimal regulation strategy. In both these approaches, one constructs a cost function which is the summation of the mean square of the difference between commanded and realized values of the parameters each term multiplied by a coefficient called gain bringing out the relative importance of each of the parameters. More often than not, the magnitude of the final control action is also included in the cost function. In order to set the constants, simulations are performed to obtain minimization of the cost function. Since the number of parameters included can be several, determining optimal coefficients is difficult indeed. Guidance from the linear approach is of value in such cases, even if the final model deviates from these.

The methods are mathematically well founded. Involvement in creating better and better mathematical foundations through approaches of pure mathematics is stated to be partly responsible for slow assimilation of the tools of optimal control in the industry (Balas and Hodgkinson, 2009). The control system development by many industries in the same country and in different countries seems to have taken very many different approaches as discussed in Balas (2003). It is instructive to understand the value of the LQR approach and one case study from Gangsaas et al (1986) is brought out here.

Boeing 767 in its commercial operations experienced small amplitude lateral limit cycle oscillations and could not be solved using classical synthesis. The cost function involved the square of the sum of yaw rate error, roll angle, roll
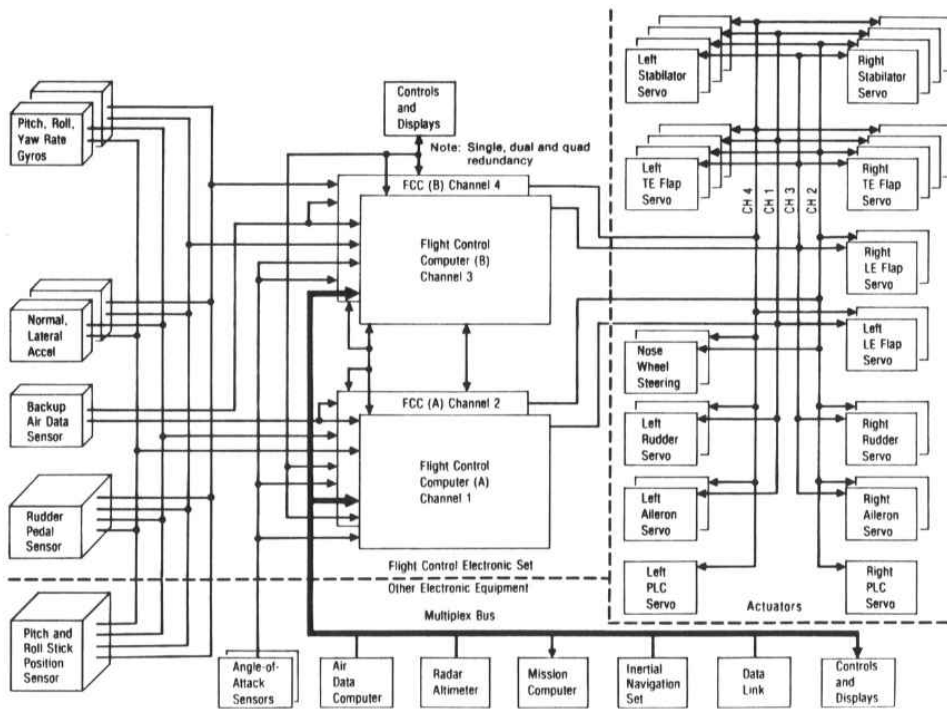
Figure 5.8.: F-18 Control system arrangement. Notice four computers and multiple inputs and outputs, drawn from Harschburger, 2002

rate, integral of heading error, dutch roll mode displacement and aileron command input with suitable gains (coefficients). Analysis and successful implementation of the new algorithm showed that satisfactory performance could be obtained through the use of gains distinctly different from the original design for yaw rate, roll angle and roll rate gains. This particular example showed that there was no possibility of obtaining good control behavior of the aircraft using classical ideas. There are other case studies that support this thinking.

A typical modern day fly-by-wire control system is as shown in Figure 5.8. Robustness and reliability demands are addressed with having redundancy - four computers with sensor data averaging and possible rejection of deviant data, processing and sending signals to actuators, measuring the positions and flight data parameters. Using this strategy is synonymous with the efforts on space shuttle system operations. In the early stages the ideas became exchanged

on avionics development between aircraft and space vehicles. A repackaged version of the F- 15 computer became the AP-101 used in Space Shuttle 2. However, the advancement in integration of all segments involved in the flight mechanics in space shuttle is being matched only slowly in aircraft avionics developments.

5.8.2. Bird and insect flight inspired control systems

It may be recalled that Chapters 1 and 2 have discussed aerodynamical aspects of birds and insects in relationship to other aeronautical vehicles. The commonalities and differences on the flight behavior between relatively fixed geometry systems and birds/insects could inspire one to build new flight systems of considerable value in critical areas to safely navigate obstacle-laden environments for surveillance, reconnaissance, and disaster prevention. Guidance and control of aerial vehicles assisted most usually by the global positioning system (GPS) and inertial measuring units (IMU) are also deployed to get a precise estimate of position and velocity. These are most suitable for open terrains that are adequately mapped. They are problematic for complex environments inadequately mapped for this purpose as also due to limitations of power available. Other tools like laser range finders to get accurate estimates of distance to the obstacles, external camera based inputs pose varying difficulties for implementation. In any case, from the fact that bats and insects maneuver so accurately with twists and turns, it appears clear that there is an intellectual invitation to mimic. What has been determined from a study of how the insects and birds navigate and control in complex environment is that they obtain a three-dimensional picture of their distance and velocity from boundaries instantaneously. The navigation is charted by approximately keeping the flight path between the boundaries by aiming at symmetry between the extremes - left and right or up and down. This strategy is entirely local and hence is an eminently appropriate for local maneuvers.

This feature is broadly termed *optic flow* (Franceschini et al, 2009; Keshavan et al, 2014). It is a measure of vehicle speed over depth to objects in the environment and therefore encompasses information on the instantaneous environment. Defined more precisely, it is the inverse of the time taken for a contrasting feature to travel between visual axes of photo-receptors in the eye separated by an angle. The ratio of the angular separation to the time taken

gives an angular speed. This information is processed in their "brain" to create the needed smaller set of motor commands. Much work has been done on insects (Raneyand Waszak, 2003; Lentink et al, 2009; Franceschini et al, 2009) to build micro– and nano– fixed wing and rotary wing class flight vehicles. The control system methodology uses LQR strategy by integrating the modeled flight dynamics in a gusty environment discussed in the earlier section to chart out the flight path. It has been applied for a quad-rotor vehicle following complex trajectories and found to be superior to other more complex procedures for navigation (Keshavan, 2014). More work in this area is expected in coming times.

5.9. Space Vehicles

The challenges of aeronautical stability and control problems are absent in space vehicles that may use control system elements and their management with similar approaches at a fundamental level.

Space vehicles can be split into launch vehicles and satellites. Launch vehicles get affected by aerodynamics in the early part of the flight path - typically for about a minute of the flight up to an altitude of about 20 km beyond which aerodynamic effects become growingly insignificant. The corrections needed for this purpose are dealt with by the control system issuing commands for operating a thrust vector control system by gimballing or injecting a reactive liquid into the divergent section of the main nozzle at specific points in the azimuth (SITVC described in Chapter 3) to create an asymmetric exit momentum flux distribution. Guidance systems measure the vehicle behavior (using GPS and gyroscope based inertial measuring instruments) on the position, velocity and orientation and provide inputs for control system to operate rocket thrust vector control systems, either on the main engine or as auxiliary elements for the vehicle to go on a programmed path. Stability of the vehicle beyond the atmosphere arise from rocket engine thrust behavior and all vehicles are equipped with switchable liquid engine based thrusters for the required duration. These liquid propellant based thrusters operate on pulse mode so that the effect of the imposed corrections can be measured from a ground control station and additional actions taken to get the satellite into position.

Issues of stability in satellites-in-orbit are related to solar pressure and occasional meteoritic hits. Station keeping is performed using multiple micro–

thrusters located such that each of them is switched on for a small duration as required by the control system.

5.10. Summary

This chapter is concerned with stability and control of aeronautical and space vehicles. Aeronautical vehicles, small and large, civil or military, fixed wing have a wide range of complexities and challenges. Rotary wing devices (not discussed here) follow similar ideas as described here. Addressing stability implies determining conditions of static and dynamic stability in longitudinal and lateral modes. Longitudinal modes are of much greater importance while lateral modes are just very "tricky" to deal with needing compromises difficult to make because of complex interactions.

The positional difference between the center of gravity and the aerodynamic center of the forces due to wing and the tail controls the longitudinal stability with center of gravity being ahead of the aerodynamic center for positive stability. Operational considerations of the demand for minimum fuel usage in flights call for setting the center of gravity as far aft as possible while still being ahead of the aerodynamic center. For conventional civil aircraft this difference kept at a minimum and fuel management is invariably adopted to keep the movement of center of gravity from the aerodynamic center the minimum. For military aircraft, the center of gravity is aft of the aerodynamic center and the aircraft is statically unstable. Thus any demand for stability due to gusts and other transient disturbances needs to be dealt with in an active manner and if this is not done, the path of the aircraft becomes unstable. This is performed through the use of fly-by-wire systems.

Longitudinal stability has two modes - the phugoid which is a long period oscillation depending on the speed of the aircraft and the damping on the L/D of the wing. Short duration oscillations are usually damped heavily. Thus longitudinal stability does not pose much challenge to deal with. Lateral oscillations involving dutch roll and spiral mode are not so easy to deal with. Dutch roll has complex interaction of all the three modes and is connected to the size of the fin. Eliminating it has been found to require strategy related to modern control theory - linear quadratic residual (LQR) and linear quadratic Gaussian (LQG) techniques that minimise the cost function composed of the sum of the error square between the current and the desired flight variable each multiplied by

coefficients (also called gains). Many reported instances of control system design have shown that advanced techniques are needed to resolve the problems caused by using classical control system ideas. These new ideas coupled with concepts such as optic flow natural to insects and birds are used in micro–air vehicle control system design to ensure stable flight in turbulent and gusty environment for a tiny vehicle.

Stability analysis, particularly the dynamic stability is a straightforward subject but one needs to keep track of numerous quantities - derivatives of forces and moments (or their coefficients) with respect to flight (speed and wing angle of attack), geometric (tail plane settings with respect to the main wing) and control (angles of deflection of tail, aileron, fin, tab) variables because the magnitude of these coefficients affects the dynamic stability. Even if some broad indications of what aspects control what can be gleaned from simpler analysis, every design house uses a computer model to deal with both stability and control issues for control law realization. While the coefficients of forces and moments are obtained from data sheets using wind tunnel and geometric data, they keep getting updated continuously with flight tests so that the predictions will need to concur with succeeding test flights to enable the test pilot to gain confidence in these data before the flights.

Stability and control of satellite launch vehicles and satellites have much reduced aerodynamic features and hence are less complex. Control is achieved using rockets either by gimballing, auxilliary fluid flow systems or small thrusters in pulse mode. Greater technological innovations in the field of control systems will occur and influence the micro– and nano–air vehicles for civilian and military use in many ways that are being explored now.

Bibliography

[1]   Carley, M (2011), Some notes on aircraft and spacecraft stability and control, Cranfield university, http://people.bath.ac.uk/ensmjc/Notes/stability.pdf

[2]   Balas, G., Flight control law design: an industry perspective, European Jour-nal of control, pp. 207 - 226, 2003

[3]   Balas, G., and Hidgkinson, J., Control design methods for good flying qualities: an industry perspective, AIAA atmospheric flight mechanics conference, AIAA 2009-6319, Chicago, 2009

[4]   Bartley, 2001, http://www.davi.ws/avionics/TheAvionicsHandbook_Cap_11.pdf

[5]   Briere, D, Favre, C and Traverse, P, 2001, Electrical flight controls, from Air-bus A320/330/340 to future military transport aircraft: a family of fault toler-ant systems, http://www.davi.ws/avionics/TheAvionicsHandbook_Cap_12.pdf

[6]   Franceschini, N., Ruffier, F., Serres, J and Viollet, S., Optic Flow Based Visual Guidance: From Flying Insects to Miniature Aerial Vehicles, Aerial Vehicles, Thanh Mung Lam (Ed.), ISBN: 978-953-7619-41-1, 2009, InTech

[7]   Gangsaas, D., Bruce, K. R., Blight, J. D., and Ly, U-L., Application of modern synthesis to aircraft control: three case studies, IEEE transactions of auto-matic control, C-31, pp. 995 - 1014, 1986

[8]   Harschburger, H. 2002, http://ocw.mit.edu/courses/aeronautics-and-astronautics/16-885jaircraft-systems-engineering-fall-2004/lecture-notes/flight_controls_1.pdf

[9]   Internet1, 2015, http://ocw.mit.edu/courses/aeronautics-and-astronautics/16-333-aircraft-stability-and-control-fall-2004/

[10] Internet2, 2015, https://courses.cit.cornell.edu/mae5070/DynamicStability.pdf

[11] Internet3, 2015, http://www.princeton.edu/ stengel/MAE331Lectures. html

[12] Internet4, 2015, http://adg.stanford.edu/aa241/AircraftDesign.html

[13] Keshavan, J., Gremillion, G., Escobar-Alvarez, H and Humbert, J. S., A µ analysis-based, controller-synthesis framework for robust bioinspired visual navigation in less structured environments, Bioinspir. Biomim, 9, pp. 1- 11, 2014

[14] Lentink, D., Jongerius, S. R., Bradshaw, N. L., The scalable design of flapping micro-air vehicles inspired by insect flight, in Flying Insects and robots, D. Floreano et al (eds), Springer verlag, 2009

[15] McCormick, B. W., Aerodynamics, Aeronautics and Flight mechanics, 1995, John Wiley and Sons, Inc

[16] Osmon, C. L., Design of flight control laws for aircraft with flexible wings using quantitative feedback theory, Thesis, M. S in electrical engineering, Air force Institute of Technology, Wright Patterson Air Force Base, Ohio, 1995

[17] Raney, D. L., and Waszak, M. R, Biologically inspired micro-flight research, SAE 2003-01-3042, http://papers.sae.org/2003-01-3042/

[18] Tomayko, J. E.,Computers take flight: A history of NASA's pioneering digital, NASA SP- 2000-4224, 2000

[19] Torenbeek, E and Wittenberg, H., Flight physics (essentials of aeronautical disciplines and technology with historical notes), 2009, Springer

[20] Wikipedia, 2015, https://en.wikipedia.org/wiki/Flight_dynamics_(fixed-wing_aircraft)

6

Structural Aspects
of Vehicles

6.1. Introduction

The aerospace vehicle, whether it is an aircraft, a helicopter, a missile or a launch vehicle is conceived for its shape, aerodynamics and performance based on a certain structural mass, the aim being always related to reducing inert mass to the neces-sary minimum. The structure of such a vehicle must then be designed to ensure that the vehicle is strong, sturdy, safe, and has adequate life. Such expectations are also expressed for on-the-land structures. If one were to think similarly, the vehicle will simply not get airborne. The mass must be brought to a minimum for the vehicle to be airborne. If it is made too flimsy, there will be catastrophic accidents. To deploying enough material of high strength or stiffness as required in appropriate locations inside the vehicle is the objective of structural design and analysis.

In this chapter, we consider the aspects related to the behavior of the aero-structures including the shapes and materials of the components to withstand static and dynamic loading. The word "dynamic" includes fatigue and aero-elastic behavior. The crucial aspect of the appropriate lightness of the aero-structure is related quite strongly to the choice of the material. Developments over the last seven decades on materials and their manufacture have dramatically contributed to the "lightness" of the structure. It is not that improvements in the analytical tools and understanding of structural behavior have not contributed – they indeed have. These can be attributed to a greater extent to the enhanced computer support – speed and architecture-wise than the software tools which have had inevitable positive inputs. To reinstate this point, the availability of composite materials –Kevlar, carbon-carbon and other composites have created enor-mous lightness without sacrifice of strength. This availability has led to a quantum jump in technology. However, how much to use and where needs structural understand-ing and there arise some new aspects here too. Also, methods of analysis need to be tuned keeping in mind the deformation behavior some of which would be orthotropic. All these are important, but not dramatic. They will be developed with the availability of the "right" material.

6.1.1. What does this chapter contain?

In the sections to follow, the aspects of how these aeronautical structures look and why so will be brought out. It might be instructive to see the relationship to birds because nature has built very efficient structures through biological evolution. The loads that the aero-vehicle has to withstand in the flight enve-lope through the classically known V-n diagram will be discussed. Materials

and the manufacturing contributing to the efficient components for various types of flight vehicles will be discussed, then. This is followed by a discussion of strength of materials - linking it to why systems look they do. This may be bypassed assuming that such information is obtained from tests and will be used in the design. A sense of incompleteness may prevail if the science behind the strength of materials remains to be understood and how the materials behave under loading. This discussion is followed by structural design principles. The first-cut design evolves from strength of materials approach to the details of the configuration. It is only then that the structure subject to finite element analysis for which several commercial codes are available. Understanding strength of materials is vital since it provides insight into the structural behavior. Even if the finite element analysis based results are available, they will need to be scrutinized for their validity. The various modes of structural deformation like bending, twisting, and buckling are then discussed. How to enhance strength by altering the structural content is brought out.

Fatigue and fracture are taken up next. These were studied for a long time and yet, their importance came out prominently with the crashes of Comet and Aloha aircraft. Much has been done to understand these aspects over the last six decades and they play a vital part in aircraft structural integrity and life. Other influencing factors like temperature, salt and moisture in the flying environment which will add to the complexity that need to be understood and factored into the design and maintenance of flying vehicles. The role of atmospheric effects like lightning and how this is factored into the design is briefly addressed.

Any aircraft flight has unsteadiness caused by the aerodynamic/fluid mechanical effects (like shedding of vortices and separated flows from the wing under certain conditions) which influences the forces on the tail region. The coupling between the aerodynamics and flexibility of the aircraft causes vibrations. Various terms like flutter and buffeting are used to indicate this behavior. To understand this behavior, the dynamics of the aircraft has to be analyzed. The idea of resonance in the structural behavior has to be understood - as to why sympathetic oscillations of "infinite" amplitude at the natural frequency arise and ways of obviating the disastrous consequences need to be explored. These form the subject of discussion next. Computer based analysis of stress, deformation and vibrational characteristics of a loaded structure using finite ele-

ment method is brought out and compared with finite volume procedure used extensively in fluid flows.

This is followed by a discussion of structures for missiles and launch vehicles, the ways they differ from those of aircraft. While the tools of understanding them are not very different, these structures are simpler in geometry and offer lesser challenges to ingenuity in design. Also, missiles and launch vehicles are one-shot events without the criticality of working life demands of aircraft. Satellites experience space environment with the need to deal with temperature cycling (~ 0 to 350 K), magnetic storms and solar flare as well as sporadic meteoritic hits in their life of 7 to 10 years in space bereft of aerodynamic effects. While system elements are introduced to take into account the effects, the methods of design and analysis are very similar. A final summary provides a view point in the spectrum of issues that are to be understood to build robust, safe and light enough structures for flying vehicles.

6.2. Aircraft Structure - Some Links with Bird Structure

Just as one derives comparisons of aerodynamic characteristics of aeronautical vehicles with birds, one can make comparisons for structures as well. The central body of the bird is the fuselage of an aircraft. The wings of a bird are wings of an aircraft. Just as a bird has to be light for flying, so should the aircraft be. If not, it would stay on ground! How light should the bird or aircraft be? In the case of bird, the evolutionary process has created hundreds of varieties from very tiny to large. The "specifications" for each bird have depended on the environmental and genetic factors. In the case of an aircraft, it is possible to specify and create one. If one assumes that the central body of a bird is the principal component and the wings are an accessory to help the bird maintain its living style, one can interpret that in an aircraft, what will be in the fuselage is primary and the wings help it maintain the flight. Fuselage carries payload – passengers, their baggage and the crew including the pilots. One can very quickly see that for a given payload which is specified externally (as also flight requirements), if the structural mass is lower, the aircraft will be better airworthy – it will need "much less" effort to maintain the flight. The precise question would be: how can we make the structural mass lower without affecting its integrity – that is the ability of the structure to carry out its role of flying the people or other payloads around without a unsafe failure (what does this mean? - safe life or fail-safe idea is discussed later).

To illustrate how important the subject of "extra structural mass" would be, let us take the two examples. During the development of Boeing 777, the aircraft was weighed once the prototype was completed. If the aircraft weighed more than the promised weight (or design weight), the user had to be paid a certain amount of USD/kg extra weight as this would impinge on the economics of commercial operation (because of extra fuel to be used to carry the "flab"). Similarly, the presence of an extra kg in the upper stages of a launch vehicle may imply as much as 150 to 200 kg extra mass in the lower stages and thus to the total mass of the vehicle.

In order to determine the structural details, two things are important – loads and materials along with their properties. The flying loads come from aerodynamic considerations – pressures on different parts of the aircraft in a steady flight and acceleration loads in other conditions – take off, climb, turn, landing, maneuvers and other critical modes of flying like gust and low speed stall that may arise under adverse conditions. These loads take different forms – some opposite of what gets experienced at other conditions. For instance, during taxiing just before take-off, the entire force which is the weight is acting downwards, particularly on the wings. In steady flight, the wing under-surface experiences higher pressure than the upper surface and so, the forces act upwards. Thus, it is important to consider many conditions of the flight and assure that the structure is safe while meeting all the expected requirements. All these will ultimately translate into costs and what people pay for their travel (in the case of civilian aircraft). This is an important principle in aircraft design – of remaining in a narrow range of margin of safety, something vastly different from design of civil structures where, a larger factor of safety is not frowned upon because the penalties are not high. Thus, the design must take a pathway in which the factors of safety should neither be too small nor too large. The second thing that affects the design is the choice of the material. The material must be strong, but not weigh much. This translates to a criterion, namely strength-to-density ratio. A heavier material should be stronger if it has to qualify for being accepted. A lighter material can afford to have lesser strength, only the ratio (strength-to-density or such a related parameter) should be higher.

One other point of comparison would be insightful. Suppose we wish to compare the loads between a bird flying at sea level at say $36\ km/h$ ($10\ m/s$) and

an aircraft flying at 10 km altitude at speeds of $M = 0.8$ (250 m/s), the dynamic pressure ($\rho V^2/2$) ratio between the flight of an aircraft and a bird is 250. This implies that the loads on an aircraft flying at 10 km altitude at $M = 0.8$ could be 250 times higher than a typical bird (the size of aircraft is maintained same in this argument). This is the reason why an aircraft designer has to invent complex materials, create structural components appropriately and put them together to give an integrity comparable to what the bird does for itself or rather, what evolution has done to the bird.

What the loads do, as can be imagined, would be to compress, extend, bend, twist and cause buckling of different parts. If the structure is made very stiff, then deformations would be very small. This implies that the factor of safety is high. If the structure is too flexible, deformations would be very large and the factor of safety may be below acceptable value. Thus the essence of the structural design is to maintain a factor of safety in all the components of the flying vehicle. Much of earlier design was conducted by strength of material calculations that involve several approximations. Testing was conducted with strain measurements using static loads and these were to be harmonized with the calculations and the structural integrity assessed. When computers became available, the calculation schemes became more sophisticated with finer details being analyzed to ensure "safe" design. The testing operation became more sophisticated with greater understanding of the structural behavior.

One of the general principles in aeronautical structural design is that if some zone experiences very low stress, one can reduce the thickness of the material in this zone or remove the material all together. This implies one can in fact use for instance, a sheet with a number of holes in it without being concerned about them. It is possible to derive a number of features of an aircraft structure from very simple considerations. If we take a fuselage of a civil aircraft, we must have space for accommodating people and baggage. Hence the structure must be surrounding a hollow inner space. This shape is somewhat like a shell. To provide stiffness to this shell which is a thin sheet, circular or oval, appropriately shaped members are located at various distances along the fuselage. These members are sized in thickness and shape and spacing to ensure strength. The wings are also made up of thin sheets and again, appropriately shaped members are located along the wing laterally and longitudinally. The longitudinal members are attached to the members on the fuselage; these

joints experience large forces coming from the wings and hence, they are suitably stiffened. Other control surfaces follow a pattern similar to the wings all sized to take the appropriate loads. These elements are like bones in the bird and muscles around them.

Figure 6.1 shows the "fleshless" skeletal structure of a bird as well as an aircraft to appreciate the similarities and differences. The space in the wing carrying the liquid fuel is the equivalent of muscles and flesh around the bones in the bird. In this particular case, the example of a pelican is chosen. It is approximately 1.5 m long and has a mass of about 10 kg, but has a skeleton mass of only 0.7 kg. This is about 7 % of the mass of the bird itself. Allowing for some other parts that have a structural value, the mass fraction is less than 10 %. This must be compared with the modern day aircraft whose structural weight is about 15 to 25 % of the total mass. Even though the comparison may be considered "improper", it shows how perfectly birds' skeleton is adapted to flight. The reason the skeleton is so light is that many bones in a bird's skeleton are hollow. The hollow bones are honeycombed with air spaces and strengthened (also stiffened) by criss-cross struts. The number of hollow bones varies from species to species, though large gliding and soaring birds and the more efficient fliers tend to have the most. Although a present-day bird has fewer bones than its ancestors, its skeleton is strong and stiff enough for flight due to fusion of many of its bones, reminding the welded construction in an aircraft. Forming rigid girders and platforms, fusing together for rigidity, and others that are not, allows for mobility. Vertebrae in the lower back are joined, as are the bones of the hip girdle, forming a light but strong plate that rests on the thigh bones and supports the bird when it is on the ground. Overlapping projections (similar to cartilage) near the backbone, add strength to the rib cage. Formed by fusion of the collarbones at their base, the bone offers structural support for the wings. In flying birds the breast bone is fused to a deep keel (a longitudinal ridge of bone) that provides an anchor for the powerful flight muscles. Generally, deeper the keel the more powerful is the flight.

As can be seen from the cutaway view of an aircraft, the outer part is made of a thin skin. If the entire structure were to be made of such a skin, the structure would be called monocoque. The skin is retained as thin but is supported by spar (flange + web) along the span of the wing and ribs in the chord-wise direction. Both these features are described in Figure 6.2 with particular reference
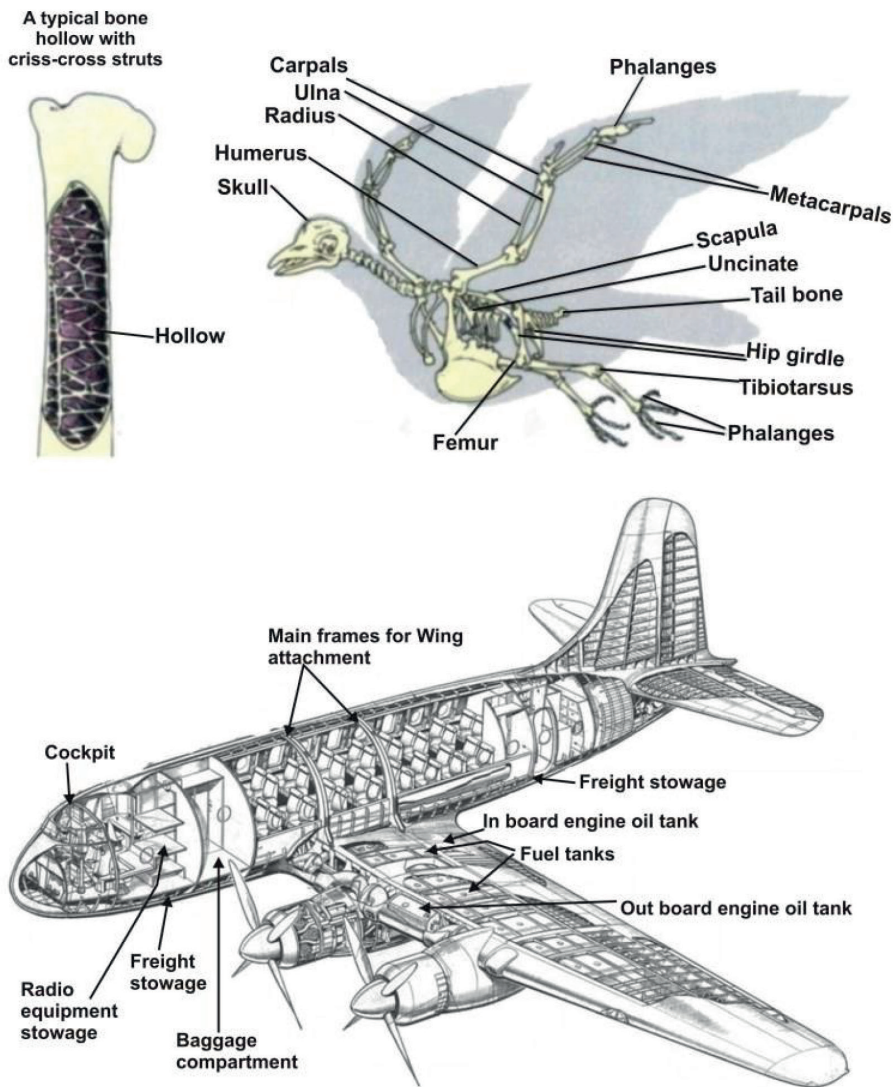
Figure 6.1.: Comparative view of the structural parts of a bird and an aircraft (The figures on bird drawn from Internet1, 2011)
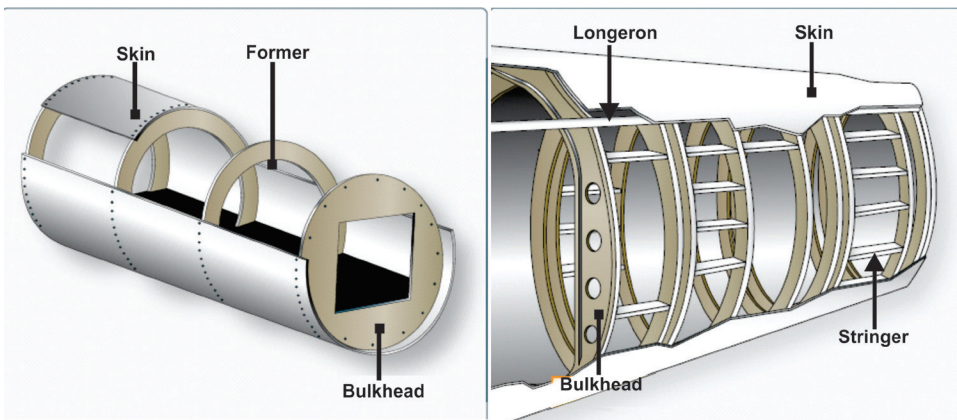
Figure 6.2.: Schematic of the elements of a monocoque and semi-monocoque construction adopted for fuselage of an aircraft, adopted from FAA, 2016

to fuselage. In the monocoque construction, formers (rings essentially) and bulkheads are used to provide support to the skin that covers them. At concentrated points of load such as connections to wing stiffer and stronger bulkheads are introduced. Since other primary loads (bending) have to be withstood, the skin is made thicker adding to weight and so heavier. To reduce the weight, a semi-monocoque construction in which longerons and stringers are added as shown. The construction of the wing as a semi-monocoque structure that is universally adopted is shown in Figures 6.3 and 6.4. The skin forms an impermeable aerodynamic surface, transmits aerodynamic forces to ribs and stringers, resists shear torsion loads (with spar webs) and reacts axial bending loads (with stringers). Spars form the main span-wise beam, transmit bending and torsional loads, and produce closed-cell structure to provide resistance to torsion, shear and tension. Within the spar, webs resist shear and aerodynamic loads and inertial loads during landing, acceleration and deceleration. They also stabilize the skin and flanges resist axial loads due to bending of the wing. The stringers themselves increase skin panel buckling strength by dividing into smaller length sections and react to axial bending loads. The ribs help maintain aerodynamic shape, act with skin to resist distributed aerodynamic pressure loads, distribute concentrated loads into structure and redistribute stress around discontinuities (like undercarriage wells, access panels, fuel tanks, etc.), increase column buckling strength of stringers through end rest-
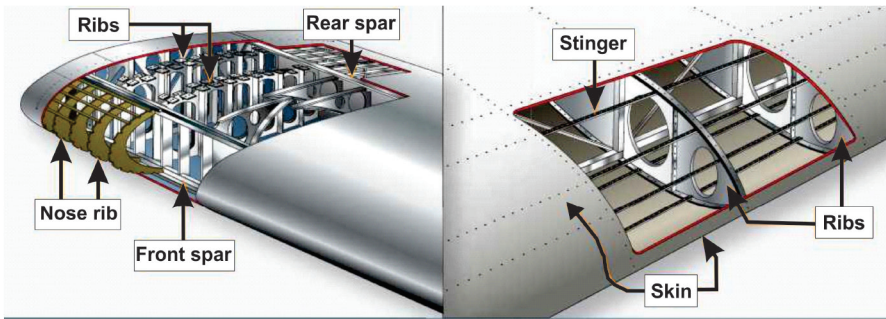
Figure 6.3.: Schematic of the elements of wing structure with outer form of airfoil, adopted from FAA, 2016

raint, and increase the skin panel buckling strength. There are a number of holes made at various locations in the ribs to reduce the material in zones where the stresses are calculated and measured to be low. The cutouts are made with smooth and suitably turned edges to reduce the stress concentration and add stiffness. The wing box can be arranged in a multi-spar arrangement as in Figures 6.3 and 6.4. The wing loads are transferred to the main bulkhead (as it is called) in the fuselage which is considered a reference for relative movements because this is occupied by the flight crew and passengers. The ribs themselves can be arranged with respect to the leading edge in various ways – nearly parallel to the main aircraft axis or nearly normal to the leading edge of the wing.

It is now useful to examine what kinds of structural elements can withstand what kinds of loads and also see how to enhance the load carrying capacity as well reduce the material content. The interesting aspects of geometry as they influence the selection of shapes for withstanding loads arise in bending, buckling and torsion.

The aspects of compression and tension are straightforward. The wing can be treated as a beam fixed at the wing root to the fuselage. If a cantilever beam is loaded with self weigh and forces of wind, the ellipsoidal pressure distribution over the wing surface (see the pressure variations in Figures 2.3 and 6.8) creates bending moment in the clockwise direction when the aircraft is taxiing

and in the anti-clockwise direction when it is in steady flight (as illustrated in Figure 6.5. The force distribution would be symmetric in the above conditions. However, with coordinated turn or side-slip there will be asymmetric distribution of loads. The twist on the wing cross section will be very severe during landing and takeoff because of loads from the extended wing surfaces with substantial curvature and the forces themselves being far away from the aerodynamic centre of the wing. These overall loading on the aircraft is expressed in a diagram called V −n diagram that describes the load factor ($n = L/W$ where L is the lift and W the weight of the aircraft) as a function of the speed of the aircraft.

6.3. The *V − n* Diagram or the Flight Envelope

Every aircraft has to fly over a speed-acceleration envelope. There are also occasional sharp loads due to gusts and buffet, both of which refer to brief but wild fluctuating winds. These impose loads on the aircraft. There are limits to allowed acceleration depending on the speed of the aircraft particularly because the aircraft is structurally stressed to these loads. The loading on an aircraft structure includes air loads (i) due to steady flight, maneuver, gust, buffet, and deflection of control surfaces, (ii) inertia loads due to acceleration and deceleration also affected by the flexibility of the aircraft leading to aero-elastic vibration (also called flutter),(iii) landing including possible emergency crash landing as well as take-off and (iv) impact or bird strike.

It is demanded that the aircraft structure withstand a (proof) load 1.0 − 1.25 times the design limit load without detrimental distortion and not fail until a design ultimate load is exceeded (usually 1.5 times the design limit load). In addition, one determines the margins of safety. For instance, the structure fails at a load, FL say, then the margin of safety (on ultimate load) = (FL − design ultimate load)/design ultimate load. One can also talk about the margin of safety based on proof load. Different parts of the aircraft use either of these depending on what is perceived as appropriate for the element considered.

Once the flight speed is selected a fact that depends on the mission for which the aircraft is designed, airworthiness requirements of the kind described above (the design limit load and ultimate limit load and the speeds at which these are allowed) are represented on the V − n diagram (also known flight env-
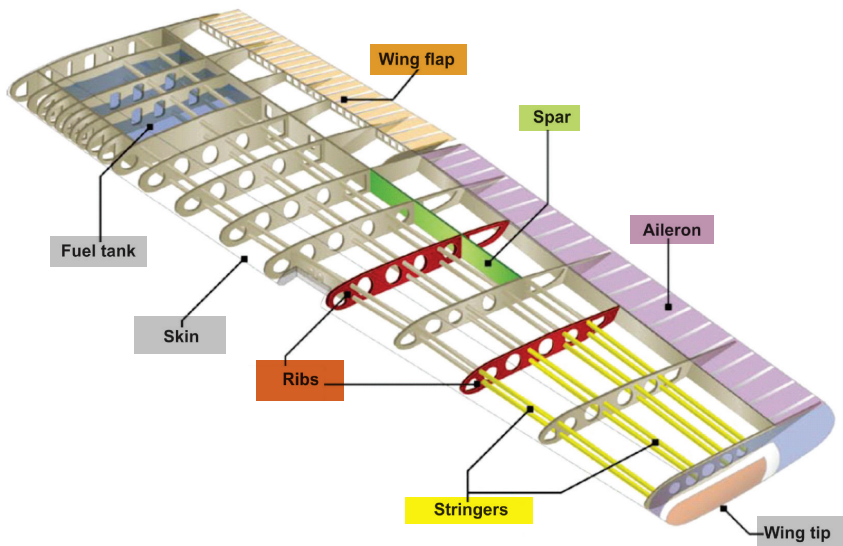
Figure 6.4.: More details on the elements of wing structure with outer form of airfoil, adopted from FAA, 2016
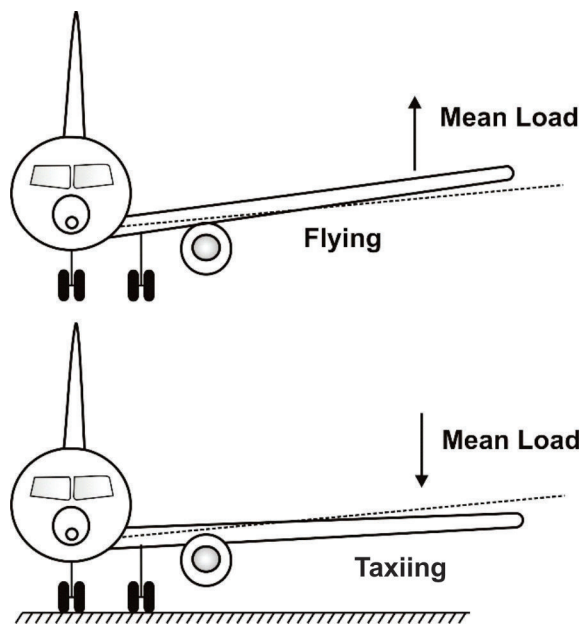
Figure 6.5.: Schematic showing the way the load distribution changes between the conditions of taxiing and in flight. What is shown is for one side. The other side is mirror image.

elope) shown in Figure 6.6. It is important to appreciate what n, called the load factor is (discussed earlier in Chapter 4, section 4.14). Each occupant (as also the aircraft) will experience a force n times the weight. There is another way of expressing this feature. The load on the aircraft is the difference between the lift and weight of the aircraft. This load is expressed as Wa_y/g where W is the weight of the aircraft, a_y is the vertical acceleration and g the acceleration due to gravity. The ratio L/W can therefore be shown to be $(1 + a_y/g)$ and denoted by n which is the load factor. For steady flight, $a_y = 0$ and therefore, $n = 1$. The curved lines 0-A and 0-F on Figure 6.6 refer to positive and negative stall both of which are are due to large positive and negative angles of attack that may be cause during maneuvers and can be obtained from

$$n = L_{max}/W = \rho V^2 c_{L,max}/(2W/A_w)$$

where A_w is the wing area. This equation leads to the parabolic variation of n vs. V for both positive and negative stall regimes. On this diagram must be imposed the restrictions on the lower speeds due to take-off and landing considerations. This leads to the horizontal line AC and refers to the limit load that can be put on the structure (on the negative n side, line FE). The design speed and the maximum speed attained in diving constitute the speed limits. In order that the loads on the structure be limited to safe values, the load factor imposed on the structure is linearly brought down beyond the design speed to the maximum speed (CD$_1$ and D$_2$E). The values of n_1 and n_3 demanded by the requirements for different classes of aircraft will determine the maximum values of $c_{L,max}$. The values of n_i for different classes of aircraft are shown in Table 6.1 (drawn from Megson, 2007). The terminology "normal" refers to all civil aircraft, most fighters belong to aerobatic variety and others chosen as semi-aerobatic depending on the missions. In addition to these load factors, the effect of gust is to be taken into account. Gust is taken as a step change in the vertical velocity (V_g), typically about 15 to 17 m/s of equivalent velocity (taking into account the altitude). Since this value is usually much smaller than the flight speed (250 m/s), a simple treatment of the enhanced lift due to the gust leads to $n = 1 + \rho V U_g c_L/(2W/A_w)$.

This modifies the $V - n$ diagram by adding straight lines emanating from $V = 0$ and $n = 1$ point as shown in Figure 6.7. The hatched portion is the operating region for the aircraft. The left hatched vertical lines correspond to the minimum
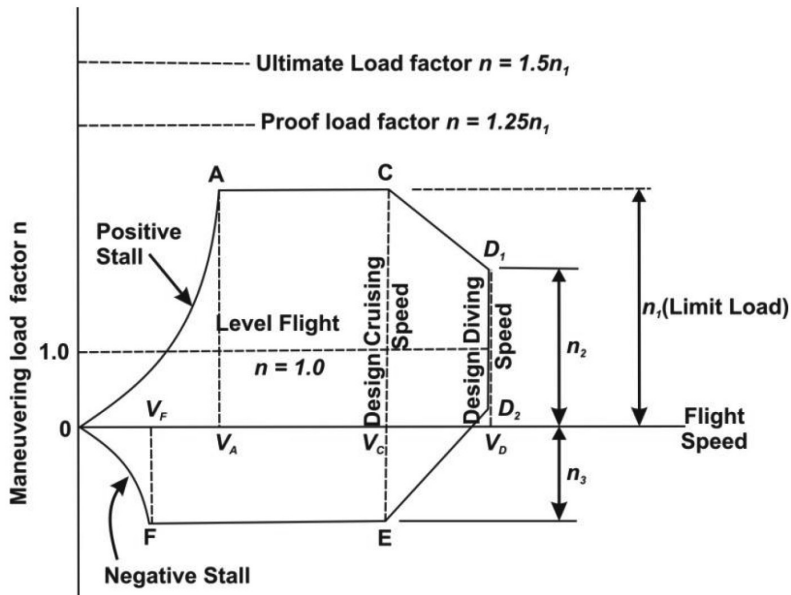
Figure 6.6.: The $V − n$ diagram ($n = 1$ is cruise condition, The various n_i represent the design limit load and VA, VC, VD and VF the speeds)

Table 6.1.: Limit load factors for different classes of aircraft

n_i	Normal	Semi-aerobatic	Aerobatic
n_1	2 to 3	4.5	6.0
n_2	$0.75\, n_1$	3.1	4.5
n_3	1.0	1.8	3.0

permitted speeds. The extended triangular regions are provided for to enable the aircraft to withstand higher loads due to gusts at these speeds. This does not mean that all parts of the aircraft are designed to same loads. Other structural aspects such as impact resistance, stiffness/structural deflection, fatigue, environmental degradation need consideration. Various parts of the aircraft will have different critical design criteria and critical load cases.

The forces acting on the aircraft include structural weight, fuel weight, and point loads (like payload, engine, and landing gear [LG]). Typical picture of these loads is shown in Figure 6.8. The lift is a primary load. It will vary depending on the flight speed, altitude and the maneuver executed. The lift com
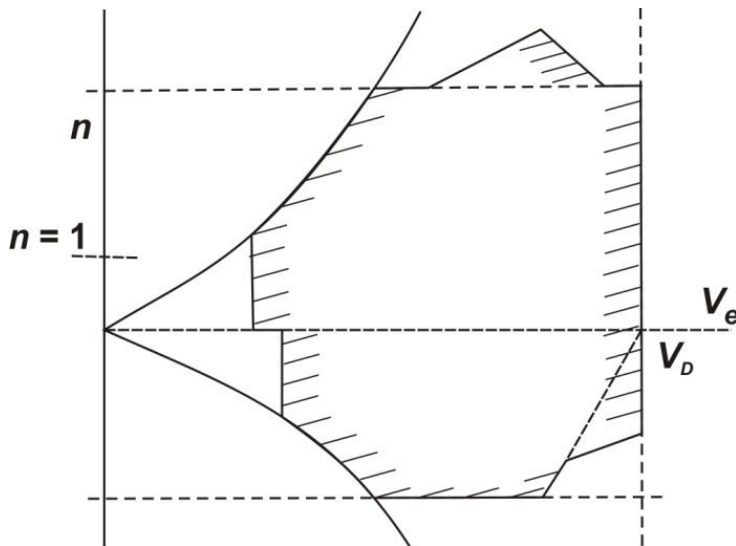
Figure 6.7.: The *V − n* diagram showing the boundaries of operation modified by gust

ponent behaves largely as an ellipse (an ellipsoid in 3–d) over the span of the wing as shown. There are point loads of the engine and the landing gear (when it is landing or taking off). *The fuel weight will continue to decrease during the flight.* The payload will remain the same through the flight if the flight is a civilian kind and may undergo changes if a military operation is conducted, like dropping of bombs, etc. These loads on the wing will be transferred to the fuselage area through the bulk heads connected to the spar. For civilian aircraft one uses 2 or 3 spar design. Typically one is located at the point of maximum thickness, since this location best counteracts the stress on the spar, and one in the aft zone and sometimes, one closer to the leading edge to provide attachments for control surfaces. Ribs are also used to join the spars and reduce wing twist. The fuselage uses a series of ring-framed bulkheads to maintain the fuselage shape and to support point loads transferred from the wing. A series of longerons (as they are called) run the length of the aircraft for providing longitudinal stiffness.

6.4. Materials and Manufacture

All flight vehicles are built up of a number of materials available at the time or developed specifically for the application (Ashby, 1999). The materials are both
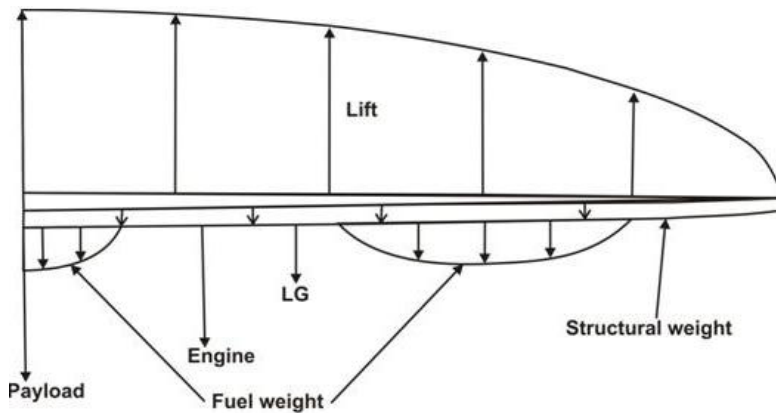
Figure 6.8.: The forces on a wing (half segment shown here)

Table 6.2.: The material composition of some recent aircraft

Aircraft	Aluminum	Composites	Titanium	Steel	Others
Boeing 777	50	12	12	15	11
Boeing 787	20	50	15	10	5
A 380	61	22	6	4	17

natural and synthetic, of course both needing processing. The range of materials includes fabric, wood, metal (iron and aluminum alloys), fiber reinforced plastics (like kevlar, carbon–phenolics and carbon-carbon). When it comes to hang gliders, metal tube – space structure covered by a fabric is a standard practice (see Corona, 2006 for a brief history of materials).

6.4.1. Recent Materials

The nature of materials used in civil and military aircraft has changed over the last thirty years. Table 6.2 composed from several sources (Johnson, 1999; Harris, 2005) shows the material composition of some aircraft built in the last twenty years. Most commercial aircraft depend on aluminum alloys significantly. Composites accounted for less than 15 % a decade ago largely because of the level of understanding of structural integrity and fire safety issues; their fraction has increased to as much as 50 % in Boeing 787.

In the case of the Airbus family, Airbus A340-600 saw the first use of compos-

Materials used in 787 body

- **Fiberglass**
- **Aluminum**
- **Carbon laminate composite**
- **Carbon sandwich composite**
- **Aluminum/steel/titanium**

Total materials used
By weight

Other 5%
Composites 50%
Steel 10%
Titanium 15%
Aluminum 20%

By comparison, the 777 uses 12 percent composites and 50 percent aluminum.
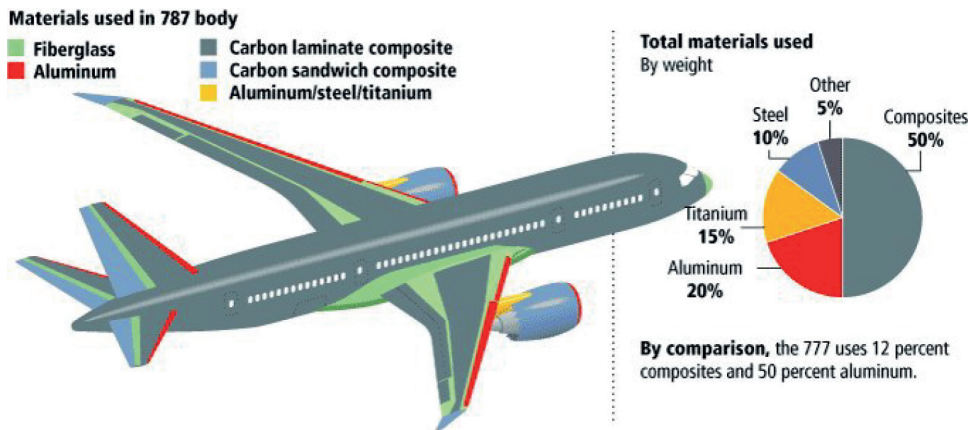
Figure 6.9.: The distribution of materials on Boeing 787 aircraft and the relative mass fractions, drawn from Internet4 (2016)

ites for crucial primary structures such as the rear pressure bulkhead and the keel beam. Other components made from composites include the fin and rudder, horizontal tail plane and wing trailing edge moving surfaces. The floor panels in the passenger deck were also made from composites. By volume, it is 80 % composite. Composites are used on fuselage, wings, tail, doors, and interior. Aluminum is used on outer fuselage skin, titanium used mainly on engines with steel used in other places. On Airbus A380, 61 % of the structure is made of aluminum alloys, 22 % composites, 10 % titanium and steel and 3 % Glare (a new material developed in 2002 made of glass fiber and aluminum as laminates; see Vlot, 2001 for the history of development). Figure 6.9 shows the distribution of various materials on the aircraft. While engine components, wing and fin leading edges and select components are of metal, most others are of composites. There have been arguments that the risks of having a composite fuselage have not been fully assessed and should not be attempted. It was also added that carbon fiber, unlike metal, does not visibly show cracks and fatigue and repairing any damage done to the aircraft would not be easy. The introduction by Boeing of an *in-situ crack detection sensor monitoring technology termed CVM^{TM}* as a standard NDT method (for the first time in aviation) is expected to deal with this concern.

Military aircraft have reached 60 % composites and military helicopters have reached 80 %. This increase in the use of composite materials in military ap

Table 6.3.: Material Selection criteria of a typical aircraft

Material	Usage	Advantages	Disadvantages
High strength unidirectional graphite/epoxy	Spar caps	High strength, low wt	High cost, low impact resistance, difficult to manufacture
High modulus $\pm 45^0$ graphite/epoxy	Skin (w/foamcore), shear web, wing ribs	High strength, low wt, low surface roughness, stealth characteristics	High cost, low impact resistance, difficult to manufacture
Aluminum 7075-T6	Bulkheads, Longerons	Low cost, ease of manufacture, good structural efficiency	Low strength, not weldable
Stainless steel (AM-350)	Landing gear	Relatively low cost, high strength, corrosion resistance	High weight
Nickel (Hastelloy B)	Nozzles and ducting	Temperature resistance	Low structural resistance
Kevlar	Internal armor	High strength, low weight, high impact resistance	High cost, difficult to manufacture

plications is because of possibilities of minimizing the radar detection (otherwise termed better stealth characteristic). A typical military aircraft may use graphite – epoxy of 55 to 60 %. 15 to 20 % aluminum alloy (7075 - T6, for instance), 12 to 15 %Hastelloy B, 3 to 4 % Kevlar and stainless steel each, and the reasons for the choice of each of these for specific components of the aircraft is clear from Table 6.3

A description of the materials used on several class of aircraft is provided in Appendix 2 to provide an appreciation of what materials go into what part of the specific kind of aircraft; it must be understood that this description is only indicative. Further, as time goes by, newer and newer materials will get introduced because operational experience will get factored into improvements and new designs.

6.4.2. More on composite materials

Composite materials, by definition, are those composed of two or more different physical or chemical constituents that can be separated. There are natural composite materials like wood or bamboo made up of cellulose and hemi-cellu-

lose fibers in a matrix of lignin (as an aside, other natural fibers include silk, wool, cotton, jute, sisal all of which are used in a woven manner by imparting better properties; dried unfired bricks into which straw fibers were introduced that were in use in Egypt are examples of a composite structural materials). In recent times, steel metal filled tires, reinforced concrete, glass fiber reinforced plastics (GFRP) have entered common use. Essentially, the development of composite materials is contemplated because it is desired to obtain properties better than what one would get from the parent materials. The principal benefits expected are: higher stiffness-to-density and better properties over a wider range of temperatures. There are three distinct composite materials in aerospace practice – metal matrix composites (MMC), ceramic matrix composites (CMC) and polymer matrix composites (PMC). The key feature of composite structures relates to having a more ductile matrix and allow-ing more brittle, but high strength dispersed phase; by creating excellent bonding between the matrix and the dispersed phase, like fibers in polymers, one derives better properties. The stress experienced by the matrix should be transferred to the dispersed phase (polymers to fibers). In the case of MMC, dispersing the brittle cementite (Fe_3C) in a α-ferrite matrix gives rise to spheroiditic steel, dispersing the stiffer carbon particles into rubber matrix leads to a stiffer tire and alumina or silicon carbide dispersed in aluminum gives better properties than aluminum. The yield strength ($Y\,S$), ultimate tensile strength (UTS) and creep resistance (minimal time dependent deformation under stress, a feature extremely important for turbine blades in a gas turbine engine, for instance) are all enhanced by this process. In the case of CMC, increase in K_{1c}, and in the case of PMC, increase in the elastic modulus, $E,\ UT\,S,\ Y\,S$ and creep resistance.

PMCs are the most used of the composites including those for aerospace. GFRPs are produced in large quantities and hence are more affordable and used in applications involving helmets, automotive bodies, industrial flooring to chemical fluid carriers. Carbon fiber reinforced polymers (CFRP) are generally used in high performance applications. Aramid fiber reinforced polymers (AFRP – Kevlar) are used in applications needing high strength, modulus and impact resistance. Polymer matrix composites are produced as thermosetting and thermoplastic materials.

Thermosetting polymers use epoxies, phenolics, polyurethanes and polyimides

in conjunction with various fibres noted above. They are mixed with a curative chosen depending on the polymer system, cast and cured in an autoclave at suitable pressure and temperature into the shape required. The product so obtained cannot be altered or reformed or recovered. As different from this, thermoplastics are produced by melting the polymer, combining with the fiber suitably, shaping the material appropriately and cooling it. It is produced by injection molding, thermoforming and blow molding techniques. Many aircraft interior elements like flooring, overhead luggage bins, bulkheads, seat components, trolleys, stairways and many such components are all produced as thermoplastics. Both these methods include other ingredients for ensuring specific properties including fire safety.

6.5. Strength Pproperties of Aircraft Materials – Metals and Composites

In order to obtain a broader picture of the material behavior, the data on elastic modulus as a function of material density is set out in Figure 6.10. A broad tendency of the elastic modulus going up with density is clear. The feature that the strength of materials increases with density is shown by the guide line of $E/\rho^3 = C$ in the Figure 6.10 (see Ashby, 1999; Ashby and Jones, 1980). However, material production and treatment will alter these significantly. More material specific data for many aircraft materials is set out in Tables 6.4 and 6.5. These data are drawn from several internet sources including Wikipedia. In the tables, E refers to elastic modulus, UTS refers to the ultimate tensile strength, YS refers to the yield strength and K_{1c} refers to stress intensity factor (a feature that arises from fatigue and fracture issues discussed subsequently).

Wood may be treated as a natural composite. Its properties vary along and perpendicular to the grain. The compressive strength along the grain (typically, 30 to 40 MPa) is about six to seven times that perpendicular to the grain (5 to 7 MPa). UTS along the grain (90 to 110 MPa) is about 10 times that perpendicular to the grain. Fracture toughness of composite materials including wood is not indicated in Table 6.4 because the failure modes of these materials under load has a complex behavior. Generally, the fatigue life of several advanced composites measured in terms of number of cycles to a residual strength for failure can be enhanced to values larger than for several metals through the choice of fibers and methods of processing.
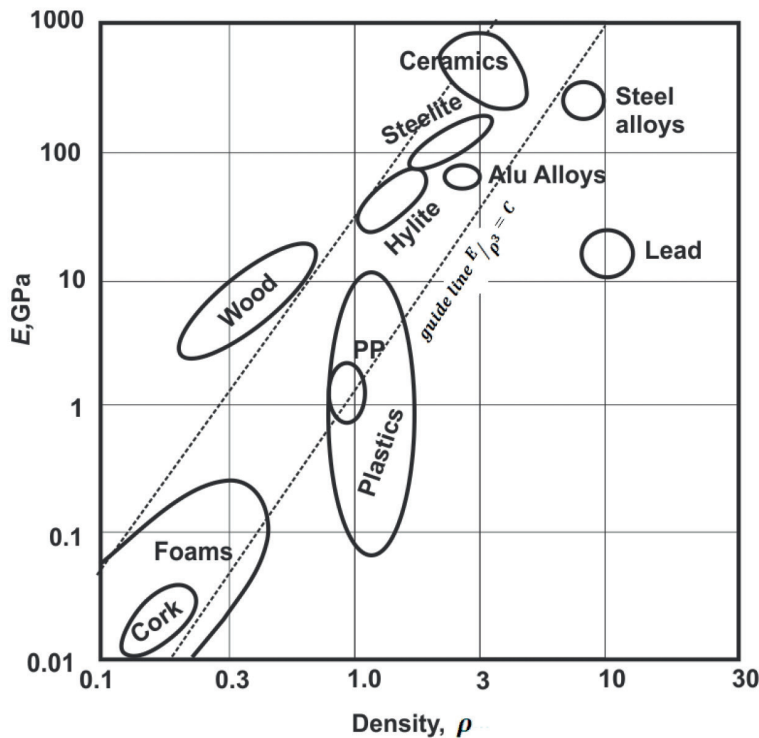
Figure 6.10.: The Elastic modulus of materials vs. density

In the case of metals and alloys, a few general features are known. Most properties follow the trends: stainless steels > titanium alloys > aluminum alloys. Yet, most aircraft use Al-alloys and composites than stainless steel. These are related to strength for a given density that will be discussed subsequently. Typical strength properties of selected aluminum alloys shown in Table 6.5 indicate that tempering the material can change the properties – the ultimate tensile strength (*UTS*), yield strength (*YS*) and the elongation at break (δ/l) drastically. Generally, increase in *UTS* is at the cost of elongation. Interestingly, tempering does not alter the elastic modulus significantly. Creating materials of low density with high strength and stiffness is a human endeavor. It can be noted that foams are very light and form candidates of sandwich composites

Table 6.4.: Density and strength properties of several materials in Aerospace applications (*UTS* = Ultimate tensile strength, *YS* = Yield strength, K_{1c} = Fracture toughness, *Ti alloy = Ti-6 Al-4 + Zr-2, Sn-0.5, Mo-0.5V; GFRP = Glass reinforced polymer, CFRP = Carbon RFP The two sets of values like 45/12 and others refer to those along the fiber and across the fiber taken from the lecture notes of Jang-Kyo Kim, Dept Mech Engg, Hongkong University)

Material	ρm	E	UTS	YS	$K1c$
	t/m^3	GPa	MPa	MPa	$MPa \sqrt{m}$
AM350	7.75	200	1400	1170	175
4340	7.80	200	1764	1530	201
AISI 403 SS	7.80	200	821	690	77
Maraging steel, 18% Ni	7.80	210	1783	–	174
Ti-6Al-4V	4.42	114	897	910	115
Ti alloy*	4.45	125	890	836	139
2219-T851 Al	2.70	70	454	340	32
2024 Al	2.70	72	480	455	26
6061-T651 Al	2.70	68	352	299	29
7079-T651 Al	2.70	70	569	502	26
7178 Al	2.75	77	670	490	33
7075 Al	2.70	75	830	650	35
GFRP	2.10	45/12	1020/40		
CFRP	1.60	145/10	1240/41		
Wood (spruce)	0.45	14	110		

Table 6.5.: The role of tempering in the mechanical properties of Al alloy (*δ/l, δ = elongation and l = length, here about 1 *mm* or less; compiled from Internet2, 2011)

Al Alloy	Temper	$UT S\ MPa$	$YS\ MP a$	δ/l^* %
	O	124.1	55.2	26
6061	T4	241.3	144.8	22
	T6	310.3	275.8	12
	O	186.2	75.8	18
2024	T3	482.6	344.7	16
	T4	468.8	324.1	20
7075	O	227.5	103.4	16
	T6	572.3	503.3	11

Table 6.6.: Properties of Carbon-Carbon Composites (From internet3, 2011)

Property	Fine-grained carbon	Uni-directional Fibers	3-D Fibers
E (*GPa*)	10-15	120-150	40-100
U T S (*MPa*)	40-60	600-700	200-350
Comp. Strength (*MPa*)	110-200	500-800	150-300
Oxidation resistance	very low	poor	moderate

structures that are indeed light but stiff. Honeycomb sandwich construction is attractive for wings of aircraft and rotor blades of helicopters.

6.5.1. Strength of composites

The strength behavior of a composite is between that of the matrix and fiber as shown in Figure 6.11. Several stages of the behavior are: (1) both fibers and matrix deforming elastically, (2) fibers continuing to deform elastically, but matrix deform plastically, (3) both fibers and matrix deform plastically and finally, (4) fibers' fracture followed by fracture of the composite material. The strength properties of GFRP and CFRP have been presented in Table 6.4. The additional point to note is that the strain at break is quite small – of the order of 2 % at the maximum. The properties of carbon-carbon composites are shown in Table 6.6. One can notice that the strength properties depend strongly on the nature of the fiber and the process for making the material. The strength of the composite is a volume weighted fraction of the strength of the matrix as well as the fiber (except requiring equal strains for matrix and fiber).

One of the problems of composites is that shock, impact, or repeated cyclic stresses can cause the laminate to separate at the interface between two layers, a condition known as delamination implying the separation of individual laminae from the matrix. This brings down the strength of the composite because the low strength matrix is forced to carry the load. Compression failures can occur at both the macro–scale or at each individual reinforcing fiber in compression buckling. Many composites are brittle while a few allow large deformation before failure. The variations in the available fibers and matrices and the blends that can be made allow a very broad range of properties for the design of a composite structure as shown in Table 6.6. The well known failure of the carbon-fiber wing of the Space Shuttle Columbia fractured when impacted during take-off. It led to catastroph ic break-up of the vehicle when it re-entered the earth's atmosphere in 2003 [Wikipedia1, 2011].
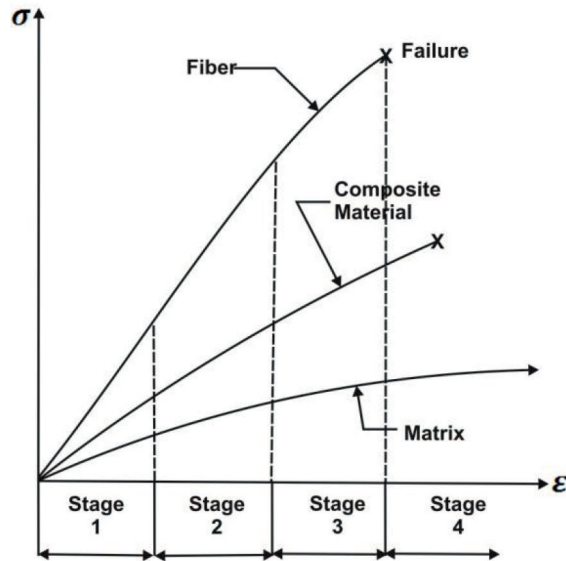
Figure 6.11.: The stress strain diagram of a composite material, (adapted from Jones, 1999)

6.5.2. Why is the strength of materials like it is?

An aircraft designer is concerned with materials that that are stronger, stiffer, tougher, degrade little with temperature and so on. Stronger implies larger ultimate strength in tension, stiffer implies resistance to buckling and tougher implies better resistance to fatigue (cyclic stress). While the issue of this section may be claimed to be outside of aerospace and rightfully belonging to material science, it is useful to understand the principles involved in the ability of a material to take up load to enable the aerospace specialist demand better from the material scientist.

The stress at break can be expressed as (see Roylance, 2001; Schreurs, 2012)

$$\sigma_{crit} \sim \sqrt{G_s E / a} \tag{6.1}$$

In this expression, σ_{crit} is the critical stress, G_s is the fracture energy, E is the elastic modulus and a is the measure of atomic distance (see section 6.9.3 for more details). If we introduce typical values for these as $G_s = 1 \ J/m^2$, $E = 200$
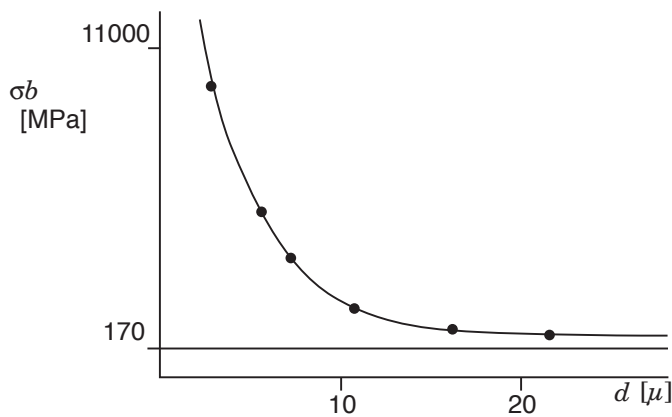
Figure 6.12.: Fracture stress as a function of glass fiber diameter, drawn from Schruers (2012)

GPa and $a = 2 \times 10^{-10}$ m, we get $\sigma_{crit} = 31.6$ *GPa* which is about 16 % of the elastic modulus. But the observed value of stress at failure for most materials is less than 6 % of the theoretical estimate. In earlier times, the strength was more close to 1 to 2 of the theoretical value. This puzzled many scientists. Griffith (of additional fame involving development of jet engines, see Wikipedia5, 2011) chose the simpler glass material as a model since it had brittle fracture (elasticity would nearly last till the end, that is why). The results drawn from Schreurs (2012) are set out in Figure 6.12. As can be seen from the figure, the strength drops from very small sizes (a few microns) to larger sizes (20 microns and above). At about 22 μm, the strength is 0.2 GPa and at 2.5 μm, it is 9 GPa, nearly 50 times higher! Subsequently, Gordon (1991) did experiments with other materials like silicon and zinc oxide by growing them in the form of "whiskers" and conducted experiments that showed similar results (the book by Gordon is one of the most readable ones in this class). These implied that if the material was prepared such that it was close to theoretical structure, the strength would be also close to theoretical (this statement may sound trivial stated this way!). But then, what is it that is happening in reasonable sized materials? These materials have defects – surface cracks in brittle materials unless the material is produced in the form of single crystals (quite large single crystals ~ 150 mm size are grown for use in gas turbine and similar applications) and disorderedatomic arrangements at several locations called dislocations in ductile materials.
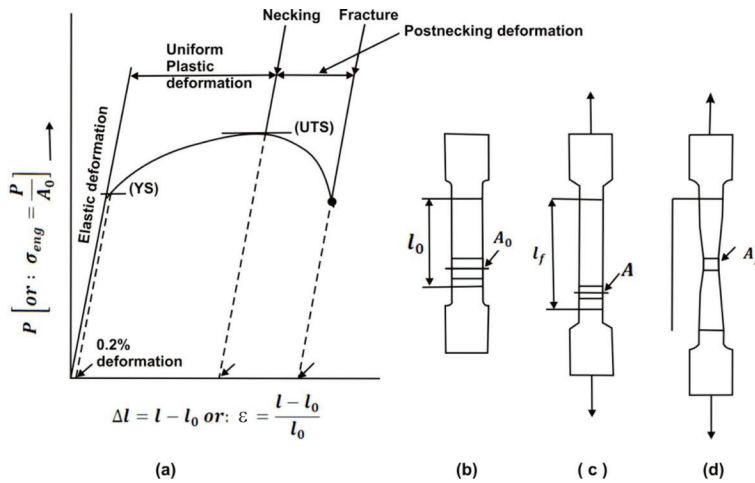
Figure 6.13.: The load extension diagram with all the principal aspects identified; (a) The load extension diagram, (b) The test sample with test section initial length, l_0 and cross section A_0, (c) Test section extension to l_f under moderate loading with cross section reduction to A and (d) Significant test section extension and reduction of cross section, called necking to A_f before fracture; $\varepsilon = (l - l_0)/l_0$

Under the action of impact load that may be small by itself, the cracks propagate in a runaway manner and break up the brittle material. In the case of ductile materials, the presence of dislocations allows plastic deformation right up to failure at loads much less than the theoretical strength of pure substances. The external force causes parts of the crystal lattice to glide along each other, resulting in a changed geometry of the material. Depending on the type of lattice, different slip systems are present in the material. Since the ductility in materials is essentially controlled by dislocations one can also say, producing a ductile, dislocation free material is contradiction in terms. Restricting the movement of dislocations leads to brittleness as it happens in cold working and allowing freer movement of dislocations allows the material to be more ductile.

6.6. Structural Design Principles

Simple approaches using ideas of strength of materials will be used to size the systems in the initial stages (see many books by Timoshenko and co-workers, Timoshenko, 1962; also Peery and Azar, 1982) and computational tools in-

volving finite element techniques and matrix algebra are used to calculate the stresses and deflections at various locations [Corona, 2006]. In any case, one must have structural sense in dealing with issues. Let us briefly review these aspects. As indicated earlier, the structures are subject to tension/compression, bending, torsion and buckling. Locally, the material experiences compression or tension, some always in one mode or the other and most of them in either of the modes depending on the flight condition.

6.6.1. Tension/compression

The behavior of materials in tension and compression is fundamental to the behavior in other modes like bending, torsion, and buckling. The behavior of materials under tension is depicted in Figure 6.13 on a load - deflection (or stress -strain) plot. The curve shown here belongs to the category of metals/alloys like steel. The first part of the load-deflection or stress-strain curve is linear.

The slope of the stress-strain curve is the elastic modulus, E. The strain, ε (extension/original length), and stress, σ (load per unit cross sectional area) are related by $\sigma = E\varepsilon$. This is good for the first part of the stress-strain plot. If we need to include the second part that is curved in nature we introduce another measure of strain $\varepsilon = ln[l/l_0]$, where l and l_0 refer to the length under deformation and the original length. This definition will cascade into the earlier one when extension is small (because $ln\ [l/l_0] = ln\ [1 + \Delta l/l_0]\ \Delta l/l_0$ for small extension, Δl and $\varepsilon = \Delta l/l_0$)). The stress – strain relation is then expressed as $\sigma = C_{sh}\varepsilon^m$ with C_{sh} and m as the strain hardening coefficient and exponent respectively. The curve is linear up to about 1 % strain, beyond which the material will undergo plastic strain that will continue with increase in load till fracture.

There is very little deformation before fracture in the case of brittle material and a necking in the case of ductile material. The material will deform elastically till the proportional limit. Beyond this point, there is plastic deformation. The transition point is called yield point, the stress at which point is called yield stress. Notionally it is defined as 0.2 % offset strength making use of a permanent yield of 0.2 % as can be noted from Figure 6.13. Beyond this, one has a peak stress around necking region called ultimate tensile strength *(UTS)* and finally, failure/fracture strain and stress.

It is interesting to compare the tensile stress strain curves of various classes of materials – metals, both brittle and ductile, polymers as well as composites.
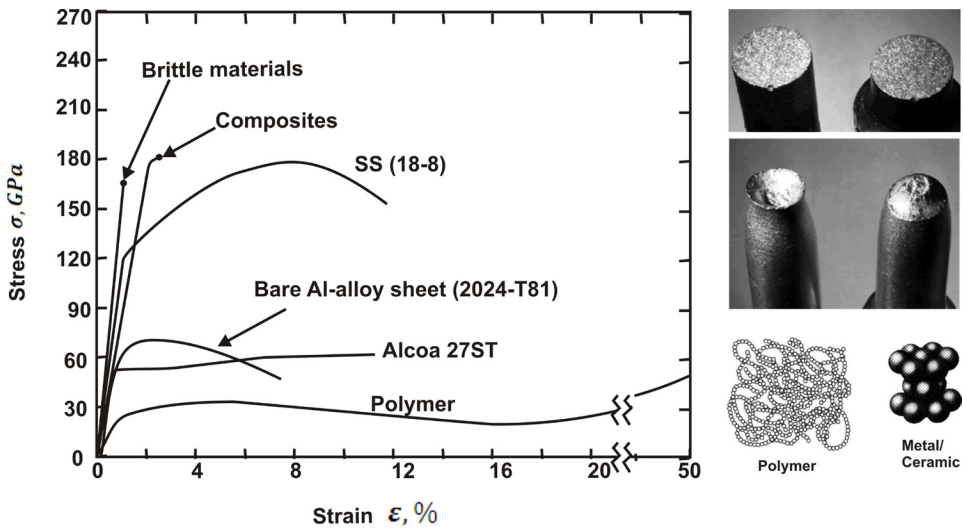
Figure 6.14.: Combined plot of stress strain curves of metals, polymers and composites. The upper portion of the picture shows the differences in stress–strain behavior between brittle and ductile materials – the sharp curve to the left has a fracture behavior of the top region. The elongated curves in the figure for SS (18-8) and Al-alloys are related to the ductile fracture at the lower part of the picture. The bottom corner shows the structure of polymers and metals, Adopted from Nelson and Odeh, 2009

As shown in Figure 6.14, brittle materials have near elastic behavior till break. Plastic materials exhibit a different behavior. There is an elastic phase and a longer plastic phase before failure. Here the yield stress is defined as the peak stress before "necking". The behavior of composites is close to those of brittle materials – small extension before break. Elastic deformation stretches atomic bonds away from the equilibrium distance of separation of bonds with energy less than that required to break the inter-atomic bonds. If it crosses into plastic domain and then is unloaded, the material will acquire some permanent deformation. In this domain, the inter-atomic bonds are broken and considerable rearrangement of atoms in a solid material will occur. If the material passes through several cycles of loading and unloading, the material undergoes what is known as "cold working". Altering the shape or size of metals by plastic deformation by rolling, drawing, pressing, spinning, extruding and heading carried out at temperatures much below the re-crystallization temperature which may also be at room temperature (re-crystallization is a process by which de-

formed grain structure allows nucleation and growth of reduced defect grain structure). Hardness and tensile strength are increased with the degree of cold work while ductility and impact values are lowered. Similarly re-crystallization leads to reduced strength and hardness, but improves ductility.

> *Any deformation – extension or compression should imply increase or decrease in the distance between the atoms in the material. These movements imply changes in forces between the atoms that are interpreted as tensile or compressive stresses. The stresses are accompanied by strains which are essentially the deformations over the length or width of the structure. Thus the stresses and strains belong to the material and not the structure. The stress at break is directly related to the force that breaks the bonds between atoms.*

At a fundamental level, the atomic level behavior is related to material defects known as dislocations (Hertzberg, 1989; Roylance, 2001; Wei, 2010; Rollett, 2015). These can be line defects in the regular crystal structure. They lead to strained and generally weaker bonds than the bonds between the constituents of the regular crystal lattice. Dislocations can also be looked upon as merely vacancies in the host medium. There are edge and screw dislocations. The strained bonds around a dislocation are characterized by lattice strain fields. There are compressively strained bonds and tensile strained bonds around the edge dislocation.

Increase in the number of dislocations is a quantification of cold working or also called work hardening. Plastic deformation occurs as a consequence of work done on a material. The energy added to the material goes into not only moving existing dislocations, but in creating a large number of new dislocations by disturbing the region sufficiently enough. Once the dislocations have been generated in the process of plastic deformation, these dislocations hinder the movement of other dislocations in the next cycle of loading.

Because dislocation motion is hindered, the stress at which plastic deformation occurs is enhanced to values beyond the first cycle. Eventually when loading is much larger, the stress is great enough to overcome the strain-field interactions

and plastic deformation resumes. In this process the ductility of a work-hardened material is decreased as can be inferred (ductility is defined as the extent to which a material can undergo plastic deformation before fracture). A cold-worked material is, in effect, a normal material that has already been extended through part of its allowed plastic deformation. Thus cold working makes the material hard and takes it towards brittleness. The relationship between cold working and dislocation density, defined as the dislocation length per unit volume has been experimentally examined – a carefully grown single crystal is estimated to have a low density of thousand mm/mm^3, but a heat treated and cold worked material have a million, and billion mm/mm^3 respectively (see for a discussion, the lectures by Rollett, 2015).

Plastics are polymeric (including rubber, for instance) have long chains as shown in Fig 6.14. Metals and ceramics, on the other hand, have molecules located at lattice points as shown in the same figure. Even alloys that have several different chemical elements in them will still have a crystalline structure as shown.

At a basic functional level, the atoms are pulled apart when a material is subject to tensile loads. The extension along the direction of pull is accompanied by contraction in the lateral direction depending on the Poisson's ratio, v. This causes the necking seen in the figure. When the stress at the reduced cross section crosses a limit, the fracture will occur. The macroscopic results of plastic deformation are essentially the result of microscopic dislocation motion.

In compression, the behavior is more complex. If the structure is short (and so called stout), the atoms that are pushed towards each other get to a stage that repulsion sets in and the material will look for opportunities to expand in the lateral direction. Aided by the requirement of volume conservation, lateral expansion becomes a consequence. The final failure controlled strongly by defects in the material can be violent in some materials – complete shattering of the material. If the structure is slender (implying large l/d, l being the length and d the lateral dimension), the part will buckle. Here again, the intrinsic asymmetry will create conditions that will bend the straight structure. Enhanced loading takes parts of the structure to tension and others to deep compression with consequent fast accentuation of the buckling process (see the buckling section for more on these aspects).

If the loading is of tensile nature, another problem can arise. Small defects, particularly the presence of inclusions, slip lines, dislocations can lead to the initiation of cracks under cyclic loading when the number of cycles is sufficiently large and the stress level is above a value that is not so large – could be as low as a quarter of the ultimate tensile strength. These cracks can further grow and lead to fracture.

> *It is useful to keep in mind the meaning of a few terms used in the above discussion. If a material has a higher elastic modulus (E), it is called stiffer, because for the same stress, the deformation is smaller. If a material is stronger, it implies that the strength at break (UTS) is higher. These two aspects are independent. Many brittle materials like glass, porcelain and other ceramics are stiff, but not strong. Plastics like Nylon are not stiff, but are strong. Several metallic alloys are both stiff and strong. Carbon fibers belong to the category of the stiffest and the strongest of materials.*
>
> *A structural geometry is stiffer because its sectional moment of area (I) is larger.*
>
> *Thus, structural stiffness is represented by EI which one wishes to maximize.*

6.6.2. Bending

A simple analysis of bending of beams under loading assuming that the material bends preserving the plane surfaces as planar using the geometry of the bent beam in relationship to the original one along with the bending moments that the section is subject to leads to the classical relation (see Timoshenko, 1955, 1956)

$$\frac{M}{I} = \frac{\sigma}{y_d} = \frac{E}{R}$$

(6.2)

where M = bending moment, I = the moment of inertia, σ, the stress, y_d = the distance of the fiber from the neutral axis (neutral axis is the axis along the

beam at which the strain is 0), E = the Elastic modulus and R = the radius of curvature of the beam bend under any load. The deflection is obtained from the relation

$$\frac{1}{R} \sim \frac{d^2y}{dx^2} = \frac{M}{EI}$$

(6.3)

where y is the deflection of the neutral axis at any axial distance from a support. It is elementary to note that higher flexural rigidity (implying larger values of EI) leads to smaller deformation. If we take a rectangular section, the moment of inertia can be written as $I = bh^3/12$, where b is the breadth and h is the height. In this case, the bending is taken to be occurring about an axis parallel to the breadth.

We note from this that $I \sim L_l^4$ where L_l is a length scale of the cross section. The bending moment can be expressed as a load (P) multiplied by distance (L). Thus we can express the stress as

$$\sigma = \frac{PLL_l}{L_l^4} \sim \frac{PL}{L_l^3}$$

(6.4)

The stress developed varies strongly with the characteristic size. In a large plate, this would be the thickness and the stress can be expressed as $\sigma = P/t_h^2$ with one length scale as of unit size (true for a sheet where the thickness alone is a variable). Thus by varying the plate thickness even slightly, one can move from a strong to weak structure and vice-versa.

There is a simple and clear example of the role of moment of inertia in a metal measuring tape. It is made slightly curved so that even when pulled out over half a meter length, the tape remains stiff and flat. An analysis of the moments of inertia of the curved tape in comparison to a flat tape will illustrate this feature. If w is the width of the tape and t_h is the thickness, moments of inertia can be worked out as

$$I_{flat} = wt_h^3/12 \quad \text{and}$$

(6.5)

$$I_{curved} \sim (w^5/R^2)(t_h/720)$$

(6.6)

where R is the radius of curvature of the tape cross section (getting this result requires lot of simple algebra on the expressions). The ratio of the two can be expressed as

$$\frac{I_{curved}}{I_{flat}} \sim \frac{w^4}{R^2} \frac{1}{60\, t_h^2} = \frac{1}{60} \frac{w^2}{R^2} \frac{w^2}{t_h^2}$$

(6.7)

For a typical tape with *w = 30 mm, R = 40 mm, t_h = 1 mm, I_{curved}/I_{flat} ~ 9*. Thus, the strength of the tape to withstand bending loads is increased by 9 times by just curving the tape.

The analysis of bending of beams shows that the stress distribution over the cross section is linear with the largest tensile stress in the top most fiber and the largest compressive stress in the bottom most fiber. Thus to withstand bending it is important to put more material at the top and the bottom and not as much in the middle region. Theoretically an "X" shaped object has the same stresses throughout the material. Of course in practice "I" sections are the ones normally used to endure bending stresses. Somewhat same view emerges when one considers torsion, of say, circular cylinder. The stress is largest at the periphery and falls rapidly inside (as will be seen later) with radius. Thus a tube is more optimized geometry compared to solid cylinder for enduring torsion.

6.6.3. Torsion

The pressure loading on the wing is such that there is torque imposed on all the sections along the wing span. We first look at what torsion does to a structure. We consider solid and hollow circular shafts for illustrative purposes.

A torque applied on the shaft produces shear stress that varies linearly from zero at the axis to a maximum at the outer surface given by

$$\sigma_T = \frac{Tr}{J}$$

(6.8)

where σT is the shear stress (MPa) due to the torque T (N-m) and r is the radius (m) and J is the polar moment of inertia (m^4) for circular cross section. This rise in shear stress with radius tells us that adding material to the core is not important when designing for torsion because most of the stress is in the outer

layers. The polar moment of inertia of a hollow circular tube with outer and inner diameters d1 and d2 respectively is given by

$$J = \frac{\pi}{32}(d_1^4 - d_2^4)$$

(6.9)

The maximum shear stress is therefore given by

$$\sigma_{T,max} = \frac{16Td_1}{\pi(d_1^4 - d_2^4)}$$

(6.10)

This equation can be turned around to answer a question as to what the maximum torque that a hollow shaft can carry. By taking a allowable maximum shear stress ($\sigma_{T,\max} = \sigma_{allowable}$) we get

$$T_{max} = \frac{\pi(d_1^4 - d_2^4)}{16d_1}\sigma_{allowable}$$

(6.11)

If we are to examine the implications of the use of hollow shaft vis-a-vis a solid shaft, the ratio of sizes required to take a torque varies as

$$\text{Ratio} = 1 - \left[\frac{d_2}{d_1}\right]^4$$

(6.12)

Since there is a fourth power on d_2/d_1 in the above expression, changes in the size (d_2/d_1) from 0.6 to 0.54 (10 %) causes a mass increase by 11 % (based on square of diameters) but strength improvement as measured by the change in the ratio from 0.87 to 0.92 (6 %). This goes to show a hollow cylinder is the more appropriate choice for carrying torques in shafts. This is consistent with the choice of thin sheets for carrying torque in wing structures of aircraft.

Aircraft structures particularly in the wing are built of open channel, T, Γ and L sections. These sections, when subject to bending loads will have only bends when the load passes through a certain line through a point called shear center. When the sections have symmetry, one can locate a point along the symmetry line. When the sections have no symmetry, a calculation procedure will help locate the shear center. A simple experimental procedure can also be visualized in which bending loads can be imposed at points that are varied to
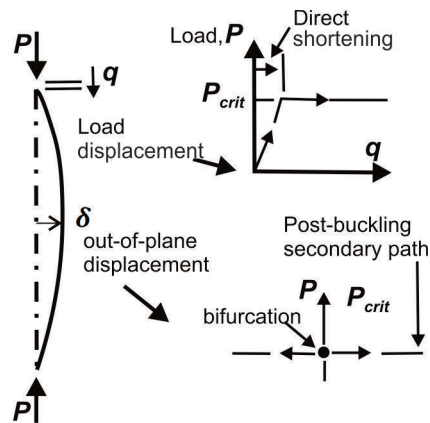
Figure 6.15.: Schematic of buckling. Till a critical load is crossed, the strut will undergo compression. Beyond this value, the lateral deflection will become significant. The lateral deflection occurs on a side that is "weaker"

assess physically whether there is a point in the cross section where if load is applied, there is no rotation.

Aircraft box sections with thin sheets and stringers can be analyzed for both bending and torsion by relatively simple procedures that use approximations –sheets and webs carry shear and the stringers carry axial loads. The shear stresses are taken as uniform across the thickness and the product of the shear stress and the thickness is called shear flow; elaborate approximate procedures have been used to analyze the stress distribution in wing sections. the thickness is called *shear flow;* elaborate approximate procedures have been used to analyze the stress distribution in wing sections. A problem closely related to the restrained torsion of rectangular section beams is what is generally known as *shear lag*. Torsion induces shear stresses in the walls of beams and these cause shear strains which produce warping of the cross-section. When this warping is restrained, direct stresses are set up which modify the shear stresses. In a similar manner, the shear strains in the thin walls of beams subjected to shear loads cause cross-sections to distort or warp so that the basic assumption of elementary bending theory of plane sections remaining plane is no longer valid. The direct and shear stress distributions predicted by elementary theory therefore become significantly inaccurate. These days, the solution
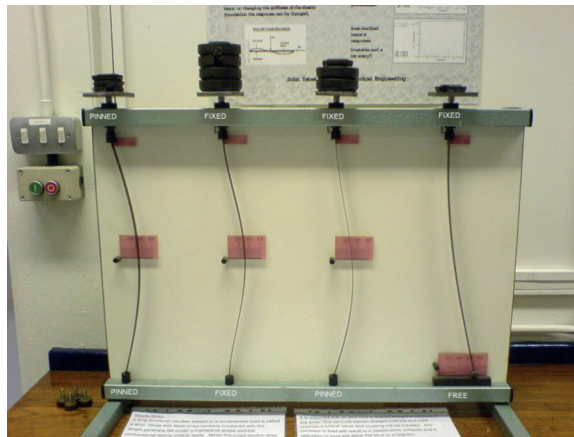
Figure 6.16.: Demonstration model illustrating the different buckling modes. From left: first - both ends pinned; second: fixed both ends; third: one end fixed and another pinned; fourth: top fixed and bottom free; the loads at the indicated state are shown at the top (drawn from the Buckling – Wikipedia2, 2011)

of the equations of equilibrium and compatibility with finite element procedures on the structure discretized into a very large number of elements of fine size have overcome the inaccuracies with these approximations. However, a simple approximate calculation (see Megson, 2007) can provide insight into the relative effects.

6.6.4. Buckling

Suppose, a plate or a rod (or a strut) is subject to compressive load under certain boundary conditions – ends pinned, ends fixed and one free or pinned and one fixed. Increase in compressive load causes a reduction in length (that can be measured). Let us say, this goes on till fracture occurs. This is the first experiment. Now we can increase the length between the ends and carry out the same experiment. Beyond a certain length depending on the cross section, the plate or the rod shows tendency towards a non-axial shape. It may show a slight lateral deflection with a maximum at the center. Any increase in load at this stage can cause substantial lateral deflection and the plate or the rod loses the ability to take the load (see Figure 6.15).

This load is much lower than the compressive fracture load. This load is called
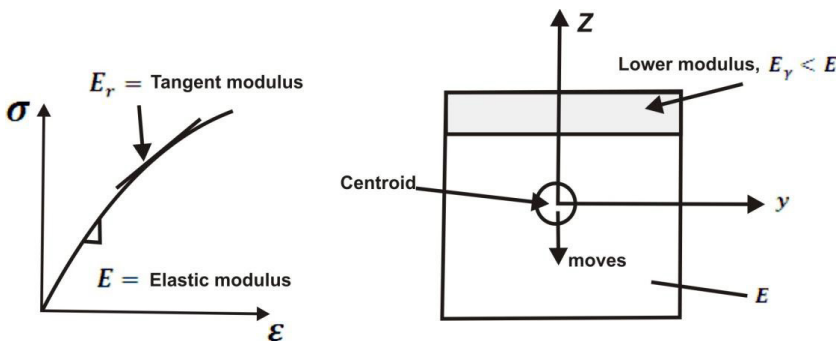
Figure 6.17.: The behavior of the critically stressed cross section during buckling

the buckling load. The fact that at a load just below the critical value, the system can remain laterally un-deflected and at a slight increase in load, the lateral deflections can be large is interpreted to mean that the equilibrium of the system is not stable. This process of transition is such that as load is increased, the strut reduces in length till a point when the lateral deflection increases suddenly and this can happen in either of the lateral directions. Such a point at which the transition can occur is mathematically termed a bifurcation point. The consequences are due to asymmetry – inherent material differences at any cross section and perhaps loading, most usually both (see later).

Figure 6.16 shows how the buckling process occurs with different boundary conditions, but with identical struts. The first one is pinned at both ends, second fixed, third one end pinned one end fixed and the last one fixed at one end and free at the other. What should be noted is that the black colored weights indicate the magnitude of the buckling load. Thus the strut fixed at both the ends has the highest buckling load. And for the case with top fixed and bottom end free, buckling load is the smallest - it buckles very easily. Other cases are in between. Better appreciation of why these happen can be obtained with the analysis of buckling phenomenon described below.

A basic question that arises is: what is that actually happens under conditions of buckling. How is it that the material "knows" it should deform substantially instead of undergoing small deformation as it happens with other kinds of loading? For this purpose, we examine the changes that occur as the load is in-
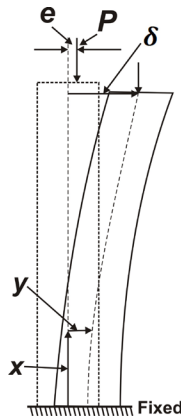
Figure 6.18.: Schematic of the way buckling is mathematically modeledincreased.

creased Figure 6.17 shows the way the cross section behaves during bucking. As the strut with a geometrically symmetric section gets compressed, due to defects and in-homogeneities across the section (natural to any real material), the compressive strains on one side (the shaded part in Figure 6.17, positive z) of the centroid would be higher than the other side (negative z).

As load increases, the strains on the positive Z will cross the yield point. Beyond this point, the slope of the stress-strain curve will be lower (and hence, the local slope representing the elastic modulus will come down) causing larger deformation. This process effectively shifts the centroid to outer zone (towards the opposite side). An accompanying effect is the increase in bending moment. The last set of changes has a bootstrapping effect and occurs rapidly as load approaches the critical value and causes a sudden large lateral deflection. Buckling will generally occur slightly before the theoretical buckling strength of a structure, due to plasticity of the material.

In order to determine the critical buckling load, there are two approaches. (1) Treat a problem with asymmetry in loading (or eccentricity in loading) leading to a solution in which peak deflections, or stresses are dependent on the eccentricity and examine how a small eccentricity, no matter how small, but non-zero can lead to approach to critical conditions or (2) treat a symmetric loading problem as an eigen-value problem (see below). It is insightful to ex-

amine both (see Timoshenko, 1955 or page 328+ of Peery and Azar, 1982). The problem of a vertical column fixed at the bottom and loaded eccentrically at the top is classical, also called the beam column problem (see the section on eccentric compression of a slender symmetrical column in Timoshenko's book on strength of materials) is posed as an equation for the moment balance at any section leading to

$$EI\frac{d^2y}{dx^2} = P(\delta + e - y)$$
(6.13)

Where y is the deflection at any height x, δ, the deflection at the top ($x = l$) and e, the eccentricity (see Figure 6.18). The solution subject to the conditions that y and dy/dx (fixed end) are both 0 at $x = 0$ yields

$$\delta = e[\sec(pl) - 1]$$
(6.14)

where $p = \sqrt{P/EI}$ and l = length of the column. The maximum compressive stress is obtained as a combination of compressive and bending stresses as

$$\sigma_{comp,max} = \frac{P}{A} + Pe\frac{\sec(pl/2)}{Z}$$
(6.15)

with $Z = I/(h/2)$, where Z is called the section modulus and is the ratio of the moment of Inertia to the distance of the neutral axis from the outer most fiber experiencing the compressive stress ($h/2$, in this case).

The above equations are revealing. The deflection at the top is proportional to e; yet, for any non-zero e, however small, $\delta \to \infty$ at $pl \to \pi/2$. This condition that leads to large deflections is called critical condition. It also leads to large stresses. The condition $pl = \pi/2$ (with $p = p_{crit}$) can be expressed in dimensional terms as

$$P_{crit}l^2 = \frac{\pi^2}{4}EI \text{ or } P_{crit} = \frac{\pi^2}{4}E\frac{I}{l^2} \text{ and so } \frac{\sigma_{crit}}{E} = \frac{\pi^2}{4}\frac{I}{Al^2}$$
(6.16)

For various end conditions, it can be generalized as $P_{crit} = \pi^2 kEI/l^2$ where k is a constant which is 1.0 for both ends pinned (hinged, free to rotate), 4 for

both ends fixed, and 0.25 for one end fixed and other end free to move laterally. These results support the features visible in Figure 6.16.

Generally, in most aircraft situations, it is suggested that $k = 2$ would be a good conservative value. The ideas indicated above can be easily extended to plates; the broad conclusions are equally valid there. If, in any column or a plate that is fixed at both ends, say, we create fixity at half the length, then, the buckling load increases four times. This is in fact the strategy that is used to strengthen thin wing sheets. By providing stringers and ribs, the overall dimensions of a panel undergoing buckling are reduced and buckling stiffness of the panels is increased. We will turn attention to the second approach of treating the buckling problem as an eigenvalue problem.

The starting point is a just-buckled condition with the load being $P = P_{crit}$. The moment balance gives very simply

$$EI\frac{d^2y}{dx^2} + P_{crit}y = 0$$

(6.17)

The moment is the product of the critical load, P_{cri} and the moment arm which is the lateral deflection, y. We render the coordinates dimensionless using the length, l to get

$$\frac{d^2y_n}{dx_n^2} + [p_{crit}l]^2y_n = 0$$

(6.18)

where y_n and x_n are y/l and x/l; the equation is solved subject to $y_n = 0$ at $x_n = 0$ and 1.

As can be noted, the equation and boundary conditions are homogeneous and hence the problem qualifies for being of eigenvalue nature (all physical problems governed by total or partial differential equations of the above type with a parameter are called eigenvalue problems). These have non-trivial solution for specific values of the parameter. The non-trivial solution to the above problem is possible for $p_{crit}l = n\pi$. This result is similar to the one obtained above excepting for the difference in the presence of n instead of 0.5. This is related to the boundary condition as well as the mode of buckling. The beam can buckle in various modes with one maximum deflection at the center in the first mode,

two peak deflections and zero deflection at the center in the second mode, etc. A distinction between the two approaches described above is that the former approach allows for the determination of actual deflections and stresses with the knowledge of the eccentricity.

It is interesting to know that a Dutch physicist van-Musschenbroek conducted buckling experiments on wooden columns and published his results in 1729 (see Chapter 4, Timoshenko and Gere, 1961) and after fifteen years, Euler provided the first derivation of the formula for buckling.

The problem of greater relevance to aircraft applications is two-dimensional buckling behavior of thin plates. This can be analyzed by solving the 2-dimensional deformation of a plate under loads with appropriate boundary conditions. This can be carried out mathematically by solving the governing equations of equilibrium (and compatibility). The results come out in the form of summation of double Fourier series and the requirement of satisfaction of boundary conditions leads to eigenvalues and eigenmodes of deflection (like in the case of one-dimension). The critical stress σ_{crit}, can be expressed as

$$\frac{\sigma_{crit}}{E} = \pi^2 \frac{1}{12(1-\nu^2)} \left[\frac{t_h}{b}\right]^2 k(a/b, \text{ boundary conditions})$$

(6.19)

where k is a constant whose dependence is indicated above. Since the deformation is two-dimensional, it is affected by the Poisson's ratio, ν. The square dependence of the critical stress (and so, the load as well) on the thickness of the plate is to be noted.

The value of the constant k decreases with the ratio a/b and asymptotes at a/b ~4. This fact is used in the sizing the panels of wings and fuselage. The stiffeners provide enhance the critical buckling load and are chosen with thickness comparable to the sheet to allow for comparable buckling capabilities between the sheet and the stiffener. This strategy optimizes the structural mass.

6.7. Sandwich Structures

Sandwich structures are constructed exactly like a sandwich that is eaten – two outer sheets with a core bonded to the outer sheets with adhesives. The objective of these structures is to achieve high strength performance. Historically, the idea of using two cooperating faces with a distance between them
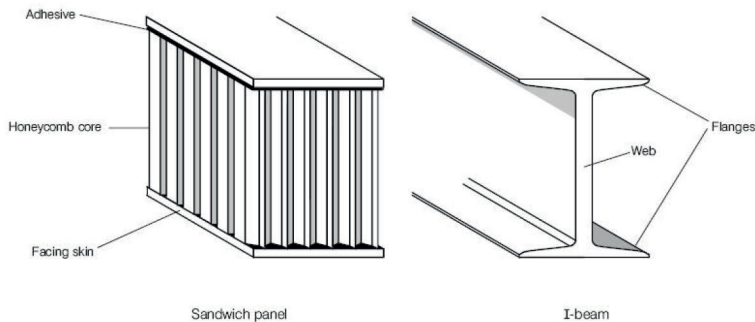
Figure 6.19.: Comparison of a sandwich construction with a I beam

was introduced as early as in 1820. However, more extensive use of sandwich panels was during World War II. In the "Mosquito" aircraft sandwich was used, mainly because of the shortage of other materials in England during the war. The faces were made of veneer and the core of balsa wood. Following this, structural analyses were presented. In the fifties, the development was mainly on honeycomb materials. Honeycomb was mainly used as core material in the aircraft industry and one problem that was encountered was corrosion. However, towards the nineteen sixties, other plastic alternatives for the core were produced.

Quite often, the facing skins of a sandwich panel can be compared to the flanges of an I-beam, as they carry the bending stresses to which the beam is subjected (see Figure 6.19). With one facing skin in compression, the other is in tension. The properties desired of the outer sheets or facing skins are high stiffness, tensile and compressive strength, impact resistance, good surface finish, environmental and wear resistance. The materials used are metals like aluminum and its alloys as well as fiber reinforced plastics (FRPs) and prepregs.

Prepregs, a short name for "PRE-imPREGnated sheet materials" are fibrous materials impregnated with reactive resins. The fiber is pre-impregnated with resin and frozen to prevent the resin from curing prematurely. This material is then thawed and laid into a mold to the proper thickness and cured. The resulting laminate has a precisely controlled resin volume and will be stiffer and
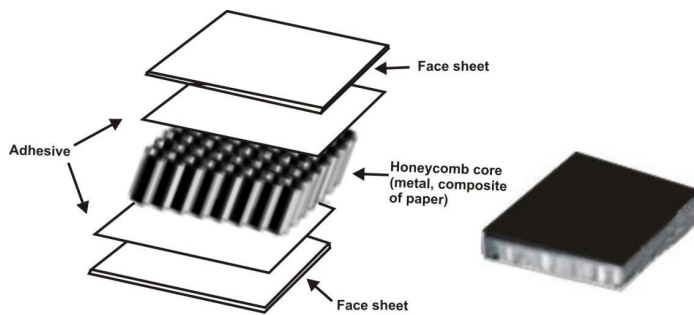
Figure 6.20.: A typical sandwich construction using honeycomb core and an actual product

stronger than a wet laminate of equivalent thickness. The prepreg method has been developed over the past 50 years to create stiffer, stronger laminates with controlled, predictable results.

Similarly, the honeycomb core corresponds to the web of an I-beam. The core helps resist the shear loads and increases the stiffness of the structure by keeping the facing skins apart. As an improvement over the I-beam, it gives wider support to the flanges or facing skins to produce a uniformly stiffened panel. Its role is to enhance the moment of inertia so that bending and bucking stiffness can be enhanced greatly (as will be seen later). The cores can be structured around rigid foams, honeycombs, or thermoplastic materials. Foam cores consist of either metallic, polymeric or ceramic foams filling three-dimensional space, in contrast to the two-dimensional patterns of truss cores. Sandwich panel incorporating a foam core can be made simply by bonding the face plates to the foam using adhesives or by pure metallic bonding. The core-to-skin adhesive rigidly joins the sandwich components and allows them to act as one unit with a high torsional and bending rigidity. The honeycomb structure as the name suggests uses hollow thin-walled sheets shaped into hexagonal or triangular or other geometries. The hexagonal geometry distinguishes itself by needing minimum surface area to cover a given plan form, a feature practiced by honey bees in the construction of honey combs. Structural considerations seem not to specially favor hexagonal over triangular geometries. Currently, most of the sandwich panels used in the commercial and military aircraft are made of metal or FRP facings with honeycomb cores. Boeing 747, 757 and 767

aircraft make extensive use of honeycomb panels in their construction up to 50 % of the structural mass. A typical constructional breakup is shown in Figure 6.20.

The core materials for a sandwich construction must be light and are usually arranged so as to be sufficiently stiff in the direction normal to the plane of the face sheets to always keep them at the correct separation. They must also possess good shear strength, to ensure that the face plates do not slide over each other when a bending loads are to be resisted and they must be stiff enough to keep the face plates nearly flat, to prevent the face plates from buckling locally (wrinkling) under the influence of a compressive stress (that may occur even under bending loads). A specific material extensively used on aircraft is made of Kevlar fibers produced in the form of paper. The honeycomb made of this material is called Nomex honeycomb. The paper is dipped in phenolic resin and cured in specific shapes of the honeycomb. It is particularly used on the interior panels of aircraft. Figure 6.21 presents the relative compressive and shear strengths of typical core materials as a function of their density. Table 6.7 shows the data of strength in compression and shear as well shear modulus as a function of density with possible service temperature for these materials. It can be taken that the properties vary linearly with density as shown in Figure 6.21 drawn from an excellent book on advanced materials by Lukkassen and Meidell (2007). Amongst the composites, it is the polymethacrylimide (PMI) foam that has the largest strength in compression and shear. The service temperatures are all below 200 °C for most foams except carbon-graphite foam. To understand the value of sandwich structures, it is necessary to evaluate EIsandwich since this directly controls the bending and buckling performance (see DIAB handbook, 2011). It is given by

$$[EI]_{sandwich} = [EI]_{core} + 2[EI]_{sheet} = \frac{E_{core}bt_{core}^3}{12} + \frac{E_{sheet}bt_{sheet}^3}{6} + \frac{E_{sheet}bt_{sheet}d^2}{2} \quad (6.20)$$

Where b is the width (arbitrary here), t_{core} is the thickness of the core, t_{sheet} is the thickness of the sheet, d = t_{core} + t_{sheet}. The last equality is obtained by introducing the expressions for moments of inertia; the first two terms on the right hand side are those with reference to their own centroids and the last term refers to that of the sheets with reference to the centroid located within the core.
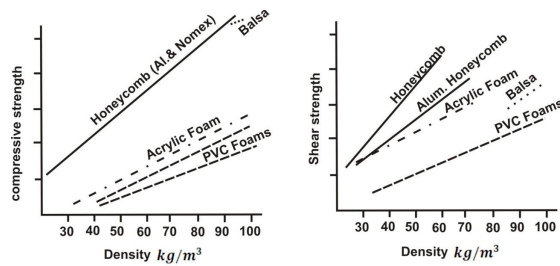
Figure 6.21.: Qualitative variation of compressive and shear strength of typical core mate-rials as a function of the density, drawn from Lukkassen and Meidell (2007), p 134

Table 6.7.: Density, compression strength, shear strength and shear modulus of core materials of composites in Aerospace applications (PU = Polyurethane, PS = Polystyrene, PVC = Polyvinyl chloride PMI = Polymethacrylimide, PEI = Polyetherimide, str. = strength, mod. = modulus)

Core Material	ρm	Comp. str.	Shear str.	Shear mod.	Service temp
	kg/m^3	MPa	MPa	MPa	^0C
Balsa wood	96 - 250	7.0 - 27.0	1.8 - 4.9	108 - 312	165
PU foam	21 - 400	0.2 - 0.4	0.1 - 3.1	1.5 - 104	135
PS foam	30 - 60	0.3 - 0.9	0.2 - 0.6	4.5 - 20	100
PVC foam	30 - 400	0.3 - 6.0	0.3 - 4.5	8.3 - 108	55 - 120
PMI foam	30 - 300	0.8 - 16.0	0.8 - 7.5	19 - 290	140
PEI foam	69 - 110	0.7 - 1.4	0.8 - 1.4	18 - 30	190
Epoxy foam	80 - 320	0.6 - 7.4	0.4 - 5.2		180
Phenolic foam	5 - 160	0.01 - 2.7	0.01 - 1.5		140 - 200
C-Graphite foam	30 - 560	0.2 - 60.0	0.05 - 3.9		2500

If we take $t_{core} \gg t_{sheet}$, a feature that is realistic (note that tsheet is about 0.5 to 2 mm, tcore about 5 to 15 mm and the ratio t_{core}/t_{sheet} is about 10 to 20), we can write an approximate expression for $[EI]sandwich$ as

$$[EI]_{sandwich} = \frac{E_{core}bt^3_{core}}{12} + \frac{E_{sheet}bt_{sheet}d^2}{2} \qquad (6.21)$$

The stiffness ratio of the sandwich to the sheet (one can also call instead of sheet, monocoque structure since the monocoque structure consists only of a sheet) is given by

$$\frac{[EI]_{sandwich}}{[EI]_{sheet}} = \frac{E_{core}}{E_{sheet}} \frac{1}{2} \left[\frac{t_{core}}{t_{sheet}} \right]^3 + 3 \left[\frac{t_{core}}{t_{sheet}} \right]^2 \tag{6.22}$$

In the above expression, the second term on the right hand side can be ignored since square dependence on the thickness ratio is weaker than the cubic dependence. Further, if the material of the sheet and the core are same (like aluminum, say or FRP), we can further simplify the relation as

$$\frac{[EI]_{sandwich}}{[EI]_{sheet}} = \frac{1}{2} \left[\frac{t_{core}}{t_{sheet}} \right]^3 \tag{6.23}$$

For the thickness ratio, t_{core}/t_{sheet} of 10 to 20, the rigidity ratio is 500 to 4000. This is so substantial that the choice of sandwich construction instead of monocoque construction is obvious. Even though the above calculation has not rigorously accounted for the difference in density, the direction of the result is not altered significantly. A simple case of similar materials arranged in three different ways to benefit from the ideas of sandwich shows the relative benefits in terms of stiffness and rigidity is shown in Figure 6.22. The *only crucial issue is the bonding between the core and the sheets.* The part that experiences compressive stress in the sheet will be unable to withstand the stress if the bond is weak. There will be local crum-pling of the sheet in such cases.

6.8. Stress Concentration

Building large structures requires holes in specific parts and joints that require riveting to be done. The stresses around the holes and sharp edges would be much larger than in plane smoothly rounded structural elements. The canonical problem that is analyzed is a plane sheet with circular or elliptic hole under tensile load. This problem of elasticity has been solved with the result that the maximum stress occurs at the edge of the major axis of the elliptic hole given by $\sigma_{max} = \sigma_0(1 + 2a/b)$ where σ_0 is the far field stress and a and b are the half-major and minor axes of the elliptic hole (see for instance, Corona, 2006).
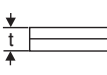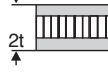
	Solid Material	Core Thickness t	Core Thickness 3t
Stiffness	1.0	7.0	37.0
Flexural Strength	1.0	3.5	9.2
Weight	1.0	1.03	1.06

Figure 6.22.: The benefits of a sandwich construction against a simple beam. Note that stiffness and flexural strength improve maining the weights at about the same value, drawn from Internet5 (2016)

One can define $\rho = b^2/a$ as a measure of the ellipticity of the shape and express the maximum stress expression as

$$\frac{\sigma_{max}}{\sigma_0} = 1 + 2\sqrt{\frac{a}{\rho}}$$

(6.24)

As the ellipse becomes tight, implying $\rho \rightarrow 0$, the ratio of the maximum stress to far-field stress, called the stress concentration factor increases to large values. When the stress goes beyond the ultimate strength or the yield strength of the material, material will begin to fail – cracks will develop at these points or the material begins to yield at these locations. *This mode of failure is different from what is discussed due to fatigue and failure as will seen subsequently.* Even though the behavior beyond the development of crack is the same as what happens here, the mechanism of crack initiation is different in the two cases.

One can reduce the stress concentration by increasing ρ or smoothening the sharp corners and sharp holes. These effects will guarantee reduction of stress concentration, but do not assure remedy for fatigue failure for it lies more deeply in the structure of the material. *In fact a new material property will emerge an account of it.*

6.9. Fatigue and Fracture

Fatigue is a feature associated with cyclic loading. The cyclic loading may have a mean value as well as the maximum much smaller than the ultimate tensile strength of the material with no visible stress concentration area and yet, the structure may suffer fatigue related fracture. The fracture mode does not spare either brittle or ductile materials. Brittle fracture has been known from over two centuries. Many structural failures from this period that reported mysterious cracking of steel were investigated (see Wikipedia3, 2011).

6.9.1. Lessons from failures

The more famous of the tank failures was of the Boston molasses tank containing more than 7.5 million liters of molasses. It failed in 1919 with a number of deaths and injuries to men and horses. The lawsuit that followed carried with it more words than scientifically defended arguments, apparently.

The most famous of the ship disasters that owes to fatigue related cracks is that of Titanic in 1912 with the loss of 1500 of the inmates with the hit from a large Iceberg being seen as the cause for the breakage. However, extraction of the wreckage in 1985 using undersea robots, and analysis of the samples showed that this was not as simple; the lower grade steel with impurities was brittle, particularly in the cold waters of Atlantic (just about 0^0C) and the collision with the iceberg generated cracking through which water entered the interiors. If the steel used was more tough (in the present language, higher fracture toughness, K_{1c}), the cracking could have been more ductile than brittle extensive allowing, perhaps, for more effective rescue operation reducing casualties. There are studies on the subject from many viewpoints (see Wikipedia10, 2016).

There is also a story of a cook on a ship bringing to the attention of the technicians on a ship of a small crack on the steel deck and being assured of its irrelevance to the safety of the ship. Perhaps for the fun of it, the cook kept track of the increasing size of the crack with time with suitable markings. Beyond a point, the crack must have led to the break of the ship and subsequent analysis of this piece of information led to unraveling of the cause of failure as fatigue related.

During WW II, more than a thousand ships carried brittle fractures; the reasons were traced to sharp edges and corners, weld joints and the poor quality of steel. Some design modifications were made and crack arresters were introduced. Despite all these, some ships broke completely into two parts in the subsequent period. These have generally been brittle fractures. The feature related to the brittle fracture is that it propagates slowly until some time and grows fast with the final failure moving at a fraction of sonic speeds which in metals reaches about 2 km/sec.

Most aircraft design till the early nineteen fifties was carried out using static features of the loading partly because the materials used were ductile. The failure of the Comet aircraft in the mid fifties (in fact two of them in flight) well documented in aeronautical literature was traced to fatigue problem after an extensive study. This provided an important focus for a fundamental study of fatigue and fracture by scientists and structural engineers. Apparently, a novel named "No Highway" (by Nevil Shute) sought a similar theme in 1948 and this was made into a movie with the aircraft named "Reindeer". Only a few years later, as though the predictions were to be proved, the Comet failure took place. Both these became a subject of intense discussion among specialists at that time. The central issue was that while the fuselage was designed for a pressure differential of 1.4 atm, the failure took place with the actual pressure differential not exceeding 0. 6 atm (less than half the design value). The subject was investigated in depth and it was uncovered that the cyclic load even though small led to the formation of cracks that grew significantly leading to a failure particularly near the window openings.

Subsequent aircraft designs included "tear straps" to stop rapidly growing cracks. Typical design of the tear strap is shown in Figure 6.23. Tear strap is simply a strip of material attached circumferentially to the fuselage skin. It reduces the circum ferential stress for an axial crack length less than the axial crack length without the tear strap. They can be of the parent material, namely aluminum alloy, steel or titanium. That it was perhaps not very effective was shown up by B737 transport aircraft operated by Aloha airlines. It was thought that this is because of the cold bonding technique deployed. The roof of the first class cabin was torn away as shown in the photograph (Figure 6.24). This aircraft was analyzed later to have had stress corrosion problem at a number of rivet joints that allowed multiple small cracks to join up into a catastrophic
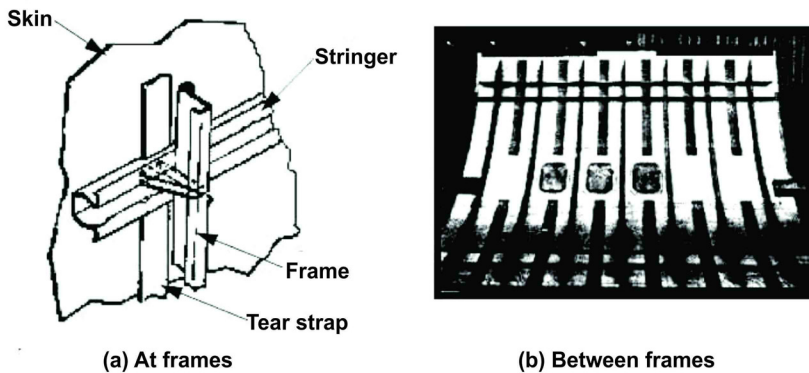
Figure 6.23.: Schematic of tear strap at a sheet-stringer interface area and between stringers, drawn from open internet sources

Figure 6.24.: The photograph of the crashed Boeing 737 air plane flown by Aloha airlines

damage (Wikipedia4, 2011). Subsequent to this, hot bonding technique was adopted. The failures of F-111 aircraft were attributed to brittle fractures of members with preexisting flaws. From this point onwards, it has been recognized that strength design is necessary but by no means sufficient. Aspects related to fatigue need to be accounted in the design. This subject is far more serious for aircraft and helicopters, particularly those meant for civil use as

the number of take-offs and landings is the largest (leading to a large number of cycles of loading) than for missiles or launch vehicles or satellites that may experience just one loading cycle.

6.9.2. Nature of fatigue failure

Initiation of cracks is identified as due to local plasticity, often caused by stress concentration, local surface roughness, wear damage at contacts, particularly at joints. Welded joints are well known sources of residual stresses and lower yield stress, *a primary reason for trying to avoid welded joints in aerospace structures.*

The actual process of failure usually begins with micro-slip in shear between adjacent planes of atoms in the crystal structure of a single grain, and usually oriented 45^0 to the normal (perpendicular) load culminating with the propagation of a macro-crack many times larger than the grain size, and oriented normal to the load (see Figure 6.25). The difference between pure metals and alloys is that there are grain boundaries that get formed during the cooling process. The grain size and orientation affect the mechanical properties directly. Typical size of the grains is about 10 to 100 μm. Finer grain sizes provide better strength as the grain boundaries impede the movement of dislocations. New nano-materials being contemplated in recent times are produced with grain sizes between 0.01 and 0.1 μm with promise of greatly enhanced mechanical properties.

6.9.3. A simple analysis of fracture

Fracture occurs because the energy made available by stressing a part in opening a crack of size, say, a, is more than the energy of the surfaces created. The energy for breaking is estimated as the work done for this purpose = (1/2) (Load x deflection) = (1/2) [(stress x area) x (strain x length)] ~ (1/2) [($\sigma a t_h$) × (εa)], where t_h is the thickness of the sheet. The strain, ε can be taken as stress/elastic modulus, a feature that is very accurate for brittle materials (up to fracture). Thus by replacing ε by σ/E, we get the work demanded to create the crack as (1/2) $\sigma^2 a^2 t h/E$. This must equal the energy obtained in creating the new surface as the product of the surface energy per unit area, G_s, and the area, $2a t_h$. This gives the energy as $2G_s a t_h$. (note that G_s is the same as surface tension, N/m or J/m^2). Figure 6.26 shows the features just described.
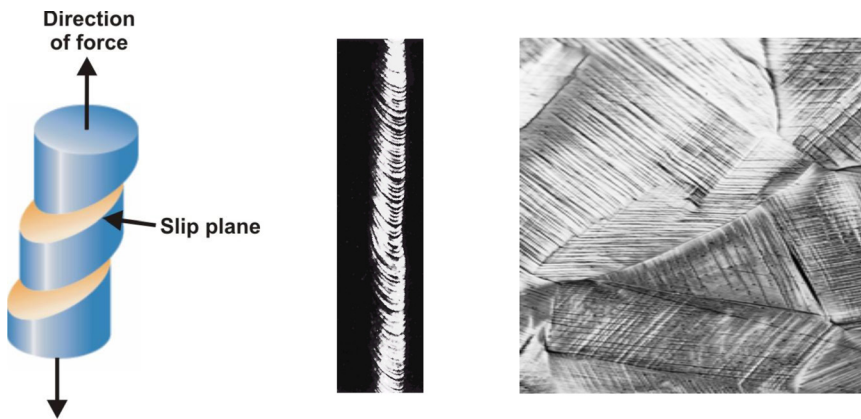
Figure 6.25.: The schematic representation of failure (left) and an actual one (middle) and the structure of the grain boundaries in a metal – scale of 10 to 100 *μm* (right)
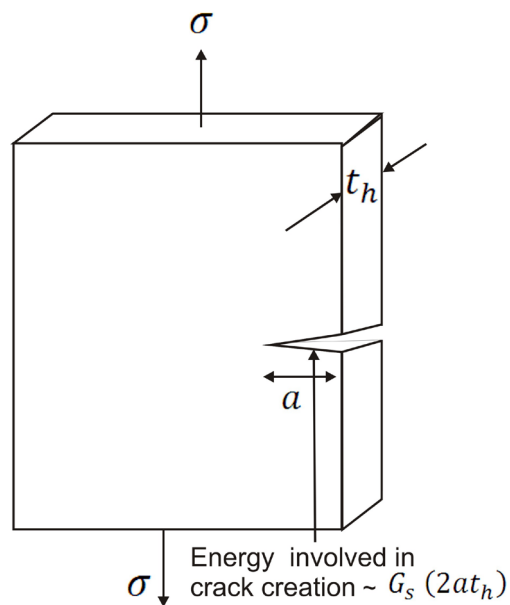
Figure 6.26.: The schematic showing the opening of the crack and the surface energy required to cause it

By requiring the two to be of the same order of magnitude we get

$$\sigma^2_{crit}a^2t_h/E \sim 2G_s at_h \tag{6.25}$$

In actual materials the amount of energy required (per unit area) to cause the break or cleavage is well described by G_s (in honour of Griffith brought out earlier in section 3.4, Chapter 3). In addition to the energy needed to create the two new surfaces, other molecular arrangements will get disturbed; perhaps, other bonds are broken or more dislocations get created. The energy required for this is called the work of fracture, W_s. It is about 6 $G_s \sim$ 6 J/m² for glass in which the disturbances are small, about 10 J/m² for many metals. In fact cold working or other thermal treatments can alter this value significantly. These imply that the crack length allowed in glass is very small, but in metals it can be very large (sometimes, even up to a meter). It is this factor that makes selection of metals far more appropriate than glasses or other ceramics even if the strength properties alone are comparable. We now plot the left and right hand side terms of the above relationship with respect to a as in Figure 6.27.

The first part, namely the energy required to create a crack varies quadratically with a and the surface energy, linearly with a. The point of tangency gives an estimate of the critical stress, σ_{crit} as $\sigma_{crit} \sim \sqrt{G_sE/a}$ or more appropriately $\sqrt{W_sE/a}$ If perchance, the crack grows to $a + \delta a$, then the energy required to create the new surface is lower than the energy available to create the crack and the crack grows further. This is a runaway condition. Equally well, if the crack decreases in size, the surface energy available is larger and the crack closes up. The expression for critical stress is composed of two terms - $\sqrt{G_sE}$ and $\sqrt{1/a}$. The former term is a property of the substance. It is called stress intensity factor, K_I. Its units are *[M P a m^0.5]*. Its value for several materials was presented in Table 6.4. Arguments of stability are made by requiring that the net energy,

$$U = \sigma^2_{crit}a^2t_h/E - 2G_s at_h \tag{6.26}$$

should be minimum with respect to the crack size. Thus $dU/da = 0$ gives σ_{crit} = $\sqrt{[2G_sE]/a}$ a result which is the same as stated earlier. This expression is written in a more usable form as $K_{1c} = C_{fr}\sigma_{crit}\sqrt{a}$ with the constant C_{fr} dependent on the geometry of the crack. It is important to recognize that the above
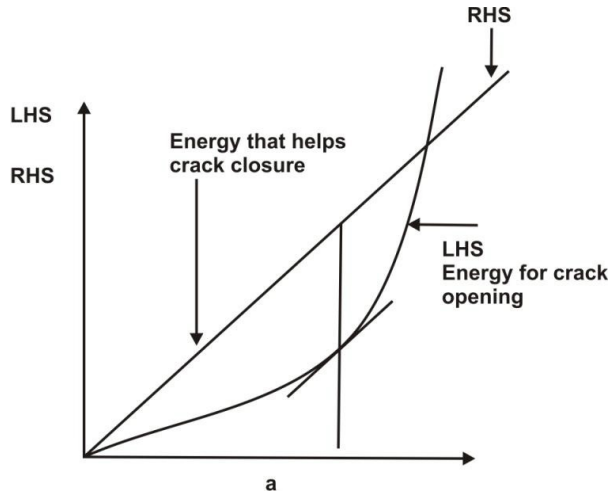
Figure 6.27.: The variation of the energy for closing and opening cracks with the crack length

analysis was first performed by Griffith in 1920 (Wikipedia2, 2011) based on scaling information provided by Inglis as early as in 1913.

There are three modes to describe different crack surface displacement schemes. Mode I is opening or tensile mode where the crack surfaces move directly apart. Mode II is sliding or in-plane shear mode where the crack surfaces slide over one another in a direction perpendicular to the leading edge of the crack. Mode III is tearing and anti-plane shear mode where the crack surfaces move relative to one another and parallel to the leading edge of the crack. Mode I is the most common load type encountered in engineering design and will be discussed now.

The tensile stresses in x and y or equivalently, in polar coordinates, r and θ directions with r measured from the crack tip and θ in the clock wise direction, and the shear stress, σ_{xy} can be solved in terms of K_1 and position mode 1 as:

$$\sigma_y = K_1/\sqrt{(2\pi r)}f_1(\theta) \tag{6.27}$$

$$\sigma_x = K_1/\sqrt{(2\pi r)}f_2(\theta) \tag{6.28}$$

$$\sigma_{xy} = K_1/\sqrt{(2\pi r)}f_3(\theta) \tag{6.29}$$

where *f1(θ) = cos(θ/2)[1 + sin(θ/2)sin(3θ/2)]* etc
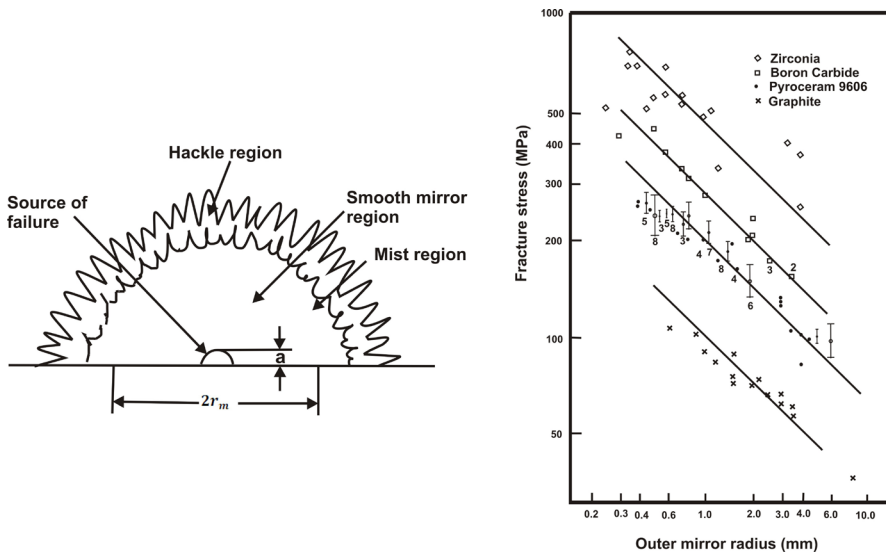
Figure 6.28.: Experimental data supporting the inverse root radius dependence of stress near a crack tip (drawn from Hertzberg, 1989)

It can be seen that all the stresses behave as $1/\sqrt{r}$. The fracture surfaces have been photographed and show a mirror like surface followed by a mist like region. The radius of the mirror like region has been correlated with the fracture stress and it behaves like $\sigma_{frac} \sim 1/\sqrt{r_{mirror}}$ (see Figure 6.28, right). This behavior is also consistent with the simple analysis due to Griffith described earlier. Fatigue tests are conducted by loading samples in cyclic loads with a mean stress level and amplitude at a certain frequency. The results are controlled by several parameters: mean stress, $\sigma_m = (\sigma_{max} + \sigma_{min})/2$, stress range $\Delta\sigma = \sigma_{max} - \sigma_{min}$, stress amplitude $\sigma_a = (\sigma_{max} - \sigma_{min})/2$, Load ratio $= \sigma_{min}/\sigma_{max}$, frequency, f. These are displayed in an $S - N$ diagram, that relates stress, σ_m (or for that matter, strain, s) and number of cycles up to failure, N. All engineering $S - N$ curves use a logarithmic axis for cycles. A typical plot is shown in Figure 6.29 (left) for steel and aluminum alloy. Some materials have the fatigue limit typically at about half the ultimate strength. Others like Al-alloys do not have a limit below which fatigue life is infinite. It is also seen that larger mean stress lowers the fatigue life. In these cases, the stress at 107 cycles is taken as the indication of the life of the component.

There are two important terminologies associated with fatigue – High Cycle Fatigue (HCF) implying local cyclic stresses that are small producing predom
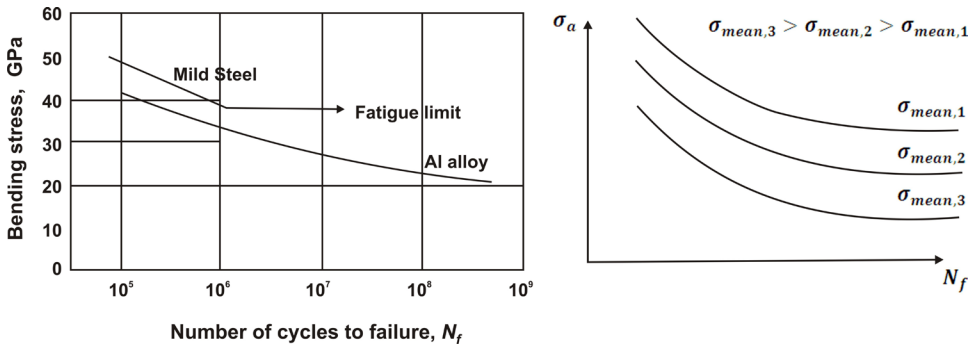
Figure 6.29.: The effect of mean stress level on fatigue life. In the left part, notice there is a lower limit for steel below which fatigue life in infinitely large, but no such limit for Al-alloy. The right part one shows the $S - N$ plot of fatigue data. Larger mean stress levels reduce the fatigue life, drawn from Rollett, 2002

inant elastic straining and the resulting fatigue life is more than 10^4 cycles and Low Cycle fatigue (LCF) that has high local cyclic stresses with significant cyclic plastic straining with fatigue life less than 10^4 cycles. While engine components experience LCF, wings, fuselage and other components experience high cycle fatigue. Figure 6.29 (above) shows the effect of mean stress level on the fatigue behavior. Larger mean stress level lowers the fatigue life.

The stress range correlates with the number of cycles as $\Delta\sigma = C_0 N_f^{-b}$ with b 0.05 to 0.1 (Suresh, 1998). This is called the Basquin law as shown in Figure 6.30. In this description, the stress range is taken with the mean stress as 0. When the mean stress is not zero, one uses one of the empirical relationships due to Sodeberg, Goodman, or Gerber (see Suresh, 1998). There are also questions about ways of dealing with different amplitudes imposed for different durations as will happen in real life. Again there are empirical approaches for this (one for instance is called the Palmgren-Miner damage summation rule).

There are questions of how to deal with cases of significant plastic deformation important to high cycle fatigue situations. In this case one uses strain relations rather than stress relations. In the elastic region, the stress approach and the strain approach are equivalent. Only in the plastic region, the novelty of the use of strain is clear. To exemplify this, the law that is a combination of Bas-
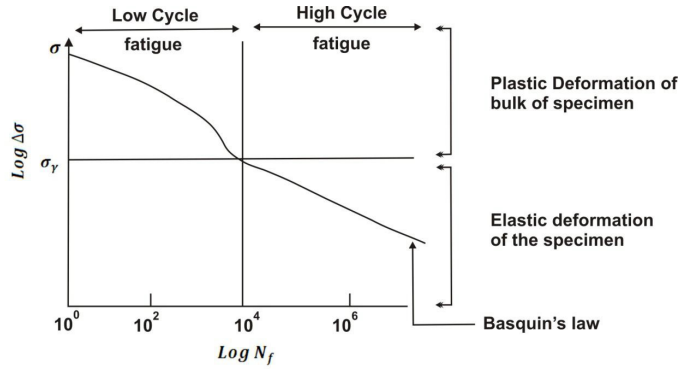
Figure 6.30.: The plot of stress range with number of cycles to failure in a fatigue test adapted from Ashby and Jones (1980)

quin law for high cycle fatigue and what is known as Coffin-Manson law for low cycle fatigue becomes $\Delta\varepsilon = (C_0/E)N{-}^b{}_f + C_1 N_f^{-c}$, with the constants determined from suitable experiments is used for life estimation.

The more important aspect that needs to be addressed is the growth rate of the crack with the number of cycles. Using the data of ΔK and the crack length, a, one gets ΔK from $\Delta K = a\Delta\sigma$. The rate of growth of the crack per cycle is plotted against the stress intensity factor range as in Figure 6.31 based on the work of Paris and colleagues (see Paris et al., 1999). The first part of the curve the crack growth rate is immeasurably small. It is the second part of the curve where the growth rate is significant and the curve is represented by $da/dN = C_k(\Delta K)^m$. The constants, C_k and m are determined from experiments. The value of m is about 2 to 4 for metals and 4 to 100 for ceramics and polymers). The large value of m for ceramics shows that once the crack achieves a minimum size, under stress it will dramatically increase for every cycle of stress. The representation above is called the Paris law. Further manipulation of this expression leads to a relationship for the number of cycles to failure, N_f with the stress range, $\Delta\sigma$ and initial and final crack lengths, a_0, and a_f as

$$N_f \sim \frac{ln[a_f/a_0]}{C_k\Delta\sigma^2} \quad \text{for} \ \ m = 2$$

(6.30)

and more complex algebraic expression for $m > 2$. The initial crack length is measured by experimental techniques and if it not measurable, it is taken as the resolution of the measuring instrument. The final crack length, a_f is the crack length allowed for design is determined from the experimentally known value of K_{1c} and $K_{1c} = \sigma_{max}\sqrt{\pi a_f}$. It is taken that the structure or the structural component is un-serviceable when the crack reaches this size (a_f). These are illustrated in Figure 6.32. As can be seen, the structural component that is subject to a cyclic stress carries a continually decreasing residual strength. The cracks keep growing in size with time that is counted in terms of flight hours. When the crack reaches a critical size (a_f), the specific structural component fails. The implications of these ideas are very significant. One can address components of a whole structure (an aircraft, for instance) individually and assess their life even if there is crack. One can think whether the remedial measure could be to: (a) allow it to continue without intervention because it is in a non-critical area, (b) make suitable repairs locally and allow the total system to function in a natural course, or (c) remove the part and replace it by another part or (d) reject the whole system as an appropriate last measure. These concepts gave rise to new ideas of damage tolerant design as against the earlier ideas of safe life that implied that even if a small component of a system failed, it was necessary to reject the entire system. The ideas of damage tolerant design are strongly coupled to the ability to monitor the structure during its operating life. New sensors that are tiny and yet reliable using quartz and nano-systems are being developed and deployed on systems for evaluation.

This important development is due to the concepts that were evolved by Paris and colleagues. An interesting historical aside is the difficulty in having this accepted by "traditionalists". In the words of Paris, "Though that method is widely accepted today, in the late 1960s at Boeing it was rejected by an outside review panel for federal supersonic transport exploratory studies as "it simply won't work". Moreover, the federal agency funding the most extensive fatigue studies on multiple occasions stated "no interest" in such work, although since 1970 they have funded more work than any other source. It was a study of rejection by authority with preconceived notions and blind self-interest, with a total reversal after more than 10 years. This was an interesting personal and historical lesson on 'radical' discoveries" (see for an interesting narrative of the historical developments, Paris et al, 1999).
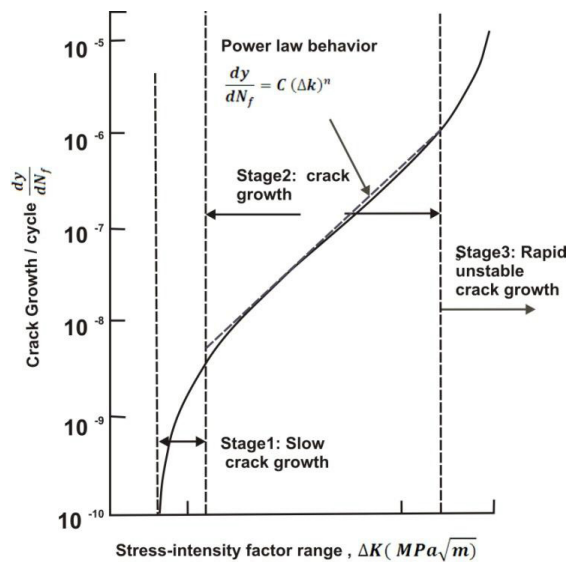
Figure 6.31.: The Paris plots of crack growth rate per cycle with stress intensity factor, drawn from Paris et al, 1999
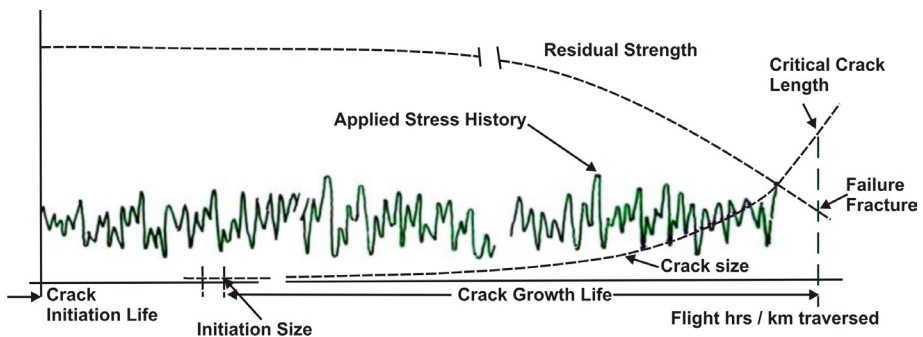
Figure 6.32.: The variation of residual strength of structure when an initial crack is growing under an applied cyclic stress in a flight situation

It is important to address how to deal with the fatigue problems of materials. For this purpose, the point to recognize is that it is principally a tensile stress related problem – tearing metal apart. Hence anything done to ensure reduction in tensile stresses would help. A well known procedure that is adopted is
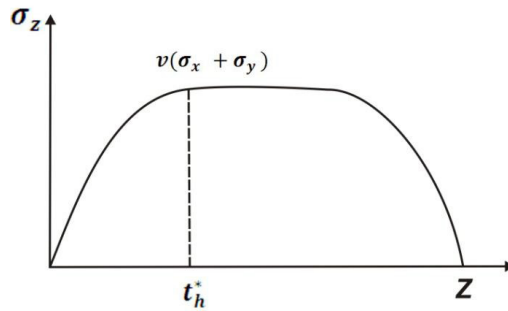
Figure 6.33.: The variation of lateral stress along the thickness, t_h

called "shot peening". Shot peening is essentially a cold working process in which the surface is bombarded by small spherical particles. The hitting by a particle is somewhat like the hit from a hammer causing a small dimple. The net effect of multiple shots is that the material on the surface undergoes compression. One can interpret this operation as leading to creating residual compressive stress, typically about half the yield strength of the material in a zone of 100 to 200 μm thick. This technique is used in the manufacture of many metal components for ground based applications as well as aircraft including engines.

Newman, Jr (1998), O'Down (2003) and Wei (2010) provide a historical perspective and the fundamentals related to fatigue and fracture. One can also benefit from Anand and Park's (2014) narrative on defect-free fatigue.

6.9.4. Plane stress and plane strain

The stress or strain state is always in three dimensions. But in most cases, they can be simplified to either plane strain or stress by ignoring either the out of plane strain or plane stress. Plane stress condition refers to the approximation in which the stress distribution is planar with zero stress across the thickness, as in the case of a thin sheet in pressure vessels or rocket motor cases. Plane strain refers to the approximation in which the strain along one direction is zero compared to those in two other orthogonal directions. This strain is ignored as in the case of long cylinders in solid propellant grains in rockets. With specific reference to fracture behavior, we need to consider the stress distribution ahead of the crack tip. The parameters that matter are the

radius plastic zone ahead of the crack in relationship to the plate thickness. To understand fracture toughness derived for plane stress and plane strain conditions we need to examine the stress distribution ahead of the crack tip.

We first note that the stress in the direction z is zero at the sides of the plate since there is no force applied there. The strain in this direction, ε_z is due to Poisson contraction. In a thin plate, the stress does not have opportunity to rise to larger values within the material. Hence it is taken as zero and this is the plane stress case. When the plate is thicker, the material in the central zone cannot contract laterally due to constraint of material in the lateral direction. Hence the strain is taken as zero. This will build up stresses that attain a uniform value in the middle as shown in Figure 6.33.

The principal stresses in the material yield

$$2\sigma_p^2 = (\sigma_x - \sigma_y)^2 + (\sigma_x - \sigma_z)(\sigma_y - \sigma_z) \qquad (6.31)$$

The stresses σ_x and σ_y are obtained from expressions described earlier (eqn. 6.29) and $\sigma_z = 0$ for plane stress and $\nu(\sigma_x + \sigma_y)$ for plane strain. If we now introduce these into the above equations, it will show that the principal stresses are higher for plane stress than plane strain [due to terms $(\sigma_x - \sigma_z)$ and $(\sigma_y - \sigma_z)$]. The actual distribution of stresses is shown in Figure 6.34 (right top).

Fracture toughness decreases from plane stress value to plane strain. Since the fracture toughness is independent of thickness beyond a certain value as shown in Figure 6.34 (top right), the value obtained under plane strain conditions (called K_{1c}) is considered as material property. In practice, for small thicknesses, one can use this value as a conservative estimate on the effect of thickness. But for part-through cracks such as surface defects and cracks in corners, contraction is nearly always constrained and thickness does not have any influence. In such cases, K_{1c} value is the correct value to be used irrespective of the thickness. The fracture toughness of most materials vs. *UTS* is set out in Figure 6.35 (bottom right).

6.10. The Material Choice – Structural Design and Material Property Combined

The choice of the material has been brought up earlier several times and it has been indicated that it should be light – light enough and carry the load as well.
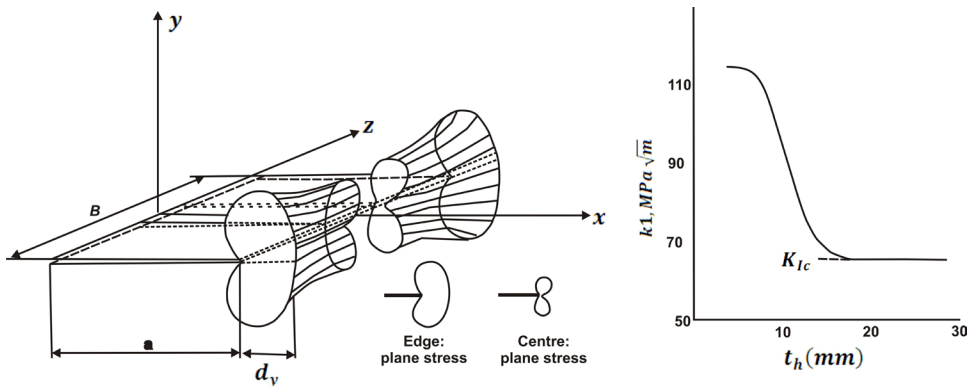
Figure 6.34.: Stress distribution in a plate (thickness B) near the crack tip. At the edges, the state of the stress is close to being plane stress. In the center it is close to plane strain. The right side of the figure shows the dependence of fracture toughness with thickness. Only for large thicknesses does fracture toughness become a material property
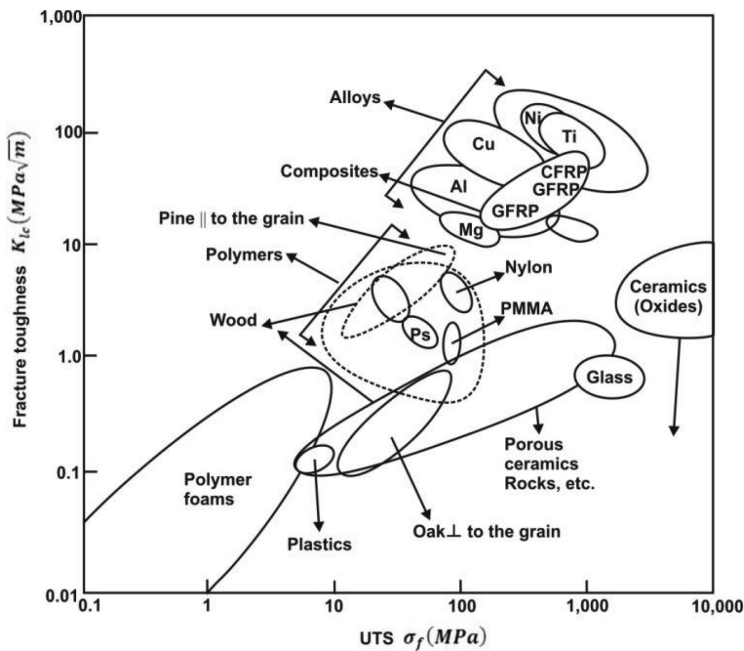
Figure 6.35.: The fracture toughness vs, *UTS* of most materials, PS = Polystyrene, PMMA = Polymethyl methacrylate, adapted from Ashby and Jones (1980)

Table 6.8.: Derived strength properties (* $MP\ a/(t/m^3)$); GFRP: Glass reinforced polymer; CRFP: Carbon RFP; the two values for GFRP and CRFP refer to those along the fiber and across)

Material	ρ_m t/m^3	E GPa	UTS MPa	E/ρ_m *	UTS/ρ_m *
AM350	7.75	200	1400	25.8	180.6
4340	7.80	200	1764	25.6	196.1
AISI 403 SS	7.80	200	821	25.6	105.2
Mar.steel, 18% Ni	7.80	210	1783	26.9	228.6
Ti-6Al-4V	4.42	114	897	25.8	203.0
Ti alloy*	4.45	125	890	28.1	200.0
2219-T851 Al	2.70	70	454	25.9	168.1
2024 Al	2.70	72	480	26.6	177.7
6061-T651 Al	2.70	68	352	25.1	130.3
7079-T651 Al	2.70	70	569	25.9	210.7
7178 Al	2.75	77	670	28.0	243.6
7075 Al	2.70	75	830	26.2	307.4
GFRP	2.10	45/12	1020/40	21.4/5.7	486/19
CFRP	1.60	145/10	1240/41	90.6/6.2	775/25
Wood (spruce)	0.45	14	110	31.1	244.4

It is somewhat simplistically thought that the parameter that should be maximized is not just the strength, but strength-to-density ratio. This is not quite true. In fact, if this alone were true, the choice of the material does not come out quite sharply. We will examine these issues presently. Table 6.8 shows many parameters of importance. It can be noticed from Table 6.8 that if we take $UTS/\rho m$ the values for most aluminum alloys are comparable to or lower than of stainless steel making the argument for aluminum alloys tenuous to justify. The choice is even more difficult if we take $E/\rho m$ as the parameter.

It is important that we examine the mass of the structure to withstand various classes of loads – bending, torsion, buckling and as a pressure vessel. Let us take the case of a beam of length l fixed at one end with cross section $b \times t_h$ subject to a bending load P. The mass of the beam is given by $m = \rho_m lbt_h$.

With the loading along the thickness, the peak stress is $\sigma max = Pl(t_h/2)/(bt^3_h/12)$. The thickness is therefore given by

$$t_h^2 = 6P\frac{(l/b)}{\sigma_{max}}$$

(6.32)

We can set the value of σ_{max} as UTS/FS where FS is the factor of safety (in some cases σ_{max} is set as a fraction of the yield strength). We can now obtain the mass of the structure by introducing the expression for t_h. This is

$$m = \rho_m lb\sqrt{[6P(l/b)/\sigma_{max}]} = lb\sqrt{[6P(l/b)FS]} \times \rho_m/\sqrt{UTS} \sim \rho_m/\sqrt{UTS}$$ (6.33)

Thus for a given size of the panel (or sheet) under bending, maximizing $\sqrt{UTS}/\rho_m$ minimizes the mass of the structure in this case. If the structure consists of a beam cross section $t_h \times t_h$, maximizing $(UTS)^{2/3}/\rho_m$ minimizes the structural mass.

We can now consider a sheet to withstand buckling load. The expression for the mass is $m = \rho_m lbt_h$. We use the expression for the stress in the buckling mode to be (see section 6.6.4)

$$\sigma_{crit}/E = \pi^2 k(l/b, \text{boundary conditions})\frac{1}{12(1-\nu^2)}\left[\frac{t_h}{b}\right]^2$$

(6.34)

We can identify the σ_{crit} with UTS/FS and extract the thickness for withstanding buckling as $t_h \sim \sqrt{[E/(UTS/FS)]}$ The mass of the structure will now become

$$m \sim \rho_m lb\sqrt{[E/(UTS/FS)]}$$

(6.35)

Hence maximizing the parameter $\sqrt{[UTS/E]}/\rho_m$ minimizes the mass of the structure under buckling. The parameter UTS/E varies between 4 to 11 for most metals, but varies widely for composites.

We now consider the design of a pressure vessel. The mass of the vessel is given by

$$m = \rho_m \pi(dl + d^2/4)t_h$$

(6.36)

The diameter d and the length l are fixed by how much of gas/liquid would be needed to be stored. The thickness t_h is now to be estimated by some criterion. The criterion of design can be yield before crack, the reason being that a benign

failure mode allows yield before fracture. The stress caused by fracture (see the section on fatigue and fracture presented earlier) is given by $\sigma_{max} = K_c / \sqrt{(\pi a_c)}$ where a_c is the crack size and K_c is the fracture toughness. The stress caused by the application of pressure, p_c inside the vessel is $\sigma = pc^d/2t_h$. The stress can be made equal to the yield stress when the crack size is just about the wall thickness. This means $\sigma_{yield} = p_c d / 2t_h = K_c / \sqrt{(\pi t_h)}$ This gives the wall thickness as $t_h = \pi[p_c d / 2K_c]^2$ which when introduced into the expression for the mass of the vessel leads to

$$m = \rho_m \pi^2 (dl + d^2/4)[p_c d / 2K_c]^2$$

(6.37)

Minimizing the mass of the vessel demands that we maximize K_c^2/ρ_m. The above discussion clearly points to the fact that different conditions require different criteria for minimizing the mass of the structural component. We can calculate the parameters (1) $\sqrt{UTS}/\rho_m$, (2)$(UTS)^{2/3}/\rho_m$, (3) $\sqrt{[UTS/E]}/\rho_m$ and K_c^2/ρ_m to check on which materials are more suitable for withstanding bending loads as well as pressure in a vessel. These are presented in Table 6.9. The values of the parameters vary even across each of the principal materials (Steel, Titanium and Aluminum alloys), but the distinction between these classes of materials is very clear. For instance with $\sqrt{UTS}/\rho_m$ the maximum for steels is 5.4 and for Ti-alloys 6.8 and for Al-alloys is 8.8 indicating clearly that aluminum alloys score over others significantly. The situation is true for buckling as well. However, when it comes to pressure vessels where fracture behavior is the strategy for design, Ti-alloys score over Al-alloys. Some stainless steels perform just as well. But strength properties at high temperature of Ti alloys are superior to stainless steel even though both material and fabrication costs are higher. Military aircraft like F15 and F16 benefit from its use as already indicated. The only problem appears to be degradation of properties in salt environment. This calls for special handling in sea borne aircraft carriers.

As explained in section 6.4.2, composite materials provide excellent fatigue endurance concerning number of load cycles as also residual fatigue strength as some of them retain more than 60 % of their residual static strength, which is far higher than with metals. This makes them excellent candidates for many components on an aircraft, much more for subsonic aircraft than for aircraft flying in high supersonic range.

Table 6.9.: Derived strength properties of importance in structural design (*MP*a m$^{0.5}$); all derived parameters use the units shown.

Material	ρ_m t/m^3	E GPa	$\sqrt{UTS}$ MPa	UTS $/\rho_m$	$UTS^{2/3}$ $/\rho_m$	$\sqrt{UTS}$ $/\sqrt{E}$	K_{1c} *	K^2_{1c} $/\rho_m$
AM350	7.75	200	1400	4.8	16.1	0.083	175	3951
4340	7.80	200	1764	5.3	18.7	0.094	201	5179
AISI 403 SS	7.80	200	821	3.7	11.2	0.064	77	760
Mar.steel,18%Ni	7.80	210	1783	5.4	18.8	0.092	174	3881
Ti-6Al-4V	4.42	114	897	6.8	21.0	0.088	115	2992
Ti alloy*	4.45	125	890	6.7	20.7	0.086	139	4341
2219-T851 Al	2.70	70	454	7.9	21.8	0.080	32	379
2024 Al	2.70	72	480	8.1	22.6	0.082	26	250
6061-T651 Al	2.70	68	352	6.9	18.4	0.072	29	311
7079-T651 Al	2.70	70	569	8.8	25.4	0.090	26	250
7178 Al	2.75	77	670	9.4	27.8	0.093	33	410
7075 Al	2.70	75	830	10.7	32.7	0.105	35	453
GFRP	2.10	45/12	1020/40	15.2	48.2	~ 0.05		
CFRP	1.60	145/10	1240/41	22.0	72.1	~0.08		
Wood (spruce)	14	110	23.3	51.0	51.0	0.089		

6.11. Environmental Factors

6.11.1. Temperature

Most of the discussion presented till now refers to ambient temperature (25 to 30^{0}C). Aircraft, helicopters, experience much wider ambient conditions near take-off in traditional airports in summer and winter apart from those near deserts as well as on sea and even harsher conditions in flight. Supersonic aircraft experience higher temperatures on most outer parts due to aerodynamic heating. Missiles experience harsh conditions in field deployment. Launch vehicles also experience varying ambient conditions that may be less harsh, but decidedly quite wide needing attention.

Materials used on gas turbine engines experience varying temperatures: compressors – 200^{0}C, combustors~ 1000^{0}C, Turbines ~1300^{0}C, Nozzles – up to 1200^{0}C with reheat systems, otherwise, 700^{0}C (the actual gas temperatures are usually higher; but cooling systems limit these temperatures). In most instances, there are cyclic and some random variations.

Temperature changes cause expansion or contraction (with increase or decrease of temperature). The fractional expansion is given by $\alpha \Delta T$, where α is the coefficient of thermal expansion and ΔT is the change in temperature. Typical values of α are 7 ×10⁻⁶/*K* for aluminum, 3.3 ×10⁻⁶/*K* for steel, 2.8 ×10⁻⁶/*K* for titanium, ~ 0.1 ×10⁻⁶/*K* along the fibers of graphite-epoxy composite and 9 ×10⁻⁶/*K* perpendicular to the fibers. This expansion or contraction will cause tensile or compressive stresses whose magnitude in the linear range is $E\alpha\Delta T$ This magnitude must be accounted for in the stress analysis. A general way of expressing this in the stress analysis is by the following elasticity equation (Timoshenko, 1961).

$$\nabla^4 \phi = -E\alpha \nabla^2 \Delta T - (1 - \nu) \nabla^2 V \tag{6.38}$$

Where ϕ is the Airy stress function, ν is the Poisson's ratio and V is the potential function for body forces.

The temperature distribution inside the structure required in the above equation is determined by solving the conduction equation with appropriate temperature dependent thermal conductivity and of course suitable boundary conditions.

Temperature controls the mechanical properties namely, *E, Y S, UTS, K_{1c}*; all these decrease with increase in temperature. Lowering the temperature makes the material stronger but brittle. Increasing the temperature increases the ductility of the material, but decreases the strength of the material and most properties take an adverse hit. This is the reason why some materials which show less degradation with temperature are specially developed using the science of materials.

6.11.2. Corrosion

Corrosion resistance is a need that arises in a far more severe way in naval applications as well as in tropical climate. Military aircraft on aircraft carriers experience the salt laden moisture and it has been known that corrosion related fatigue and fracture are serious problems. This fatigue behavior in the presence of salt and moisture is due to electrochemical action. Those materials that provide cathodic protection (that is, protection against the electrochemical corrosion) help reduce pitting. Classical treatment procedures like electroplating, cladding, and nitriding are helpful in improve the corrosion resistance
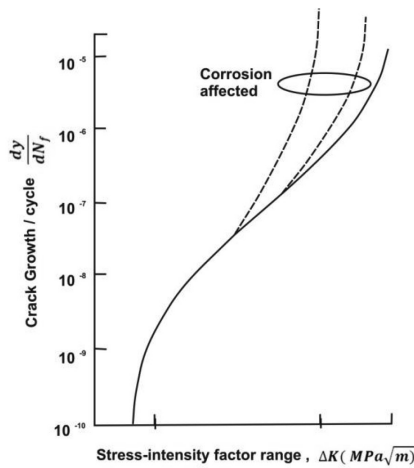
Figure 6.36.: The Paris plot with and without corrosion

since corrosion fatigue cracks get normally initiated at the surface. The way Paris law gets altered due to corrosion effects is shown in Figure 6.36. The sharp deviation in the curve occurs when the stress intensity range exceeds a critical value affected by corrosion and the crack growth rate is dramatically large. A situation like this is what occurred on Comet aircraft (Wikipedia11, 2016). While composites provide excellent protection against corrosion, some composites create difficulties with moisture and are to be specially taken care.

6.11.3. Creep

Creep is the tendency of a solid material to undergo time dependent deformation under the influence of stresses. It occurs as a result of long term exposure to levels of stress that are below the yield strength of the material. Creep is more severe in materials that are subjected to heat for long periods, and at elevated temperatures. Thin walled gas turbine combustors, and turbine blades in gas turbines are particularly affected by creep. Components of supersonic aircraft are also affected by creep. Cyclic temperature variations add the dimension of creep fatigue. A common example of creep deformation relates to tungsten light bulb filaments. Sagging of the filament coil between its supports

increases with time due to creep deformation caused by the weight of the filament itself. Too much deformation leads to touching of adjacent turns of the coil leading to electrical short and local overheating reducing the life of the filament. The coil geometry and supports are so designed to limit the stresses caused by the weight of the filament at high temperatures; a special tungsten alloy with tiny amount of oxygen in the crystallite grain boundaries helps slowing down creep that is strongly affected by diffusion of atoms along the grain boundaries.

Creep is described by the strain rate as a function of stress and temperature. While there are several mechanisms for creep, the prominent one is related to the movement of dislocations. At high temperature, the dislocations are greatly mobile and under stress, their movement has been surmised to be somewhat like chemical reaction. The more energetic of the dislocations causes movement. In this movement it has to overcome obstacles that may include other dislocations.

Creep is modeled by $d\varepsilon/dt \sim (\sigma - \sigma th)^n exp(-Q/kT)$ where $d\varepsilon/dt$ represents the strain rate, σ, the stress, Q, the activation energy, k, the Boltzmann constant, T, the temperature. The value of the threshold stress, σ_{th} is 0 for pure metals and is non-zero for alloys that have greater ability to resist movement of dislocations. The constant n is about 5 for pure metals and goes up to 10 for alloys. The dependence on the temperature is such that until some temperature, the strain rate is marginal and becomes very significant after that. A simple rule of thumb proposed is that for metals, the temperature at which creep begins to affect is about 40 % of the melt temperature (K).

6.11.4. Lightning, Rain, Hail, etc

Lightning, rain, and hail intrinsic to thunderstorm are all a part of a global atmospheric electric circuit. The solar radiation that includes elementary particles, electrons and ions interacts with the outer atmosphere to create an ionosphere blanket over the earth that also helps in the absorption of cosmic radiation. This electric potential between the ionosphere and the earth leads to thunderstorms as a natural occurrence. These thunderstorms average about 100 lightning strikes per second. The question of whether aircraft experiences natural event of lightning strike or is responsible for it has been answered by much research on several research aircraft and incidences occurring in flight. It appears that nearly 90 % of the lightning strikes are caused by the aircraft

Figure 6.37.: The electrical discharge tests in a wind tunnel (left) and wing tip electrical discharge wicks on Boeing 737 aircraft (middle), electrical conduction paths on a wing with composite structure (right) (drawn from lightning, 2011)

themselves. The actual process involves the two sides of the wing (top and bottom) developing opposite charges. Every commercial aircraft experiences a direct lightning strike about once in a year and the damage is usually confined to burn marks on the aircraft skin and the trailing edges of wings or tail surfaces. This minimal damage is attributed to the widespread use of aluminum (an excellent electrical conductor) for the skins and primary structure.

Careful attention to ensure that electrical paths are not disrupted by gaps in the skin, and the use of mechanical and hydraulic flight control systems, makes aircraft relatively immune to the adverse effects of lightning. The charge that is created on the surface is dissipated through static discharge wicks or rods arranged generally at the tips of the wings, stabilizer or fin. It must be understood that they are not for lightning protection in the sense that they do not draw away a potential lightning strike from other parts of the aircraft. They will help discharge the accumalated charge on the aircraft. If the static build-up on the airframe is allowed accumulate one can surely expect radio interference, particularly of several electronic devices like the automatic direction finder. Any damage to these is expected to be checked out in a walk-around inspection of the aircraft by ground personnel before clearance for take-off. Generally, there are a few on each wing tip and one each on horizontal and vertical stabilizers.

Figure 6.37 shows the tests being made on a research aircraft in a wind tunnel and the discharge wicks on a Boeing 737 aircraft. Uman and Rakov (2003) provide a authoritative review of the mechanisms of the interaction between lightning and airborne vehicles. Some lightning strikes have splintered the non-conductive plastic radar domes on the nose of some aircraft. Current flow-

ing through the aircraft structure can also result in isolated arcing or sparking and heating. If this occurs in a fuel tank, explosion, fire, and catastrophic structural damage can result. Fuel vapor ignition leading to explosions and consequent structural failure has been identified as the cause of over 10 fatal lightning accidents in the past with many fatalities. Since then, it is mandatory for civil aircraft to undergo a rigorous lightning certification tests and hence, accidents of the above kind are very rare these days.

The use of poorly conducting composite materials for aircraft structures and low-voltage digital avionics for flight and engine controls and other displays occurring rather simultaneously in the development history, have posed new challenges to ensure electromagnetic protection. Improvement of composite materials is contemplated through metallization of exterior surfaces or incorporation of fine metallic wires into carbon fiber composite skins to provide adequate conductivity for lightning currents as seen in the last part of Figure 6.37. A special facility has been created for lightning tests on the light combat airraft, being built at the Aeronautical Development agency in India (Rao et al, 1997)

Avoidance of the effects of rain and hail is usually accomplished by bypassing the zone of intense activity. Using ground radar generated inputs and/or on-board radars that present the picture of rain and hail affected zones, decisions are made on the flight routing that also demands specific aircraft-to-aircraft spatial separation decided by ground air traffic control. It is useful to note that such an avoidance strategy does not assure avoidance of lightning effects, for lightning discharges are more often found at the edge of a storm rather than in its interior.

6.12. Safe Life, Fail Safe, Damage Tolerant Design

Safe-life is a traditional concept in which the life is decided at the time a product is released for use and the product is expected to be discarded after the safe-life period. It is decided based on the life of some critical element in the product. Any life extension process has to go back to the designers who may initiate some tests on samples or conduct some non-invasive tests and decide on limited life extension. For instance, if the component has undergone some damage in its life, the life extension possibility may be compromised. Many equipment, particularly reactive components, like solid propellants in missiles

belong to the safe-life category. Life extension process is made difficult by the fact that such an act is in conflict with business interests. Occasionally, brave action is initiated to understand the causes for setting the safe-life, initiate the conduct of separate tests to determine why life extension should not be provided. Since safe-life concept is found to be very expensive to practice and particularly when it is realized that it is too conservative, ideas of fail-safe and damage tolerant design have emerged.

The idea of fail-safe is that even when some critical element fails, such a failure should not be catastrophic. The way it is implemented is as follows: Critical and highly stressed parts and those where the stresses that the component has to withstand could exceed the limits are first identified. These are then designed with more than one path for carrying the stresses. Should one path fail, the other path comes into play and would be able to maintain the minimum structural integrity required to complete the mission implying safe landing before further examination. Flight strategies are arranged to be fail-safe. A simple example is aircraft landing on aircraft carriers. In aircraft landing procedures, it is recommended that full throttle be maintained at touch down so that in case the arresting wires fail to hold on to the airplane, the airplane should have the ability to take off. In flight operations of an aircraft or a space launch vehicle, usually, the flight data acquired from sensors is received on several computers and processed to give inputs for decision making by pilots or flight directors. When the results from the individual computers differ, a voting scheme is implemented to enable robust decision making. This strategy in which decision is made even if some pathways have failed is essentially a fail-safe concept.

Damage tolerant design (see for instance, Woods and Engle, 1979), by its definition is tolerant to damage. Damage begins to show up in structural deformation or a crack that was not present earlier. One might interpret that this deformation is non-critical functionally or a crack too small to cause any problem. Both need examination and study that could involve an additional FEM calculation or a non-invasive test that may support this conclusion. But then, these features are noted for subsequent periodic check. The deformation may lead to a crack or the crack might have grown from its earlier condition. These facts, again, are subject to study and with this information it would be possible to predict the life of the component and also indicate the time duration of further safe-life and examination. Thus, the structure is being monitored for its

behavior during its operating life. It may be possible that at a future point in time, the component may need be repaired or replaced. Thus that segment of the total system alone is dealt with retaining other parts as they are since they are completely functional.

The damage tolerant design calls for a structural arrangement that helps access, examination and repair of critical elements. If the critical components are made inaccessible, the idea of damage tolerant design may be compromised ab-initio. Therefore, there must be adequate sensors to assess the strain, temperature and other parameters of importance. A continuous recording and analysis of these on-board will give indication to the health of the system and such an effort is called health monitoring system. These ideas are new in some ways and practicing them with new sensors that provide reliable data on a long term basis has not been widespread yet. Coming times will see significant deployment of health monitoring systems. As pointed out earlier, the use of composites in aircraft has become more significant even though the damage mechanisms are not known as well as in metallic alloys because it has been felt that continuous health monitoring would overcome this deficiency.

It would be fitting to examine the developments in gas turbine engines as an example of the changing philosophies over time. The early design strategy followed safe-life concepts. The entire engine was discarded when some serious malfunction occurred. It was known that the hot section – combustion chamber and the turbine will have much less operating life compared to the compressor and yet the situation of safe-life was practiced for want of an approach that was better founded. The working parts of the rotating machinery that would be discarded in such a situation would be very expensive. Subsequently, the engine design was made modular with compressor – combustion chamber and turbine sections that could be separated and replaced when needed. This made operations far more comfortable since the elements with lower life alone could be replaced when failure occurred or its life expired and the other active components could be retained for operation. The third phase of the development is periodic examination of most active elements. The compressor blades are examined using a "boroscope" to check on the integrity of blades – compressor or turbine. Decision to allow continued operations or replacing the system to allow off-line repair could be made. Sensors to determine rotor-rub or enhanced vibration would help diagnose any problems for similar decisions. These de-

velopments have made the operations of gas turbine engines far more safe for passengers and also operator-friendly. There are extensive guidelines on how to practice damage tolerance in design. These are now practiced in most aircraft design offices.

6.13. Smart Materials and Structures

Much of the current flight operation is dependent on feed back inputs from various systems for navigation and safety and these are "smart" compared to such operations three decades ago. Yet, the structures have generally remained passive. It is assumed that during a flight the structural components are safe. This is assured by ground inspections.

Typically, any major airline requires over a thousand employees to service their aircraft with checks - routine, ramp, intermediate and major - to monitor the safety and usage of the aircraft. Routine checks involve large number of tasks carried out under approximately a few hundred headings. Ramp checks increase in thoroughness every week to month, hanger checks occur every two to three months, 'inter-checks' every 12 to 15 months, and major checks every 20000 to 25000 flying hours. In addition to manpower resources, hanger checks require the aircraft to be out of service for 24 hours, inter-checks require about a week to ten days and major checks five weeks. All these procedures were developed at a time when science and technology advances in sensors, communication and analysis were at a rudimentary stage. Developments in these areas due to inputs from fundamental science have occurred substantially in the last three decades and hence the aspiration to do things left undone hither-to have arisen. The aim is to mimic human system in terms of design, but do better in terms of monitoring and decision-making for repair and maintenance on a continuous basis (the point made here is that even though the evolution of the human system design is incredible, it should be periodically checked for the performance of its elements, most of which that are critical are generally not visible to or understood by the individual or others unless instrumented and data acquired).

Thus, a smart structure is a system containing multifunctional parts that can perform sensing, control, and actuation, the source of stimuli being external or internal. Smart materials are used to construct these smart structures, which can perform both sensing and actuation functions. An introduction to smart

structures can be found in Summerscales (2010). The examples of smart materials are as follows.

At one end, we have (i) a low melting point wax in a fire sprinkler that blocks the nozzle until it gets hot, (ii) photo-chromic glass that adjusts the light intensity received at the eye by absorbing more light in a bright light environment, and (iii) microporous breathable fabrics that provide comfort for the person who wears these fabrics, (iv) shape memory alloys that undergo shape changes due to phase transformation when subject to a thermal field, ferromagnetic shape memory alloys that get influenced by magnetic field and (v) magneto-rheological fluids in which liquids mixed with fine iron powder respond to magnetic field by becoming stiff solid and a somewhat similar behavior for electro-rheological fluids (see Koma and Zimcik, 2003).

At another end, materials that can be used even as sensors are: (a) strain gauges that change the resistance when extended, (b) piezoelectric materials that undergo mechanical change when subject to eletrical charge or voltage and vice versa, (c) electro-strictive and magneto-strictive phenomena in which mechanical change is due to to electrical and magnetic fields, (d) smart gels that shrink or expand because of small changes in pH, temperature or electric fields, (e) acoustic emission sounds emitted under high stress, (d) embedded optical fibres, and (e) giant magneto-impedance wires in which the impedance changes substantially under the influence of a magnetic field.

The actuators can be of several kinds: (a) the conventional hydraulic, pneumatic and electric types that usually turn out to be heavy occupying large volumes,(b) piezoelectric crystals whose shape changes when voltage is applied, (c) shape memory materials whose shape changes at a specific temperature, (d) magneto-rheological fluids whose viscosity changes with magnetic field, and (e) electro-rheological fluids whose viscosity changes with electric field.

The basic idea of using these smart materials is that the miniature size devices can be embedded in the structures at various locations, stress/strain, temperature or pressure can be measured and transmitted to on-board computers that can process the information to provide the heath status of the structure. What is very important is the reliability of the sensors and data transmission chain over substantive periods of time to be able to make useful sense of the new approach. These approaches have made inroads into many aspects of

life including aerospace; there are more examples in general life situations. These include vibration reduction in vehicles and sporting goods, buildings and bridges, and smart-skin.

Piezoelectric devices have been used in vibration control on aircraft. These devices generate voltage signals that are then processed to provide a feedback to another set of piezoelectric actuators that cause control of vibrations.

Amongst shape memory materials discussed earlier, shape memory alloys (SMA) occupy an important position; they are alloys that can change their shape, stiffness, position, natural frequency, and other mechanical characteristics in response to temperature or magnetic fields (Wikipedia8, 2016). The use of shape memory materials help in creating lightweight solid-state alternatives to conventional actuators such as hydraulic, pneumatic, and motor-based systems. There are several materials that have the shape memory effect. For instance, Ag-Cd at 44/49 % Cd, Cu-Al-Ni at 14/14.5 % Al and 3/4.5 % Ni, Cu-Sn at 15 % Sn, Fe-Pt at 25 % Pt, Fe-Mn-Si, Co-Ni-Al, Co-Ni-Ga, Ni-Fe-Ga, Ti-Pd in various concentrations and the most famous one namely Nitinol, Ni-Ti (~ 55 % Ni).

The discovery of shaped memory alloys has an interesting aside. When a few deeply bent pieces of Nitinol were shown in a lecture demonstration, one of the scientists held a flame below the material only to discover the pieces returning to the original shape. The process of shape change is directly related to an internal structural transformation from the martensite to the austenite phase. If the material encounters resistance during the phase transformation it can generate extremely large forces and displacements (400 MPa and 8-10 % respectively for Nitinol). When they cool down their original shape can be easily recovered, due to their low yield stress (around 80 MPa). Transition temperatures fall in the range of 50 to 100⁰C and the repetition life is over 100. Other useful properties of Nitinol are its excellent damping characteristics at below the transition temperature, corrosion resistance, non-magnetic nature, low density and high fatigue strength. Nitinol is also to an extent impact- and heat-resistant. These properties have enabled its multifarious use including military, medical, safety, and robotics applications.

The military has been using Nitinol couplers in F-14 fighter planes since the late 1960s. A space application concerns making the routine tasks automatic

while astronauts are busy performing research projects in space. During space experiments samples need to be turned off regularly. One way of doing this is to make clutches or hinges from SMA that will turn a sample when it reaches a certain temperature. Further applications include the deployment of space structures by means of electric impulse which heat the SMA through Joule effect.

There are examples of SMAs used in safety devices like anti-scalding devices and fire-sprinklers that are already on the market. The anti-scalding valves can be used in water faucets and shower heads. After a certain temperature, the device automatically shuts off the water flow. The main advantage of Nitinol-based fire sprinklers is the decrease in response time. Nitinol is being used in robotics actuators and micromanipulators to simulate human muscle motion. The main advantage of Nitinol is the smooth, controlled force it exerts upon activation. An engaging presentation on smart materials and structures has been provided by Akhras (2008); Summerscales (2010) provides insights into structures including biomimetics (biomedical applications).

6.14. Vibration and Aeroelasticity

Classical vibration problems follow the elementary understanding of pendulum and spring-mass systems (see for instance, Wikipedia6, 2011). The equation

$$m\ddot{x} + c\dot{x} + kx = F = F_0 sin(\omega t)$$ (6.39)

where m is the mass of the system, c, the damping coefficient, k, the stiffness (force per unit deflection of a spring, for instance), F, the imposed force that could depend on time, x is the deflection and $\prime$ represents derivative with respect to time, t. The first term is the inertial force, the second term is that of damping force, the third term spring force. These features are illustrated in Figure 6.38.

The equation $m\ddot{x} + kx = 0$ represents the un-damped ($c = 0$) free vibration of a linear spring – mass system. If it is taken that the initial amplitude at which oscill on started is A_1 and the velocity zero, the solution is $x = A_1 cos(\omega_n t)$, where $\omega_n = \sqrt{(k/m)}$ is the undamped natural frequency proportional to the square root of the ratio of the stiffness to mass (the frequency in Hz is obtained from this simply: $f_n = \omega_n/2\pi$; note that ω_n is in *radians/s*). Increased mass reduces the frequency. A stiffer spring has a higher frequency. These elementary facts
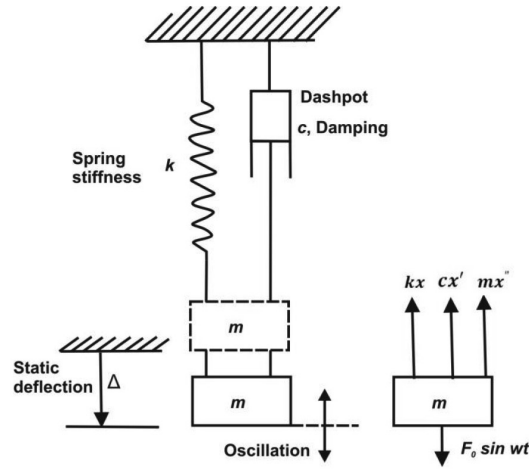
Figure 6.38.: A typical damped spring mass system with a sinusoidal forcing

are of great value in making judgments about the vibration behavior of even complex systems. The system with damping can be solved similarly. One defines a non-dimensional damping $\zeta = c/2\sqrt{(k/m)}$ Typical value of ζ for metal airplane structures like fuselage is about 0.05, and for automobile suspensions as high as 0.3. The solution to the problem is

$$x(t) = A_1 exp(-\zeta\omega_n t)cos\omega_n t\sqrt{(1-\zeta^2)} - \phi]$$

(6.40)

The amplitude and velocity at $t = 0$ will decide A_1, the initial amplitude and φ, the phase shift. The first thing to recognize is that for $\zeta = 0$, the above result cascades into the earlier result. With non-zero ζ, the behavior is different. The amplitude keeps decaying in an oscillatory manner. The time to half-the-amplitude is taken as another measure of damping. The time for halving the amplitude, $t_{1/2}$, is given by $t_{1/2} = 1/(\zeta\omega n)$. If the frequency is say, 10 Hz, ω_n is 62.8 rad/s and at $\zeta = 0.05$, the time to half the amplitude is 0.32 s.

One can analyze the problem of vibration with forcing. We consider $F = F_0 sin(\omega t)$ as a simple harmonic forcing function. The solution to this problem is given by

$$x(t) = F_0 cos[\omega t - \phi]/[k\sqrt{q}]$$

(6.41)

with $q = (1-r^2) + (2\zeta r)^2$, $r = \omega/\omega_n$ and $\phi = tan^{-1}[2\zeta r/(1-r^2)]$
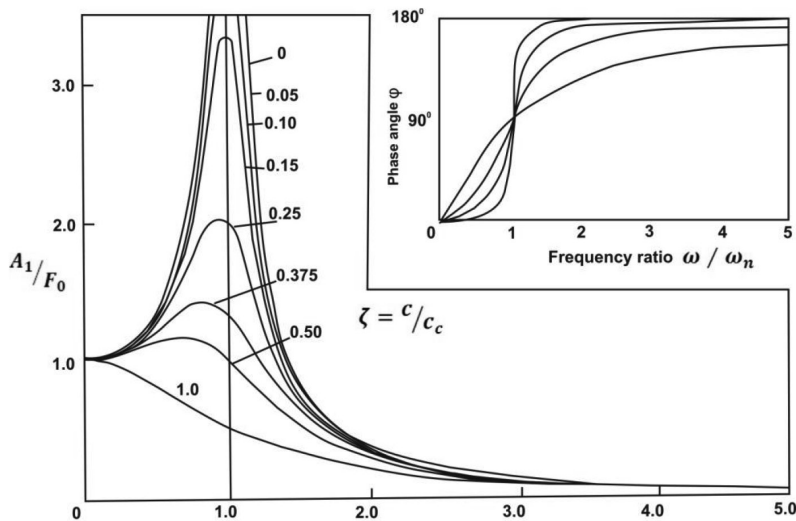
Figure 6.39.: The response of a spring-mass system to forced oscillations – amplitude and phase based on Vibrations, drawn from Wikipedia6, 2011

The results of amplitude and phase are shown as a function of frequency ratio, r, in Figure 6.39 for various values of damping. For $\zeta = 0$, the behavior is simple. The amplitude increases to ∞ from both sides of natural frequency. The moment there is some damping the amplitude becomes limited at frequency equal to natural frequency, but the amplitude is large indeed. This is roughly what we observe when structures are excited at the undamped natural frequency. These amplitudes are indeed to be avoided. Increasing the damping may appear a directly visible solution. When there is inadequate control on this aspect, one usually ensures that the natural frequency is kept away from possible disturbing frequencies by making it much lower or higher.

There is one curve marked $\zeta = 1$. This corresponds to a response with amplitude not overshooting the initial value. It is called critical damping condition.

6.14.1. Why is there resonance?

An examination of Figure 6.39 indicates that at very low levels of damping the amplitude of the vibrating system at the natural frequency is very large compared to the initial amplitude? It looks as though the system is drawing energy and pumping it away by creating high amplitudes! But let us remember that

this result is a consequence of the solution of a simple force balance – between inertia, viscous damping (that can be kept aside in these arguments), spring force and the input force. Since the increase in amplitude is much larger than the initial amplitude, one can keep input force aside as well. This implies that the answer must lie in the balance between inertial and spring forces or stated in energy terms, kinetic and potential energy. When a load is added to the pan held by the spring, there is some static deflection. This deflected position is the mean position around which oscillations occur. Now let us say, we just draw the pan down to cause extension of the spring and leave it (as is the usual way this is done). When the spring stays in extended manner, the energy is stored as potential energy. When the pan is released this potential energy gets converted to kinetic energy and the mass accelerates towards the equilibrium position. At the time the equilibrium position is reached, the potential energy is exhausted and the kinetic energy is at the peak. The mass then continues to move up using the kinetic energy till all of it is transferred to potential energy of compression in the spring. This motion keeps on and on if there is no damping and the amplitude that the system attains is limited to the initial value as this determines the total energy. The presence of damping will result in continued reduction in the peak amplitude till the system comes to rest.

We now consider explaining the high amplitudes in the case of forced oscillation. The simple undamped spring mass system oscillates with the amplitude equal to the initial amplitude. Now the presence of external forcing keeps adding energy in phase when the frequencies are equal during the entire oscillation cycle. This builds up the amplitude significantly and in theory, to infinity. One might, at this stage ask: why should it go to infinity? Why not some large value? The answer is that can be expected under idealized conditions since a finite large value must have a basis and there is none that can be found.

If the frequency of the external forcing departs from the natural frequency, the addition caused by the external forcing will aid in part and go against other times. The net effect is that the amplitude will be large but finite. In all cases, the presence of damping will further bring down the peak amplitude of the oscillations.

6.14.2. Complex systems

Every real system is complex. It is usually modeled by using a number of spring mass systems (as also damping where required) suitably arranged.

Such a system will have many natural frequencies depending on the number of spring–mass elements (see Laglace, 2001). The lowest of the frequencies is usually very important since exciting higher frequency modes needs larger energy. There are nonlinear systems with soft and hard springs whose behavior is such that the spring stiffness changes with deflection *[k = k₀(1 + αx)]*. This leads to nonlinear differential equation that has multiple solutions. The response curve seen in Figure 6.39 gets modified with the vertical region near $\omega/\omega_n = 1$ bending over to the left or right. And for every frequency, there are two amplitudes. It turns out that one of these is unstable. If the damping is nonlinear – implying that *c* is replaced by *c(x² – 1)*, say, one has nonlinear differential equation. This is called the forced Van-der-Pol oscillator. This oscillator is known to mimic the heart beat. The oscillator has oscillations called the limit cycle oscillations. These are essentially periodic nonlinear oscillations, somewhat similar to the electro-cardiogram (ECG) of the human heart. The nonlinear differential equations, with certain class of coefficients and values of parameters lead to solutions that are chaotic. Chaotic solutions imply that in the resulting output, there is a presence of large number of frequencies not directly traceable to any particular feature in the input. Another way of stating this is that the output signal has white noise (there are other noises - like pink, blue, brown, violet and grey noises – the power spectrum has all the frequencies with frequency dependent amplitudes). Chaotic solutions and fluid turbulence are thought to be intimately connected. Oscillatory systems occupy large interest beyond aerospace structural applications in electrical engineering, telecommunications and quantum physics.

6.14.3. Aero-elasticity

Coming back to flight applications, if the force *F* in the equation stated above is related to instantaneous deflection, *x*, as might happen with systems with feedback, the system behavior will mimic aero-elasticity where the deflection of the lifting surfaces can cause changes of loads (see Wikipedia7, 2011 and Dimitriadis, 2009).

There are four classes of problems coming out of structure – flow interaction. These are (a) divergence which is a static aero-elastic interaction, (b) flutter which is a dynamic aero-elastic phenomenon (c) limit cycles which are the asymptotic state of non-linear oscillators, and (d) vortex shedding, buffeting, galloping which are essentially unsteady aerodynamic phenomena.

In a flying vehicle increased speed leads to larger forces. One needs to apply the control forces to maintain a steady flight. Also, when a maneuver is performed, the control surfaces need to be deflected. Under conditions of being at the boundaries of flight, demand for increase in control surface angle may be countered by the forces on the surface playing upon the elasticity of the material, a feature normally ignored in the discussions up till now. In this situation, any further command for the movement of the control surface will not lead to change of forces. This is called control reversal. It is a consequence of the structural deformation to the enhanced load distribution. This is therefore called static aero-elasticity.

Flutter, on the other hand can be understood as a spring mass system that we have discussed above except that the coefficients are related to dynamic fluid forces. In the equation that we started with earlier, namely, $m\ddot{x} + d\dot{x} + kx = F$, we represent the various additional terms as follows. The first inertial term is modified to include what is termed "added mass" to account for the mass of the air moved by the oscillation. This implies that m is replaced by $(m + \rho b^2 \bar{c})$ where b is typically the span of the wing, $\bar{c}$ is the chord. The damping term is expressed as $d = \rho V\, B_0 + S_d$, where ρV is the flow mass flux (the product of the density of air stream and flight speed) and B_0 is a constant and S_d is the structural damping constant. The spring constant k is defined as $\rho V^2 C_0 + S_k$, where the first part is due to aerodynamics and the second part is due to structure per-se. The term F on the right hand side is due to gusts and control inputs. Restating the equation,

$$(m + \rho b^2 \bar{c})\ddot{x} + (\rho V B_0 + S_d)\dot{x} + (\rho V^2 C_0 + S_k)x = F \text{ (gust, control commands)} \quad \textbf{(6.42)}$$

When steady fluid flow past an object occurs, there will be vortex shedding from the edges. At smaller Reynolds numbers $(= \rho V\, \bar{c}/\mu)$, the vortex shed is regular termed Karman vortex street. As flow velocity increases, Reynolds number increases and the flow field has a complex vortical shedding. The aero-structural effects are characterized by a non-dimensional number called Strohal number defined as $S_{th} = \omega_{vs} D / V$, where ω_{vs} is the frequency of vortex shedding and D, the characteristic dimension of the body which in this case could be $\bar{c}$. The control surfaces, particularly those at the tail part – the horizontal and vertical stabilizer (the elevator and the fin) experience the "downwash" of

the main wing containing these complex vortical structures. These can alter the fluctuating forces that would be induced on the control surfaces, a condition called buffeting.

A more appropriate model has two sets of equations for aerodynamics and structural dynamics with terms of interaction in each of them. The coupled set of equations will provide the solution that explains the aerodynamic and the structural situation with time as well as the overall effects – flutter and buffeting.

The famous Tacoma bridge failure discussed extensively in aeronautical and fracture literature belongs to the category of flutter. The collapse occurred in November 1940 in the morning (see Wikipedia9, 2016). The account of a driver who narrowly managed to escape the bridge before the collapse is interesting – "Just as I drove past the towers, the bridge began to sway violently from side to side. Before I realized it, the tilt became so violent that I lost control of the car... I jammed on the brakes and got out, only to be thrown onto my face against the curb... Around me I could hear concrete cracking... The car itself began to slide from side to side of the roadway.

On hands and knees most of the time, I crawled 500 yards [450 m] or more to the towers... My breath was coming in gasps; my knees were raw and bleeding, my hands bruised and swollen from gripping the concrete curb... Toward the last, I risked rising to my feet and running a few yards at a time... Safely back at the toll plaza, I saw the bridge in its final collapse and saw my car plunge into the Narrows".

Even before this failure, it was uncovered that the bridge would sway and buckle dangerously in relatively mild windy conditions. The failure of the bridge occurred when a twisting mode occurred from winds of 67 km/h which may be considered mild. It was analyzed to be the second torsional mode, in which, the midpoint of the bridge remained motionless while the two halves of the bridge twisted in opposite directions.

The torsional disturbance in the structure increased the "angle of attack" of the bridge. The structure responded by twisting further. Eventually, the angle of attack increased to the point of stall, and the bridge began twisting in the opposite direction. The entire oscillatory motion had an effective negative damping

and the oscillations increased till the suspender cables gave way in a cascading sequence. This failure must not be interpreted as a simple forced resonance that we discussed above as there was no periodic external forcing. Subsequent calculations showed that the frequency of the destructive mode, 0.2 Hz, could neither be identified with a natural mode of the isolated structure nor that resulting from the blunt-body vortex shedding of the bridge; what is for sure is that it was a complex aero-elastic effect.

The first ever incident of flutter occurred on an aircraft occurred on Handley page bomber in 1916 during WW I. It was analyzed that a torsional mode of the fuselage got coupled to the anti-symmetric elevator mode The problem was solved by coupling the elevators. There have been many aircraft that have experienced flutter and buffeting particularly during maneuvers. Military aircraft like F16 and F18 had experienced buffeting and limit cycle oscillations due to external stores (bombs, rockets etc). The methods of overcoming the flutter and buffet problems need a careful investigation of the flows over the control surfaces that emanate from wing in the maneuver envelope of the aircraft; in some aircraft the flutter associated with the control surface has been solved by adding a mass around the hinge line of the control surface and in others changing the shape of the exit of the flow from the engines (Wikipedia7, 2011 has additional information and links to studies).

Gas turbines are composed of rotating machinery with blades, axial or radial flow. The rotating machinery is usually mounted on a hollow shaft. Also several pumps used in aerospace applications have rotating machinery. Such machinery can exhibit serious vibration and flutter problems during development. The analysis of vibration proble follows a procedure outlined for spring mass system. It can be recalled that $\omega_n = \sqrt{(k/m)}$. For the case of a rotor mounted on a shaft between bearings, the spring stiffness can be written as $k = mg/\delta$ where δ is the deflection of the shaft. The deflection is dependent on the mass distribution about the bearings and the bearing stiffness. The deflection can be calculated as $\delta = mgL^4/C_{bc}I$, the constant C_{bc} depends on the boundary conditions. Reducing the deflection helps raising the critical speed to levels that allow smooth operation at speeds contemplated. For fixed boundary conditions at the bearing, C_{bc} is 192 and for pinned condition it is 48. Perhaps, the actual value is between the two limits. It is these conditions that also dictate the critical speed (or critical natural frequency). Since the deflection is strongly dependent

on the distance between the bearings (~ L4), attempts are made to make this distance as small as is possible and in addition, to make it close to fixed conditions without having to pay for frictional losses. In earlier times the number of bearings was 4 to 5. All round technological choices and developments in recent times have brought down the number of bearings to 3. Modern developments in bearings – foil bearings, magnetic levitation are currently going on (as an aside, it is useful to note that the small fans that are used on computers have allowed the creation of a new technology of magnetic levitation for reducing frictional losses in bearings).

Apart from the basic aspects that one can handle by design procedures, there are other issues like mass imbalance on the shaft that accentuates the vibration problems in rotating machinery. It is due to the principal axis of inertia of the rotor not being coincident with its geometric axis. The use of higher speeds that has become the order of the day due to better compactness leads to greater centrifugal imbalance forces and therefore, calls for greater care in balancing. Traversing into territories dominated by aeroelasticity can result in disastrous consequences for the hardware. Resolving vibration problems in gas turbines is tedious, time consuming and expensive.

While computation of flows through the blade passages, even if involved, can provide guidance to the needed changes, there is no escape from well instrumented test bed runs at increasing speeds up to the rated condition evaluating the results at each stage. Generally, the presence of vibrations with harmonics embedded in the output signal is taken to be simply due to the flexibility of the rotating system. The presence of signals with odd frequencies is then taken to be due to aero-elastic coupling. The consequent pathway for modification would then be related to tuning the flow behavior due to altered geometry of the blades because of flexibility.

Extensions to the study of aeroelasticity with thermal effects is termed aero-thermo-elasticity and the study of aeroelastic problems including control systems is termed aero-servo-elasticity. It is normally understood that aero-elastic study becomes relevant in advanced high performance aircraft where control systems have necessarily to be more finely tuned. It is entirely possible that the control system action induces aero-elastic problems and that is why the subject of aero-servo-elasticity becomes important.

6.15. Computational Aspects

Aircraft structural analysis includes statics and dynamics as well as non-linear behavior. There are also subcomponents like the landing gear that need analysis. Each of the structures needs to be modeled to some level of detail. The degree of detail depends on the questions needing answer. At one level, it is sufficient to use blackbox like ideas and get the broad behavior. Slowly, as design and realization of component hardware goes along, sub-components need to be modeled, some for statics and others, dynamics. Aspects like aeroelastic analysis need serious consideration at some time when the vehicle development has progressed. Most tools are used separately many a time. The discussion on the computational aspects addresses these separately.

All approaches underlying static analysis are expressed in a matrix form

$$\left[\begin{array}{c} Q_i \\ Q_2 \end{array} \right] = \left[\begin{array}{cc} k_{ii} & k_{ij} \\ k_{ji} & k_{jj} \end{array} \right] \times \left[\begin{array}{c} q_i \\ q_j \end{array} \right]$$

[Force $(n \times 1)$] = [Stiffness $(n \times n)$] [nodal displacement $(n \times 1)$]

This equation whose size is dependent on the number of finite elements chosen to discretize the structure is solved by matrix computational approaches to give the displacements and local stresses. When it comes to buckling as well as vibration problems the problems are structured in an eigenvalue format to lead to critical buckling loads, frequencies as well as mode shapes. In problems of material fracture, one uses the numerical calculation procedure in which the given structure has some initial crack distribution to obtain a quantity called the J-integral. This represents the stress energy release rate for small crack extension. From this estimate, the stress intensity factor is calculated. One can compare this value with the fracture toughness value to determine the state of the system in so far as fracture issues are concerned. There are also problems of non-linear behavior in fracture that need modeling of the structural behavior. Several of these problems have been addressed over the last two decades and much has been understood about the material behavior near fracture. In many cases, experiments and computational approaches are used in a supportive manner to both understand the phenomenology and predict better the behavior of complex structures. A large number of commercially available software to solve structural problems use largely the finite element method
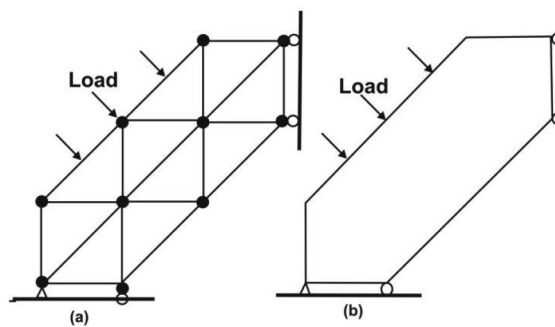
Figure 6.40.: Historical aspects of FEM: The truss and a continuous structure, adapted from Anon (1992)

(FEM). We shall examine below the history and comparative status vis-ï£¡-vis finite difference and volume methods adopted in fluid flow problems.

6.15.1. Finite element method (FEM) and its history

A number of aspects related to the response of the structure to loads can be mathematically modeled and computationally dealt with. Excepting a few cases related to wave propagation in structures, in fatigue and fracture that are perhaps in the frontier research area, most other aspects have been addressed, largely using Finite Element Method (FEM). A readable account of the history and practice of the FEMs is found in Anon (1992). It was first developed in 1943 by Courant utilizing the Ritz method of numerical analysis and variation calculus to obtain approximate solutions to vibration systems. Subsequently, M. J. Turner and colleagues established a broader definition of numerical analysis with a paper centered on the "stiffness and deflection of complex structures" in 1956 (see Anon, 1992).

Physical intuition brought finite element concepts to engineering design. In the 1930s when a truss problem such as the one shown in Figure 6.40 was encountered, it was clear how to deal with obtaining component stresses and deflections of the unit; first, the truss was recognized as an assembly of rods whose force – deflection characteristics were known. Then these would be combined invoking the laws of equilibrium and the resulting system of equations was solved for the unknown forces and deflections of the total system (strength of materials approach).

This procedure worked well whenever the structure in question had a finite number of interconnection points, but then the following question arose: What can be done with an elastic continuous structure such as a plate that has an infinite number of freedom or interconnection points? For example, in Figure 6.40, if a plate replaces the truss, the problem becomes considerably more difficult. Intuitively, Hrenikoff (1941) reasoned that this difficulty could be dealt with by dissecting the continuum structure into elements or structural sections (beams) interconnected at a finite number of node points. With this simplification the problem reduced to a conventional structure handled by the known methods. This method called the "framework method" was considered successful. Later, piecewise continuous functions defined over triangular domains were adopted with an assemblage of triangular elements and the principle of minimum potential energy to study the St. Venant torsion problem by Courant (1943). Continued developments of mathematical and computational aspects led to the popularity of FEM techniques for structural analysis.

6.15.2. Structural and fluid flow problems – FEM, FDM and FVM

As different from FEM, fluid flow calculations started with finite difference schemes, since finite difference methods (FDM) have root in the elementary statement of equivalence between differentials and differences: $\partial u / \partial x = (u_i + 1 - u_i)/(x_i + 1 - x_i)$. Extension to three dimensional problems also appeared simple to appreciate. It is only later that they evolved into finite volume methods (FVM) to account for complex geometry and ensure conservation of flow properties in individual cells. Thus, FDM is a point method and FVM is a cell technique akin to FEM. It (FVM) is based upon an integral form of the partial differential equations of conservation of mass, momentum, and energy. The equations are written in a form which can be solved for a given finite volume. The resulting system of equations usually involves fluxes of the conserved variable making the calculation of fluxes very important. The basic advantage of this method over FDM is it does not require the use of structured grids or its transformed curvilinear grids. Currently, the most widely adopted strategies incorporated into several classes of commercial software use FVM for fluid flow problems and FEM for structural problems. Some problems like conduction are handled by both methods. Aero-elastic problems use combined strategies – FEM for structural aspects and FVM for fluid flow aspects with supervisory software dealing with interface aspects.

There has been a large debate on FDM, FVM and FEM for structures and fluid flows on the internet and in literature (see for instance a discussion in Peiro and Sherwin, 2005). It is to be recognized that fluid flow problems present a wider range of mathematical behavior – nonlinear due to convective terms, subsonic (elliptic), supersonic and hypersonic (both hyperbolic) regimes of flow, turbulent modeling issues that enhance the complexity in terms of number of equations to be solved and heat release effects due to complex chemistry and chemistry-turbulence inter-action that contribute to enhanced number of equations and stiffness (due to wide time scales of individual steps of reaction), and finally, thermal radiation that is inherently three-dimensional. The words elliptic, hyperbolic used above imply the following. Problems in which a certain disturbance – pressure/stress in any one zone influences the entire zone are called elliptic. Those in which any local disturbance affects only downstream (as in the case of a flow) are termed parabolic. Those in which there is a zone of influence (cone of influence more precisely) even when the disturbance propagates downstream are termed hyperbolic. Most structural static stress behavior is governed by elliptic behavior, just as subsonic fluid flows are. Wave propagation is essentially a hyperbolic behavior, generally in the case of supersonic and hypersonic flows. Issues of wave propagation in structural analysis occupy a small segment of the demand on solutions to problems of importance, since most materials used are ductile and fracture in these materials occurs after much plastic deformation.

Several advantages claimed only by FEM for structural analysis have been evolved and made available for fluid flows – the important aspect of FEM being able to deal with complex geometry has been dealt with a whole range of software tools for grid generation allowing body-fitted grids and multi-block approaches in FVM. It is claimed that desired accuracies being achieved with smaller number of elements in FEM in comparison to the number of elementary cells/volumes in FVM. But the use of multi-gridding and adaptive gridding strategies in FVM have made this claim a weak point of debate; faster computers and better storage and retrieval methods have made the arguments even weaker.

Mathematical level equivalence has been established with these techniques in specific cases. Chung in his book "computational fluid dynamics" has shown the equivalence between (a) explicit FTCS (forward time central space) finite

difference schemes and generalized Galerkin schemes with suitable choice of temporal parameters for parabolic type problems and (b) Lax-Wendroff finite difference schemes and generalized Petrov – Galerkin methods, again with specific choice of convection and temporal parameters for first order hyperbolic partial differential equations. In summary, this debate of FVM vs. FEM that has occurred in literature has had less essential content than emotion and the debate should truly be converted to "how much of FVM with FEM" so as to make it more convenient for the user to get correct results with less computational effort both in preparation and resources, as discussed in Chung's book.

6.16. Structures for Missiles, Satellites and Launch Vehicles

A good description of the structural aspects of launch vehicles and satellites is found in Nasser et al (2004). The structural arrangement for small missiles generally used in tactical applications consists of cylindrical body with a conical tip. Fins at the back are used for controlling the missile. The cylindrical body with a dished end on one side and the nozzle assembly on the other is a pressure vessel designed to withstand anywhere up to 150 atm (generally, smaller the missile, higher is the chamber pressure). The space between the rocket combustion system and the front nose tip is filled with war head and control and guidance systems.

Since field deployment is the demand on many classes of missiles, all the com-ponents are designed to withstand an ambient temperature of - 40 to +40⁰C and a wide range of relative humidity up to nearly 100 %. Most missiles fly at supersonic conditions, typically up to $M = 3$ and burn duration does not exceed a few tens of seconds. Several missiles are made in thousands. Hence, quality assurance of the product demands rigorous control on the quality of input materials. The design procedures for these systems are classical and strength of materials approach itself is adequate in many cases.

Launch vehicles for satellites and military payloads (strategic missiles) are about the same. The propulsion system is generally very large in size, going up to 3 m in diameter and 30 to 40 *m* long. Solid propellant combustion chambers that need to withstand chamber pressures up to 70 *atm* have reasonable wall thickness (up to 8 *mm*) and their design needs to account for fracture related issues. Liquid propulsion combustion chambers have also to withstand high pressures (for instance, 200 *atm* in the case of space shuttle main engine,

SSME) and high and very low temperatures. For instance, a full cryogenic engine (based on liquid oxygen and liquid hydrogen) has a combustion chamber inner wall temperature of 800 K and in the coolant tubes a few mm away the temperatures will be about 100 K. The choice of metallic materials for these cases is complex, but cost criterion is not the limiting feature here. The liquid propellant tanks are huge carrying several hundred tonnes of propellants. The liquid oxygen tank of SSME is 8.4 m dia and 16.6 m long. The liquid hydrogen tank is of much larger volume even though the mass of hydrogen carried is low – 8.4 m dia and 29.5 m long. The inside pressures are 1.5 and 2.5 atm respectively. Hence the wall thicknesses are small. Building these tanks is done by maintaining inert gas pressure inside to prevent bucking. The mechanical design should also account for significant shrinkage in the tanks that occurs because of substantial reduction in temperature. The building of these systems is arranged in such a way that even the painting of the outer surface is limited to the rust colored primer to save the mass, as much as several hundred kg.

The structural design of the payload for satellites or advanced warheads needs to take into account the external and g-loads on the flight path – both longitudinal and lateral. Typical g-levels are about 5 to 7 for short durations towards the end of burn of each stage (in a typical multi-stage vehicle). There are also shock loads that arise during launch and stage ignition that need to be accounted for.

Satellites have special demands on their design. The satellites that reside either in sun-synchronous or geo-synchronous orbit have to have long life – seven to ten years. They cannot be attended to after their launch. Either they function or they become space debris. This imposes significant demands on the design, construction and testing before their launch. In the space home, they experience near-hard vaccum (1.3×10^{-9} atm) at 200 km altitude and 1.3×10^{-14} atm at altitudes beyond 6500 km) and surface temperatures of the order of $\pm70^{0}$C. The loss of material by sublimation from the surface should be accounted for. A similar problem of out-gassing – release of adsorbed gases from the surface in vacuum leading to deposition of some of the gases in unwanted locations that further leads to reduced or loss in performance is a problem. A solution to out-gassing problem is to condition the system under the same or more rigorous environment on ground.
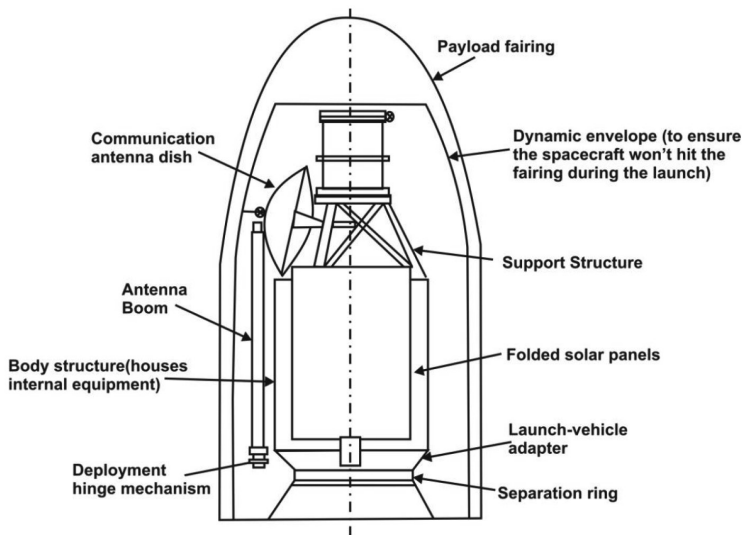
Figure 6.41.: Typical structural arrangements of a satellite inside the outer casing

Another problem concerns the dimensional stability of antenna dish needing to have high pointing accuracy throughout the life time of the satellite. Of course, corrections to the attitude of the spacecraft will be possible because of micro-thrusters on the body of the satellite. Yet, any possible distortion should be within the range for correction to be enabled. Use of composite structures with very low thermal expansion coefficients will help overcome the problem. A typical structural layout of a satellite in the outer casing that will be fixed to the launch vehicle is shown in Figure 6.41. A further problem common to all satellites and launch vehicles is vibration. The natural frequency of most launch vehicles is about 15 to 40 Hz in the longitudinal mode and 8 to 15 Hz in the lateral mode. The satellite and its structure must be designed so as to be outside of this natural frequency range. The rule of thumb called the octave rule is that the natural frequency of the systems should be twice the natural frequency of the supporting structure (implying the launch vehicle).

6.17. Comparison between Structures for Aero-vehicles, Missiles, and Others

Among the various aerospace vehicles, civil aircraft occupies the highest position in terms of complexity of performance demands: wide operating conditions

from an ambient temperature of - 40 to + 40^{0}C, wide range of relative humidity up to nearly 100 %, saline atmosphere, high speeds with aerodynamic heating and a large number of take-offs and landings some of which occur in desert areas with unprepared runways. Even if all the conditions do not occur with the same aircraft, most critical ones are common and these problems are indeed very severe. They impose critical demands on the materials, design and manufacture since performance, life and cost impinge on the final product.

The only other aeronautical system of comparable or higher complexity is the gas turbine engine. Designed to be compact, rotating at high speeds with unsteady flow through the system at temperatures up to 1700^{0}C with turbine blades having very small clearances between the edge of the blade and the outer casing both of which undergo thermal cycles of no mean measure is an outstanding achievement of human ingenuity.

Helicopters operate over a less severe setting, lower altitudes, lower speeds and yet experience repeated take-offs and landings, some which could be on unprepared helipads. The severity in the demand on the structural performance is less demanding than in an aircraft in many parts, but in some parts higher – like in the main rotor responsible for propulsion.

Missiles and launch vehicles are one shot affairs (except for reusable launch vehicles, which share the features of an aircraft). The demand on the design of the elements of a missile is much less severe than in an aircraft.

Satellite structures can be thought of more as support systems for electronic and propulsion hardware. The structural stressing issue from flight related operations is largely the g-load that appears during the launch sequence. Once the satellite arrives at its orbital home, the structure experiences much less loads in the orbit. Stresses that appear due to differential thermal loading because of radiation from sun are still small compared to those experienced during the launch.

The procedures used in the design of all aerospace structures are similar both for static loading as well as dynamics (vibrations). The number of aspects on which the aircraft structure undergoes check in the design is far, far more than for the rest. Also, aircraft components undergo far more severe testing compared to others to ensure structural integrity.

6.18. Summary

This chapter is concerned with aerospace structures: how they are similar to birds, what materials are chosen for various parts, what structural design principles govern the choice of the geometry, what classes of materials are more appropriate and why? What problems do cyclic loading create in terms of fatigue? Why materials behave under stress the way they do? What are the environmental factors that structures experience taken care of? How ideas of safe life have been replaced by damage tolerant design?

Aircraft and birds share a common feature of arranging their structure for optimizing the strength-to-weight ratio. Changes in birds occur due to following the evolutionary biology and changes in aerospace structures follow science and technology inputs arising out of deeper understanding of the behavior of both the material and the structure. Adding just the right mass of the right shape at the right place with the right material provides for the optimal design. While birds fly very much within the atmosphere at low speeds, aircraft have a much wider range of al-titudes and speeds providing greater challenges in all spheres – materials, design, and manufacture.

While fabric and wood were the primary material in the early development stages, metals with other alloys of aluminum, iron, and titanium began to be used in varying proportions depending on a compromise between performance and cost. Fatigue and fracture entered the fields of design going beyond the dominant aspect of stress analysis in structure and materials design. The way the material is required to resist loads through an analysis of stress behavior in tensile, compressive, bending, buckling, or torsion or a combination modes along with material properties decided wh h class of materialp would fare better – for instance, materials with maximum of $\sqrt{UTS/\rho_m}$ and $\sqrt{[UTS/E]/\rho_m}$ minimize the structural mass in bending, and bucking as discussed in section 6.10. These justify the choice of aluminum alloys as more appropriate materials and wood is not a material that can be discarded by light arguments.

New materials continue to be developed and deployed for superior performance. One of these, called Glare is a laminated material made of alternate layers of aluminum and glass fiber, 'Glare' standing for Glass fiber Reinforced Aluminum. Developed in cooperation between the Delft University of Technology and the Netherlands National Aerospace Laboratory (NLR) it is currently deployed

on Air bus A380 to the extent of 3 %. Its choice is due to reduced susceptibility to fatigue (what may be interpreted as high fracture toughness; the crack growth behavior of Glare is different from other materials)

Demand for even more light structures has led to the development of composites, principally, glass, kevlar and carbon fiber based composites. Sandwich structures that promise even better performance have been deployed up to 50 % in modern aircraft. The major issues that have been overcome are the methods of manufacture that give repeatable properties of structural integrity. Analysis methods that would use properties depending on the alignment of fibers in different layers of a composite structure, predicting deformation even under conditions of fatigue are other developments that have helped adaptation of these new materials. While lightness for a given strength demand is one important property, the other property enjoyed by these materials is the minimal radar cross section that helps "stealth" operations very important in military applications.

The most important development that is bound to take place in the coming decades is related to health monitoring of all the subsystems. New sensor principles and technologies for reliable data acquisition and transmission from critical locations inside the aircraft for continuous health monitoring would become the order of the day in the forseable future.

In the early times (implying the nineteen thirties to fifties) the knowledge base was built from scratch because nearly all segments were being explored simultaneously for the first time. These days, so much is known in public domain that it can be stated with certainty that the number of cycles of modifications required to realize an aircraft or launch vehicle is much smaller. Once the specifications are laid out, the schematic design of the entire system based on a simplified approach can be set out. The availability of materials and critical components will pose issues to be resolved before launching the project to realize the system.

In the hierarchy of complexity of the systems, tactical missile hardware is the simplest. Launch vehicles for satellites and strategic missiles are the next in complexity. In both these systems, strength of materials approach is considered for the preliminary design. It is usually followed by detailed analysis using FEM for specific critical components. In the case of solid propulsion systems,

the solid propellants are considered visco-elastic structural elements and analyzed for strength and to determine the boundaries of safety. For missile systems that have to withstand high temperatures (up to 70^0C), this analysis is considered essential. For large systems (up to 3 m diameter) with propellant geometry usually having sharp corners (like in star shaped cross section), possibilities of stress concentration related problems need to be studied. Of course, such studies are carried out along with experiments; the material characterization is also crucial to getting meaningful results.

Aircraft design is far more complex than missile and launch vehicle systems because aircraft is man-rated. Similar features are present for launch vehicles carrying astronauts - the Apollo mission with higher demand on physical fitness and space shuttle missions with less critical demand on physical fitness. But space operations involve much less number of civilians compared to aircraft operations. While part of the design accounts for the man-rating by enhancing the factor of safety, the reliability of components selected must be much higher. User satisfaction, firstly of the pilots and then, of passengers is a very significant new element here. Therefore, the number of cycles of review of design and associated modifications is much higher. Consequently, time to realize an acceptable product is also higher. Cost and time overruns cannot also be ruled out.

This situation will get altered once the first system is flown to satisfaction. Improvements in design will be made to the design as measured flight data on relevant parameters (like strain at several locations) becomes available. Factors of safety will get fine-tuned and the inert mass comes down making the structure more efficient.

While aero-structural design adopts strength-of-materials approach to start with, later studies are all dealt with using FEM. Large segments and the entire aircraft will be mapped for their structural content with finite elements and analysis carried out with the aerodynamic loads at all critical points on the *V-n* diagram. Structural performance is also verified for environmental conditions - low and high temperatures. Aero-elastic checks are made initially and if deviations are noticed in early flight test data, the design is revisited including these effects. Since there are long established procedures for ascertaining the validity of the design through codes, these are followed throughout (after the preliminary design).

Structural design of gas turbine engines has additional complexity of high temperatures in various segments. Compressors experience temperatures up to 400^0C, combustion chamber walls experience up to 1000^0C and turbine blades as high as 1500^0C. While turbine blades are cooled with air from one of the stages of the compressor, the temperature gradients will be high. These impose thermal stresses. All calculations must include thermal effects in the case of gas turbine engines. The development of aircraft and the engines is strongly linked to materials whose development is critical to realizing the hardware in the first instance and achieving structural efficiency subsequently. All these imply that aeronautical and aerospace developments involve a culture that includes graded levels of analysis, materials development and manufacture to high levels of accuracy.

Bibliography

[1]   Anand, L and Parks, D. M. (2004) Supplemetary notes on Defect-free fatigue, MIT opencourseware ocw.mit.edu

[2]   Akhras, G. (2008) Smart composites for smart structures, www.polymtl. ca/spequebec/documents/Expoplast_2008/Akhras.pdf

[3]   Anon. (1992) http://media.wiley.com/prouct_data ex cerpt/89/04713707/0471370789.pdf

[4]   Ashby, M. (1999) Materials Selection in Mechanical Design, 3rd edition, Burlington, Massachusetts: Butterworth-Heinemann

[5]   Ashby, M. F and Jones, D. R. H (1980) Engineering materials I, Pergamon press

[6]   Corona, E (2006) Notes on Aerospace Structures, AME 30341, University of Notredame http://web.itu.edu.tr/ mecit/uck328/kaynaklar/asdn.pdf

[7]   Courant, R (1943) Variational methods for the solutions of problems of equi-librium and vibrations, Bull. Ame. Math. Soc., V. 49, pp. 1 – 23.

[8]   DIAB handbook, 2011 http://www.zjgxx.com/search-DIAB-pdf.html

[9]   Dimitriadis, G (2009) Introduction to Aeroelasticity, AER00016, Universite de Liege http://www.ltas-aea.ulg.ac.be/cms/index.php?page=aero-elasticity-course

[10]   FAA, (2016) https://www.faa.gov/regulations_policies/handbooks_manuals/aircraft/amt_airframe_handbook/media/ama_ch01.pdf

[11]   Grantadesign, 2009 CES EDUPACK - Material and process selection charts http://www.grantadesign.com/education/edupack/index.htm

[12]   Gordon, J. E (1991) The new science of strong materials or why you don't fall down through the floor, 2nd edition, Penguin books.

[13]   Harris, R (2005) Report on A380, Boeing 747, 777, 787 aircraft; also see the Boeing and Air bus details on websites noted below

http://home.iwichita.com/rh1/hold/av/avhist/abs/a380flys.htm

http://www.boeing.com/commercial/777family/background/back5.html

http://www.globalaircraft.org/planes/airbus_a380.pl

[14] Hertzberg, R. W (1989) Deformation and Fracture Mechanics of Engineering Materials, Third edition, John Wiley and sons, p 277

[15] Hrenikoff, A (1941) Solution of Problems in Elasticity by the Framework Method, J. Appl. Mech., v. 8, pp. 169 – 175

[16] Internet1 (2011) http://www.paulnoll.com/Oregon/Birds/Avian-Skeleton.html

[17] Internet2 (2011) http://www.engineersedge.com/manufacturing_menu.shtml

[18] Internet3 (2011) http://composites-by-design.com/?page_id=17 ; also see Composite materials: testing and design (tenth volume), Editor: Grimes, G. C., (1992) ASTM Publication STP 1120, 04-011200-33

[19] Internet4 (2016) http://modernairliners.com/boeing-787-dreamliner/boeing-787-dreamliner-specs

[20] Internet5 (2016) http://www.hexcel.com/Resources/DataSheets/Brochure-Data-Sheets/Honeycomb_Sandwich_Design_Technology.pdf

[21] Johnson, E (1999) Introduction to structures, AE 1350 course notes of Georgia Inst. Technology, USA soliton.ae.gatech.edu/people/ejohnson/ae1350-Spring2011/10.structures.pdf

[22] Jones, R. M (1999) Mechanics of Composites Materials, second edition, Taylor and Francis, 1999.

[23] Koma, A. Y., and Zimcik, D. G (2003) Applications of smart structures to air-craft for performance enhancement, Canadian Aeronautics and space Journal, v.49, pp. 163 - 172

[24] Laglace, P. A (2001) Vibration of multio degree-of-freedom and continuous suystems, units 22 and 23, MIT opencourseware, ocw.mit.edu

[25] Lightning (2011) http://oea.larc.nasa.gov/PAIS/Concept2Reality/spin_re-sistance.html and www.aerospaceweb.org/question/design/q0234.shtml

[26] Lukkassen, D and Meidell, A (2007) Advanced Materials and Structures and their Fabrication Processes, Book manuscript, Navrik university, http://www.scribd.com/doc/24165910/Advanced-Materials

[27] Megson, T. H. G (2007) Aircraft structures for engineering student, fourth edi-tion, Elsevier

[28] Nasser, L A., Bonifant, R., Diggs, C., Hess, E., Homb, R., McNair, L. and Moore, E (2004) Spacecraft structures and launch vehicles, http://www.aoe.vt.edu/ cdhall/courses/aoe4065/FDReports/SLV04.pdf

[29] Nelson, E. A., and Odeh, D, J., (2009) High performance structures, Course Arch 2168, RISD, Rhode island

[30] Newman Jr, J. C (1998) The merging of fatigue and fracture mechanics con-cepts: a historical perspective, Progress in Aerospace Sciences v. 34, pp. 347 -390

[31] O'Down, N (2003) Advanced Fracture Mechanics, lectures on fundamen-tals of elastic, elastic-plastic and creep fracture, Imperial college, London http://www.docin.com/p-81841283.html

[32] Paris, P. C., Tada, H. and Donald, J. K (1999) Service load fatigue dam-age - a historical perspective, International Journal of fatigue, v. 21, pp S35 - S46 www.elsevier.com/locate/ijfatigue

[33] Peery, D. J and Azar, J. J. (1982) Aircraft structures, Second edition, Mc-Graw-Hill Book Co.

[34] Peiro, J. and Sherwin, S., (2006) Finite difference, Finite element and Fi-nite volume methods for partial differential equations, Chapter 8, Hand-book of ma-terials modeling, V. 1: Methods and Models, pp. 1 - 32

[35] Rao, P. N. A. P., Shamanna, K. N., and Nagabhushana, G. R., (1997) Lightning test facility for light combat aircraft, Proc. of the Int. Confer-ence on electro-magnetic interference, Bangalore, http://ieeexplore.ieee.org/xpl/login.jsp?tp=&arnumber=669837

[36] Rollett, R. D (2015) A range of useful lecture material including micro-structure property relationship http://pajarito.materials.cmu.edu/rollett/27301/27301.html

[37] Roylance, D (2001) Introduction to Fracture Mechanics, MIT open course-ware lectures in the department of materials science and engineering-http://ocw.mit.edu/courses/materials-science-and-engineering/3-11-mechanics-of-materials-fall-1999/modules/frac.pdf

[38] Schruers, P. I, G., (2012) Lecture notes http://www.mate.tue.nl/ piet/edu/frm/pdf/frmsyl1213.pdf

[39] Summerscales, J. (2010) Smart materials, intelligent structures and bio-mimet-ics, www.scribd.com/doc/49256221/MATS324A14-smart

[40] Suresh, S (1998) Fatugue of materials, 2nd edition, Cambridge university press; also see his lectures on fatigue in MIT opencoursewaremit. nelc.edu.eg/OcwWeb/Materials-Science-and-Engineering/3-35Fall2003/LectureNotes/index.htm

[41] Timoshenko, S. P., Strength of Materials, Part I, Elementary Theory and Prob-lems, D. Van Nostrand Company, 3rd Ed. 1955; Strength of Materi-als, Part II, Advanced Theory and Problems, D. Van Nostrand Company, 3rd Ed. 1956.

[42] Timoshenko, S. P., and Gere, J. M., Theory of elastic stability, 2nd edi-tion, Dover Publications, 1961

[43] Wei, R. P (2010) Fracture mechanics - integration of mechanics, material sci-ence and chemistry, Cambridge University press

[44] Uman, M. A and Rakov, V. A (2003) The interaction of lightning with airborne vehicles, prog. Aerospace Sciences, v. 39, pp. 61 - 81

[45] Vlot, A (2001) Glare: History of the Development of a New Aircraft Mate-rial, Kluwer Academic Publishers

[46] Wikipedia1 (2011) http://en.wikipedia.org/wiki/Space_Shuttle_Colum-bia_disaster

[47] Wikipedia2 (2012) http://en.wikipedia.org/wiki/Buckling

[48]   Wikipedia3 (2011) en.wikipedia.org/wiki/Fatigue_(material)

[49]   Wikipedia4   (2011)   http://en.wikipedia.org/wiki/Aloha_Airlines_
       Flight_243

[50]   Wikipedia5 (2011) http://en.wikipedia.org/wiki/Alan_Arnold_Griffith

[51]   Wikipedia6 (2011) http://en.wikipedia.org/wiki/Vibration

[52]   Wikipedia7 (2011) http://en.wikipedia.org/wiki/Aeroelasticity

[53]   Wikipedia8 (2016) https://en.wikipedia.org/wiki/Shape-memory_alloy

[54]   Wikipedia9   (2016)   https://en.wikipedia.org/wiki/Tacoma_Narrows_
       Bridge_(1940)

[55]   Wikipedia10 (2016) https://en.wikipedia.org/wiki/RMS_Titanic

[56]   Wikipedia11 (2016) https://en.wikipedia.org/wiki/De_Havilland_Comet

[57]   Wood, H. A., and Engle Jr, R. M., (1979) USAF damage tolerant design
       handbook: Guidelines for the analysis and design of damage tolerant air-
       craft, Technical report AFFDL-TR-3021, Wright Patterson Air force base
       www.dtic.mil/dtic/tr/fulltext/u2/a078216.pdf; also see Gallagher's docu-
       ment at http://www.dtic.mil/dtic/tr/fulltext/u2/a141899.pdf

7

Navigation and Guidance

7.1 Introduction

Navigation and guidance are closely linked functions in which guidance constitutes the strategy to move from one location to another with the help of necessary control systems. Early aircraft navigational approaches depended on what has been known as "pilotage" implying looking out of the aircraft, seeing the land marks, identifying known areas and moving towards the destination. Of course, compass and maps in hard copy were always in the cockpit for guidance. The map would have various land marks indicated prominently to help the pilot identify features on ground.

A follow-up strategy was what is known as dead reckoning where initial position, direction and speed of flight were used to determine one's position and move from one place to another. Celestial navigation was used in aircraft till the arrival of inertial and Doppler based navigational systems; it was not exactly pilot-friendly because the time available for navigation would be very limited As a matter of history, Boeing 747 had an sextant port in the roof of the cockpit for celestial navigation that was phased out in the early nineteen sixties. While these approaches needed visibility of the environment, unanticipated clouded weather conditions that caused many accidents needed an alternate approach for flight safety. The demand for "blind" flight and greater accuracy of location as well as motion was dealt with by invoking radio based instruments.

The First World War (1914 - 1918) saw the development and use of two-way radio communication from ground-to-air as well as between aircraft. Radio beacons got established and were used by pilots to know where they were and plan out the route on their maps. Navigator was an important part of the cockpit in trans-Atlantic flights in the early nineteen-thirties. On-board communication equipment, radar based navigational aids were introduced during the World War II period; solid state electronics followed. Beyond this point, communication, navigational and guidance tools were considered very important. Theoretical advancements of ideas in inertial navigation, global positioning systems with satellites and practical realization using digital electronics enabled size, weight and cost reduction of the devices and the achievement of greater accuracy in the information on location, speed and environment. The benefits have flowed into civilian and military aircraft, into tactical and strategic missiles, and launch vehicles for both civilian and military use.

Bird and insect navigational skills of flights over long distances have provided challenging questions in biology and navigational strategy with one skill directly related to quantum mechanics (see section 7.8). These will be discussed in some detail in the following sections.

7.2. Navigational Aids for Aircraft

Several kinds of radio aids have been in practice for a long time. Radio waves are more than a million times longer in wave length compared to visible light (radio waves have a wave length of 1 mm to 100 km and visible light has a wavelength range of 0.35 to 0.8 microns). Low frequency radio waves using large antennas and with wavelengths of the order of a km follow the curvature of the earth. Higher frequency waves travel straight and hence line-of-sight reception is the solution. However, they can also be received as a reflected wave since these waves get reflected from several layers (D, E, F1, F2) of the ionosphere as frequency is increased. Higher the frequency, greater is the penetration and reflection from higher and higher layers. This different layers were briefly alluded to in Chapter 1, section 1.1.1.

Navigation becomes possible due to two sets of equipment - on ground and/or in space and on-board the aircraft. Some approaches are passive and others active. Passive implies that the information broadcast from ground is received on-board the aircraft and inference is made inside the aircraft. Active implies, there is a signal generated by the aircraft and sent to the ground and on interrogation response is received from the ground station. Further, when air-traffic control station on ground monitoring the status of aircraft sends a signal, the "transponder" on-board the aircraft responds. Radar in the air-traffic control station with "plan position indicator" is an active system since it scans the sky for aircraft using a transmitted signal, and the reflected signals are set out on the screen. Basic procedures of estimation of distances and location use the time of travel of electromagnetic waves with a speed of 300,000 km/s. Signal-to-noise ratio management requires many techniques and these have evolved over a time.

Most of the navigational aids are set out in Table 7.1. As the table indicates, beacons are found in large numbers to enable any aircraft to receive a signal with its code to enable locating the relationship of the aircraft (as well as other vehicles) with those of the beacons on the ground. The non-directional beacon

Table 7.1.: Radio based navigational aids G/S = Ground stations/Satellites; VOR = very high frequency omni-range; LORAN = Long range navigation; ILS = Instrument landing system; DME = Distance measuring equipment; TACAN = Tactical air navigation; GPS = Global Positioning Satellite(American); GLONASS = GLObal NAvigational Satellite System (Russian)

System	Frequency	Hz, Band	No. G/S
Beacon	200-1600	kHz, LF	4000
VOR	108 - 118	MHz, VHF	1500
LORAN	100	kHz, LF	50
ILS	108 - 112	MHz, VHF	1500
	329 - 335	MHz, UHF	
DME	962 - 1213	MHz, L	1500
TACAN	962 - 1213	MHz, L	850
Radio Altimeter	4200	MHz, C	-
Weather radar	10	GHz, X	
Airborne Doppler radar	13-16	GHz, Ku	
Weather radar	9.4	GHz ,SHF	-
GPS-GLONASS	1227, 1575	MHz, L	24 + 24

signals follow the curvature of the Earth, so that they have a much longer reach at lower altitudes unlike higher frequency aids like the very high frequency omni-range (VOR) system. However, the beacon signals will be affected by electrical storms, coastal reflection and mountainous terrain. The automatic direction finder (ADF) that is a part of the airborne equipment determines the direction or bearing to the beacon relative to the aircraft by using a combination of directional (cardioid pattern) and non-directional (sinusoidal pattern) antennae to sense the direction in which the combined signal is strongest. The very high frequency device (VOR) is sometimes combined with distance measuring equipment (DME) when it is termed VOR/DME and with tactical air navigation (TACAN) in which case it becomes VORTAC. Figure 7.1 shows the ground system arrangement for VOR and TACAN systems. TACAN was designed so that a small team could put a system into unprepared field for use; it is a military option that can be made available or denied for civilian use. The DME part provides for pulse distance measurements at a different frequency. The time delay for an aircraft to interrogate a VORTAC station and receive a reply is multiplied by the velocity of electromagnetic wave (velocity of light in the medium) to provide distance information. TACAN is a more accurate ver-

Figure 7.1.: The beacon is a combination of a Doppler VOR with a circle of orange balls and a TACAN identified by the cylinder in the centre. The ground station emits directional radio signals all around. The communication is line-of-sight dependent. Triangulation of position requires information from multiple stations

sion of the VOR/DME system that provides bearing and range information for civil aircraft.

Space shuttle was designed to use TACAN navigation but later was upgraded with GPS as a replacement. Some of these capabilities have been upgraded over a period of time to include an air-to-air mode where two airborne users could get relative slant-range information. Depending on the system installed, this mode may provide range, direction and relative velocity of the other aircraft. The non-directional beacon is considered a last resort if other systems like VOR and GPS fail.

LORAN (meaning Long Range Navigation) that functions as a beacon with a long range because of the use of even lower frequencies (up to 100 kHz). Also it is also used for non-precision approaches to airports without much cloud cover with typical accuracies of about 0.4 km, limited by propagation uncertainties over the terrain between the transmitting station and the aircraft. The measurement of 100-microsecond time differences is possible with low quality clocks (one part in 10,000) in the aircraft.

LORAN can be considered a coarse precursor of GPS and a stand-alone navigation aid whenever GPS is out of service. Navigational support is also provided by European or Russian navigation satellites and private navigation-commun-
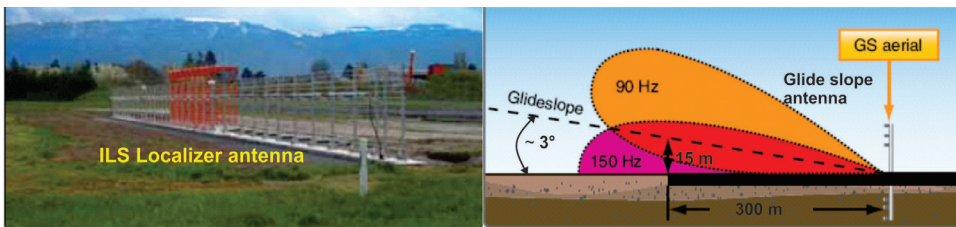
Figure 7.2.: ILS antenna system: The localizer provides guidance to horizontally align the aircraft to the runway. The glide slope antenna provides signals to be along the glide slope of about 3^0 from the horizontal

ication satellites. India has also recently established an independent navigational system called IRNSS - Indian Regional Navigation Satellite System that is composed of seven satellites, three satellites being located in suitable orbital slots in the geostationary orbit and the remaining four in geosynchronous orbits with the required inclination and equatorial crossings in two different planes; all the satellites are of identical configuration. Chapter 1, section 1.2.13 describes aspects connected with IRNSS in some detail. All satellite based systems are more accurate than LORAN but are subject to outages due to solar flares and jammers. On short over-ocean flights, the inaccuracies in the estimation of speed can be up to 4 km/h. When an aircraft approaches shore, the VORTAC network updates the inertial state vector and navigation continues to the destination using VORTAC. On long over-ocean flights either trans-pacific or polar, GPS can be used alone but is usually used with one or more inertial navigators to protect against failures. With respect to the Instrument Landing System (ILS) (see Figure 7.2), transmitters are set adjacent to the runway create a horizontal guidance signal near 110 MHz and a vertical guidance signal near 330 MHz. Both signals are modulated and transmitted from antennas whose nulls intersect along a line in space 2.7 - 30 above the horizontal and on a vertical plane through the runway centerline, that may lead an aircraft from a distance of about 30 km to a point 15 m above the runway.

ILS gives information on the aircraft location along the beam at two or three vertical marker beacons. Navigational aids and associated operations form an important part of pilot training and many manuals are produced by each aircraft and equipment manufacturer. Hence, many details of navigation systems are outlined in the training manuals (internet1 - internet4, 2015).

7.3. Inertial Navigation - Gimballed and Strap-down

Inertial navigation is related to the direct integration of the acceleration as d^2X/dt^2 where X is the position vector. The measured acceleration is integrated once to give velocity and twice to obtain position. This gives the movement of the vehicle as a mass point. In order to obtain the attitude of the vehicle, the rotational motion is measured using gyroscopes. Accelerometers (for measuring linear acceleration), rate gyroscopes and integrating gyroscopes are the instruments that are mounted in (a) a gimballed frame inside a frame using three gimbals for isolating the interior from external rotations about the bearing axis. This is also called stabilized platform, the measuring instruments will be set in a space fixed coordinate system, also called inertial frame of reference or (b) fixed to the vehicle, also called strap-down system where the vehicular motion directly influences the measurements. These are pictorially set out in Figure 7.3.

There are several varieties of gyroscopes. Ordinary attitude gyros indicate angular displacement, bank or pitch. Rate gyros indicate rotational speed. Rate integrating gyros indicate the product of the rate of turn and the time that the rate is active, and therefore provide rotational distance or angular displacement. Rate integrating gyros are used in special cases where greater output accuracy over a small angular movement is required. There are different kinds of gyroscopes developed over the last six decades, the more recent ones that have found great use in aerospace systems are fiber-optic gyros (FOG, see internet2, 2016 on gyroscopes for details) as well as ring laser gyroscope (RLG). The fiber-optic gyro uses a coil of fiber optic cable about 5 km long. A laser beam passes through a beam splitter and the two split beams pass through the cable in oppositer directions. The light beams after they have traversed the length of the fiber are collected in a detector. There will be interference of light due to different passage lengths of the laser beam when the coil is subject to rotation. This interference is proportional to the rate of rotation of the coil, and is a direct measure of the rotation of the vehicle on which the coil is mounted. Figure 7.4 shows schematically the details of an RLG.

A small fraction of light from the two laser beams passes through one of the mirrors. The beams are combined by the optics to produce a beat frequency. This takes the form of a fringe (interference) pattern. This beat frequency of
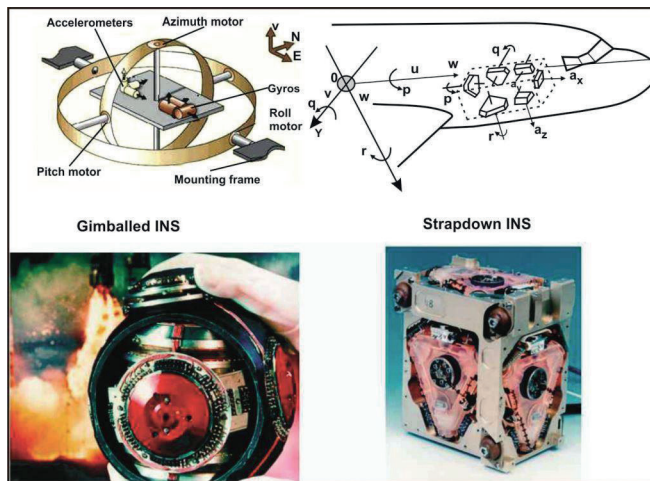
Figure 7.3.: Gimballed and Strapdown inertial navigation systems, drawn from Tempere, 2015
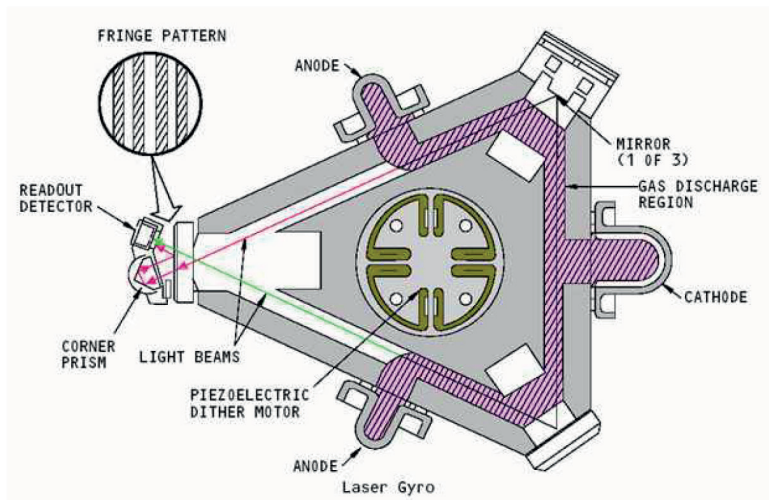
Figure 7.4.: Schematic of ring laser gyro, adopted from Makris, 2016

light is very similar to beat frequency in acoustics. The final result is a fringe pattern of alternate dark and light stripes. Photo-diodes sense the fringe pattern rate and direction of movement. The frequency and relative phase of the

two outputs indicate magnitude and the direction of the gyro's rotation. At low rotation rates, the small frequency difference between the laser beams leads to beam coupling. This locks the frequencies together at a single false value. Compensating for this effect calls for the use of a peizo-electric dither motor (shown in Figure 7.4) that is used to vibrate the laser block through the lock-in region. Dither vibration is set such that there is no net inertial rotation.

The interference effect which is the basis of both RLG and FOG is called the Sagnac effect after French physicist Georges Sagnac. The principles behind the conventional gyroscope and fiber optic or ring gyroscope are different. A conventional gyroscope relies on the principle of conservation of angular momentum whereas the sensitivity of the ring interferometer to rotation arises from the invariance of the speed of light for all inertial frames of reference. Regarding the last point, there has been much debate whether the Sagnac effect is classical or relativistic and if it is the latter, does it disprove theory of relativity (see internet3, 2016), even if its use based on the experimental work of Sagnac is not affected by relativistic effects. That it is classical is the conclusion and it is deployed even in GPS system design (Ashby, 1979). With the development of RLG and FOG, the bulky mechanical gyroscope is replaced by one having no moving parts in many modern inertial navigation systems. Most aircraft and long range missiles use ring laser gyroscopes primarily because their "bias stability" is better than 0.01 degree per hour an important requirement in military and civil transportation vehicles. They have been used in Airbus 320, Boeing 757 and 777, as well as Agni missiles III, IV and V developed in India.

INS navigation systems are autonomous and do not rely on any external aids. They are immune to jamming and inherently stealthy. They neither receive signals nor emit detectable radiation and require no external antenna that might be detectable by radar. On the negative side, the time required to initialize the position and attitude is large and the navigational errors increase with time. The answers to these problems lie in coupling the INS with the GNSS (GPS). If GNSS becomes unavailable, INS continues to be available and when available helps align fast and increase the accuracy of measurements.

Display of the flight data acquired by the instruments would be with mechanical gadgets. Gyroscopic motions and pitot-static pressure sensors would be mechanically acquired and translated on to an analog dial or guage. The de-

velopment of miniaturized sensing systems and digital electronics has made it possible to display the data on rightly sized LCD screens. This cockpit display arrangement is termed as "glass cockpit" as against the earlier version of "steam cockpit". This changeover has helped reduce the number of flight crew and has allowed pilots to focus only on the most pertinent actions. Many early versions of Boeing 757 and 767, as well as Airbus A300 and A310 had electronic systems to display attitude and navigational information and traditional mechanical gauges for airspeed, altitude, vertical speed, and engine performance. Later, aircraft have nearly completely replaced the mechanical gauges and warning lights of earlier generations of aircraft, although some analog instruments are retained as backups.

7.4. Navigational Aids for Launch Vehicles and Long Range Missiles

One of the key aids in navigation for launch vehicles and long range missiles is the global navigation satellite system (GNSS) apart from INS. GPS (one example of GNSS) functions through three segments: space, ground control and user. The space segment consists essentially of 24 satellites carrying atomic clocks. There are four satellites in each of six orbital planes inclined at 55^0 with respect to earth's equatorial plane, so distributed that from any point on the earth, four or more satellites are almost always above the local horizon. The satellites send out navigation and timing signals. The ground control segment is comprised of a number of monitoring stations which continually gather information from the satellites. These data are sent to a Master Control Station in Colorado Springs (USA) where analysis is performed of the needed astronomical events and updating various user related information into the satellites. The user segment has aircraft pilots or launch vehicle operators who have a system that uses the signals from the satellites to determine their position and velocity.

Nearly every aircraft is fitted with GPS along with other navigational aids these days. This multi-option arrangement is considered essential as the pilot may need to rely on others in times when GPS or a few others become unavailable. The information from these aids and sensor data on speed, local ambient conditions are all presented to the pilot and co-pilot to help them fly the aircraft to the destinations. Advances in sensor science and technology, on-

board computers, materials and manufacturing processes have all contributed to reduced weight and volume of the systems and greater use of them in all aircraft. The accomplishment of higher safety in air travel has led to the cost of advanced aircraft these days being significantly influenced by avionics.

7.5. Radars

Radar meaning radio detection and ranging is one of the extensively developed and used radio based device for aeronautical and other civilian applications. It uses a wavelength of about a millimeter to about hundred meters (implying frequency of 300,000 MHz to 3 MHz). While early ideas on radio detection were explored in the early nineteen hundreds, engineering practical systems for aircraft applications is credited to Robert Watson Watt (UK) in 1935 during World war II. Over the last seventy years, many technological innovations with variants have occurred. These variants are classified as pulsed or continuous wave systems depending on the wave form, operating frequency (UHF, L, S, C, X and Ku), mono-static, bi-static or multi-static depending on the separation of the transmitter and receiver, primary or secondary depending on whether it is aided by the target, and coherent, non-coherent or phased array depending on the type of radiators, receivers, processing and applications. Radar frequencies (with designations) used in a variety of applications are set out in Table 7.2.

In the case of a mono-static radar, both the transmitter and receiver are in the same location; in the case of bi-static radar, the transmitter and receiver are in different locations and in the case of multi-static radar, there is one transmitter, but several receivers placed in different locations or several bi-static radars spatially distributed. Distributed arrangement allows for data fusion from different radars and hence better target characterization or surveillance as demanded.

Primary radars send out a signal that will be reflected by aircraft and this reflection is received by the radar (at much reduced intensity). This is presented on a screen to indicate the aircraft (or an aerial object). In secondary surveillance radar, the aircraft has another aid (called transponder) that transmits back a signal on receiving an interrogation from a ground station. This interrogation may occur at one frequency (1.03 Ghz) and the transponder on the aircraft transmits back its signal at another frequency (1.09 GHz) and higher

Table 7.2.: Typical features of radars (very long range surveillance
~ 10000 km; Medium range ~ 3000 km short range ~ 400 km)

Band Designation	Frequency range	Usage
HF	3 to 30 MHz	OTH surveillance
VHF	30 to 300 MHz	Very long range surveillance
UHF	0.3 to 1 GHz	Long range surveillance
L	1 to 2 GHz	Long range surveillance
		Air traffic control (ATC)
S	2 to 4 GHz	Medium range surveillance
		Terminal traffic control
		Long range weather
C	4 to 8 GHz	Long range tracking
		Airborne weather
X	8 to 12 GHz	Short range tracking
		Missile guidance
		Marine applications
Ku	12 to 18 GHz	High resolution mapping
		Satellite altimetry
	27 to 40 GHz	Very high resolution mapping
		Airport surveillance

power. This transmission can contain the identification of the aircraft and its altitude in some instances. Such system is also termed IFF (identification friend or foe). Air traffic control radars function for the purpose of IFF, to help precise approach under conditions of very low visibility, to provide surveillance cover for take off, landing and taxiing, for monitoring weather to measure rain and strong wind-shear, and to help enroute check for a long range (nearly 500 km). Somewhat similarly, air defence radars act as early warning systems to detect enemy aircraft or missiles, to guide air patrol aircraft and to help defence against medium range ballistic missiles. They are also used by army and navy in similar applications. Battlefield radars are used in various modes. For surveillance, to alert combat troops of hostile and unknown aircraft, cruise missiles and unmanned aerial vehicles, for navigation to fix the position of a ship with sufficient accuracy to allow safe passage and for weapon control by providing information used to guide missiles/weapons to an enemy target.

They are composed of an antenna that radiates electromagnetic energy into the surroundings and also receives radiation from the surroundings. The radiation received is processed along with the radiated signal to get results that can be displayed. In pulsed systems, a sharp energy pulse of the energy is directed by the transmitter for a short time, and the switch is turned to reception mode to a sensitive receiver for another brief while during which the response from the surrounding is received. The radar antenna is to be directed to the segment of the sky to be scanned physically or otherwise. What is received depends on how much of energy is reflected back from whatever object lies in its path at the time the pulse was sent. Figure 7.5 shows the features of signal transmission and reception. The time difference between the moment radiation is sent out and the moment some fraction of it received multiplied by the speed of light in the medium gives double the slant distance between the source of radiation and the object.

The design issues are the choice of the frequency of transmission, pulse width, accounting for radar clutter (unwanted echoes from surrounding medium), distinguishing between different flying objects and their speed. The radar can be mounted on ground or on the aircraft surveillance of objects on ground or atmospheric features including rain. In all these cases there is need to use mathematical tools and so, the on-board computer to process the signals to extract many features and enhance the signal-to-noise ratio. Several technical details of radars for a variety of applications are set out in Table 7.3. As can be noted the capability of the range varies over two orders of magnitude. The mean power required for good radars is in the range of several MWe. The peak-to-mean power ratio also varies from about 10 to 1000 depending on the specific use.

Antenna is basically a conducting structure into which alternating current of specific frequency is introduced. This oscillating current of electrons in the antenna creates an oscillating magnetic field around the antenna, while the charge of the electrons also creates an oscillating electric field along the elements. These time-varying fields radiate away from the antenna into space as a moving transverse electromagnetic field wave. During reception, the oscillating trons in the antenna elements, causing them to move back and forth, creating oscillating currents in the antenna. The design of the antenna directly controls the way energy of radiation gets distributed over the surrounding space. The right hand side of the Figure 7.5 shows the radiation intensity distribution over the azimuth for a omni-directional antenna as well directed antenna. Directed.
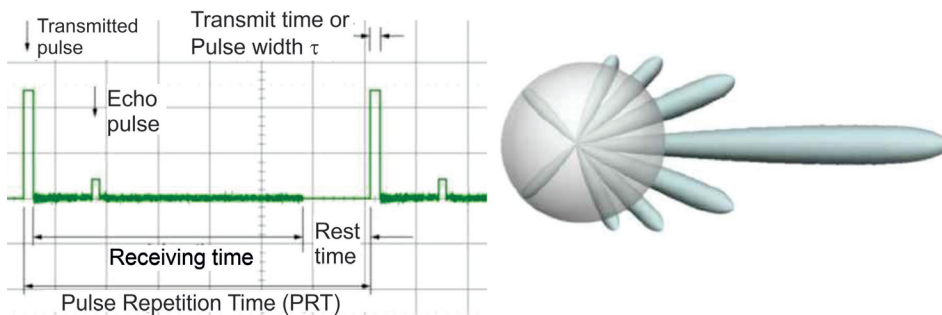
Figure 7.5.: Principles of functioning of radar - signal transmission and reception times (left); radio transmission intensity in the azimuth - the circular radiation pattern from an omni-directional antenna and lobed intense radiation from a directed antenna

Table 7.3.: Technical aspects of radars

Parameter	Long range	Medium range	Surveillance	Short range	Units
	10000	3000	400	100	km
Peak power	50	100	30	0.0013	MWe
Mean power	2	1	0.03	0.0001	MWe
Frequency	0.03 - 1	1 - 2, 2 - 4	4 - 8	8 - 12	GHz
Designation	VHF, UHF	L, S	C	X	
Pulse duration	2	0.1	0.005	0.001	ms
Pulse rep.Freq	20	100	200	1000	kHz
Duty cycle	0.04	0.01	-	-	

antenna is far more used option in most applications.

While early developments deployed klystron based transmitters that were large with large sized receiver electronics, the development of solid state (based on gallium arsenide) micro-electronics in later times brought down the size very drastically.

In a normal transmission-reception situation, the signal strength during reception is much lower than in transmission. The reason for this is that when radiation is transmitted, the flux received at any surface far away is $RCS/(4\pi r^2)$ where RCS is the radar cross section of the intercepting surface and r is the radial distance of the surface from the source. If the antenna beam is shaped such that the peak beam radiation is larger than the mean radiation, The flux

received will now become $RCS\ G_T/4\pi r^2$ where G_T is the antenna gain for transmission being the ratio of the peak to average power. The radiation that the surface at a distance r responds to will be diffuse and will also generate a flux at the reception point as $RCS GT\ A_{eff}/(4\pi r^2)$ where A_{eff} is the effective cross section of the receiver (in area terms). The effective antenna area is related to the wavelength of the radiation through the expression Antenna Gain = G_R = $4\pi Aeff/\lambda^2$ obtained from antenna theory (one can obtain large reading material from internet. see for instance, Ray Kwok, 2016). Thus the ratio of the power received to power injected varies as $G_T\ G_R\lambda^2 RCS/(54\pi^3 r^4)$. The electromagnetic wavelength, $\lambda = cf$ where c = the velocity of electromagnetic radiation and f is the frequency of the radio wave. If we now factor loss coefficient, L_s, we can write the "Radar equation" (Budge, Jr, 2011) as

$$\frac{P_{recd}}{P_{peakinp}} = \frac{G_T G_R \lambda^2 RCS}{4\pi^3 r^4 L_s}$$

(7.1)

where P_{recd} and $P_{peakinp}$ are the peak received power and peak input power respectively and L_s is the factor to account for the loss of signal through atmospheric effects, beam shape and mismatch in the filters (the loss can be as much as 30 %). If the transmitter and the receiver are the same or have identical antennas, $GT = GR = G$. By selectively directing the antenna radiation, implying that G is made large, the strength of the signal received can be enhanced. The antenna on the ground radar is rotated horizontally and vertically to cover the volume of space and enable higher reception signal strength from individual targets. If the radar is in a track mode, the antenna is moved in order to point to the target continuously or frequently.

For a typical set of parameters: $P_{peakinp}$ = 1 MW (same as $10\ \log_{10}[10^6 W/1W]$ = 60 dB), G = 1900 (32 dB), λ = 0.11 m, RCS = 1 m², L_s = 128 W (21 dB), if the minimum detectable signal is 0.005 μW, we get the maximum distance at which the aircraft of a RCS of 1 m² can be picked up is 76 km.

One can derive significant conclusions from the radar equation 7.1. Detecting flying objects at large distances is very tough indeed. Improving the antenna gain is very essential in such cases. Radar cross section plays such an import
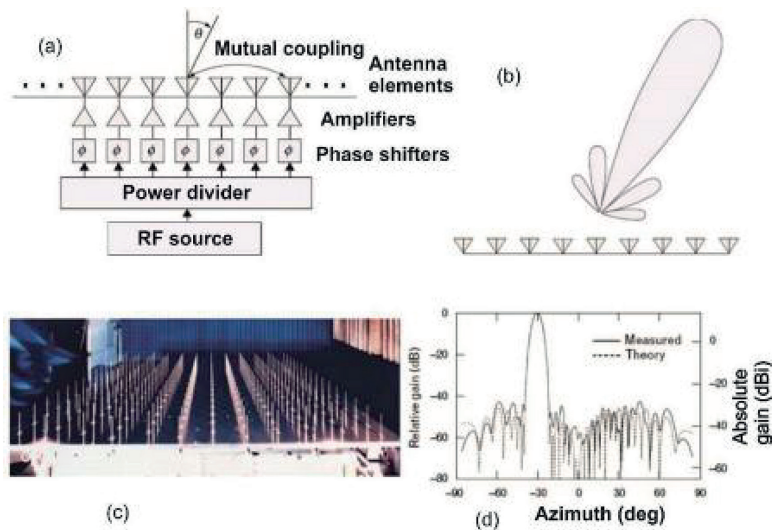
Figure 7.6.: Phased array radar (a) The system arrangements with antennas, individual amplifiers, phase shifter and power supply, (b) The radar beam with main and side lobes,(c) An L-band 96 mono-pole radiating phased array radar on a test bed and (d) A comparison between theoretical and experimental measurements of radiation

Table 7.4.: Radar cross section of several vehicles

Flying vehicle	RCS (m²)	RCS (dB)
Boeing 747 - 787	80 - 120	19 - 21
Boeing 737 class	20 - 40	13 - 16
Large fighter class	6 - 8	8 - 9
Helicopter	3 - 4	5 - 6
Executive aircraft	1.5 - 2	2 - 3
Small aircraft	~1	~0
Stealth jet	0.01 - 0.1	- 10 to - 20

ant role that for civil aircraft it is desirable to have a large RCS and for military aircraft and missiles it is very desirable (considered essential) to reduce the radar cross section. Typical values of RCS are set out in Table 7.4.

7.5.1. Phased array radar

Phased array radar (see Figure 7.6) performs electronic scanning using an array of antennas with radiation injected at slightly different phases. The elec-
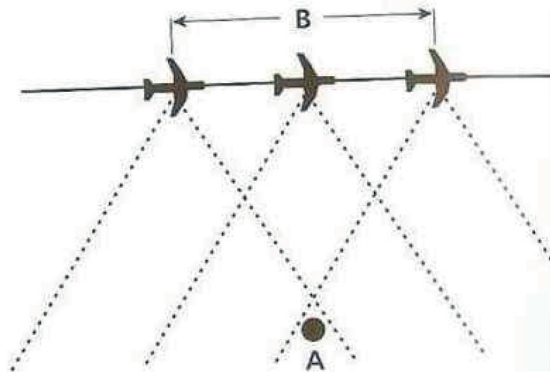
Figure 7.7.: Synthetic Aperture Radar - The signals from the region denoted A will arrive at the radar on-board over a period of time in which the aircraft moves through region B. This constitutes the "antenna" since the object is observed over this space and time

tronic switching overcomes the limitations of mechanical scanning reducing the time scale of operations. On a two-dimensional array, electronically controlled operation creates beams that can be moved from one region of sky to the other, can be broadened or sharpened as desired; it is also possible to change the frequencies of transmission in different pulses. Thus a whole range of options can be exercised over very short durations enabling complex tracking as well as surveillance and combined mode operations.

One of the key problems of phased array radars is called mutual coupling by which is meant that a part of the radiation from each element is received by the surrounding elements and gets re-radiated. Mutual coupling depends strongly on the spacing of the elements. Half-wave length spacing is to be avoided to reduce the mutual coupling. Further, the phase shift angle needs to be optimized to enhance the directional beam strength in comparison to those in other directions. The history of the development of radars is enchanting (see for instance, internet2, 2016 on the history of radar) and many technologies with improved capabilities have been developed for a large range of civil and military applications on ground, sea and atmosphere and space over this period. A detailed description of the development of phased array radar can be found in Fenn et al (2000).

7.6. Synthetic Aperture Radar (SAR) and Moving Target Indicator Radar

A Synthetic Aperture Radar (SAR) is a either an airborne or spacecraft mounted radar that uses the flight path of the mounted platform to simulate a very much larger antenna electronically and that generates high-resolution remote sensing images as shown in Figure 7.7.

The process of image analysis involves storing the electronic signals and processing the magnitude and phase information over successive pulses. After a given number of cycles, the stored data is recombined including the Doppler effects to create a high resolution image of the terrain being over flown. The SAR works in a manner similar to phased array, but without the large number of physical antenna elements. The data from a single antenna is interpreted in time-multiplex mode. The size of the antenna is essentially the speed of the platform (aircraft/space craft) multiplied by time duration over which the data is acquired for a given field of view. This constitutes the synthetic aperture. Stated differently, the process can be interpreted as combining the series of spatially distributed observations as if all had been made simultaneously with an antenna as long as the beam width and focused on that particular point. The "synthetic aperture" simulated at maximum system range by this process not only is longer than the real antenna, but, in practical applications, it is much longer than the radar aircraft, and tremendously longer than the radar spacecraft. By making the period of data collection and analysis large, the aperture (antenna) appears large. While a detailed description of nearly all aspects of SAR can be found in Moreira et al (2013), brief history and details are set out in Wikipedia (2016).

7.7. Navigational Aids for Missiles

Missiles are built in a wide variety: surface-to-surface, surface-to-air, air-to-air and air-to-surface with range from a few km to ten thousand kilometers. The smaller systems usually carry conventional warheads and are called tactical and while the long range systems usually carry nuclear warheads and are called strategic. Missiles with ranges of several hundreds to a few thousands kilometers are often termed IRBMs (intermediate range ballistic missiles), those with longer ranges are called ICBMs (intercontinental ballistic missiles) and those launched from sub-marines referred to as SLBMs (subma-

rine launched ballistic missiles). There was a huge pile of these missiles both in USSR and the USA from the sixties. Mutual suspicion and buildup of a stock of nuclear-tipped missiles during the cold war after World War II and got reduced slowly through a series of bilateral negotiations and treaties that have not completed their course yet. The number of IRBMs, ICBMs and SLBMS in their stockpile is still very large (thousands). Of course, in the intervening period, other countries have developed their own strategic missile systems.

Tactical missiles use two principal guidance strategies - homing and command. In the homing strategy, the missile senses the target by some device and then guides itself on to the target by commanding the control surfaces on its own. Homing can be achieved by one of three approaches- passive, semi-active and active. In the case of passive approach, the missile senses and tracks the target using the radiation emitted by the target itself. For instance, if an aircraft is flying away, the exhaust leaving the aircraft will have temperatures of 500 to 1000^0C and at these temperatures fairly strong and characteristic infrared radiation is emitted. The seeker on-board the missile detects the radiation, measures the direction of the radiation with respect to the missile and provides input to the control system to direct the missile's trajectory towards the source of the radiation. Other electromagnetic radiation detection strategy can also be devised.

In the case of active approach, the missile tracking the target carries a source of radiation, say a radar. It transmits the radiation and receives the reflected radiation from the target and detects it. This signal is processed and serves as the input into the control system for maneuvering the missile towards the target. This strategy calls for the missile carrying a radar for transmission of signals. In the case of semi-active homing system, the active signal generation part is transferred to a ground system. The missile carries largely the target detection system. It also will have the ability to differentiate between the signal from the on ground illuminator and that from the target by reflection. One strategy is to use the Doppler frequency difference based on the fact that the missile is moving away from the illumination source and approaching the moving target leading to higher Doppler frequency of the latter. In all the three cases, the missile should have the ability to maneuver in the lateral plane - the missile should be structurally strong enough to withstand pulling so many lateral g's (as high as 25).

As different from the homing guidance strategy, one can also have command guidance system. In this approach, the ground system tracks the target and sends signals to the missile for performing the maneuvers required to reach the target.

In the case of command guidance, the missile does not carry any target tracking element with it. The tracking segment is dealt with by a ground system that may have two separate performing systems for the missile from its launch point and the target or be integrated into a single unit. Tracking can be performed with optical, infrared, laser or radar systems or some combination as needed. Tracking and generating the commands required to be fed into the control system of the missile to get to the target is performed by the ground computer aided system. The missile has a receiver for these commands and acts on them through the operation of the control surfaces. Further commands on arming the war head and detonation are all sent from the ground. These systems are good for relatively short range targets since the energy put into the radiation for tracking the target will become very large at larger distances. Also at shorter ranges larger radiation received by the target can be used by the target (an aircraft, say) to take evasive actions. Beam rider technology is a form of command guidance. The missile senses its displacement from the beam center, and uses it to derive the control signals to align itself to the beam center so that it can intercept the target. There are also variants to this approach depending on how much hardware is to be put into the missile and how much on ground. One variant of the command guidance is the command line of sight system in which the missile's displacement from the beam centerline is sensed on the ground and the missile is commanded to stay close to the line of sight between the ground system and the target.

In homing guidance, there are several possibilities of structuring the guidance law. These are proportional navigation, pure pursuit, deviated pursuit, lead pursuit and pure collision. Amongst these, the proportional navigation law and pure pursuit law are more common. The difference between the two is that in pure pursuit, the missile aims towards the current position of the target (and hence, turns at the same rate as the missile-target line of sight) while in the proportional navigation, the missile turns at a rate faster than the line of sight, the ratio called the navigational constant. In the guidance and control function of the missile is set so that its lateral acceleration is made a combination of

the navigational constant and the missile-target closing velocity. The choice is ideally made such that the final interception takes place when the rate of line of sight becomes zero. The Surface-to-Air (SAM) missile series from Russia - SA6, SA7, SA8 and SA9 have used semi-active homing, passive homing, and command and passive homing strategies. Amongst other SAMs and Air-to-Air missiles the use of various guidance strategies is spread over all the three approaches. A very detailed account of guidance systems, and the basic algorithms used on weapon systems is provided in Siouris (2004).

In respect of strategic systems, there are three segments of flight. The launch phase with guidance and control to let the payload achieve a specific velocity at a specific location. When the payload is released at this altitude (second phase), it will take a ballistic trajectory in space, and this phase takes a long time depending on the range assigned (anywhere between 15 to 30 minutes). In the third phase, the payload reenters the earth's atmosphere and travels along a path affected by aerodynamics and delivers the explosive warhead at a location whose accuracy has improved over decades to less than 0.5 km over a travel distance of 10000 km. The dynamics of injection is calculated to get to the delivery location via ballistic-aerodynamic effects. The first part of the trajectory is identical to what a satellite launch vehicle experiences. While the launch vehicle delivers the payload to an orbit circling the earth, the launch vehicle of this class of missiles stops its action at delivering the payload in atmosphere condition sufficient to help achieve a subsequent sub-orbital flight.

The guidance systems use GNSS and INS - gimballed or strap-down similar to what is done for satellite launch vehicles (discussed earlier). Control is achieved via thrust vector devices and/or thrust termination in various designs (see Chapter 3, sec. 3.18).

Celestial guidance is used on some missile systems to correct navigational errors arising out of inertial navigation systems. This is termed "astro-inertial guidance system" and is a fusion of sensor and information from both the sources. It is particularly employed on submarine-launched ballistic missiles because the navigation system of moving submarines accumulate more errors over long periods when they are away from calibration sources

7.8. Bird Navigation

Like the aspects of aerodynamics, propulsion and structures on birds presented in earlier chapters, there are also aspects about bird navigation that appear astounding and perhaps they could be helpful in evolving new designs for aeronautical navigation. A very large number of studies have been conducted on the migratory habits and the approaches used for navigation over the last several decades (for a recent relevant summary, see Bingman et al, 2006).

It is clear that navigation requires knowledge of three aspects: current location, the details of destination, and the direction of travel. The details of destination needed by birds are the location of the wintering and breeding areas. It is thought that the evolutionary process has integrated the navigation strategy into the DNA since even a very young bird navigates without being taught. Of course, with experience over a time, the navigational skills become more accurate. They use various spatially available features like familiar land marks, the equivalent of pilotage in airplane navigation, atmospheric odours with a neural representation of the mosaic and gradient maps inside the hippocampus area of bird's brain, solar orientation using polarised light particularly in the evening light, star based navigation and also use vector navigation and compass mechanisms. The curious property of their magnetic compass is that it is an unconventional polarity compass by which north and south are defined by the angle the ambient magnetic field lines make with some vertical reference like gravity. It should be brought out that these broad conclusions have been obtained through very inventive and systematic experiments with birds in the laboratory as well as in the field.

One of the key new features is that many birds have a sensing capability for weak magnetic fields. There are at least three possible directions of explanation. (i) The neurons in bird brain and inner ear seem to contain iron molecules and appear sensitive to three different aspects of the geomagnetic field: direction, intensity, and polarity, all required for self-location. (ii) There is region called cluster N in bird's eyes sensitive to the magnetic field because when cluster N is removed, the ability of the birds to sense the north is lost. (iii) TA protein called cryptochrome in the brain is split into two magnetically sensitive molecules when exposed to light. A quantum effect called "quantum entanglement" then allows pairs of molecules to cooperate, even when separated, to

detect variations in the magnetic field. This is thought to allow birds to see patterns of spots that remain stationary as they turn their heads, to indicate magnetic direction.

Which one of the mechanisms or their combination is at work in bird navigation is still being examined. Some of these, if true - like the protein, cryptochrome may be capable of being used in aviation or other technologies in times to come.

7.9. Summary

While the early developments of navigational aids in aircraft were similar to those used by birds that had the leading edge of millions of years of evolution (pilotage being the example), the developments in navigation over the last seven decades have been phenomenal. Radio based navigation in a large range of electromagnetic spectrum (from very low frequencies or long wave length to very high frequencies or short wave length) with radio beacons, radars in its various forms, like primary radar, secondary surveillance radar are most effectively used in air traffic management both by stationary systems as well as on-board systems for identification purposes as well as weather mapping. Phased array radar and inertial navigational systems with global positioning satellite-supported systems have been imbibed into aeronautical and launch vehicles slowly, but surely. Synthetic aperture radar is currently used in remote sensing applications.

Reduced weight and volume due to miniaturization of electronics have contributed to enhancement of performance over years and greater adoption in air and space vehicles. While the broad principles of electromagnetic radiation have been captured easily and well in early times, fine-tuning required to enhance the performance, development of relevant hardware like power systems and antennae for multitude of demands has also occurred in this period. The developments of ring gyro and fiber-optic gyros have contributed to improved quality of INS systems. Not the least are the analysis tools of signal processing to obtain higher signal-to-noise ratio in radars, combining theory with hardware development for phased array radars, and composing high quality pictures from time-shifted reception of signals in synthetic aperture radars.

Military developments of use of these techniques and devices to track the enemy either on ground or in the air and home on to it with a warhead has pro-

pelled these developments most of the time. While many of these technologies will continue to exploit developments in science, one area that may find greater intensity of development consists of combining biology with quantum physics as is being unraveled in the case of migratory birds.

Bibliography

[1]   Ashby, N (1979) http://areeweb.polito.it/ricerca/relgrav/solciclos/ashby_d.pdf; see also Ashby, N and Allan, D. W., Practical implications of relativity for a global coordinate time scale, Radio Science, 14, pp. 649 - 669, 1979

[2]   Bingman, V., Jechura, T. and Kahn, M. C., (2006) Behavioral and neural mech-anisms of homing and migration in birds, chapter in Animal spatial cognition, volume edited by Brown, M. F and Cook, R. G. http://www.pigeon.psy.tufts.edu/asc/

[3]   Blake, L V., (2000) Prediction of radar range http://helitavia.comwww.helitavia.com/skolnik/Skolnik_chapter_2.pdf

[4]   Budge, M. C., Jr, (2011) http://www.ece.uah.edu/courses/material/EE619-2011/RadarRangeEquation(2)2011.pdf

[5]   Cossins, D (2013) http://www.the-scientist.com/?articles.view/articleNo/36722/title/A-Sense-of-Mystery/

[6]   Dunn, R. J., Bingham, P. T and Fowlwr, C. A., Ground moving target indicator and the transformation of US war fighting, Northrum Grummon, http://www.northropgrumman.com/AboutUs/AnalysisCenter/Documents/pdfs/Ground-Moving-Target-Indicator.pdf

[7]   Fenn, A. J., Temme, D. H., Delaney, W. P., and Cortney, W. E., (2000) The development of phased-array radar technology, Lincoln Laboratory Journal, 12, pp. 321 - 340 https://www.ll.mit.edu/publications/journal/pdf/vol12_no2/12_2devphasedarray.pdf

[8]   Internet1,   (2016)   http://www.theairlinepilots.com/forum/viewtopic.php?t=908

[9]   Internet2, (2016) https://en.wikipedia.org/wiki on Radio_navigation, Avionics, Gyro-scope, History_of_radar

[10] Internet3, (2016) http://mathpages.com/rr/s2-07/2-07.htm; http://www.physicsinsights.org/sagnac_1.html

[11] Internet4, (2016) http://www.pilotfriend.com/training/flight_training/nav/rad_nav_overview.htm

[12] Internet5, (2016) http://www.langleyflyingschool.com/Pages/CPGS%20Radio%20Navigation.html

[13] Internet6, (2016) http://aviation.stackexchange.com/questions/2589/how-do-airliners-cross-the-ocean-without-gps

[14] Internet7, (2016) http://www.ixys.com/Documents/Appnotes/IXAN0015.pdf

[15] Moreira, A., Prats-Iralola, P., Younis, M., Kreiger, G., Hajnsek, I., Pap-athanassiou, K. P., (2013) A tutorial on synthetic aperture radar (2013) http://elib.dlr.de/82313/1/SAR-Tutorial-March-2013.pdf

[16] Ray Kwok, (2016) Antenna fundamentals, http://www.engr.sjsu.edu/rk-wok/EE172/Antenna_Fundamental.pdf

[17] Singh, H and Jha, R. M., Active radar cross section reduction - Theory and Applications, Cambridge University Press, 2015

[18] Siouris, G. M., 2004, Missile guidance and control systems, Springer

[19] Tempere, 2015 http://aerostudents.com/files/avionics/InertialNavigation-Systems.pdf

[20] Tutorial, 2015 http://www.radartutorial.eu/druck/Book1.pdf

[21] Wikipedia (2016) https://en.wikipedia.org/wiki/Synthetic_aperture_radar

[22] Makris G. R (2016) http://www.k-makris.gr/AircraftComponents/Laser_Gyro/laser_gyro.htm

8 Overview

Six different components involving different disciplines from solid and fluid mechanics, aerodynamics, thermodynamics, electromagnetics, materials and manufacture are required to create functional aeroplanes, helicopters, missiles, launch vehicles and satellites. These vehicles operate differently and need emphasis of different aspects of the disciplines. Low speed flight vehicles need aerodynamics for shaping and structural analysis and design for strong light weight construction but need little of thermodynamics. Propulsion system, which in itself needs thermodynamics, but as a system element will have an impact on the design of the system, is connected to other elements in a feature that is usually dealt with under the title vehicle-propulsion integration. Civil aircraft can choose engines from different manufacturers with similar broad specifications but some aspects specific to their aircraft; hence, the relationship of the rest of the design with propulsion is weak. However, when speeds increase, the connection between the vehicle elements becomes tighter and when designing a hypersonic vehicle, the vehicle elements with propulsion have to be dealt with together because enthalpy changes due to flow are comparable to heat addition due to fuel energy. Chemical thermodynamics of high enthalpy air stream plays acrucial part in this development.

Tactical missile realization requires greater emphasis on propulsion optimization and avionics and guidance as important aspects with other fields playing the auxiliary role. Launch vehicle design too is similarly dependent on propulsion (and staging), and navigation and guidance systems to achieve the orbits. The role of aerodynamics is far less than for aircraft and is related to the early part of the flight through the atmosphere. Satellites function outside the atmosphere and need space mechanics contributed largely by Newtonian gravitational theory. While aircrafts can be checked out for maintenance on the ground, satellites in orbit cannot be reached for repair in any similar sense. The amount of work to be done on the ground before launch to ensure safe life for seven to ten years is very significant.

Cost is a matter of concern for all vehicles. But it is of the greatest concern for civil aircraft. Designing and manufacturing techniques need to keep the cost in mind. If we recognize that the processes driving down the cost without any reduction in quality and full aspects of safety cannot be achieved in one design

cycle, we conclude that building variants of a given aircraft – for instance, an aircraft for freight in addition to passenger transport will provide opportunities to improvise.

Building a Boeing 747, then the later aircraft, 757 to 787 all provide experiences that many times cannot be implemented in one current aircraft, but will get into the next generation aircraft. This is why building a new airliner from scratch is an extraordinarily difficult task. The learning required is long and hard. This is also why only a few companies that have built up the knowledge base for design and manufacture continue to build better ones, costs being lower for making incremental crucial advances and thus maintain leadership.

The situation for tactical missiles and launch vehicles is not very different. Building one working system, reviewing and identifying aspects in design or mission profile to reduce the weight of the system elements usually leads to the next set of superior systems. Also successful vehicle development for air force application may lead to variants for navy or army with demands for better elements than in the first version. It is this constant and continuous engagement in design and development that provides leadership to an industry or country in specific areas.

Since much learning has been accomplished over the last six decades or more, a majority of future developments will be incremental. Yet, it is possible that one country doing it ab-initio may redo or re-engineer systems known elsewhere and learn on its own what has been known very well otherwise. But it takes all that one has done over a wide platform for radically new developments to come by. One area that will see many dramatic developments will be in micro- and nano-vehicles drawing analogy from bird and insect flight. These areas will find integration of ideas from biology far more significantly than in the past.

A. Appendix 1

Equilibrium properties - Pressure (p) and Temperature (T)

As one moves from lower layers of the atmosphere to altitudes beyond 1000 km, the ambient density comes down significantly. Close to the surface of earth, the density is about 1 kg/m³, at 100 km altitude it is 10^{-8} kg/m³, and at 1000 km altitude it is 10^{-17} kg/m³. At these conditions, the number of molecules per cm³ is about 10000 where as ambient conditions it would be about 2 x 10^{19}. Because the number of molecules are very small their collisions that are directly responsible for the thermodynamic properties p and T become inadequate to cause average properties.

The ideas of pressure and temperature are based on the fundamental idea of it continuum and equilibrium. The idea of continuum is that the fluid which is composed of molecules or atoms can be treated as whole indivisible substance whenever the scale of objects over which the fluid moves or interacts is much larger than the molecular dimensions. This feature is described by invoking a dimensionless quantity called Knudsen number (K_n) defined as the ratio of mean free path to the size of the object or more appropriately, a characteristic physical dimension becomes relevant. For all K_n < 0.1 (more typically K_n~0.01), the flow is considered a continuum. For K_n > 1, molecules are so dispersed, ideas of statistical mechanics need to be brought in. These ideas are important when gas-to-gas interactions alone are important or when interactions occur with a physical surface.

The connection with ideas with equilibrium need a more careful understanding.

Suppose we consider a container (could even be a room) into which ambient or hotter or colder air can be introduced and a pressure transducer and a thermometer or a thermocouple are placed at the wall to measure the pressure and temperature. Let us take it that both the instruments respond and reasonably fast when cold or hot gas is introduced into the container. Whenever the valve of inlet air is opened, the pressure gages starts responding. They respond because the molecules inside the room are collide with each other and with the surface of the wall. They transfer their momentum to the wall and this is recognized as pressure. They also transfer energy of random motion and this is interpreted

as temperature. Once a new set of conditions are set, the gages acquire and remain steady at new values. These are the equilibrium properties of the gas inside. It should be noted that the processes inside the container are dynamic. There will be continuous exchange of momentum and energy. It turns out that the net change due to this exchange is negligible and so a state of equilibrium can be taken to be established.

The aspect we should recognize is that molecular collisions must occur "frequently" and averaged over a meaningful period, they must remain same. There can be changes with time leading to unsteady behavior of the equilibrium quantities, pressure and temperature.

There is a spatial scale associated with this collision dynamics. Since the molecules are moving at some speed between collisions, the mean distance between collisions is called the mean free path (λ). The mean free path is related to molecular dimensions and number density by

$$\lambda = \frac{1}{\sqrt{2}\pi d^2 n}$$

(A.1)

where d is the molecular diameter and n is the number density of the molecules. The number density follows the equation of state $n = p/kT$ where k is the Boltzmann constant. Thus

$$\lambda \sim \frac{T}{pd^2}$$

(A.2)

Thus increased temperatures and reduced pressures cause the mean free path to increase. Typical mean free path in low earth atmosphere is about 0.07 microns and is several kilometers at these altitudes (100 km) due to very low pressures and higher temperatures. This regime of flow is called free molecule flow and needs the use of kinetic theory of gases (Boltzmann equation) to analyze the flow behavior. The mean speed of the random molecular motion is given by

$$v_{rms} = \sqrt{\frac{3kT}{m}} = \sqrt{\frac{3RT}{\mathcal{M}}}$$

(A.3)

where m is the molecular mass, R, the universal gas constant and $\mathscr{M}$ is the molecular weight of the gas. Typical random velocity of oxygen is about 480 m/s at $T = 300$ K.

Thus, when averaging of momentum and energy transfer of random motion of molecules is discussed, the scale of averaging must be much larger. And indeed, the size of most objects is much larger, typically a few mm to meters. Averaging properties over a few microns should be adequate to resolve the flow behavior in the low atmospheric flows. However, when one wishes to discuss the meaning of atmospheric pressure and temperature for flight vehicles at altitudes several hundred kilometers and beyond, the averaging sizes that must be considered are much larger. So also the averaging times for the data must also be higher.

This does not take away the meaning of temperatures of solid objects like the body of a satellite. The interaction of the satellite with solar radiation leading to substantial changes in the temperatures during day or night would still be appropriate and meaningful.

A further point of importance is that in all flows where there are changes in pressure and temperature, like for instance in flow through flames and rocket nozzles, the idea of equilibrium needs to be understood as follows. The flow transition through the flame or nozzle goes through a sequence of equilibrium states even if the overall flow is in non-equilibrium. These become questionable only in cases like a high Mach number flow goes through a shock across which temperatures and pressures rise (see Chapter 2) is only a few mean free paths in thickness.

B. Appendix 2

How are forces generated over air-foil like objects?

Literature has several descriptions of the force generation mechanisms when there if flow over airfoil-like objects. Wiki (2016) contains a good discussion of the subject. NASA (2016) carries a discussion of the incorrect approaches to the lift generation mechanisms.

First, the flow that comes in, say horizontally, flows past the wing and moves off downstream. If the wing cross-section, an airfoil, as it is called, is symmetric and axially symmetrically located, the airfoil is set to be at zero angle of attack and the flow leaves the airfoil axially as shown in Figure B.1. There will be no vertical force (or lift). Viscous effects close to the surface of the airfoil dissipate some momentum and there will be a resistance (called drag). To keep the airfoil in position one needs to apply some force (thrust). Now we position the airfoil at an angle to the mainstream as shown in the bottom of figure B.1. The exit stream leaves the trailing edge at a downward angle to the horizontal in-flow line. This implies that the airfoil has imparted a downward momentum to the air-stream. The reaction to this is an upward force on the airfoil (following Newton's third law). This naturally implies non-zero lift. Also there will be drag that will now be composed of direct viscous effects and inviscid effect called profile drag (that is viscosity inspired, see discussion in succeeding paragraphs).

While this picture is adequate to appreciate how lift is generated, we need to examine the fluid dynamics over the airfoil to elucidate the dependence of lift and drag on flow parameters and fluid properties.
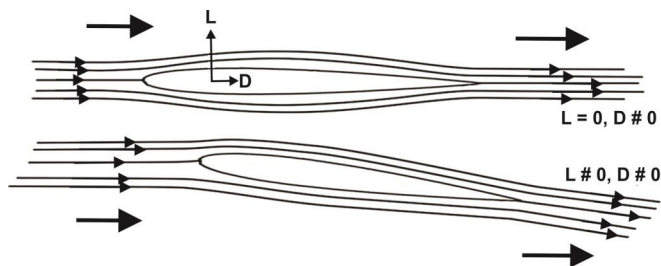
Figure B.1.: The stream lines over an airfoil at zero and non-zero angles of attack. The flow exits axially in the first case and leaves the trailing edge at a downward angle
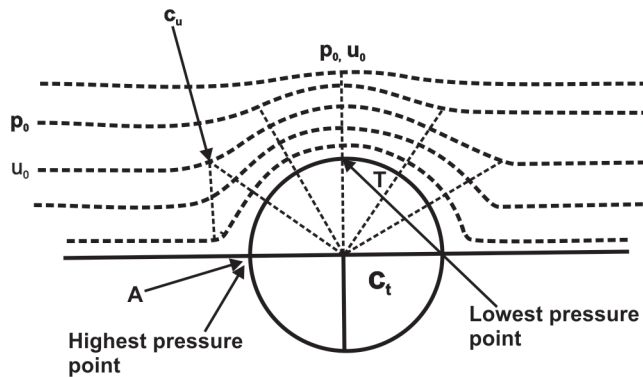
Figure B.2.: The stream lines over a cylinder. Note that in the upstream region the centre of curvature is in the stream and towards the top region, T, it is inside the cylinder.

We therefore, look at the flow past an infinite cylinder first. The uniform flow going over the cylinder has a pressure P_0 and stream speed U_0. If we enquire as to how the flow takes place it will appear as shown in Figure B.2. As can be seen, the stream lines approaching the cylinder have a curvature whose center is outside the cylinder and so, inside the flow (C_u) and those going over the top region of the cylinder have a center inside the cylinder (C_t) (Mathew, 2011). Since the flow is turning around this movement causes a centripetal acceleration (pressure gradient normal to the stream lines $\sim v_t/R$, where v_t is the velocity tangential to the flow lines or streamlines, as they are called and R is the radius of curvature). The stream lines have a large radius far away from the cylinder and become smaller as the cylinder is approached. This leads to rise in pressure from the free stream value to larger values towards the cylinder. In fact the streamline on the axis divides itself into the top and bottom regions (at A). At this point the pressure will be the highest. Towards the top part marked by T, since the center of curvature is inside the cylinder, the regions far away from the cylinder along C_t - T experience little pressure change and this pressure is close to P_0. As the radius of curvature comes down towards T, the *pressure drop* must increase. This therefore brings down the pressure at the top of the cylinder and in fact it will be the lowest. The behavior of the pressure over the cylinder with an ideal fluid (inviscid) is shown in Figure B.3. It is higher than the free stream in the upstream zone and lower than the free stream value on the top region. The flow is symmetric about the horizontal and vertical lines through C_t because the flow is inviscid and the geometry is sym-
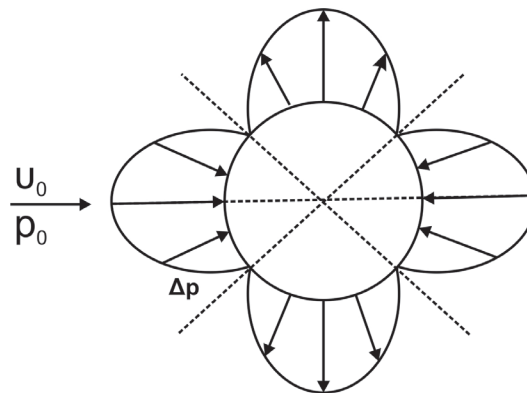
Figure B.3.: Pressure variation over the cylinder with an inviscid flow past it. Notice that the pressure distribution is doubly symmetric
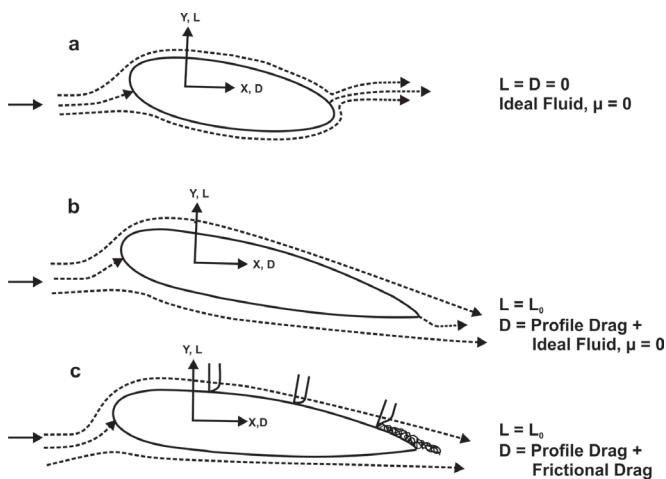
Figure B.4.: Flow behavior over objects modified from a circular cylinder with the first two cases (a and b) involving geometric change but zero fluid viscosity and the third case, b involving a viscous fluid

metric. It is important to understand that the variation in pressures also leads to accompanying changes in velocities.

This follows from momentum conservation equations that lead to $p + \rho V^2/2 = P_0$ along a stream line. Here p is the static pressure, ρ is the density of the

fluid, u is the local velocity of the fluid, P_0 is the stagnation pressure. For the ideal fluid, the stagnation pressure remains constant. Therefore when static pressure increases or decreases, the velocity decreases or increases.

We now examine the flow field in three cases (a) the circular cylinder elongated into long ellipsoid with an ideal fluid, (b) the ellipsoid being converted into an object with sharp trailing edge with an ideal fluid and (c) the object as in (b) experiencing a real fluid with viscosity. These are depicted in Figure B.4. The fluid will have a forward stagnation point (or line, to be correct since the geometry is two-dimensional) and a downstream stagnation point. The front stagnation point refers to the location at which the streamline divides into two - one going over the top part and the other bottom part. The aft stagnation point refers to the merging of the stream lines and its moving off into the stream. In (a), the stream line from the bottom area bends around the end of the body and reaches the stagnation point. For this configuration, the force balance leads to zero forces, as obtained from a mathematical analysis of the flow. The generality of this result is established for any general two-dimensional wing shape by converting the geometry through "conformal transformation" into flow over a cylinder. This is contradictory to experience and is termed d'Alembert's paradox (see Bertin and Cummings, 2009). As the trailing edge is made sharper, the flow turn over leads to very large velocity gradients ultimately needing infinite velocity gradient for a turn around when the trailing edge is very sharp. This causes the flow to move off from the trailing edge itself as shown in case (b) in Figure B.4. The stagnation point moves from the position in case (a) to the trailing edge. This leads to a readjustment of pressure forces such that one component of the net force is non-zero lift and the other profile drag, a drag component that results from a readjustment of pressure forces. The role of viscosity in this readjustment is only to the extent of shifting the stagnation point from over the aft region to the trailing edge. This condition in which the rear stagnation point moves to the sharp trailing edge is termed a Kutta-Joukowski condition. In case (c), viscous effects come into play to much larger extent.

The role of viscosity near the surface is to equalize the velocity of the fluid at the surface with that of the body. The velocity will be zero if the body is stationary and equal to the speed of the body if the body is moving. The viscosity of air is very small and the zone affected by viscosity is a small layer next to the surface of the body. In this case, the flow and the pressure forces are about
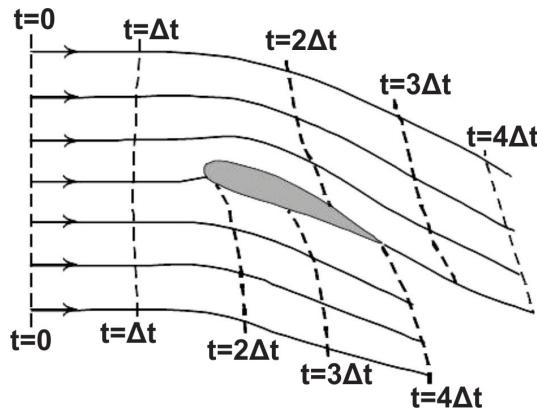
Figure B.5.: The position of the "particles" at various locations on the vertical positions with time in a steady flow. Note that the particle tracks in the top of the airfoil move far ahead of the airfoil at the time the particles at the bottom reach the trailing edge, adopted from Torrenbeek and Wittenberg (2009)

the same as in case (b). However, the viscous effects dissipate momentum near the body and this leads to additional defect of the momentum. Since this momentum loss occurs largely in a direction aligned to the flow, an additional component to drag is introduced. Thus drag has two components - profile drag and viscous drag. Lift that is obtained from inviscid calculation with smooth flow at the trailing edge is little affected by viscosity.

There is an alternate explanation that when the flow goes over the airfoil, the flow has to start at the leading edge and reach the trailing edge at the same time and this requires that the air flows at a higher speed over the top of the airfoil than the bottom. In order to explore this question particle tracking technique was used to compute the flow. Figure B.5 shows the particle tracks at different positions of the incoming stream over the airfoil in a steady flow over the airfoil (from Torrenbeek and Wittenberg, 2009). The particle tracks on the top of the airfoil move far ahead of the airfoil when the tracks on the bottom have reached the trailing edge of the airfoil. This means that the average stream speed over the top of the airfoil is more than in the bottom region and it is not that this arrangement has somehow to bring the particles in the top region match with those in the bottom in reaching the trailing edge.

Bibliography

[1]   Bertin, J. J., and Cummings, R. M., (2009) Aerodynamics for Engineers, Pear-son Prentice-Hall

[2]   Mathew, J (2011) Personal communication

[3]   NASA (2016) https://www.grc.nasa.gov/www/k-12/airplane/wrong1.html

[4]   Torenbeek, E and Wittenberg, H., (2009) Flight physics (essentials of aero-nautical disciplines and technology with historical notes), (Fig. 4.14 on p144) Springer

[5]   Wikipedia (2016) https://en.wikipedia.org/wiki/Lift_(force)

C. Appendix 3

Materials on different components of aerial vehicles

In the following is provided a description of materials in various parts of transport and supersonic aircraft as well as helicopters. In general, the typical aluminum alloys used are 2024-T3, 2024-T4, 2014-T6, 7075-T6, 7079-T6, 7178-T6, 2219-T81, 2219-T87, 5052-H39, 5056-H39, 3003-H19, in various physical shapes and some in the form of foils – 5052-H19, or 5356-H19. These alloys are composed of several alloying elements – Zn, Mg, Ti, Cr, Cu, Fe, Si, Mn and others. The most used 7075 alloy has 5 to 6 % Zn, 2 to 3 % Mg, 1 to 2 % Cu, whereas the 2024 alloy contains 4 to 5 % Cu, 1 to 2 % Mg, and others in smaller quantities. In these specifications, the second alpha-numeric designation refers to tempering. Symbol O implies annealed, T implies thermally treated and H refers to strain work hardened. The digits refer to the cycle that the system must go through. For instance, T3 implies solution heat treated and cold worked; T4 refers to solution heat treated and naturally aged to substantially stable condition; T6 refers to solution heat treated and artificially aged.

Transport Aircraft

Most aircraft are generally of semi-monocoque and sheet-stringer aluminum construction. The alloys primarily utilized today are 2024-T4 and the alloys having still higher strength (2014-T6, 7075-T6, 7079-T6 and 7178-T6). Where sheet is used, the alclad form is preferred (alclad is the aluminum alloy bonded to pure aluminum on the outside to prevent the corrosion problems) The upper skins and spar caps of wings often are of 7075-T6 and 7178-T6, because the critical requirement is high compressive strength, and tension loading or fatigue strength are not the most important one.

For wing tension members, shear webs, and ribs, alloys 2014-T6, 2024-T4, and 7075-T6 are used extensively. For these applications, fatigue performance and frac-ture toughness (see later for a discussion on this), combined with high strength, are the characteristics of chief concern.

Rolled sheet and plates 1 to 10 *mm* thick are employed for wing skins by several manufacturers. Fail-safe design in this type of construction is achieved by many separate stiffeners, formed from sheet or milled from standard extrusions, or machined from stepped extrusions to accommodate integral end

fittings. Adhesive bonding, instead of riveting, is employed by some designers for attaching doublers and stiffeners to the skin sheet.

Fuselages on aircraft are pressurized to the pressure at 8000 ft (2.4 *km*) altitude, but this value is being brought to the pressure at 6000 ft (1.83 *km*) altitude for greater passenger comfort (Boeing 787 dreamliner). The pressurization cycles and safety requirements dictate the design parameters of high-load, fatigue-resistant and fracture-resistant structures for this application. For this design, fracture toughness has the largest influence on the weight of the structure. Tempered alloys with good combination of static strength, fracture toughness, and corrosion resistance are the best for this application. Al clad sheets typically, 1 to 5 *mm* thick are used.

Landing gear structural parts for heavy airplanes are often produced as aluminum alloy forgings. The main cylinders are made on hydraulic presses as conventional closed-die forgings, with a parting plane at the center of the cylinder. In the past, alloy 2014-T6 was employed extensively, but in recent years alloy 7079-T6 or T611 has been used. Tempered 7075 Alloy is also considered due to its good resistance to stress-corrosion cracking. Other landing gear members, attached to the main cylinders, also are produced as aluminum forgings, including structural forgings in the fuselage and wings, which distribute the landing gear loads into other structures, and forged parts for the retracting mechanism.

Wheels for heavy civilian or military airplanes generally are designed on a safe-life basis. They are replaced at regular intervals during the life of an airplane, allowing use of lighter-weight designs than are required for long-time fatigue resistance.

Supersonic Aircraft

Supersonic aircraft, designed to withstand aerodynamic heating to 120^0C for over 100 *hr* (the time in service is accumulated in small increments), generally utilize the 2xxx series alloys in artificially aged tempers for skin sheet. The 2024-T81 and T86 alloys are the most extensively employed; 2014-T6 and 2024-T62 or T81 are used for extruded members. Alloys 2014-T6 and 2618-T61 are employed for forged products located in heat-affected areas; alloy 2024, which can be forged, also can be considered for parts of this type. Alloy 2219 has had limited application in engine pods as sheet, rivets, and forgings.

The designers of one supersonic bomber (B58) have made extensive use of honeycomb core sandwich construction for wing panels, to achieve a stiff structure that does not buckle when stressed in compression near the yield strength of the material. The honeycomb in these sandwich panels is 5052 aluminum foil, except where fiber glass is applied to further insulate the fuel from aerodynamic heating.

Honeycomb panel frames are predominantly 7075-T6, machined from plate to eliminate corner joints. Aluminum honeycomb is also used in the beaded areas of skin doublers, to help stiffen the fuselage skin. At elevated temperatures, 2024-T81 foil provides higher strength than is obtained in work hardened alloys, such as 5052-H39 and 5056-H39. The supersonic transport aircraft developed by British and French Aerospace companies (Concorde that is currently phased out) made general use of alclad and bare 2618-T6 for the structure.

Helicopters

Helicopters have critical structural requirements for rotor blades. Alloys 2014-T6, 2024-T3, and 6061-T6, in extruded or drawn hollow shapes, are utilized exten-sively for the main spar member.

The blade skins, typically 0.5 to 1 mm thick, are primarily alclad 2024-T3 and 6061-T6. Some blades have alloy 3003-H19 or 5052-H39 honeycomb core; others depend on ribs and stringers spaced 120 to 300 mm apart to prevent excessive buckling or canning of the thin trailing edge skins. Adhesive bonding is the most common joining method. The cabin and fuselage structures of helicopters generally are of conventional aircraft design, utilizing formed sheet bulkheads, extruded or rolled sheet stringers, and doubled or chemically milled skins.

INDEX